

**UNIVERSITÀ DEGLI STUDI DI PADOVA**

Dipartimento di Ingegneria Industriale

Tesi di Laurea Magistrale in INGEGNERIA ENERGETICA



&

**CERN**

Technology Department, Vacuum Surfaces and Coating Group,  
Vacuum Studies and Measurements (TE-VSC-VSM), Geneva, Switzerland



**COMMISSIONING OF  
THE CERN LARGE HADRON COLLIDER  
“VACUUM PILOT SECTOR”**

*Supervisor: Prof. Piergiorgio Sonato*  
*Co-supervisor: PhD. Vincent Baglin*

*Student: Elena Buratin*  
*Identification Number: 1080468*

Academic Year 2015/2016



Ai miei genitori, Anna e Francesco,  
con Amore e Riconoscenza







# CONTENTS

ABSTRACT .....	1
PREMESSA .....	2
1. INTRODUCTION .....	3
1.1 The Structure of CERN Accelerators Complex .....	3
1.2 The structure of LHC Accelerator .....	5
1.3 Vacuum in accelerators .....	6
1.3.1 Classification of vacuum .....	7
1.3.2 Production of Vacuum .....	8
2. ELECTRON CLOUD PHENOMENON .....	13
2.1 Electron Cloud Phenomenon .....	13
2.2 Remedies for multipacting effect .....	14
2.3 SEY .....	15
2.4 Structure of the beam .....	16
3. THE LHC VACUUM PILOT-SECTOR PROJECT .....	19
3.1 Introduction .....	19
3.2 Installation .....	20
3.3 Instruments .....	24
3.3.1 Pressure gages .....	24
3.3.2 Pickup .....	26
3.3.3 Calorimeter .....	29
3.3.4 Residual Gas Analyser (VQM) .....	30
3.3.5 Electron Kicker Detector (EKD) .....	31
3.4 System and data acquisition .....	32
3.4.1 PVSS .....	32
3.4.2 LabVIEW .....	39
3.4.3 SCOPE .....	40
3.4.4 VQM program .....	41
3.5 Main table of tools Of VPS .....	43
3.6 Objectives of VPS .....	48
4. STEPS OF WORK .....	49
5. SCRUBBING RUN ANALYSIS .....	53
5.1 Scrubbing Plan for LHC .....	53
5.2 First Scrubbing Run .....	54

5.3	Second Scrubbing Run.....	59
5.4	Conditioning effect .....	62
6.	ANALYSIS .....	63
6.1	Check the reliability of the electrical measurements (Keithley and SCOPE) .	63
6.2	Study of the influence of the transparency of the grids of shielded pickup.....	67
6.3	Check the effective conditioning of surfaces during the scrubbing runs in different coatings with shielded pick up.....	73
6.4	Measurement of photons with unshielded pickup .....	77
6.5	Control the influence of the voltage in the electrical signals through a High Voltage Bias .....	82
6.6	Scan the energy spectrum of electron cloud (EKD) .....	84
6.7	Analyse the power deposition on the walls (Calorimeters) .....	87
6.8	Analyse the gas spectrum (VQM) .....	93
6.9	Gas Injections .....	97
6.9.1	Injection 2014.....	97
6.9.2	Injection 2016.....	102
7.	PLAN FOR THE NEW INSTALLATION .....	109
7.1	Plan for VPS 2016 .....	109
7.2	Production of new pieces .....	113
7.2.1	Rolling of tools and making hole plates .....	113
7.2.2	Cleaning of Stain steel ribbon .....	115
7.2.3	Welding of detectors.....	115
7.2.4	Assembly of detectors on liners.....	117
7.2.5	Bake out of chambers and wires.....	120
7.2.6	Vacuum Tests in the laboratory.....	121
7.3	Installation of new system .....	132
8.	CONCLUSIONS .....	135
8.1	Achievements in brief.....	135
8.2	Next steps.....	138
9.	BIBLIOGRAPHY .....	141
10.	APPENDIX: ACRONYMS.....	147
11.	APPENDIX: DRAWINGS.....	149
12.	ACKNOWLEDGMENTS .....	167

## **ABSTRACT**

The European Council for Nuclear Research (CERN) of Geneva is one of the most well-known research center in which knowledge, competence, talent, teamwork, creativity and enthusiasm are fundamental in order to reach goals. The main area of research is particle physics which deals with the study of the matter's components and the forces acting between particles. One of the most interesting engineering and technology fields is the Vacuum system, in particular that of Large Hadron Collider (LHC), and it is the biggest in the world. It works with different levels of pressure and vacuum technologies. It has three aims: insulating the cryogenically cooled magnets, the helium distribution line and the beam pipes.

This work focuses on the last purpose, studying and understanding the phenomenon of so called "electron cloud" in order to avoid it. This issue of the machine is very widespread, but quite new.

This work is divided in three phases: the first is about the preliminary calibration of the parameters and the instruments on LHC accelerator, from remote control without beam. The second is the data analysis starting with the two scrubbing periods in which it is possible to improve the superficial behavior of the inner material, directly in contact with the proton beam. The last part is about the optimization of the tools, the plan for replacing the lines of LHC from December 2015 and the built up of themselves.

The data acquisition was carried out at the Technology Department (TE), inside the Vacuum, Surfaces and Coatings Group (VSC), within the Vacuum Studies and Measurement Section (VSM). The "Vacuum Pilot Sector", in which it has been worked, is situated in the LHC Tunnel, near the LHCb experiment, in the sector A5L8.

## PREMESSA

Il Consiglio Europeo per la ricerca nucleare (CERN) di Ginevra é uno dei piú conosciuti centri di ricerca in cui conoscenza, competenza, talento, lavoro di squadra, creatività e entusiasmo sono fondamentali per raggiungere gli scopi. Il principale settore di ricerca é la fisica delle particelle che é legata allo studio dei costituenti della materia e delle forze agenti fra le particelle. Uno dei campi piú interessanti dal punto di vista ingegneristico e tecnologico é quello dei sistemi da vuoto, in particolare quello del Large Hadron Collider (LHC), ed é il piú grande al mondo. Opera con differenti livelli di pressione e tecnologie da vuoto. Esso ha tre scopi: l'isolamento dei magneti raffreddati in maniera criogenica, l'isolamento delle linee di distribuzione ad Elio a l'isolamento dei tubi dove passa il fascio.

Questo elaborato si focalizza sull'ultimo obiettivo, studiando e capendo il fenomeno del cosí detto "electron cloud", col fine di evitarlo. Questo problema della macchina e' molto diffuso, ma abbastanza nuovo.

Questo studio é diviso in tre fasi: la prima riguarda la calibratura preliminare dei parametri e degli strumenti acquisendo dati dall'Acceleratore LHC, da remoto senza la presenza del fascio. La seconda e' l'analisi dei dati a partire dai due periodi di "scrubbing" in cui é possibile migliorare il comportamento superficiale del materiale interno, direttamente a contatto col fascio di protoni. L'ultima parte riguarda l'ottimizzazione degli strumenti, il progetto per fabbricare nuove linee in LHC a partire da Dicembre 2015 e la costruzione delle stesse.

L'acquisizione dei dati é stata fatta al Technology Department (TE), all'interno al gruppo Vacuum, Surfaces and Coatings (VSC), nella sezione Vacuum Studies and Measurement (VSM). Il "Vacuum Pilot Sector", in cui si é lavorato, é situato all'interno del tunnel di LHC, vicino all'esperimento LHCb, nel settore A5L8.

# 1. INTRODUCTION

CERN is one of the most important research place in which lots of students work with illustrious people and researchers from all over the world. It was founded in 1954 in the Franco-Swiss border near Geneva. This site contains many departments in which people with different backgrounds collaborate in order to investigate particle physics.

## 1.1 The Structure of CERN Accelerators Complex

The instruments used at CERN are accelerators and detectors. At first accelerators boost two beams of particles before collisions take place. They can be circular or linear. These accelerator are joined together in sequence to reach higher energies and speed. The bigger is LHC (Large Hadron Collider) in which detectors are placed. The detectors, instead, gather clues about the particles (mass, speed, charge) created after the collision between the two beams (see *Figure 1-1*). (1) (2) (3)

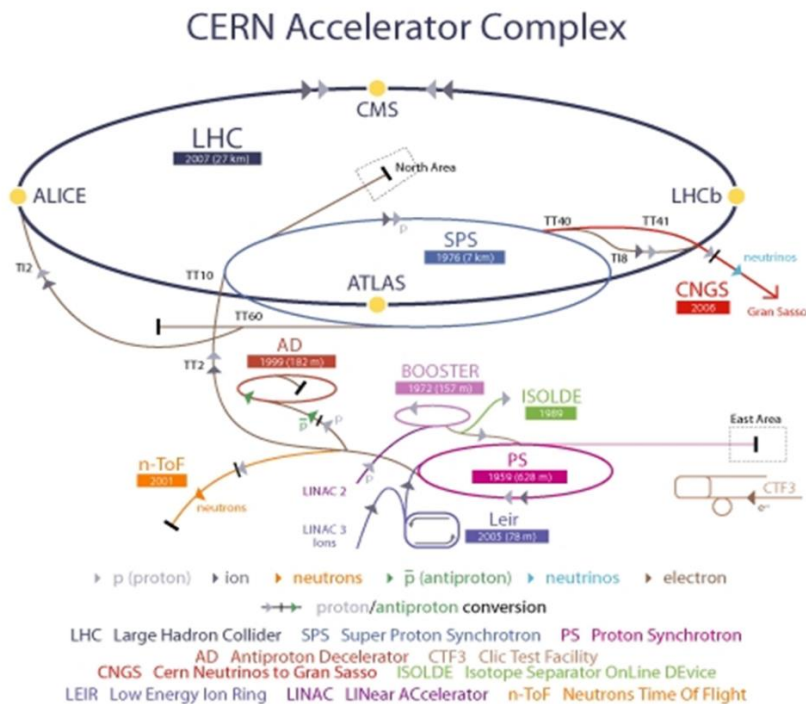


*Figure 1-1: The image shows the particle accelerators (circular and linear) and the detector existing at CERN (ATLAS, ALICE, CMS, LHCb).*

As you can see, there are several machines to reach LHC accelerator, in which the experiment studied in this report takes place. Each machine boosts the energy of beam, before injecting the beam into the next machine. The speed of particles is very close to that of light and the beams travel in pipes, kept under ultrahigh vacuum. The type of particle used depends on the experiment. They mainly are neutrons, ions, neutrinos, electron, protons and antiprotons. LHC, for example, accelerates mainly protons and sometimes heavy lead ions. (4)

The first step is to create protons from a bottle of hydrogen, using an electric field in order to remove the electrons from the hydrogen atoms. It is replaced twice a year only for pressure problems. *Linac 2* is the starting point, in which protons are accelerated and injected into *Booster (PSB)*, made up of four superimposed synchrotron rings. Subsequently there are *Proton Synchrotron (PS)*, *Super Proton Synchrotron* and *Large Hadron Collider (LHC)*. Inside it, there are two beams, circulating in opposite directions to permit the collisions inside four detectors: *ALICE*, *ATLAS*, *CMS* and *LHCb*.

The accelerator complex includes also the *Antiproton Decelerator* and *Online Isotope Mass Separator facility (ISOLDE)*, feeds the *CERN Neutrinos to Gran Sasso project (CNGS)*, *Compact Liner Collider* area and *neutron time-of-flight facility (nTOF)*. Here there is a summary of the accelerators and experiments at CERN (see *Figure 1-2*). (5)

Accelerator	Experiments	Overview
LINAC2		accelerates proton from the source and sends them to the booster (PSB)
LINAC3		accelerates ions from the source and sends them to LEIR
PSB		accelerates protons and sends to the PS and ISOLDE
PS	EA nTOF DIRAC CLOUD	East Area - various experiments neutron time-of-flight to observe and then measure lifetimes of Muons and Kaons to study possible links between cosmic rays and cloud formation
ISOLDE		to produce a range of isotopes for research
AD	ALPHA ASACUSA ATRAP	to make, capture and study atoms of antihydrogen and compare these with hydrogen atoms to compare anti-protons and protons using antiprotonic helium to compare hydrogen atoms with their antimatter equivalents
LEIR		accelerates ions and sends them to the PS
SPS	NA CNGS COMPASS	North Area - various experiments to send muon neutrinos to to the Gran Sasso National Laboratory in Italy to study how elementary quarks and gluons work together to give particles we observe
LHC	CMS ATLAS LHCb ALICE TOTEM LHCf	to search for the Higgs boson, extra dimensions, and particles that could make up dark matter to search for the Higgs boson, extra dimensions, and particles that could make up dark matter to understand why we live in a Universe composed almost entirely of matter, but no antimatter to study a state of matter known as quark-gluon plasma to measure the size of the proton and also monitor the LHC's luminosity to simulate cosmic rays to interpret and calibrate large-scale cosmic-ray experiments

Figure 1-2: Overview of accelerators and experiments.

## 1.2 The structure of LHC Accelerator

The most important experiment is the accelerator LHC that has started to work in September 2008. Now it is at its second running, started in April 2015.

It consists of 27 kilometer ring of superconducting magnets (arcs), which guide the beams, and accelerating structures to boost the energy of the particles, the RF cavities, the straight areas and the detectors. It is divided in 8 areas (see *Figure 1-3*).

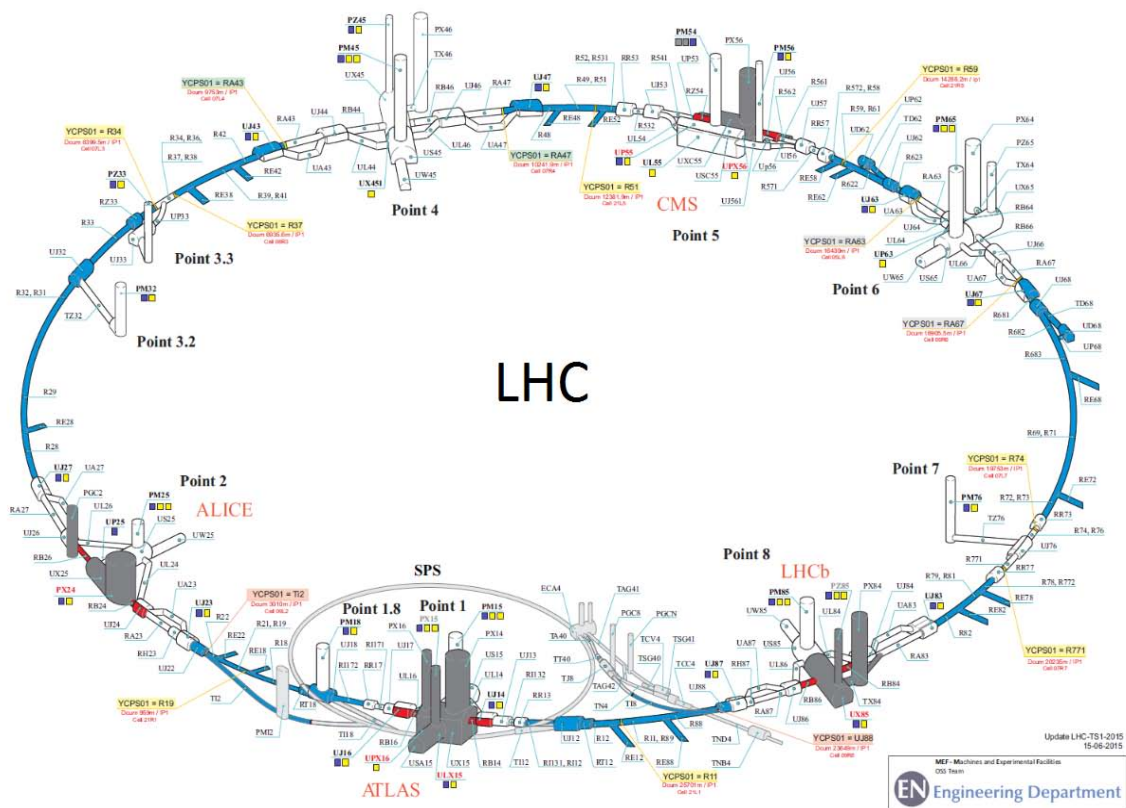


Figure 1-3: LHC accelerator.

Usually **magnets** have a temperature around  $-271^{\circ}\text{C}$ , kept by liquid helium cooling system. It is important to know that there are different kind of magnets: dipole which bend the beams, quadrupole which focus the beam, other kinds in order to squeeze the particles closer in order to increase the chances of collisions.

The **RF cavities** are metallic chambers that contains an electromagnetic field, in which radio waves interact with the beam in order to transfer some of the energy into them.

The **straight areas** usually are located between arcs (bending magnets) and detectors and they are at room-temperature.

The most important particle physics **detectors** are located in four different points of LHC accelerator: *ATLAS* in point 1, *ALICE* (A Large Ion Collider Experiment) in point 2, *CMS* (Compact Muon Solenoid) in point 5, *LHCb* (Large Hadron Collider beauty) in point 8 of the ring.

All this is controlled from CERN Control Center (CCC) in which I worked during scrubbing runs (see *Figure 1-4*).



*Figure 1-4: CERN Control Center (CCC).*

### 1.3 Vacuum in accelerators

One of the most interesting engineering and technology fields at CERN is the Vacuum system, in particular that of LHC, in which the experiment, I worked with, takes place. This vacuum system is the biggest in the world and it works with different levels of pressure and vacuum technologies. (6) (7) (8)

Vacuum is used at CERN in three different systems: first to insulate the cryogenically cooled magnets, second to insulate helium distribution pipes and third inside the beam pipes [1]. The first and second purpose is to reduce the heat deposition from the room-temperature environment into the cryogenic parts (1.9 K), while the third is to avoid the interaction between the beam and gas molecules.

This work focuses on the last purpose, studying and understanding the phenomenon of so called “electron cloud” in the beam pipes. The pressure is in the order of  $10^{-10}$  and  $10^{-11}$  mbar, a vacuum similar to that found on the Moon.



In the arcs the ultra-high vacuum is maintained by cryogenic pumping. Due to the fact that there is low temperature, the gas condenses near the wall of the beam pipe by adsorption.

In the straight areas usually two tricks are used to obtain a high vacuum. “Non-evaporable getter coating” (NEG), developed at CERN, absorbs residual molecules and “pump” them into the wall. It is a thin liner of titanium-zirconium-vanadium alloy deposited in the beam pipe. Secondly, the “bake out” of all components is a procedure in which the vacuum system is heated from the outside.

### 1.3.1 Classification of vacuum

Conventionally the vacuum is classified in rough ( $10^3 \div 1 \text{ mbar}$ ), medium ( $1 \div 10^{-3} \text{ mbar}$ ), high ( $10^{-3} \div 10^{-7} \text{ mbar}$ ) and ultra-high vacuum ( $< 10^{-7} \text{ mbar}$ ). In this work, the kind of vacuum used is the last one, ultra-high vacuum.

In the first two steps, rough and medium vacuum, the density of molecules is high and the pumping is not affected by the degassing of walls. The flow regime is viscous.

In the third step, the high vacuum, the molecules are quite all on the walls and the pumping consists on removing them. The flow regime is molecular because the molecules don't interact between them.

In the ultra-high vacuum, the time in which the experiment takes place is lower than that necessary to create a monolayer of molecules on the walls. In this way the wall is ‘clean’ and the molecules present on the volume are coming from the material of the wall. The regime is molecular.

Focusing on the explanation of flow regime, it is the way in which molecules are distributed on the vessel and interact between them. It can be viscous or molecular.

In the first the mean free path between molecules is small and they interact between themselves. This flux can be laminar or turbulent.

While, in the molecular regime the mean free path is very big comparing to the dimension of the vessel and the molecules don't interact.

In between there is a third state, the intermediate in which dimension of the free path and the vessel are in the same order of magnitude. (9)

### 1.3.2 Production of Vacuum

Pumps are used in order to create vacuum. There are several kinds of pumps, considering different ranges of pressure. The range of working pressure is indeed one of the most important parameters in order to install a pump. Another important parameter is the minimum pressure the pump is able to reach. This depends on the leaks of the pump, on the diffusion of the pumped gas and on the geometry of the system. Here it is possible to see the different ranges for the most important pumps used (see *Figure 1-5*). (10) (11)

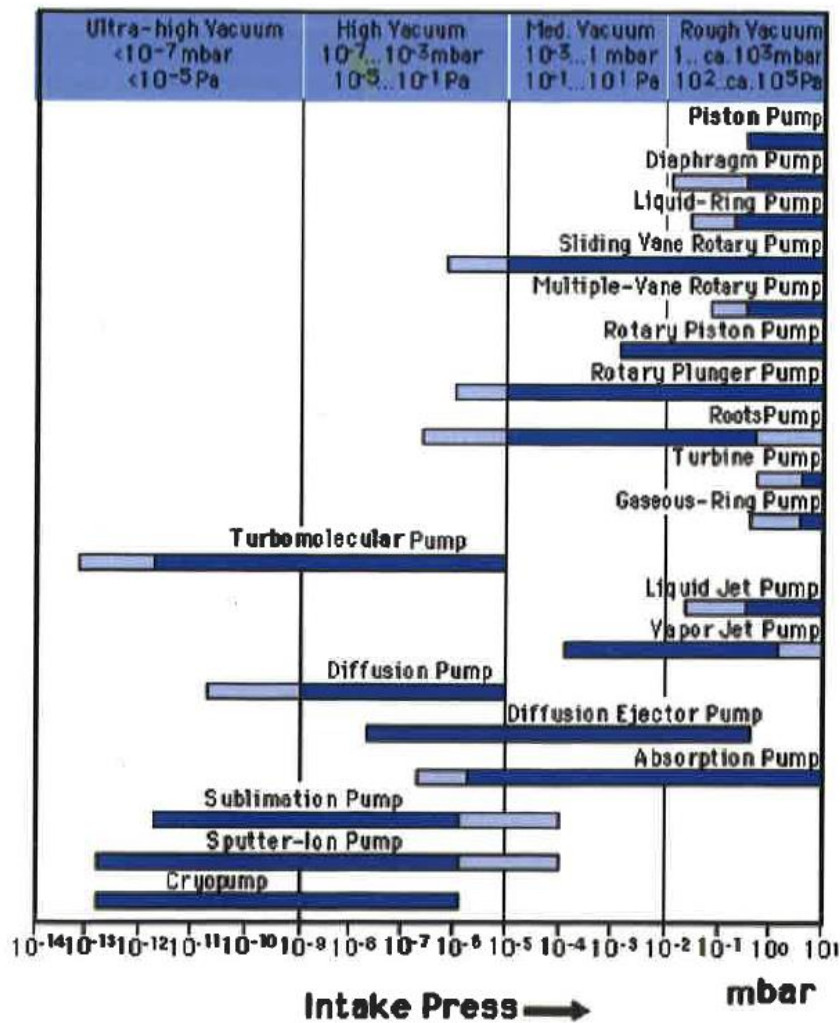
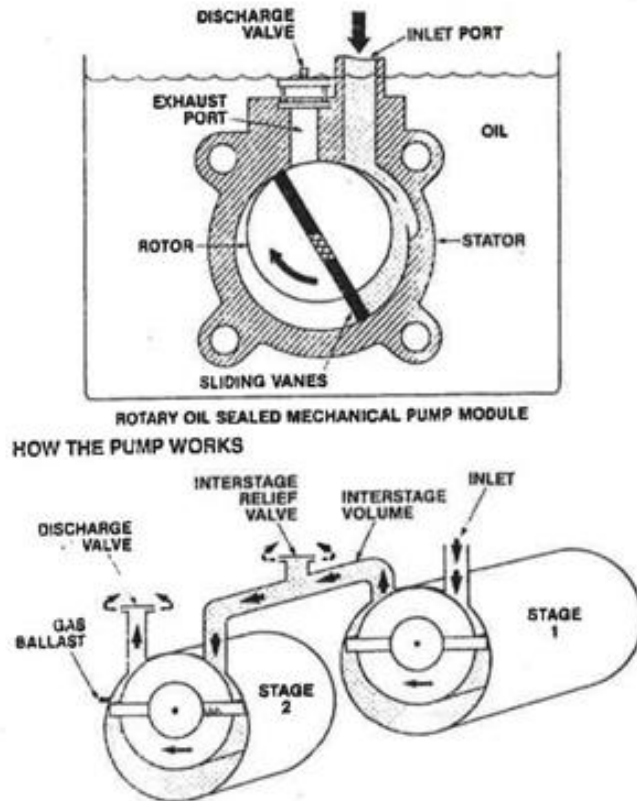


Figure 1-5: Ranges for vacuum pumps.

Multiple stages of pumps in series are necessary to reach UHV regime. A primary pump, as for example a rotary one, a turbomolecular pump and then an ion pump.

The **primary pump** is used to do pre-vacuum for pumps which needs to discharge in sub-atmospheric ambient. It works until  $10^{-3}mbar$  starting from atmospheric pressure. The speed is of tens  $m^3/h$  and usually they are “wet”, operating with oil which aim is to be a lubricant, a sealing, a heat exchanger and to protect mechanical parts. This kind of pumps has a disadvantage because of the oil used: the backscatter of oil vapour into the flange has to be minimized with filters (see *Figure 1-6, 1-7*).



*Figure 1-6: Pattern of a primary pump.*



*Figure 1-7: Primary pump.*

The **turbomolecular pump** is made up of stators and rotors which turn at very high speed (16000÷60000 rpm) with a pumping range from 10 to 3000 l/s. The ultimate pressure it can reach is around  $10^{-11}mbar$ , working in the molecular regime. It is clean, without oil. It needs the primary pump to exhaust to atmosphere. When a molecule strikes the rotor, it keeps the speed and it picks up a slightly different direction when in contact with the moving surface. In this way, the molecules move out. It is efficient with high compression ratios and for heavy gasses, but a backscatter of hydrogen can be present (see *Figure 1-8, 1-9*).

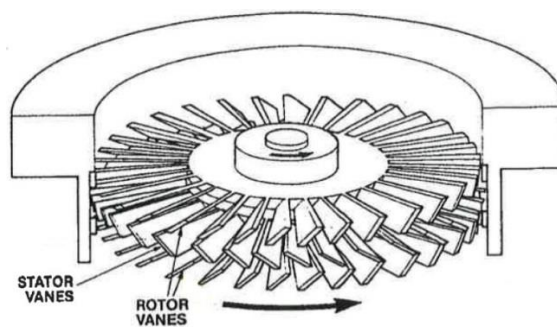


*Figure 1-8: Rotor and stator on a Turbomolecular pump.*



*Figure 1-9: Turbomolecuolar pump.*

The **sputter ion pump** operates from  $10^{-5}mbar$  to  $10^{-11}mbar$  with a pumping speed range from 1 to 500 l/s. It is used to maintain a good vacuum in accelerators. This pump is made of cathodes (two flat plates of Titanium) and anodes (many hollow cylinders). Thanks to a magnetic field, electrons do spirals and ionize molecules that become ions. The ions are accelerated to the cathode and sputter Titanium elsewhere. In turn it creates bonding with molecules from the residual gas. Only noble gasses and hydrocarbons don't react with *Ti*, but they are implanted onto the cathode (see *Figure 1-10, 1-11*).

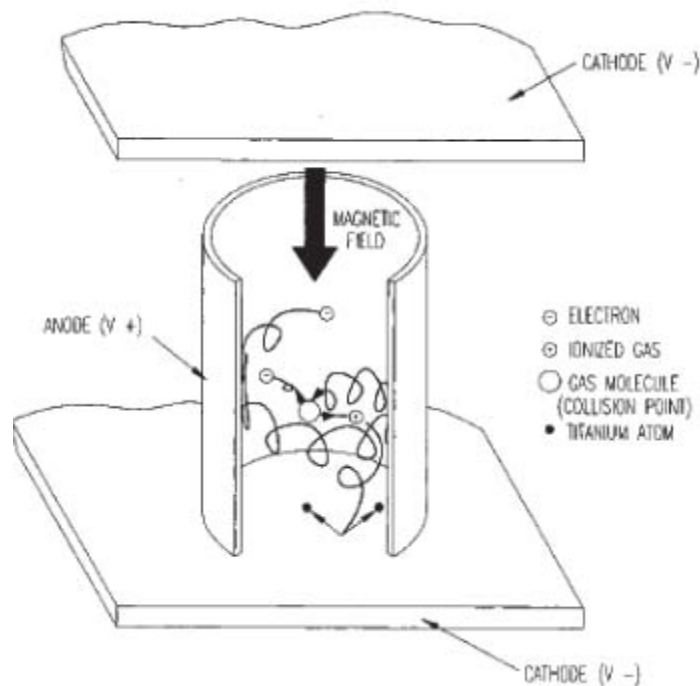


*Figure 1-10: Pattern of a sputter ion pump.*



*Figure 1-11: Sputter Ion Pump.*

There is a coating, created in CERN, which is able, after a treatment, to pump gasses. It is called NEG. **NEG** (Non Evaporable Getters) is an interesting material due to its capability to keep clean the surface and maintain the pressure at low levels. So the vacuum conditioning become faster during the scrubbing periods. The use of this kind of coating in vacuum systems is positive because it pumps without requiring additional space, can substitute a “traditional” pumping system, reduces outgassing of a surface and reduces SEY (Secondary Electron Yield). But it not possible to use NEG for systems which are frequently vented or uses noble gases.

It is needed to do a bake out process to be able to activate the coating in order to make it pumping. The activation process of this material starts when the temperature exceeds 180°C. In the case of LHC it can be used for its good response to the phenomenon of “electron cloud”.

NEG is a porous alloy or mixture of Al, Zr, Ti and Fe. These are the main elements in slightly different proportion with also other materials. These elements readily form stable compounds with active gases, if present in the vacuum chamber, and so in this way they improve the performance of the vacuum system. The film is created thanks to a magnetron sputtering deposition. (12)

## 2. ELECTRON CLOUD PHENOMENON

### 2.1 Electron Cloud Phenomenon

The phenomenon of electron cloud is the topic of this study. It reduces the quality of the beam and forms instabilities. It is created when particles, in the case of LHC are protons, create an electric field, making electrons bouncing and kicking the walls (see *Figure 2-1*). The source of primary electrons can be electrons coming from ionized gas molecules present in the vacuum chamber and photo-electrons created by Synchrotron Radiation, SR, hitting the wall. The SR is present because the beam is bended and accelerated in the arcs by the magnets, used to keep protons at the centre of the beam pipe. All the electrons and the particles (ions or photons) which hit the wall release electrons from the metal surface. Those which are created by the SR are called photo-electrons. Then all the amount of electrons generated on the next collisions with the walls are called “secondary electrons”. In turn, these electrons hit the walls and generate a multipacting effect, forming the cloud. All this is related to the surface of the vacuum chamber in which the beam passes through, this is why in this system different coating and surfaces are tested. In fact, different surfaces have several reactions to the interaction with molecules. This is why coatings are done. Electron cloud growth can limit the beam current and this causes instabilities in the beam. It also causes the rise of pressure and heat load (see *Figure 2-1*). (12) (13) (14)

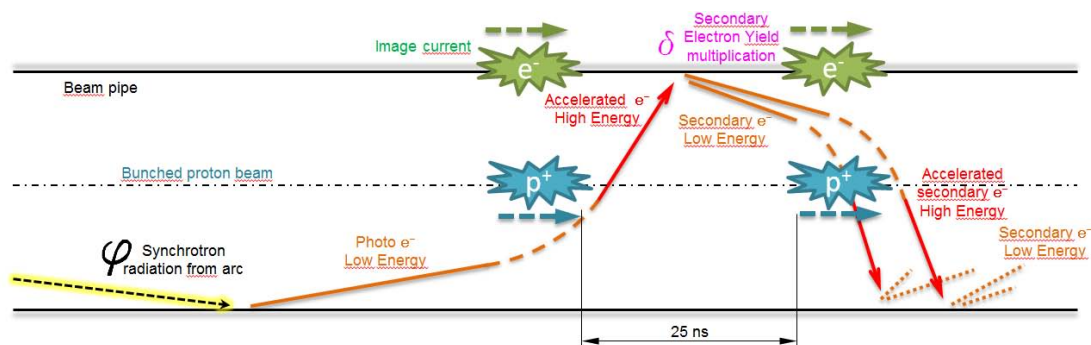
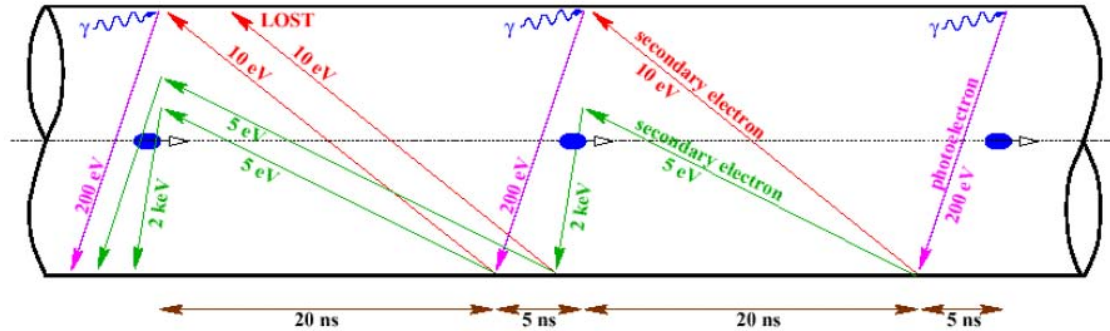


Figure 2-1: Electron Cloud phenomenon.

The blue points are bunches of protons forming the beam and  $\phi$  is the light, also called SR, created by the deflections of the protons due to bending magnets in the arcs.

When electrons are created, they have got low energy, less than 10 eV, but due to the presence of the beam, they accelerate and acquire high energy, around 100-200eV (see *Figure 2-2*). Then kicking the opposite wall, the multiplication starts.



*Figure 2-2: Schematic of Electron Cloud phenomenon and multipacting effect done by F. Ruggero et al.*

An important parameter to take care is the Image Current. It is a phenomenon that exists with the presence of the beam. It is a negative currents running on the beam pipes, all along accelerators, following the positive beam made of protons. It is needed to pay attention to make it pass through in each changing of section and components because it can heat up the system and damage tools. (15) (16)

## 2.2 Remedies for multipacting effect

In order to avoid or reduce the multipacting effect, many remedies can be used. (17)

- a) It is possible to reduce the photoelectron yield varying at the angle of incidence.
- b) Reducing secondary electron yields through different techniques:
  - Using the “scrubbing” effect. It concerns on sending a stronger beam in order to achieve a continuous electron bombardment, reaching a stable situation. This is periodically during the restart phase of the beam.
  - Thanks to a coating (Typical one are TiZrV, also known as NEG, “Non evaporable Getters”, and Carbon coating) that reduces the amount of secondary electrons coming from the wall after the collision of one particle. The ratio of the particles released per particle imping into the wall is called SEY, Secondary Electron Yield. (18) (19)
  - Changing the geometry.



- c) Reducing the amount of electrons in the system:
- Through a coil that creates a solenoidal magnetic field that can confine the electrons.
  - Using clearing electrodes.
  - Playing with material reflectivity.
- d) Adapting the structure of the beam to reduce multiplication.

In the system studied in this work, several techniques are used, such as Scrubbing run, coatings and solenoidal coils.

## 2.3 SEY

It is important to spend some words about the parameter SEY. It is a characteristic of the material but it can change if the wall is treated or after a conditioning, like the scrubbing run. It is very important to control the number of particles released per particle impinging on the wall because it creates the multipacting effect.

If the value is bigger than one, it means that for one electron impinging to the wall, more than one are coming outside from the surface. What it would be great is to find a material with SEY equal to 1, or, better, less than this.

Unfortunately the energy of the electrons impinging on the wall is around 100-200 eV that is close to the maximum pick of SEY in the curves shown above.

Here it is possible to see the big difference between several metals used in the machine (see *Figure 2-3*). (20) (21) (22) (23)

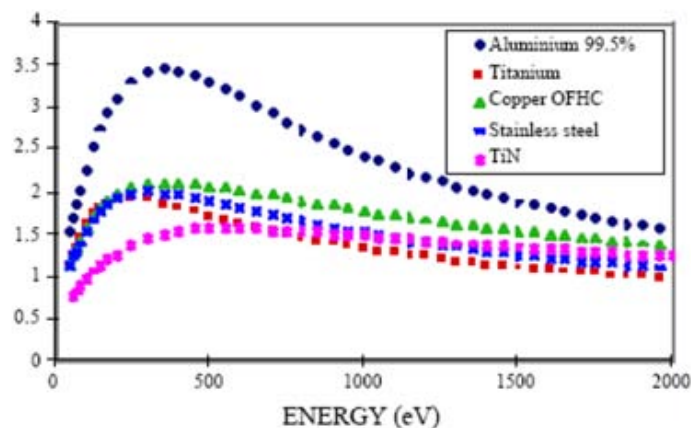


*Figure 2-3: SEY of the most common material used in accelerators.*

The standard values of SEY are more than 3 for Aluminium, 2.2 for Copper not baked and 1.6 for NEG.

Considering the same material, copper, with different treatments, it is possible to notice that the bake out can help in order to reduce the SEY. This technique concerns the heating up of the sample to degas the gasses trapped on the surface. This is usually done for each part of the machine before the installation. Another technique is the Argon Glow Discharge, AGD, that consists on Argon sputtering of the samples kept at a certain voltage. This last one is possible only in the laboratory because of the presence of a wire in the centre of the chamber (see *Figure 2-4*). (24) (25)

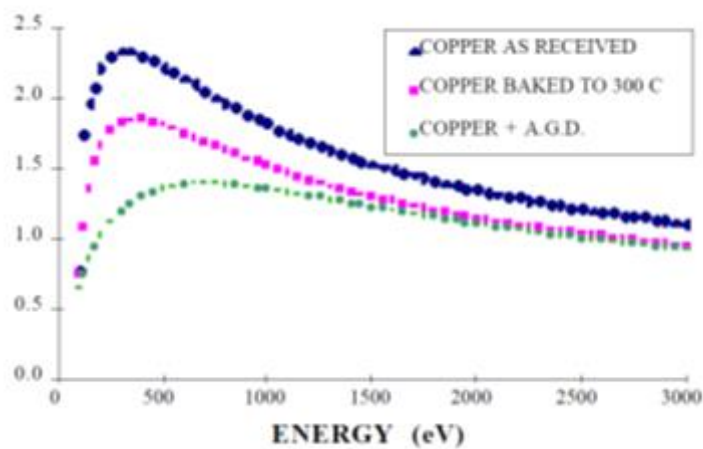


*Figure 2-4: SEY of different kind of copper.*

## 2.4 Structure of the beam

Working with LHC machine in order to study the electron cloud phenomenon it is important to know the structure of the beam, because it influences the behaviour of molecules, ions or electrons inside the vacuum chamber.

The beam is formed by bunches, pulses made up of many protons, around  $1.2 \cdot 10^{11} p/b$  per each. A group of 72 bunches is called batch and a set of many batches is called train. Usually the space between one bunch and the following is 4 ns while between a batch and the following one there are 25 or 50 ns. (26)

Usually the maximum number of bunches is 2808 on the overall 27 km of LHC, divided in 12, 24, 36, 48 or 72 bunches per batch. The maximum number of bunches in a train is 288 (see *Figure 2-5*).

## **LHC FILLING SCHEME**

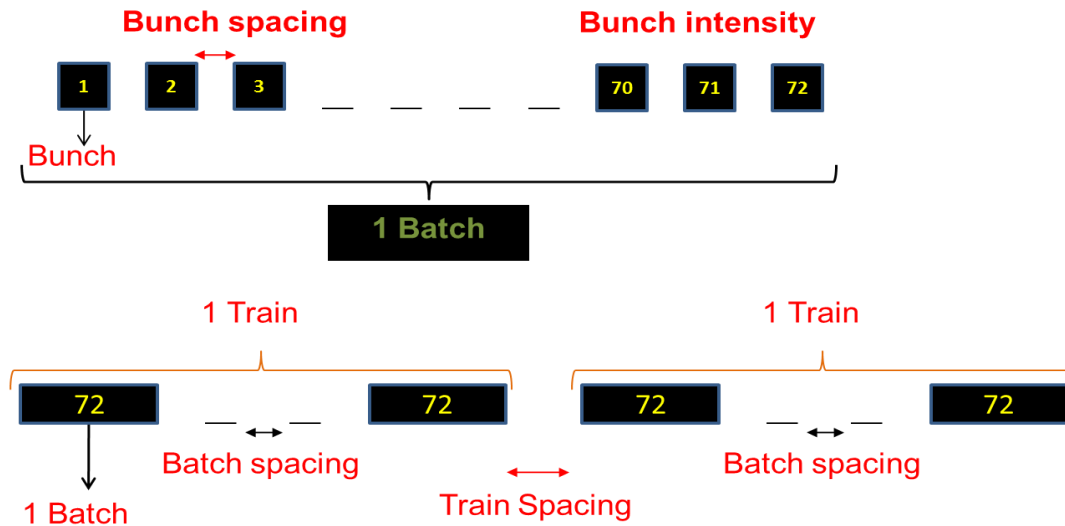


*Figure 2-5: LHC filling scheme of the beam*

This is why three circular accelerators are used: in PS 72 bunches are assembled in order to build a batch, in SPS the batches arrive and are packed, finally in LHC the beam is build thanks to the series of batches coming from the previous machine. The time spacing is very important and it depends on the aim of beam (physics, scrubbing run etc.). In order to go along the entire ring of LHC, the beam spends 88.924  $\mu\text{s}$  (See *Figure 2-5*).

Here it is possible to see graphically the same information, very useful to understand the structure (see *Figure 2-6*).

### Bunch Disposition in the LHC, SPS and PS

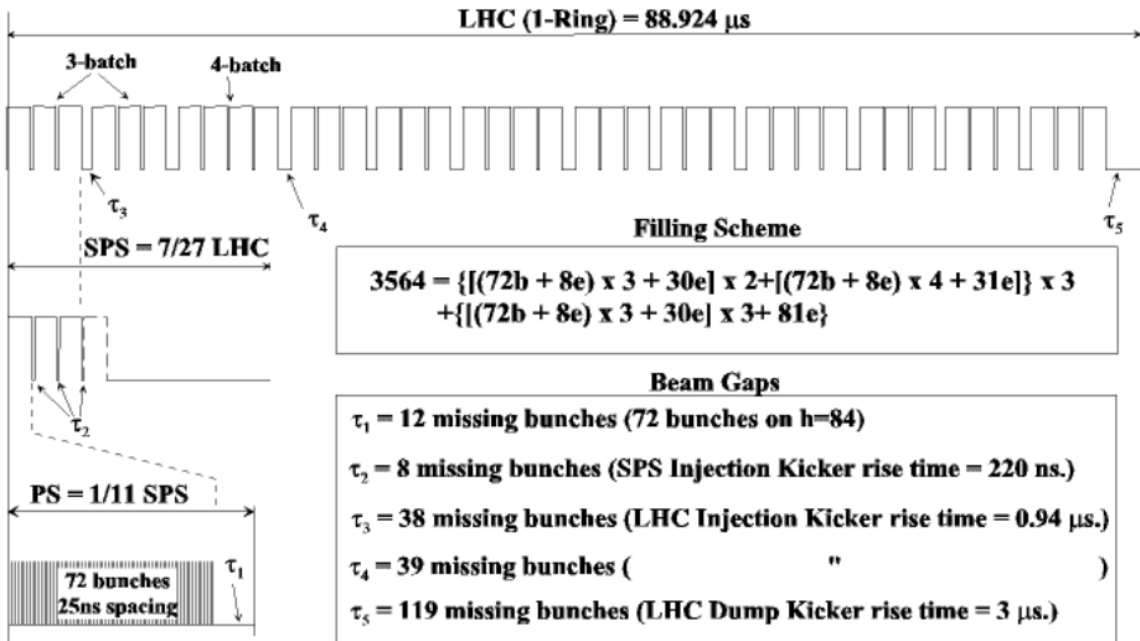


Figure 2-6: Bunch disposition of the beam structure, thanks to P. Collier 12/06/2006.

Usually the beam is identified by a code of numbers and letters. In order to be able to understand it, here there is a simple explanation.

Let consider one example like the following: 50ns\_1380b\_1331\_0\_1320\_144bpi12inj

Where:

- The bunch spacing is 50 ns,
- There is a total of 1380 bunches,
- The machine is filled by 12 injections of 144 bunches simultaneously,
- There are 1331 collisions in the collision stations of ATLAS and CMS, 0 in ALICE and 1320 in LHCb.

### 3. THE LHC VACUUM PILOT-SECTOR PROJECT

#### 3.1 Introduction

In the LHC Accelerator, just on the left side of point 8, where there is the LHCb detector, there are 18 meters of straight lines (see *Figure 3-1*). (27) (28)

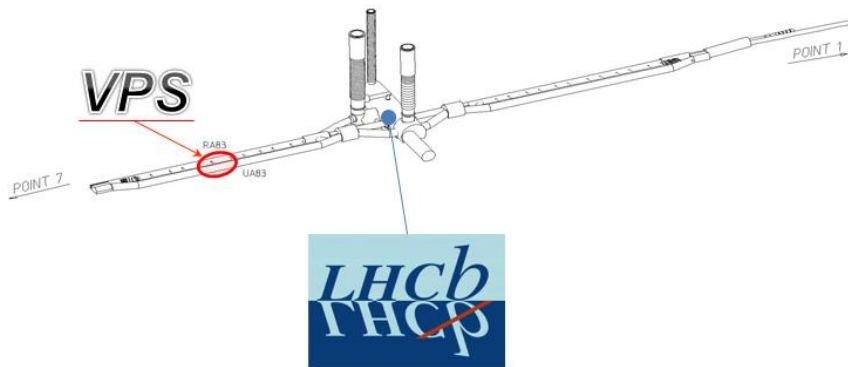


*Figure 3-1: VPS location of LHC accelerator, on left side of LHCb experiment, in point 8.*

This area is called “A5L8” in which the project “Vacuum Pilot Sector”, or VPS, takes place, between the quadrupoles Q5 and Q4, that connects the ARC 7-8 to LHCb experiment. This experiments settles in this point because of the easy access, the fact that there are low radiations, it is near to the rack side of the Tunnel so it is easier to have good connections and shorter cables, and because it is a straight area.

The aim of this project is to study and understand the behaviour of electron cloud phenomenon, due to the interaction with the beam, in different surfaces and coatings (see *Figure 3-2*).

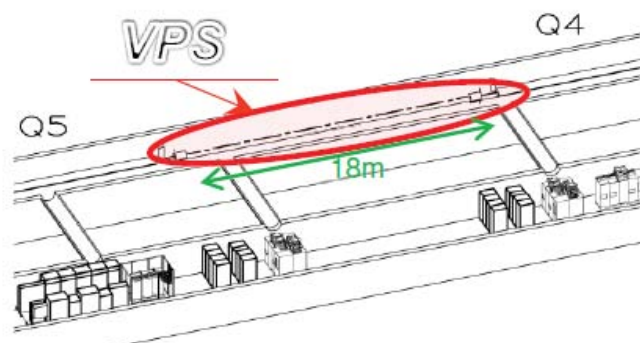


*Figure 3-2: VPS located in between quadrupoles Q5 and Q4.*

### 3.2 Installation

Vacuum Pilot Sector is an experiment in which there are two parallel beam pipes in which two beams circulate in opposite directions. The external pipe is called “Blue” beam or B1 and it comes from left side (arc 7-8), while the internal pipe is called “Red” beam or B2 and it comes from right side, where LHCb experiment is located.

Each of them consists in four standard modules (1.4 m long each). This modules are separated through buffers (five per pipe), simply NEG activated tubes of 80 mm diameter. (see *Figure 3-3, 3-4*). They avoid the influence between themselves because NEG is acting like a pump.

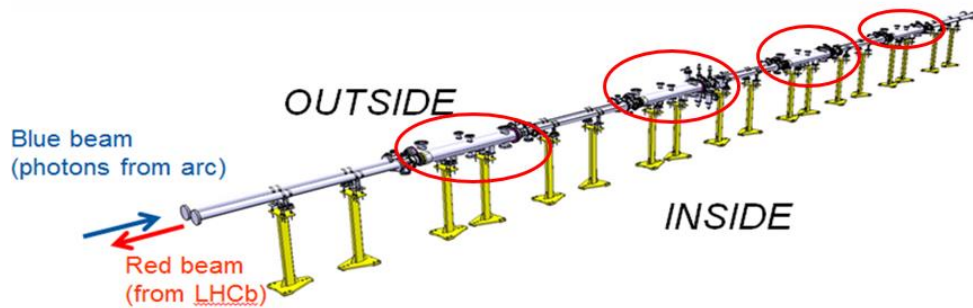


*Figure 3-3: Structure of VPS made up of four stations spaced by buffers.*

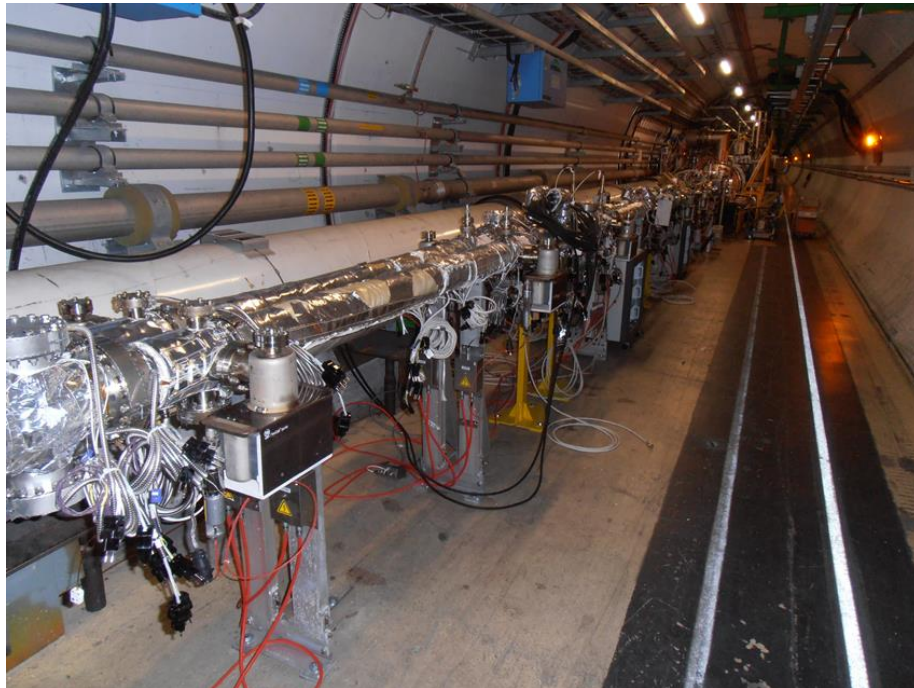


*Figure 3-4: VPS system.*

These modules are equipped with many instruments: ion pumps, a mass spectrometer called “Vacuum Quality Monitor” (VQM), Bayard-Alpert gauges (BAG), Penning and Pirani Gages, photon and electron flux monitors (pick up), calorimeters.

The first module is coated with NEG not activated, the second with NEG activated (LHC main coating), the third with Copper baked, while the fourth with Copper not baked (as cold parts of LHC). These different materials haven’t the same replay to the phenomenon of “electron cloud” that it is the goal of this study. This phenomenon limites the experiments because it consists in a raising pressure due to:

- electrons present in the vacuum chamber hitting the walls,
- residual gas that becomes ionized after the collision with electrons,
- the fact that protons beams, accelarated in the arcs, emit synchrotron radiation which, hitting the inner surface, generates photoelectrons and then the multipacting phenomenon takes place.

This phenomenon affects the ultimate pressure, so it has to be reduced through the choice of materials and through the “scrubbing” effect.

In *Figure 3-5* there is an overview of the system.

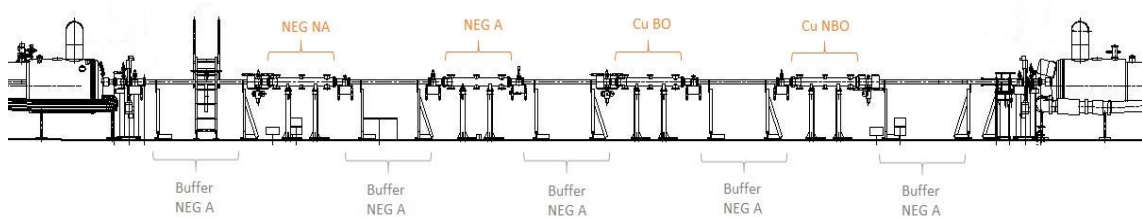


*Figure 3-5: VPS schematic specifying the surface studied.*

Going into details of each module, it is possible to see that it is made of a liner and a vacuum chamber (see *Figure 3-6*).

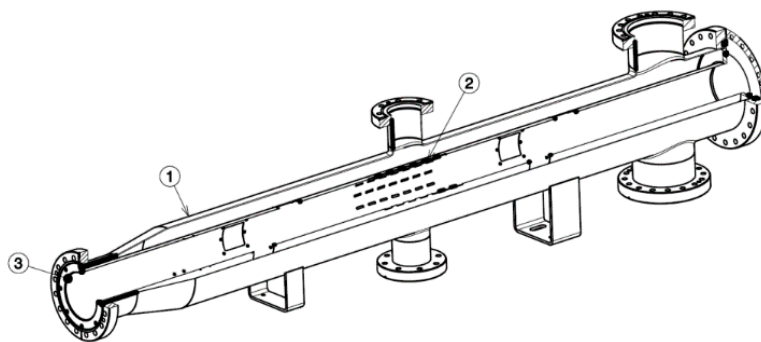


*Figure 3-6: Vacuum chamber in which a liner is inserted.*



The liner is made up of a rolled sheet of copper, 1mm thick, in which tolls, like pickup and calorimeters, are attached in some windows carved on it. Its diameter is 80 mm and the weight is around 2.96 Kg. In the middle there are some holes to permit to the pumps to create vacuum inside it. Here there is a photo and drawings of it. (see *Figure 3-7, 3-8, 3-9*).



*Figure 3-7: VPS liner with windows for pick up and calorimeters.*

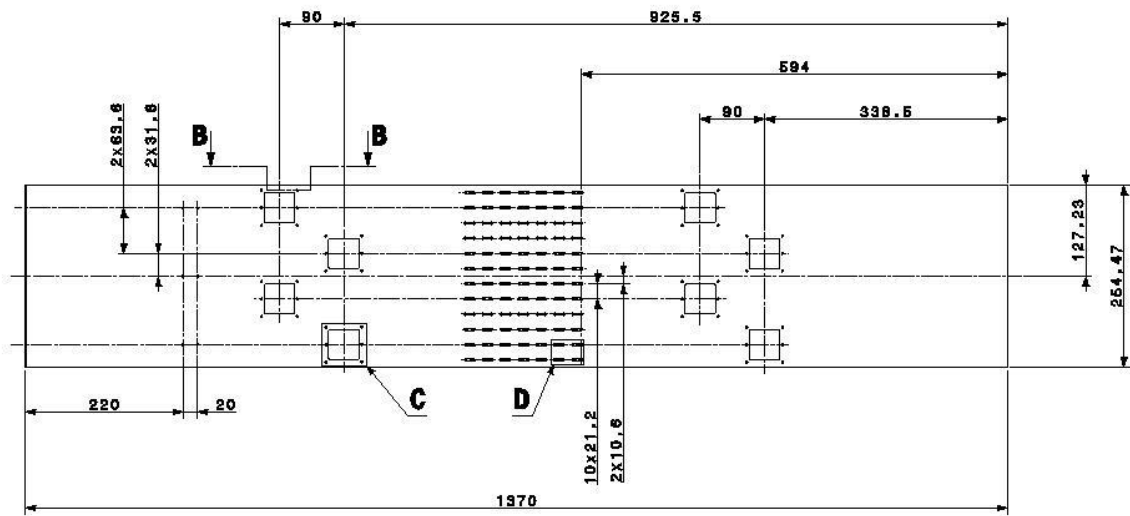


*Figure 3-8: Lateral view of the drawing of a liner.*

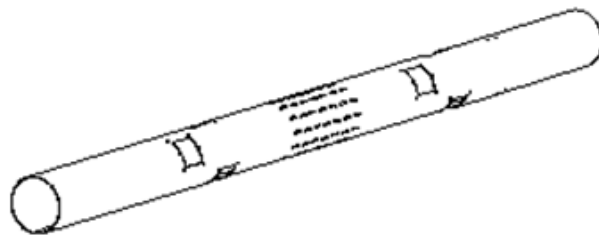


*Figure 3-9: 3D view of a liner.*



The vacuum chamber is made of stain steel, thicker than a liner, and its aim is to maintain the vacuum inside. This chamber has four vertical holes connected to flanges: the first two are used to electrically connect all the tools such as calorimeters and pickup, while in the middle there are two flanges connected to the spectrometer VQM (up - tool used to analyse the spectrum of the gasses released from the walls) and to a BAG (down - pressure gage).

Here the model of a chamber present in LHC accelerator (see *Figure 3-10*).

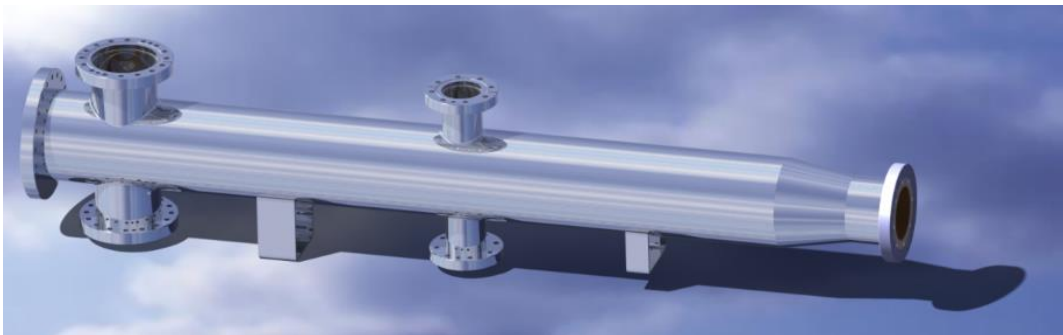


*Figure 3-10: Vacuum chamber.*

In order to compare the results from two beam pipes, it has been chosen a symmetric configuration.

In order to reduce the pressure values inside this vacuum system, some liners are treated with the bake out process. The first station is made of NEG coating activated at 230°C for 24h. The second is NEG coating only baked at 80°C for 24h. The third is Copper baked at 250 °C for 24h. The last is Copper unbaked, as the surface of the LHC arc, kept at 80 °C during the bake out.

**NEG** is already presented in *Paragraph 1.3.2*.

**Copper** (OFC, Oxygen free Copper) is a chemical element and it is a ductile metal. It has got a very high thermal and electrical conductivity and this is why it is used.

All the material tested in this system are materials used already in LHC accelerator or will be used for HL-LHC.

### 3.3 Instruments

As I said before, this system is equipped with many instruments. Now they will be presented in order to have a schematic idea of the kind of analysis is possible to do with the “Vacuum Pilot Sector”.

#### 3.3.1 Pressure gages

The first important parameter to study and to control, being a vacuum system, is the pressure. In order to measure it, it is possible to use different tools: Bayard-Alpert gages (BAG), Penning and Pirani gages. (30)

**Penning gauge** (cold cathode) is used to measure the pressure in the buffers of the system. In this kind of gage there is no filament and the measurement is not very precise. The device consists of two cathodes and a hollow anode in between. When a voltage is applied, a strong magnetic field is produced and so electrons are ejected. If the pressure is low (below  $10^{-2}$  Torr), a collision may not occur between the gas and the electrons and the ionization can't start (see *Figure 3-11*).

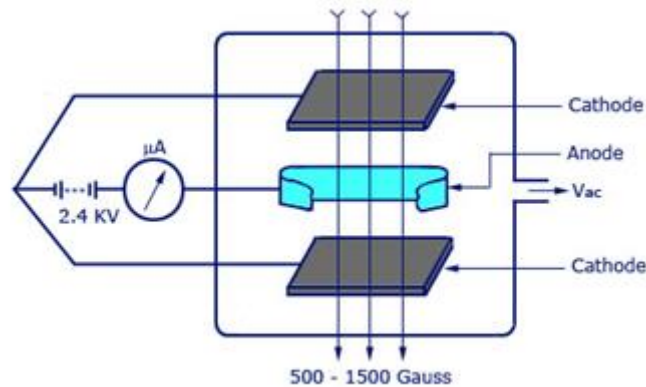


*Figure 3-11: Ionization Gauge with cold Cathode.*

**Pirani gauge** is used in the middle of the experiment, in which it is possible to inject gas. Its consists of a metal filament suspended in a tube which is connected to the vacuum system. The filament is connected to an electrical circuit that permits to convert current in pressure value, through a calibration. This doesn't work in HV or UHV conditions.

A more precise gauge is **Bayard-Alpert gauge**, called BAG or VGI (hot cathode). This kind of gauge is used in the eight stations. Here it is possible to see the internal structure of the gauge (see *Figure 3-12*). (31) (32)

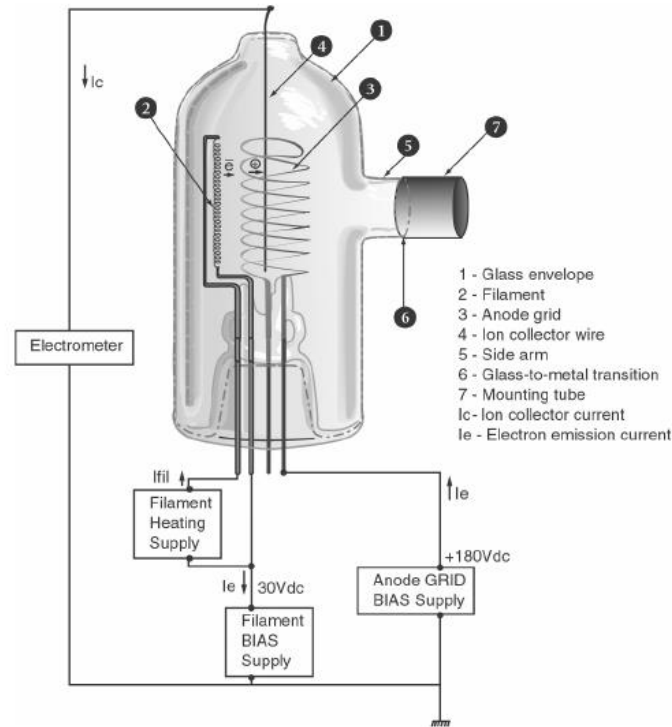


*Figure 3-12: Bayard-Alpert gage.*

The principle of operation is quite simple. The electrons, due to the hot filament, start to accelerate towards the anode grid. When the current cross the inner volume of the grid cage, the electrons ionize the molecules of gasses that they encounter in the path. The electrons that don't hit molecules are redirected back in the inner volume thank to electrostatic field. The ions created are collected by the grounded collector wire (0 V dc). There is an important parameter speaking about this kind of gage: the sensitivity. The number of molecules per unit volume, the ionization cross section for each gas at each electron energy, the number of electrons and the path length of them influence the number of ions formed inside the anode grid. The ion collector current  $I_c$  measured by the electrometer is the following:

$$I_c = \sigma \cdot L \cdot \frac{P}{k \cdot T} \cdot I_e$$

Where  $\sigma$  is the ionization cross section for a gas molecule,  $L$  the length of the ionizing space,  $P$  the pressure,  $k$  the Boltzmann constant,  $T$  the temperature in Kelvin and  $I_e$  the

electron emission current, given by  $N \cdot e$ , in which  $N$  is the number of electrons and  $e$  the electron charge.

The factor  $\frac{\sigma \cdot L}{k \cdot T}$  is called gauge sensitivity factor  $S$ , that is a function of the type of gas, the geometry of the gage and the temperature. It can be written in this way:

$$S = \frac{I_c}{P \cdot I_e} [Torr^{-1}].$$

Considering also residual currents  $I_r$ , due to X-ray that induces photo-emission of electrons from collector and envelope, electron stimulated desorption, leakage currents and errors, the equation becomes:

$$I_c = S \cdot P \cdot I_e + I_r$$

### 3.3.2 Pickup

Pickup are tools useful to measure the electron cloud phenomenon. They can be of two kinds: not shielded and shielded. In this system are both present with different goals. (33)

**Unshielded pickup** is a tool used for triggering the beam and its structure and to acquire electrical signal of photons-electrons (see *Figure 3-13*). It measures the image current that flows through the liner, due to the electrical field created by bunches. It is made of a circular button, coated with gold, which is directly inserted in the liner, around 40mm far from the beam. This button is electrically connected through wires. It uses the same principle of an antenna. This tool is made of a patch with a hole, an electrode in with a screw keeps the golden button (see *Figure 11-12*) and the cover sheet (see *Figure 11-13*).



*Figure 3-13: Unshielded pickup, used as trigger or photon pickup.*

The measurement is done through a very simple electrical circuit, 1 M $\Omega$  of resistance in which it is possible to read the voltage, and from the ratio between the voltage and the resistance to obtain the value of current, because also the vessel is earth connected (see *Figure 3-14*).

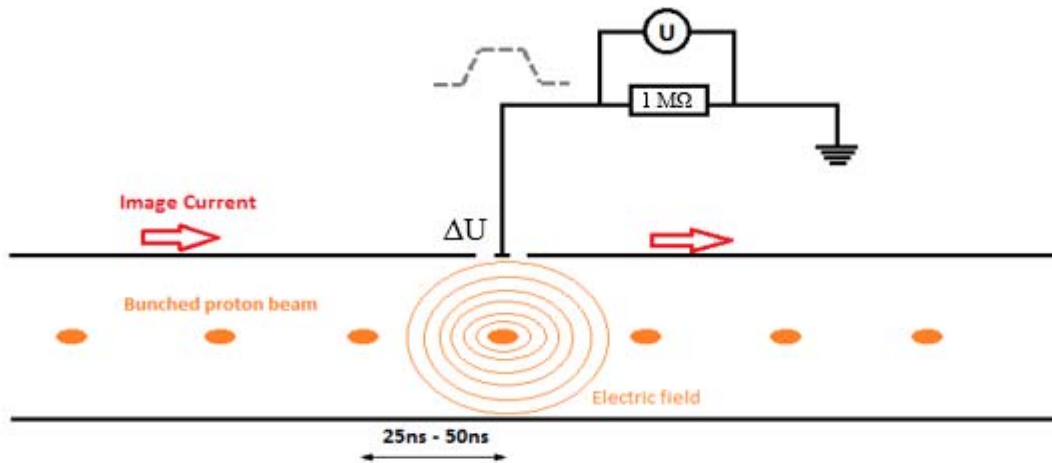


*Figure 3-14: Scheme of an unshielded pickup.*

**Shielded pickup** is used to have an electrical signal of electron cloud phenomenon, not considering the image current (see *Figure 3-15*). It is made of a grid (different transparencies are tested) that permits the image current to pass through without compromising the measurement. This shield permits to select only a part of the electrons present on the vacuum system, proportionally to the numbers of holes. (34) This tool is made of a grid welded on a patch (see *Figure 11-8*), an electrode (see *Figure 11-12*) and the cover sheet (see *Figure 11-13*).

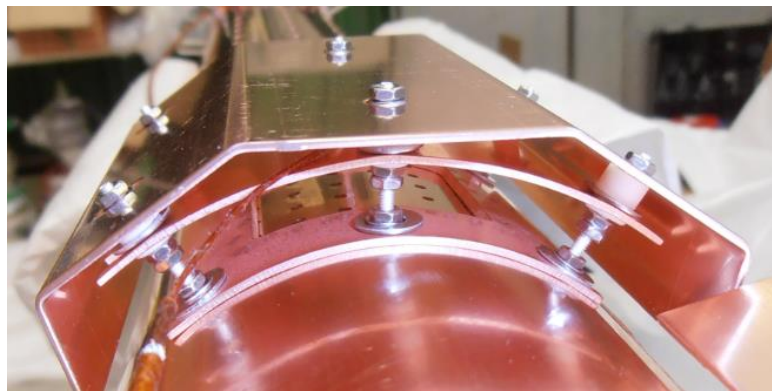


*Figure 3-15: Shielded pickup, made of a grid, an electrode to collect the current and a hood to protect.*

Different grids are tested in order to understand how the number of holes could have influence on the measurement. The more common grid used in accelerators is 7%, in which seven percent of the area of the grid is empty. Then in this system there are 0.02%, 5%, 10%, 75%.

As you can see from the electrical design, a battery of 9V is plugged in order to attract the greatest amount of electrons (see *Figure 3-16*).

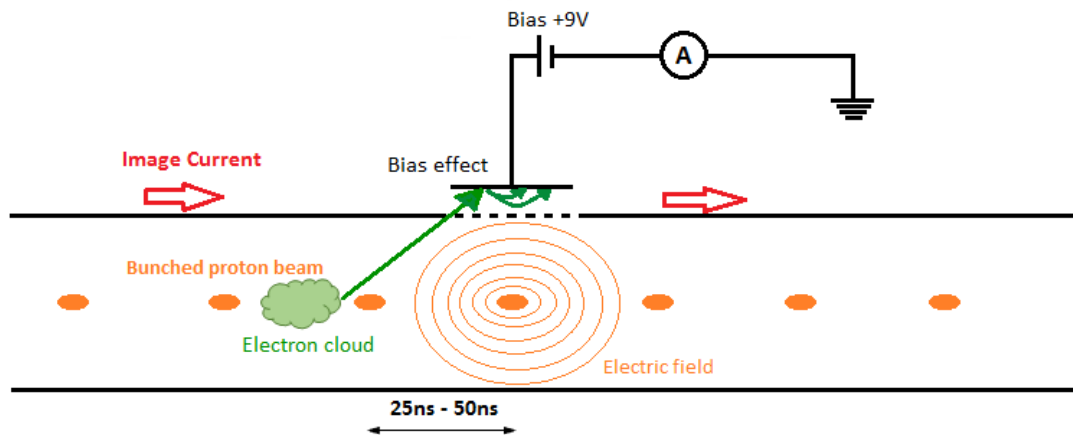


*Figure 3-16: Scheme of a shielded pickup.*

It is interesting to apply a variable voltage, not using a standard battery of 9V, in order to study the influence of the voltage on the phenomenon. This system is applicable to pickup shielded and not, and its name is **High voltage BIAS**.

### 3.3.3 Calorimeter

Another important signal is coming from calorimeters that detect the power deposition on the wall during the beams. (35) It consists of four temperature sensors Pt100. Two of them are welded through INOX ribbon to a plate of copper (thickness 0.2mm, area 30mm\*30mm). The third is attached on the liner. The last is measuring the temperature of the air of the tunnel. The first two (red and purple on the next photo) are respectively used for calibration and for the reading the temperature of the plate. The third one is the temperature reference of the liner (green mark) and the last one is useful to have a reference of the temperature of the outside part of the chamber (see *Figure 3-17*). (36)

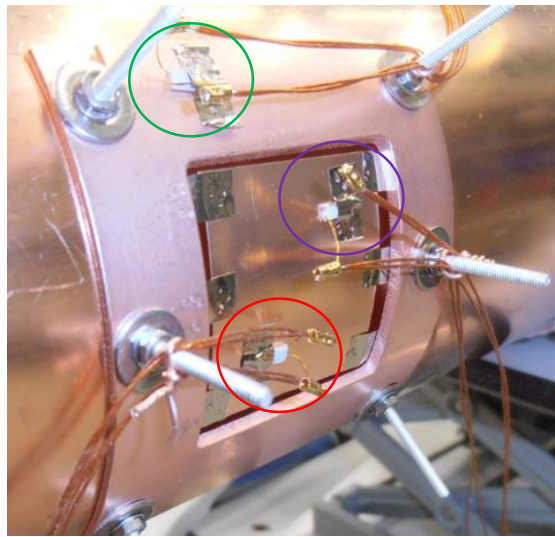


*Figure 3-17: Calorimeter.*

Here you can find a detail of the Pt100 linked to the copper plate through the INOX weld (see *Figure 3-18*).

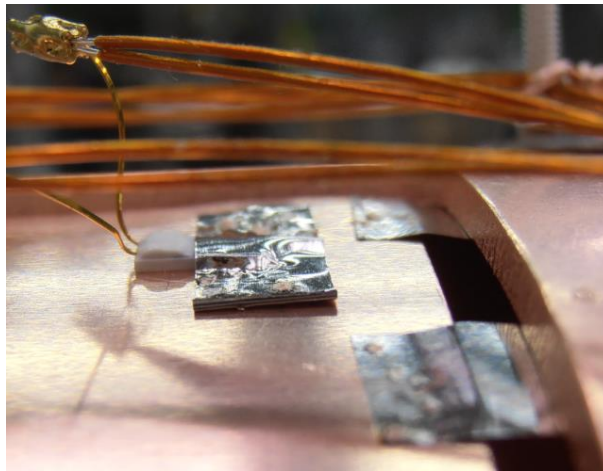


*Figure 3-18: Detail of Pt100 sensor stuck thanks to an INOX ribbon welded to the copper plate.*



Here it is possible to find the schematic drawing of the system (see *Figure 3-19*).

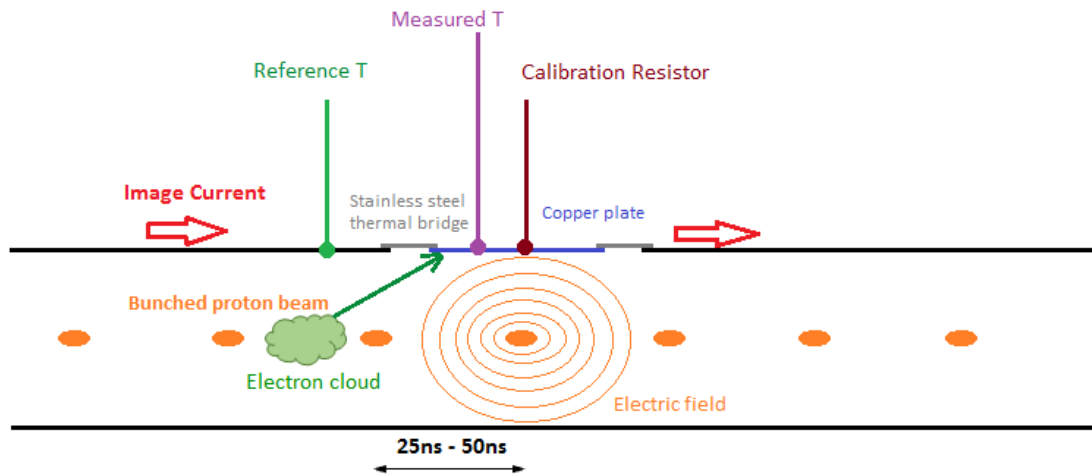


*Figure 3-19: Scheme of a calorimeter.*

Doing the calibration of this system is possible to know the main parameters, thermal resistance and capacity. This will be explained later.

### 3.3.4 Residual Gas Analyser (VQM)

There is another important instrument: the residual gas analyser called VQM (Vacuum Quality Measurement).

The aim of this instrument is to build the spectrum of gasses present in the vacuum chamber. Due to electronics problems, it is not possible to use a standard analyser of gasses and for this reason VQM is used, for the first time in LHC accelerator (see *Figure 3-20*). The use of this, an Electrostatic Ion Trap for low-mass range mass spectrometry application, is quite new. Its principle of operation consists of ionizing compounds, measuring the ratio between mass and charge and separating molecules. In this way it is possible to know how many molecules per type of gas.



*Figure 3-20: VQM instrument.*



### 3.3.5 Electron Kicker Detector (EKD)

The Electron Kicker Detector is useful for many reasons. Due to the fact that the control box was not ready to use it to kill the residual electrons of electron cloud in between two bunches, it is used to estimate the spectrum of energy of electrons.

It is made of two grids, respectively 7% in order to shield the measurement (see Figure 11-8) and 75% in which is possible to change the voltage up around +1250V (see Figure 11-11). Then there are the electrode measuring the current (see Figure 11-12) and the cover sheet (see Figure 11-8). Changing this voltage, it is possible to do a scan the amount of electrons that reaches the collector. Deriving this current is possible to find the energy spectrum of electrons of electron cloud. (37) (38) (39) (40) The next images show a photo of this tool and the electrical circuit (see Figure 3-21, 3-22).

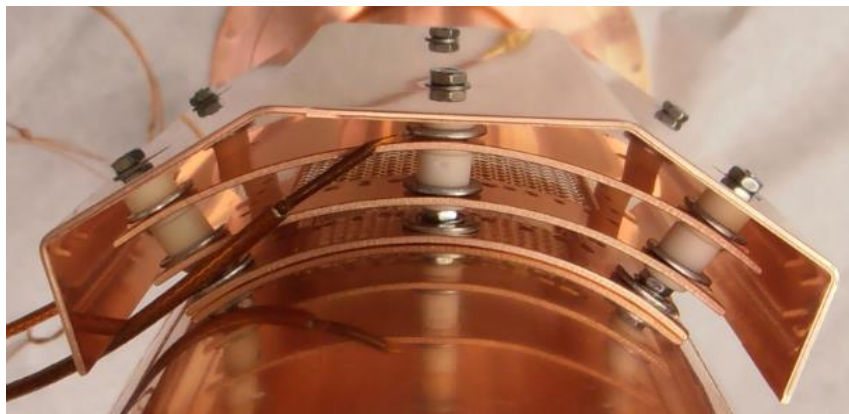


Figure 3-21: EKD, made up of two grids, an electrode and a hood.

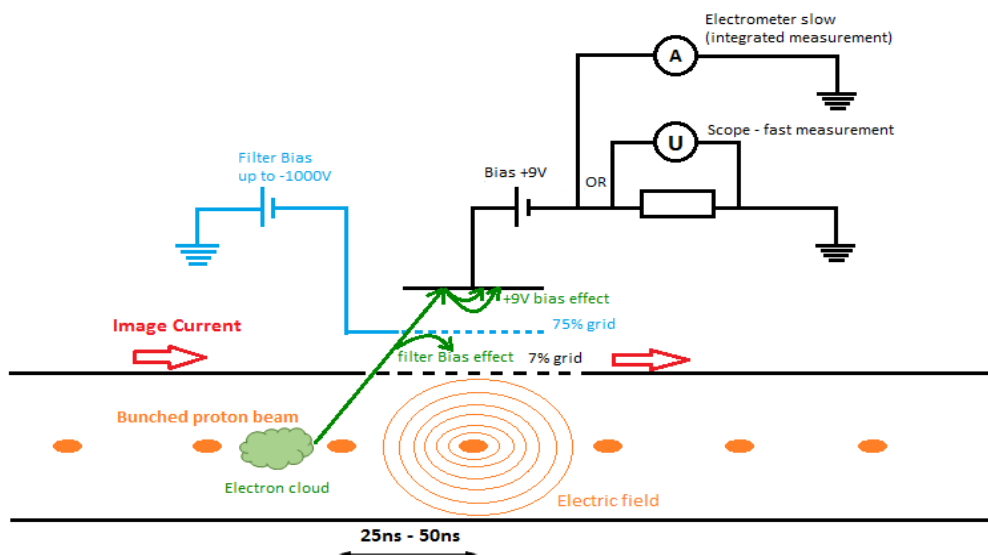


Figure 3-22: Scheme of an EKD.

## 3.4 System and data acquisition

In this subchapter it is possible to find the operational manual to be able to use the programs to acquire data.

The main programs used are four:

- PVSS – LHC Synoptic for pressure gages,
- LabVIEW for beam parameters, calorimeters, pickup, EKD and pressure gages,
- SCOPE for pickup,
- VQM program.

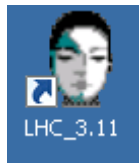
### 3.4.1 PVSS

This system was created by the vacuum group in order to manage and control all the vacuum systems at CERN. In particular, the following is the interface for LHC accelerator.

On this interface it is possible read and save many data, important for this project: beam parameters (such as Beam Energy, Beam Currents, Critical Energy, Photon Fluxes and Doses, number of Protons, structure of the Beams) and the values of all the pressure gages and Cryo-Thermometers.

In order to open this program, let do these steps from a CERN computer:

- Start
- Remote Desktop Connection
- Choose “Cerntsvac.cern.ch”
- Insert name and password
- Click the icon on the desktop: LHC\_3.11”



- The program of LHC vacuum system will open (see *Figure 3-23*):

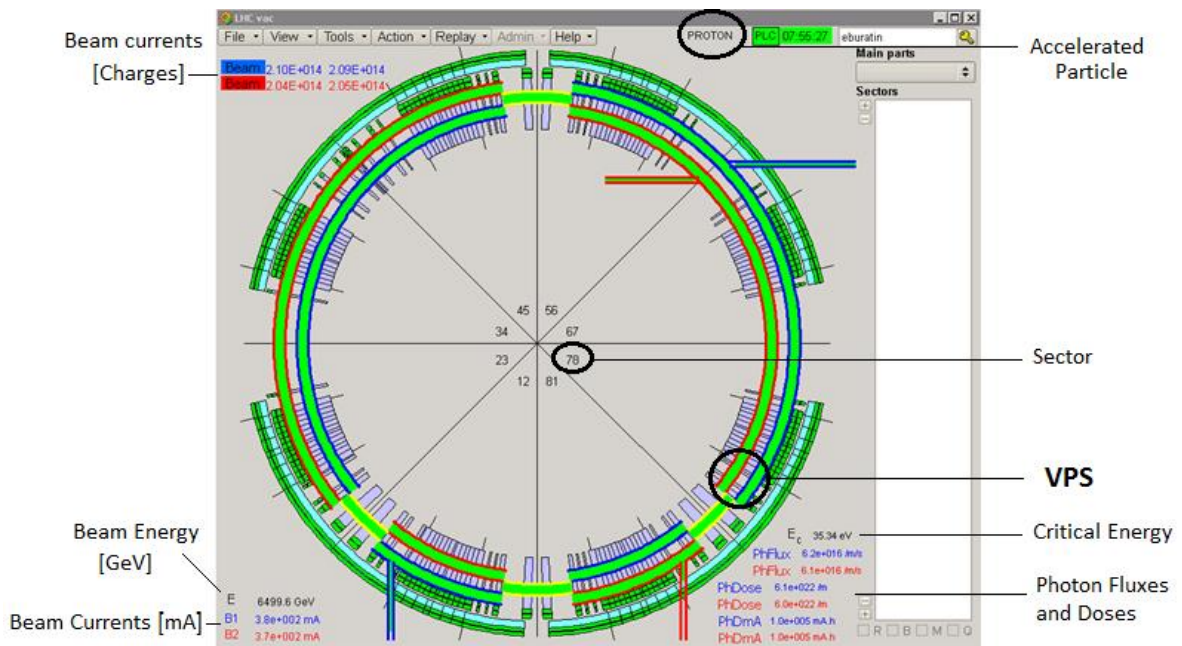


Figure 3-23: Main interface of LHC vacuum system in PVSS.

- Double clicking on one pipe, for example on the black mark for VPS, and the LHC synoptic will appear (see Figure 3-24):



Figure 3-24: A part of the synoptic of LHC vacuum system in PVSS.

This is the sector LSSV8 (Long Straight Section in sector 8), in which the VPS settles (see Figure 3-25). Going into details, next there is the explanation of the VPS vacuum system and of all the gages. It is possible to notice that there are two pipes, blue one and red one, as explained above. The blue is coming from left, while the red one from right. Each time it is said “right” or “left”, it is referred looking from the centre of the circumference of LHC accelerator.

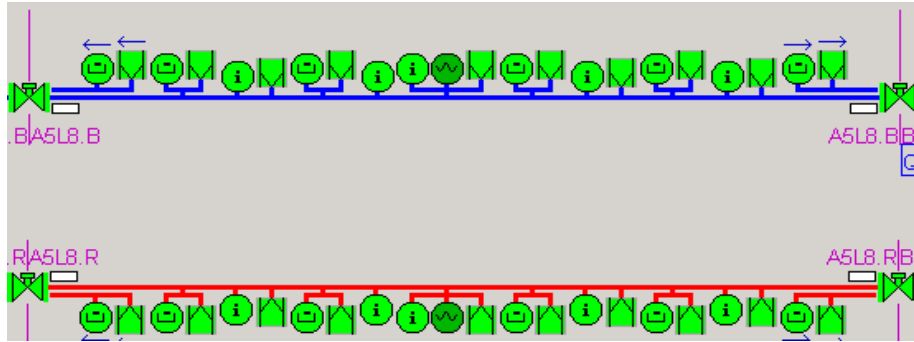







Figure 3-25: VPS Synoptic.

Where:

-  This is a VGI or BAG, measuring the pressure of the liners.
-  This is a VGPB, Penning Gage, measuring the pressure of the buffers.
-  This is a VPIA, an Ionic Pump.
-  This is a Pirani Gage, in the middle of the system.
-  This is a valve.

The colour of the gages is important: if light green it is working or open if it is a valve; if dark green it is in a state of transition, not controlled; if yellow it is in standby; if red it is not working or closed if it is a valve.

Now it is possible to see all the names of the gages and what they measure. All this is in the database of the program, investigating each gage with the right click of the mouse (see *Figure 3-26*).

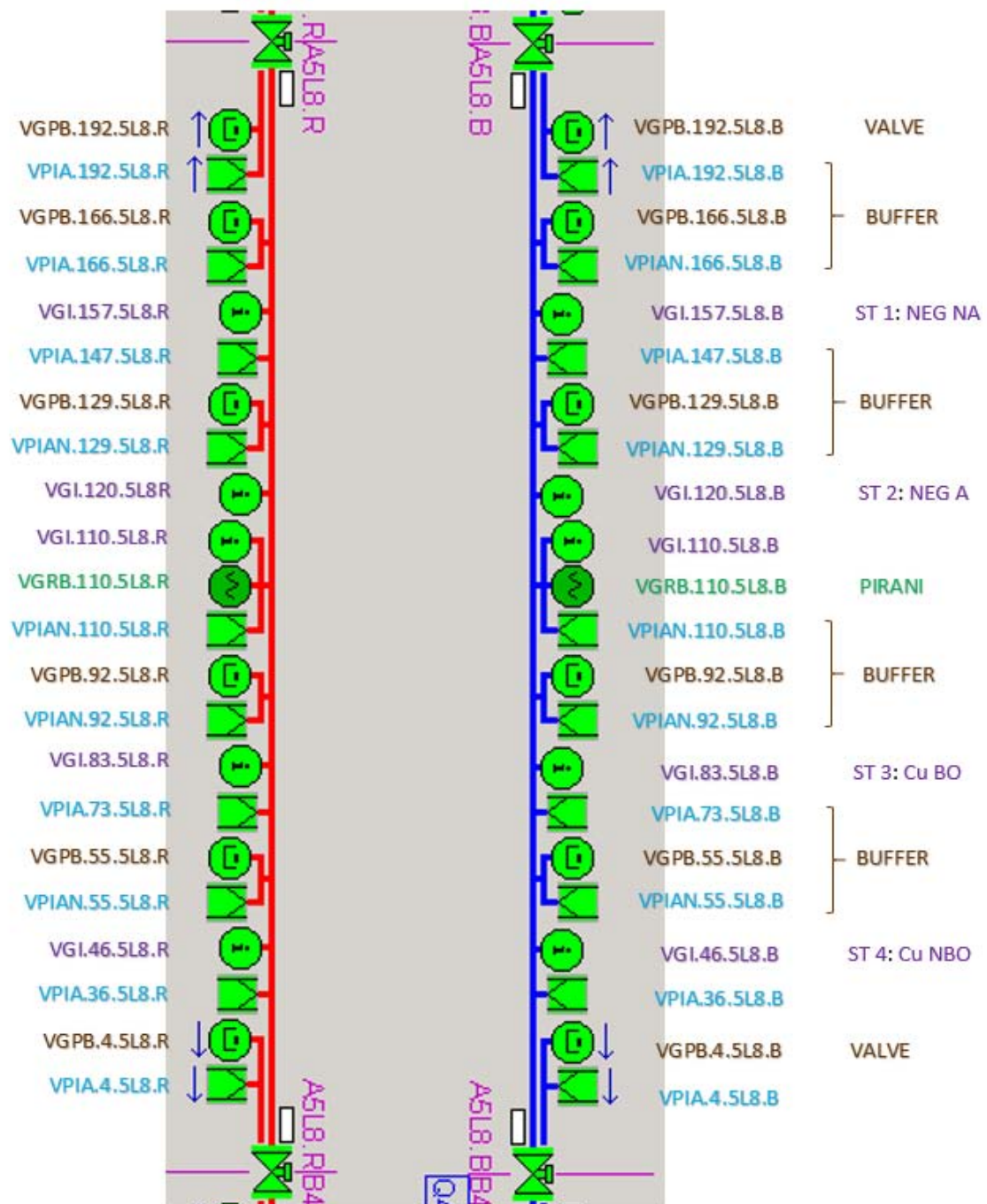


Figure 3-26: VPS Synoptic with labels of the gages.

In order to see beam parameters, it is needed to click (see Figure 3-27).

- View, in the upper left side,
- Beam Parameters,

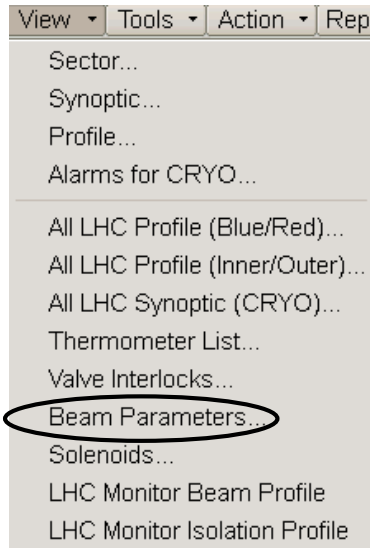


Figure 3-27: PVSS - Menu.

- This window with the parameters will appear(see Figure 3-28):

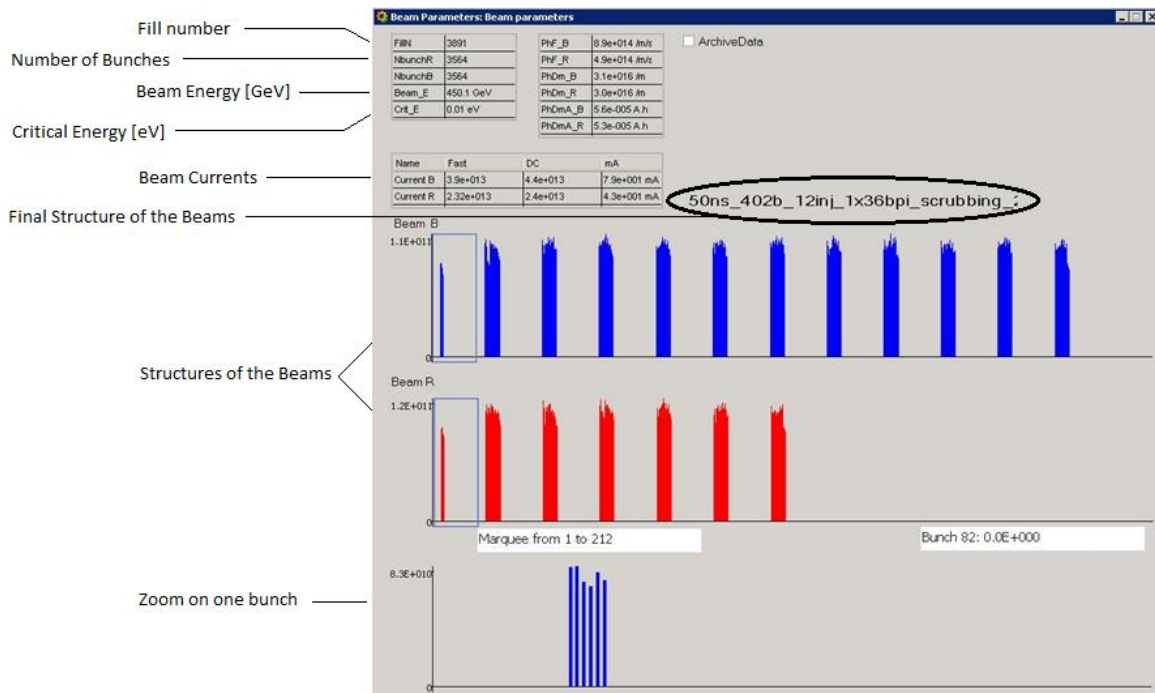


Figure 3-28: PVSS – Beam Parameters.

In order to see the pressure trends, it is needed (see Figure 3-29):

- do the right click on the gage,
- click History,

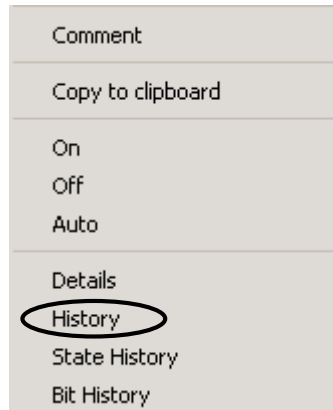


Figure 3-29: PVSS: Menu.

- then the following window will appear (see Figure 3-30):

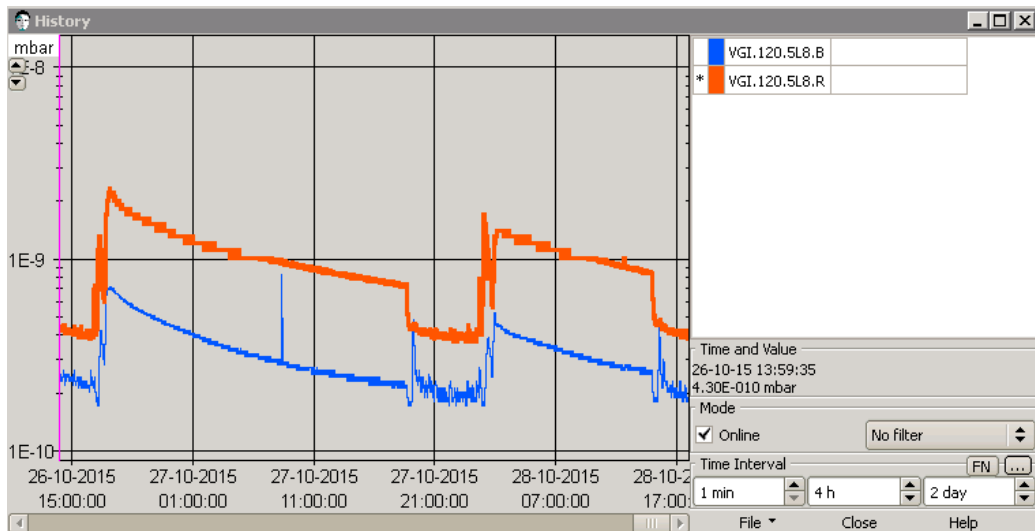


Figure 3-30: PVSS – History window in which pressure trend are shown.

I provide some configurations I built during this collaboration inside CERN in which I settled the most important parameters together, in relationship with the goal of a particular analysis.

In order to use these configuration, let click:

- Tools,
- History config
- This window will open, in which all my configuration are visible. The more useful are “VGI\_VGPB\_B\_A5L8” and “VGI\_VGPB\_R\_A5L8”, in which values of pressure of each station and buffer, Beam Energy, Current, and Fill number are present (see Figure 3-31).



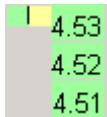




Here it is possible to play with time scale and order of magnitude of all parameters.

In order to see the trend of Cryo-Thermocouple, let click:

- View,
- Equipment on beam vacuum,
- CRYO Thermometers
- On the synoptic these windows will appear:



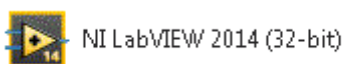
The first value is the maximum, the last is the minimum and in the middle there is the average. There is only one thermometer in A5L8, as the next picture shows, but you can take into account also the temperatures of two stand-alone magnets, that are before and after A5L8.

### 3.4.2 LabVIEW

LabVIEW is an interface that reads many values: beam parameters, electrical signals from pickup, temperatures of Pt100 used to calculate the power deposition on calorimeters, EKD signals and pressure trends (these are already recorded in PVSS).

In order to open this program, let do these steps from a CERN computer:

- Start
  - Remote Desktop Connection
  - Choose “Cerntsvac.cern.ch”
  - Insert name and password
- From the new remote desktop click:
- Start
  - Remote Desktop Connection
  - Choose “pcte24207”
  - Insert name and password
  - Look for the program “NI LabVIEW 2014”



- Chose “Lab Logger- BH Core v1.1.vi”

- The program will open (see *Figure 3-33*):

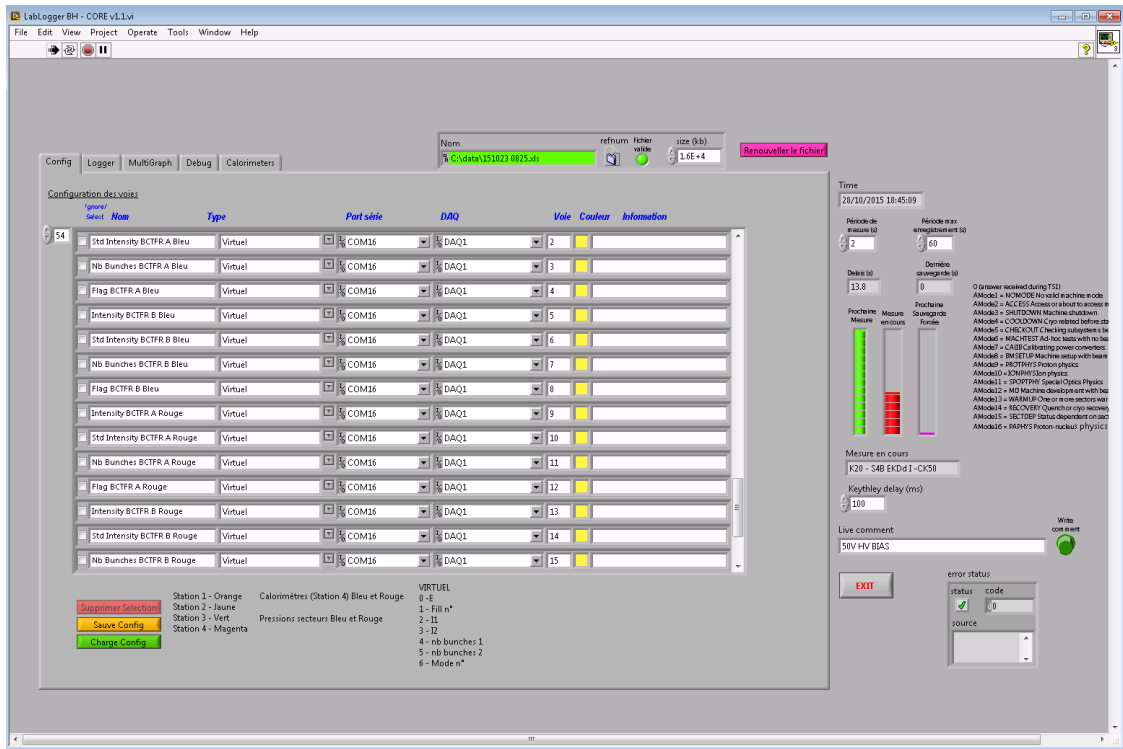


Figure 3-33: main interface of LabVIEW.

There are many pages in which values are shown in graphs and computation. The more important are these:

- “Logger” for values,
- “Multigraph” for graphs,
- “Calorimeters” for the power computation starting from differences of temperatures.

### 3.4.3 SCOPE

This program is used for values of triggering pickup (unshielded one) and some of the electrical signals (shielded pickup).

It has four channels in which are plugged the pickup. There is the possibility to change the scale of time and intensity of signals read. This is a fast measurement that is different from LabVIEW reading, which is low measurement.

In this it is possible to see the structure of the beam (bunches and batches) on unshielded pickup and build-up of electron cloud phenomenon.

In order to open this program, let do these steps from a CERN computer:

- Start
- Remote Desktop Connection
- Choose “tevscope1”
- Insert name and password
- The program will open (see *Figure 3-34*).

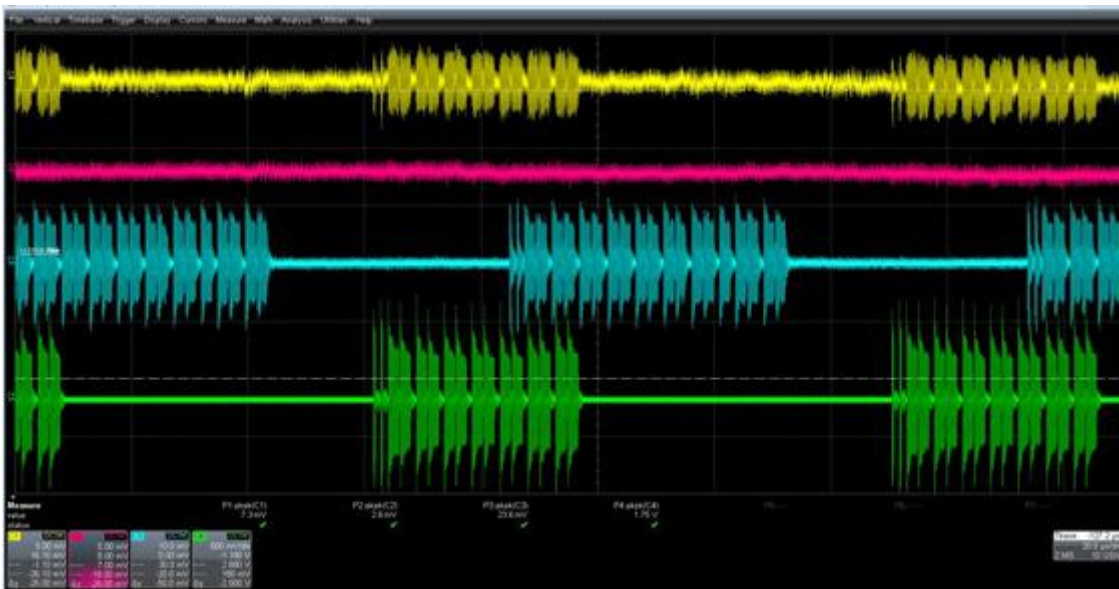


*Figure 3-34: Main interface of SCOPE.*

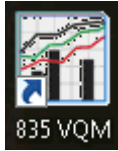
#### 3.4.4 VQM program

The VQM measurement are very new for LHC machine. This program is able to build a spectrum of gasses present in the vacuum chamber. It is not very precise because the values of picks are related between themselves.

In order to open this program, let do these steps from a CERN computer:

- Start
  - Remote Desktop Connection
  - Choose “Cerntsvac.cern.ch”
  - Insert name and password
- From the new remote desktop click:
- Start

- Remote Desktop Connection
- Choose “pcte24207”
- Insert name and password
- Look for the program “835 VQM”



- Click and then the program will open (see *Figure 3-35*):



*Figure 3-35: Main interface of VQM program.*

There are four channels, as many as VQM installed in the tunnel. Each channel is a different liner and it is possible to choose the input from the menu. All these species present in the measurement appear in the blue window with an average percentage of their presence. Once these data are saved, it is needed to evaluate also the pressure and sensitivities of the gage in relationship of the gas taken into consideration.

The four channel are connected in this way:

- 1) 835A99 10: NEG A – Red beam
- 2) 835A99 11: Cu NBO – Red beam
- 3) 835A99 20: NEG A – Blue beam
- 4) 835A99 21: Cu NBO – Blue beam

### 3.5 Main table of tools Of VPS

Considering the big amount of tools, it was necessary to build a table in which all the parameters and names of the tools were written. The following table is the current configuration of the setup (see *Figure 3-36*).

Station	Faisceau	Coté	Direction	Remarque	23155.113	23158.813	23162.513	23166.213				
					<u>1</u>	<u>2</u>	<u>3</u>	<u>4</u>				
<b>Faisceau</b>	<b>Bleu</b>	<b>Extérieur</b>		<b>Photons</b>	Connecteur	Connecteur	Connecteur	Connecteur				
	Surface				NEG NA	NEG A	Cu BO	Cu NBO				
	N° Liner				1	3	5	7				
	N° Chambre				6	3	10	12				
	N° BAG				40	703	401	50				
	N° VQM				NA	835A00676	NA	835A00679				
Equipement	Entrée (Gauche)	H			7%	1 / 111 / Sc2	7%	1 / 311 / Sc3	7%			
		B			NU		NU	NU	NU			
		E			NU	0%	2 / 212 / Sc1	NU	NU	NU		
		I			NU	NU		NU	1 trou	3 / 413 / K19		
		H			7%	2 / 112 / K17	5%	4 / 214 / K3	5%	2 / 312 / K9	Cal	
		B			NU		NU	NU	NU	Canon		
Equipement	Sortie (Droite)	E			ph	3 / 113 / K8	10%	3 / 213 / K2	10%	3 / 313 / K10	EKDK	6 / SHV1
		I			NU		NU	NU	NU	EKD	2 / 412 / K20.5 / SHV2	
		H			7%	1 / 121 / K18	5%	1 / 221 / K4	7%	3 / 323 / K13	Cal	Canon
		B			NU		NU	NU	NU	NU	NU	NU
Equipement	Entrée (Droite)	E			ph	2 / 122 / K14	10%	2 / 222 / K5	10%	2 / 322 / K12	EKD	1 / 421 / K7.5 / SHV4
		I			NU		NU	NU	NU	NU	EKDK	6 / SHV3
		H			7%	3 / 123 / KV	7%	3 / 223 / K6	5%	1 / 321 / K11	7%	2 / 422 / K15
		B			NU		NU	NU	NU	NU	NU	NU
		E			NU	0%	4 / 224	NU	NU	NU	NU	NU
		I			NU	NU	NU	NU	NU	1 trou	3 / 423 / K16	
<b>Faisceau</b>	<b>Rouge</b>	<b>Intérieur</b>		<b>Pas de photon</b>	Connecteur	Connecteur	Connecteur	Connecteur				
	Surface				NEG NA	NEG A	Cu BO	Cu NBO				
	N° Liner				10	4	6	8				
	N° Chambre				4	2	1	16				
	N° BAG				636	474	398	326				
	N° VQM				NA	835A00705	NA	835A00675				
Equipement	Entrée (Droite)	H			7%	1 / 121 / K18	5%	1 / 221 / K4	7%	3 / 323 / K13	Cal	Canon
		B			NU		NU	NU	NU	NU	NU	NU
		E			ph	2 / 122 / K14	10%	2 / 222 / K5	10%	2 / 322 / K12	EKD	1 / 421 / K7.5 / SHV4
		I			NU		NU	NU	NU	NU	EKDK	6 / SHV3
		H			7%	3 / 123 / KV	7%	3 / 223 / K6	5%	1 / 321 / K11	7%	2 / 422 / K15
		B			NU		NU	NU	NU	NU	NU	NU
Equipement	Sortie (Gauche)	E			NU	0%	4 / 224	NU	NU	NU	NU	NU
		I			NU	NU	NU	NU	1 trou	3 / 423 / K16		

Figure 3-36: Main table of VPS information.

The colour of the background is meaningful of the name of the beam, blue or red.

Going into details in one liner of one beam (see *Figure 3-37*):

	Faisceau	Coté	Direction	Remarque	23155.113		
Station					<u>1</u>	Number of the Station	
Faisceau	Bleu	Extérieur		Photons	Connecteur		
	Surface				NEG NA	Material of the surface	
	N° Liner				1	Number of the liner	
	N° Chambre				6	Number of the Chamber	
	N° BAG				40	Number of pressure gage, BAG=VGI	
	N° VQM				NA	Number of VQM	
Equipement	Entrée (Gauche)	H			7%	1 / 111 / Sc2	Windows in the first part of the liner
		B			NU		
		E			NU		
		I			NU		
	Sortie (Droite)	H			7%	2 / 112 / K17	Windows in the last part of the liner
		B			NU		
		E			ph	3 / 113 / K8	
		I			NU		

*Figure 3-37: Part of the main table, with the parameters explained.*

Where:

- “Number of the station” is an ideal number in order to understand the position of the liner: 1, 2, 3 or 4, going from left to right.
- “Material of the surface” is an acronym for the surface: NEG NA (not activated NEG), NEG A (activated NEG), Cu BO (Baked Copper) and Cu NBO (Not baked Copper).
- “Number of the liner” is a mark in order to recognize the liners once extracted.
- “Number of the chamber” is a mark in order to recognize the chamber once extracted.
- “Number of the pressure gage, BAG” is the name of the gage, in order to have a reference.
- “Number of the VQM” is the mark to recognize the tool.
- Next, there are eight rows: four for the first part of the liner, and four for the windows nearer to the end of the liner. The window are positioned in the upper part (H), bottom (B), external side (E) and internal one (I).
- The numbers with the symbol of *percentage* are the values of the transparency of the grids used for pickups. *NU* means that window is not used, so there is a patch. *Ph* means that there is a photon pickup (unshielded) while *0%* means trigger. *Itrou* means a shielded pickup with only one hole (corresponds to 0.02%). *Cal* means the presence of a calorimeter. *EKD* and *EKDK* are the Electron Kicker Detector.

- The last written is the code to recognize the cables attached to the chamber. The red colour symbolizes the connection to the SCOPE. The bold font means the use of CK50 cables. Taking into consideration one of them, for example, **2 / 312 / K9** Where **2** is the number of the connection on the flange for a certain liner (up to 6), **3** is the number of the station (up to 4), **1** is the number of the beam (1 for Blue one, 2 for Red one), **K9** is the name of the pickup connected to Keithley. The data acquisition can be expressed by a capital K and a number if it is connected to the Keithley, a Sc and a number if it is connected to the SCOPE, a KV if it is connected to High Voltage Bias.

The same is valid for each pickup, calorimeter, EKD of the system.

Now that all the detectors are presented, it is possible to recognize from the picture the tools attached on a station (see *Figure 3-38*).

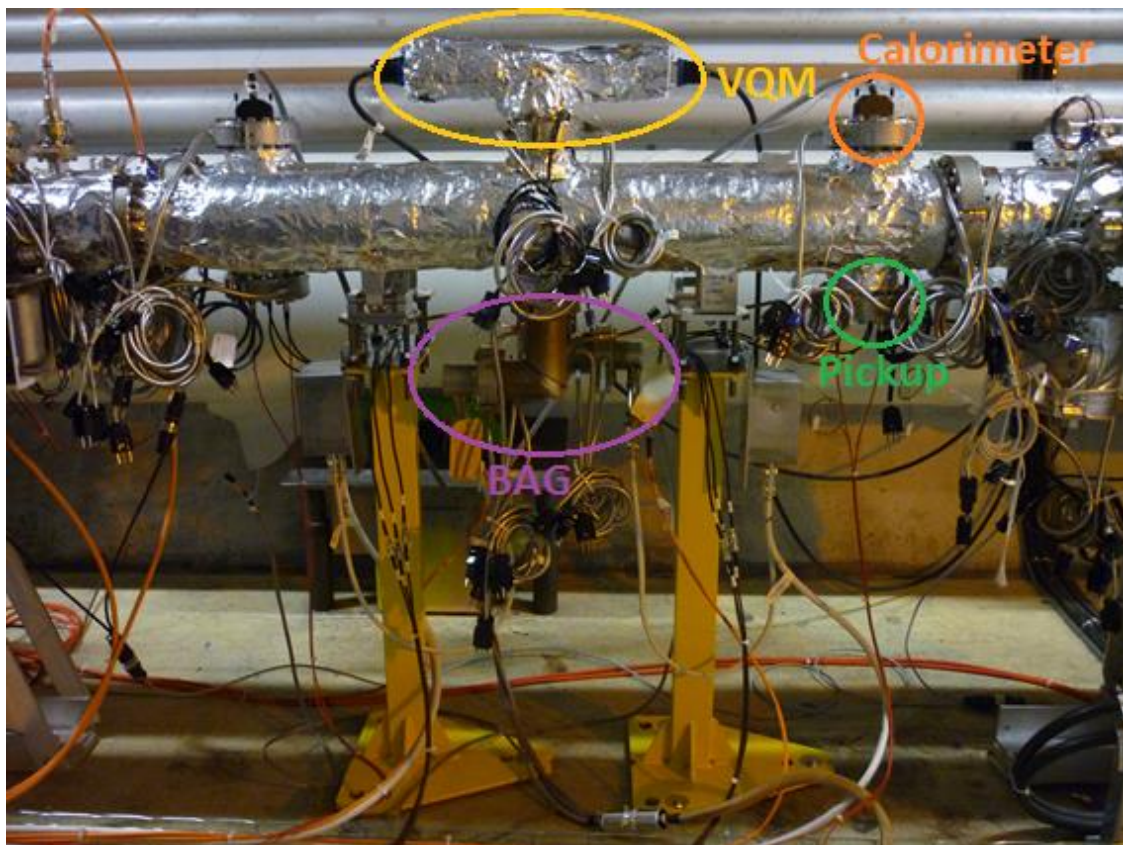


*Figure 3-38: Photo of the tools set up on a station in VPS system.*



Here it is possible to visualize the system, station by station, with all the tools installed and positioned in the right place, as in the tunnel. This is useful to have the global idea of the setup (see *Figure 3-39, 3-40, 3-41, 3-42*).

**STATION 1 – Not Activated NEG**

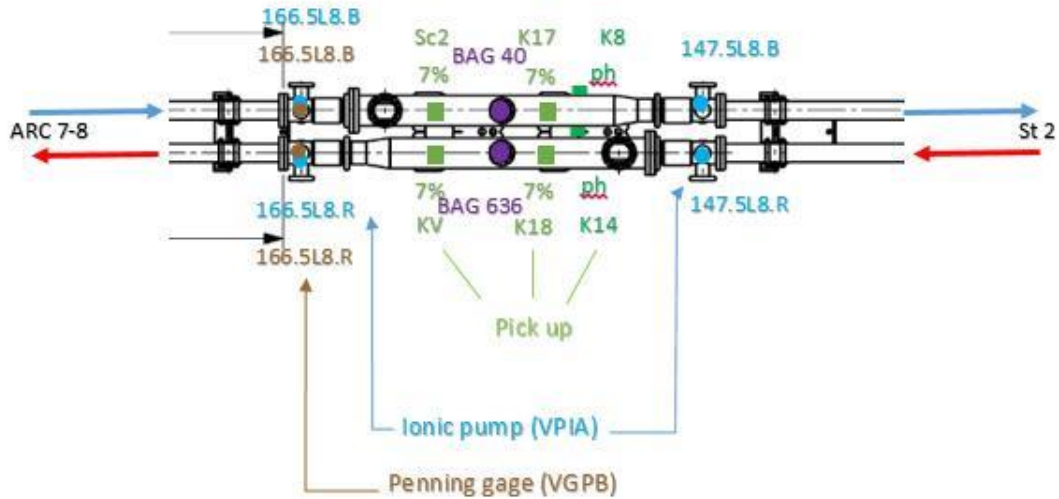


*Figure 3-39: First station of VPS (Copper coated with not activated NEG).*

**STATION 2 – Activated NEG**

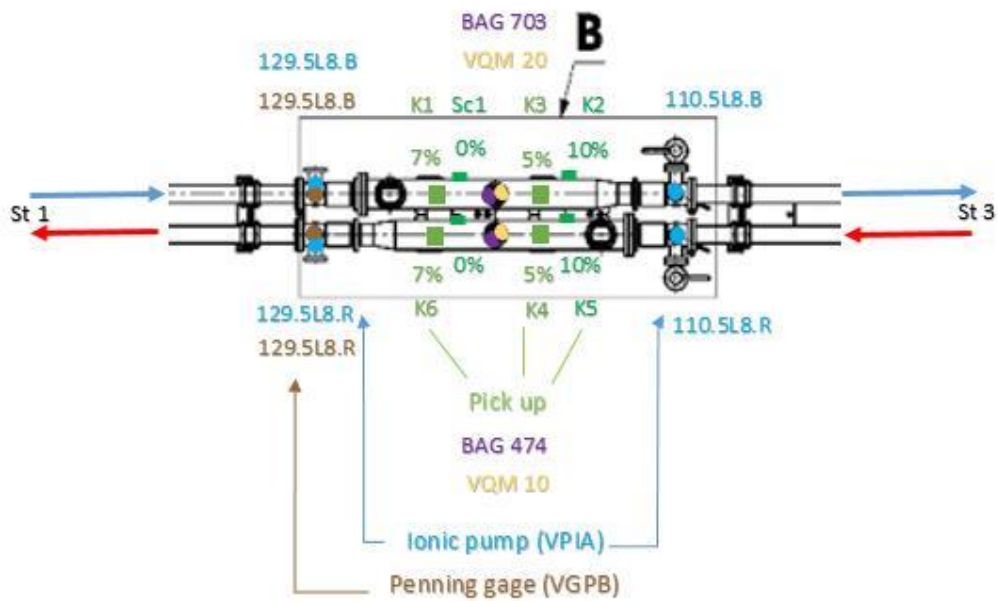


*Figure 3-40: Second station of VPS (coated with activated NEG).*



### STATION 3 – Baked Copper

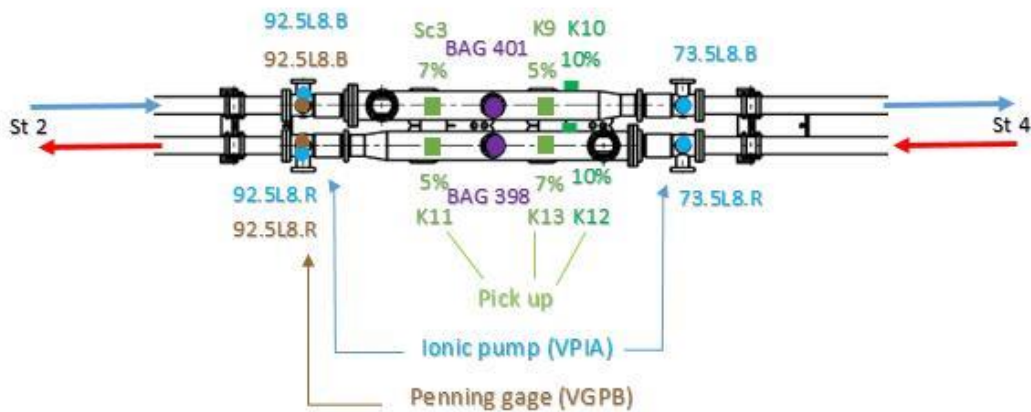


Figure 3-41: Third station of VPS (Copper baked Copper).

### STATION 4 – Not Baked Copper

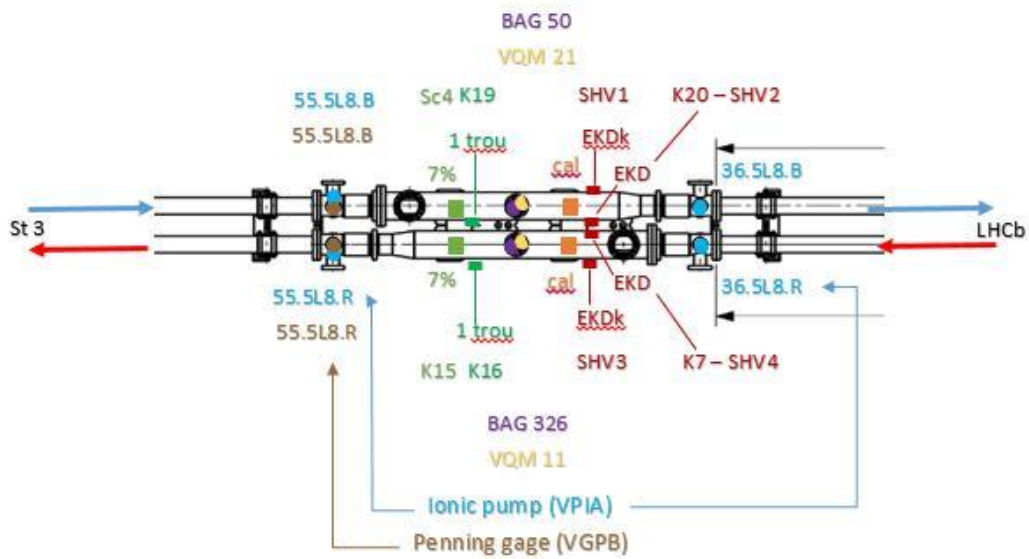


Figure 3-42: Forth station of VPS (not baked Copper).

This overview shows the names of the gages, the information about the tools attached. Also the symmetry of the system on both beams is evident.

As it is possible to see, the pumps and the penning gages are in the ends of the liners while pickup, calorimeters and EKD are all along. In the middle there are the gas analyser (VQM) and the Bayard-Alpert gage (BAG). This scheme is kept for all the liners, to be able to compare them.

### 3.6 Objectives of VPS

The main goal of this system is to understand the phenomenon of electron cloud, with different tools. This is done in order to control this phenomenon in materials and surfaces usually used in accelerators.

In order to do this it is necessary to know the instruments and the behaviour the tools show with different inputs. It is necessary to start from the signals, trying to understand the meaning of them. Once this is done and it is sure that all the signals are truthful, it is possible to analyse data.

The most important periods of analysis are the Scrubbing Runs of LHC and the following beams.

Considering the tools it is possible to use, the main purposes are the following:

- a) Check the reliability of the electrical measurements of Keithley and SCOPE (shielded pickup)
- b) Study the influence of the transparency of the grids for electrical signals (shielded pickup)
- c) Check the effective conditioning of surfaces during the scrubbing runs in different coatings (shielded pickup and pressure gages)
- d) Measurement of photons (unshielded pickup)
- e) Control the influence of the voltage in the electrical signals through a High Voltage Bias (shielded pickup and unshielded pickup)
- f) Scan the energy spectrum of electron cloud (EKD)
- g) Analyse the power deposition on the walls (Calorimeters)
- h) Analyse the gas spectrum (VQM)

For each of these questions, there will be presented results in the next chapters in order to define and optimize the new configuration to install on December 2015.

## 4. STEPS OF WORK

After this presentation of CERN and of the system, the analysis part starts. During my permanence at CERN I faced many kinds of work, from computer analysis to real handwork.

Starting from the beginning, I spent some months to understand and study the configuration of the system and all the detectors used (March-May 2015).

Then I followed from CCC the “Scrubbing Run” of LHC in order to reduce the phenomenon of electron cloud in the machine (June-August 2015). This analysis are presented on *Chapter 5*. Here I controlled directly all the parameters in parallel to check the effective conditioning of the walls of my system.

I analysed data after the scrubbing runs with the programs presented above, *Chapter 6* (August-September 2015). Here I tried to follow all the objectives, solving the questions proposed. Then the injections of gas on the system are analysed.

Thanks to the analysis done, I optimized the system, doing the new plan submitted on *Paragraph 7.1* (September 2015). It was modified and approved until the best solution.

After this I managed all the steps of manufacturing of the new liners and pieces, I built detectors, in particular calorimeters and pickup, and I assembled the liners. I took care about the bake out of the cables and the mounting of them. Then vacuum tests followed before the installation in the tunnel. This is shown on *Paragraph 7.2* (October-November 2015). Then the final installation of the new system, *Paragraph 7.3* (December 2015-February 2016).

All these jobs were done considering the LHC schedule that here is presented for 2015 and 2016 (see *Figure 4-1, 4-2*). (41) (42) (43)

**LHC Schedule 2015**  
Approved by the Research Board, December 2014

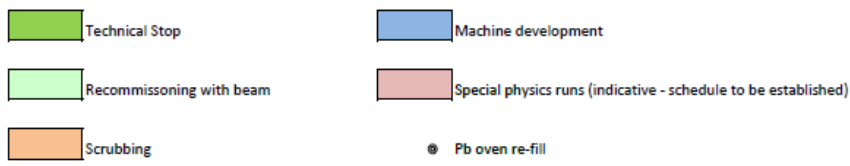
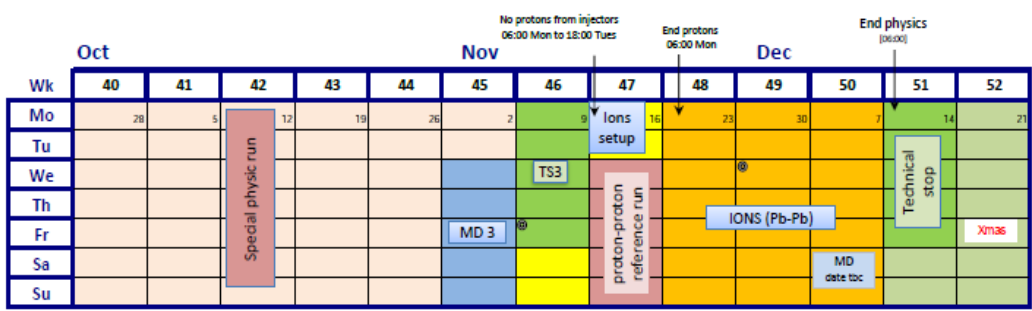
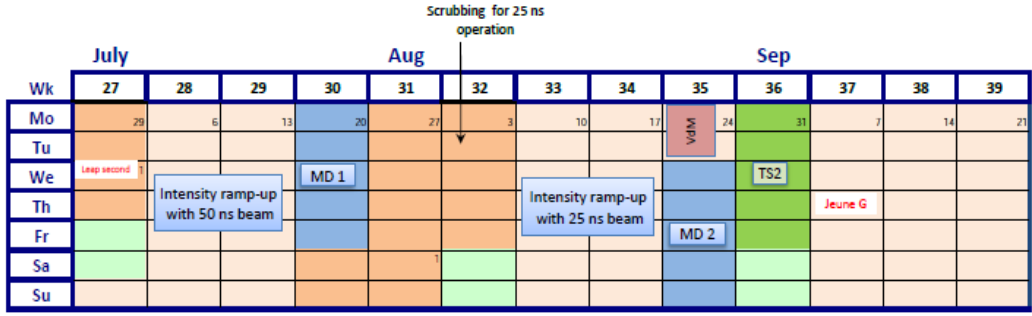
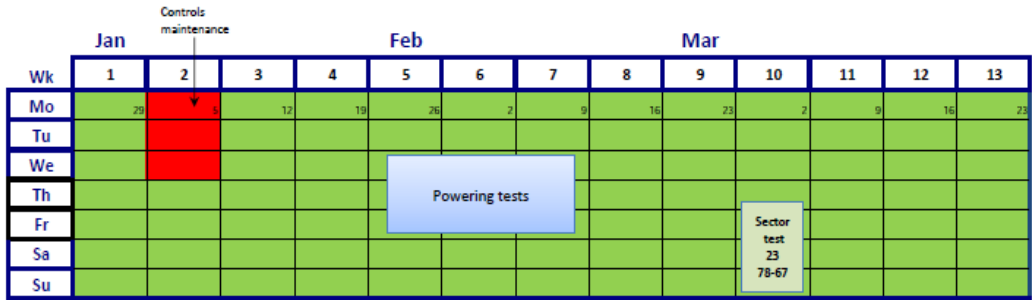


Figure 4-1: LHC Schedule 2015.

**LHC Schedule 2016**  
Approved by the Research Board, December 2015



Figure 4-2: LHC Schematic 2016.



## 5. SCRUBBING RUN ANALYSIS

As told before, the scrubbing effect is useful to reduce electron cloud phenomenon. Studying this is the first aim of this work. This procedure consists on bombarding the surface with electrons in order to decrease the number of electrons coming outside from the walls during a normal run of LHC. The goal, indeed, is to mitigate the electron cloud effect by accumulating electron dose on the beam chambers. The strategy used is to increase gradually the electron flux using at the beginning 50 ns and then turn to 25 ns, until doublets. (44) (45) (46) (47)

### 5.1 Scrubbing Plan for LHC

This wall cleaning is done in two periods for LHC accelerator in 2015. The first is in the end of June for around one week (24/06/15 to 04/07/15) using 50 ns beam and the second one from the end of July to the beginning of August (25/07/15 to 08/08/15) using 25ns beam. (48)

Considering the difference between 50 ns and 25 ns, it is important to know that less is the amount of time spacing between bunches, more the phenomenon of electron cloud takes place, because the electric field is higher and electrons receive more acceleration kicks. This is why the scrubbing start with 50 ns to reach 25 ns, the normal bunch spacing for LHC run.

The energy used is 450 GeV, instead of the maximum energy of 6.5 TeV per beam. This is due to the fact that during a scrubbing run the losses of protons are higher than a normal run because the aim is to stimulate the electron cloud phenomenon in order to release many electrons from the walls. If the maximum energy would be used, there will be too many losses and instabilities from a cryogenic point of view and this energy will be not necessary for this goal. Vice versa it is not possible to use less than 450 GeV because it is the energy used in SPS accelerator.

During these two periods I worked in CCC in order to follow, hour by hour, the strategy of cleaning. The plan of the LHC scrubbing is the following (see *Figure 5-1*). (49)

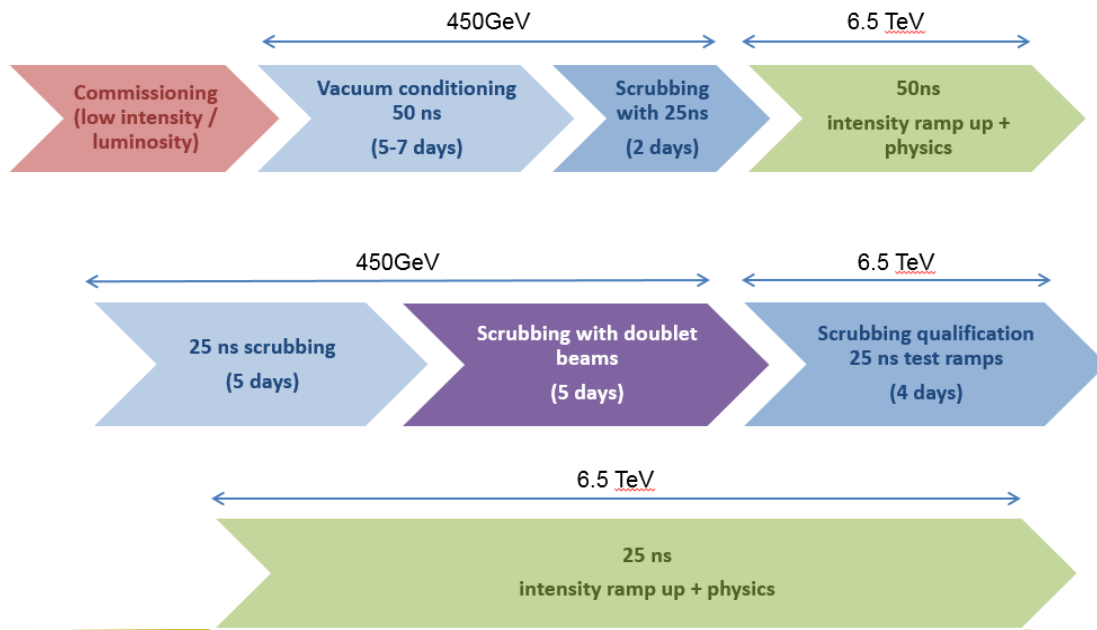
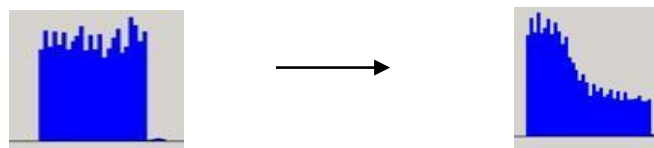


*Figure 5-1: Steps of LHC scrubbing.*

## 5.2 First Scrubbing Run

The first scrubbing run uses 50 ns in order to start the cleaning of wall surfaces of LHC. The main parameters to check are the pressures and the beam currents. The required result is the reduction of pressure, both maintaining constant the beam currents and increasing the same currents. This is mainly due to two phenomena: the loss of protons per batch and the real scrubbing effect. It is not easy to split this two contributions. But it is possible to see the effect of the scrubbing when the reduction of pressure occurs also with an increase of currents. Here it is shown an example of loss of protons per batch.





This can be verified in some minutes, usually on the first batches injected in the machine. If the loss of protons is high, it is possible to see the beam current decreasing during a stable beam.

Some examples of both beams are now shown. The colour of the beam current gives the information about the beam I am talking about. If blue, it is the external pipe, if red, it is the internal one. Here it is only shown in green the higher level of pressure that it is the station number four, Not Baked Copper. In black there is the beam energy (see *Figure 5-2*).

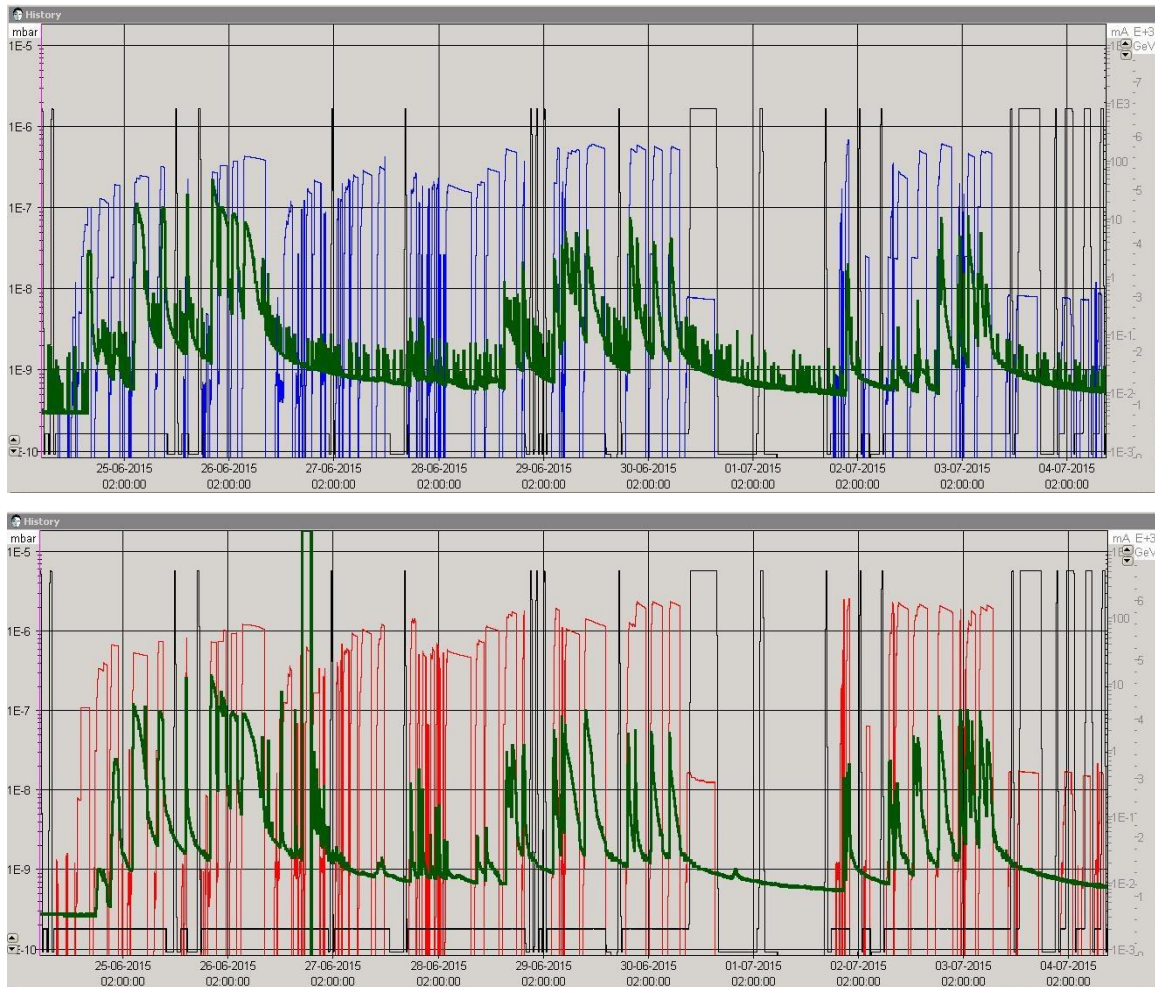


*Figure 5-2: Trend of pressure of Copper not baked (green), energy of external beam (blue) and internal beam (red), energy in LHC accelerator (black).*

It is possible to notice that the trend of the pressure of the external pipe, blue one, fluctuate more than the red one. This is due to the influence of the cooling system.

The maximum value of pressure that is acceptable is around  $5 \cdot 10^{-7} \text{ mbar}$ , above which the injections have to be stopped because of the limits of the LHC machine.

Here it is possible to see the scrubbing effect and the loss of protons which reduce the pressure with constant beam current considering one fill number. The pressure trend seems to linearly decrease with time at the beginning (first two figures). With the scrubbing, the fall of pressure becomes faster until to reach a shape with a pick and a more than linear decrease (see *Figure 5-3*).

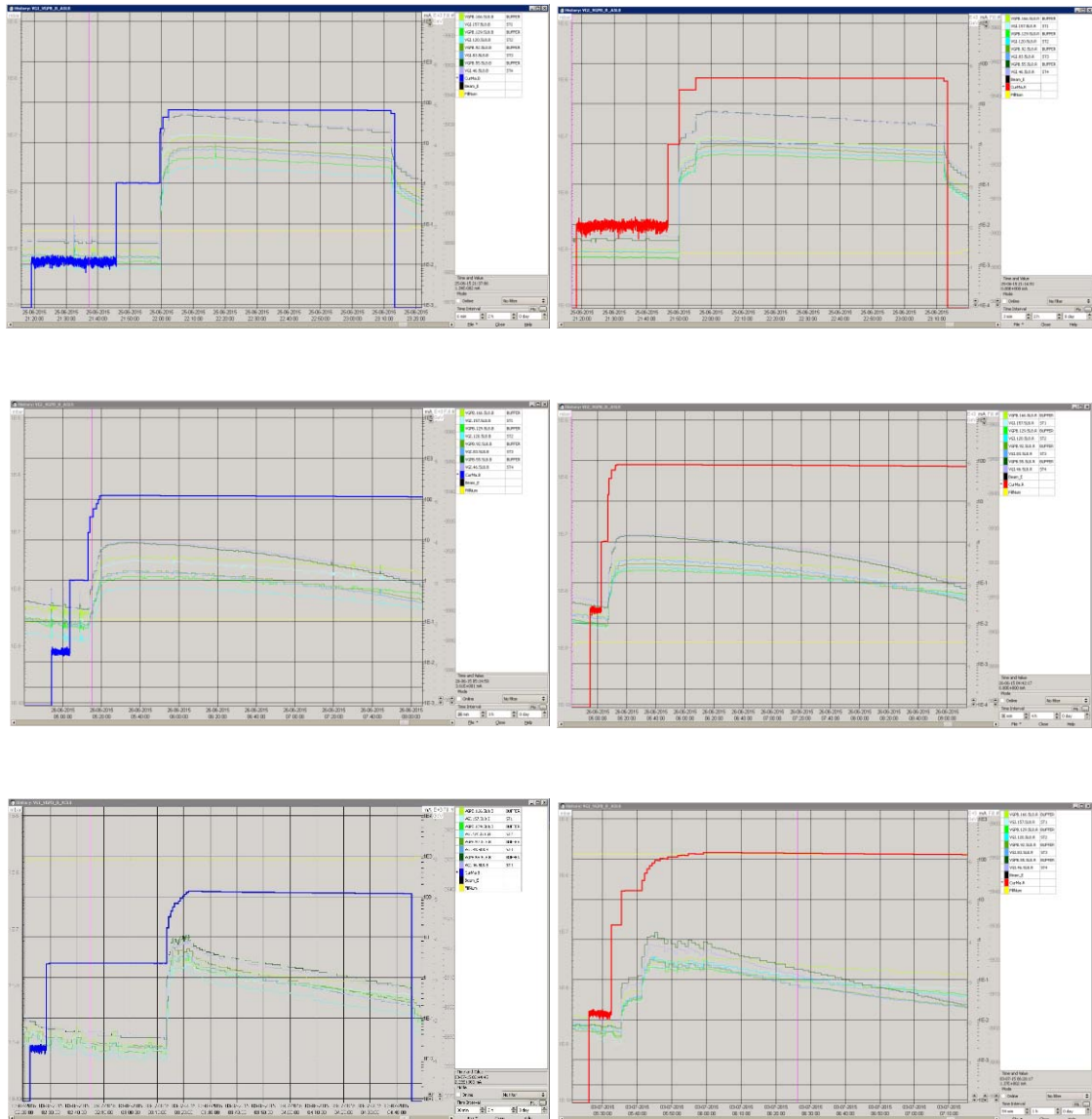


*Figure 5-3* Trend of pressure during scrubbing run.

Here it is possible to see mainly the scrubbing effect which permits to reduce the pressure with the increase of beam current (see *Figure 5-4*). (50)

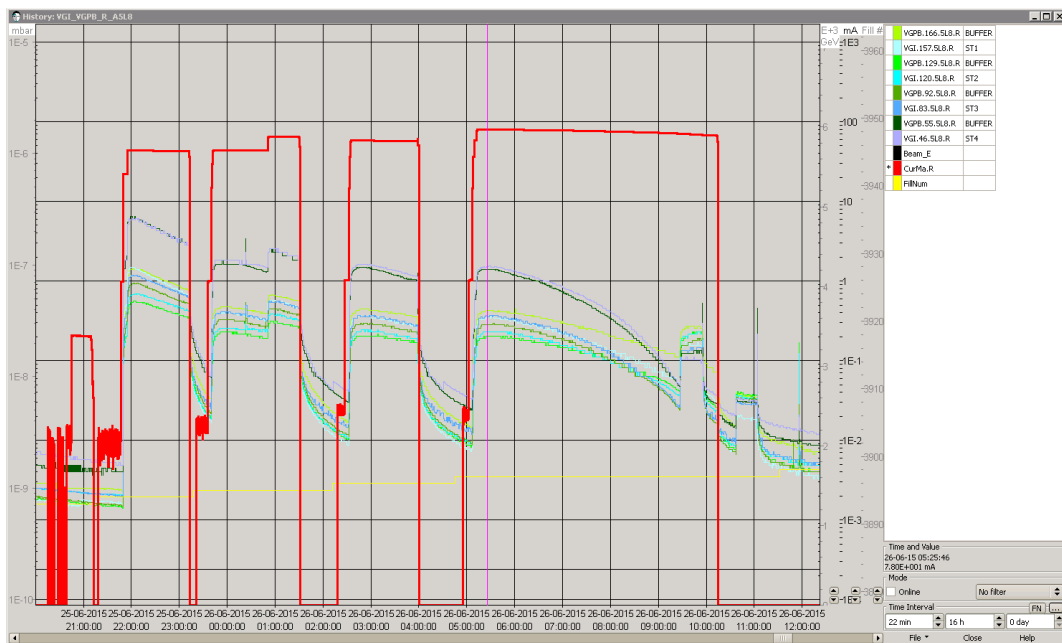
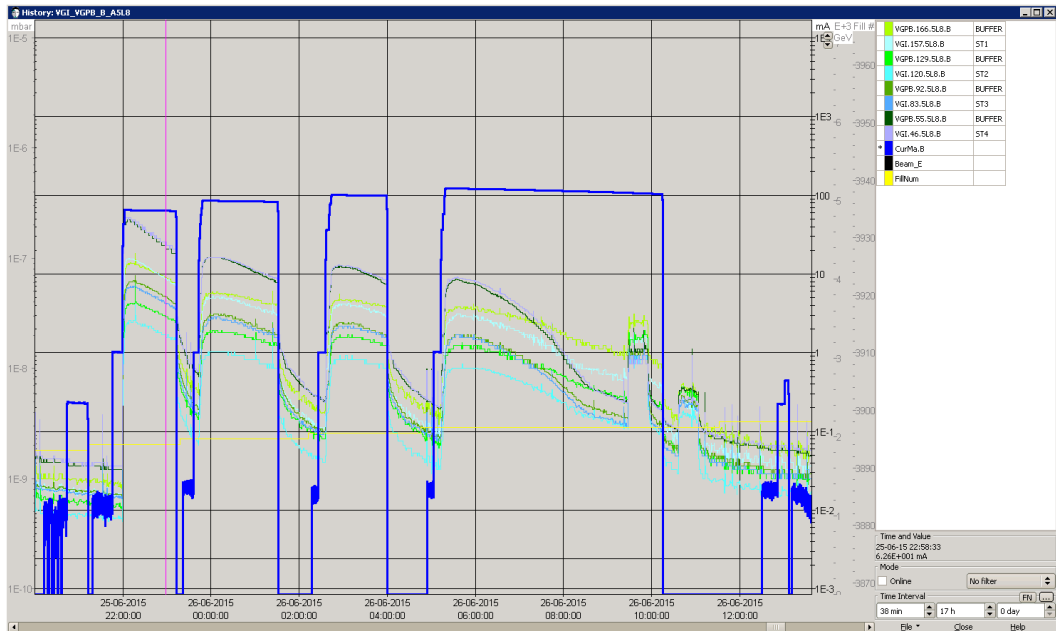


*Figure 5-4: Scrubbing effect: decrease of pressures with increase of beam currents.*

The slope of the decrease of pressure increases, with negative sign, when the scrubbing effect is more and more evident. It is possible to see this comparing the last figure, taken at the beginning of the scrubbing, with next one, taken in the middle of the first scrubbing. This is an indication of the effectiveness of the scrubbing (see *Figure 5-5*).

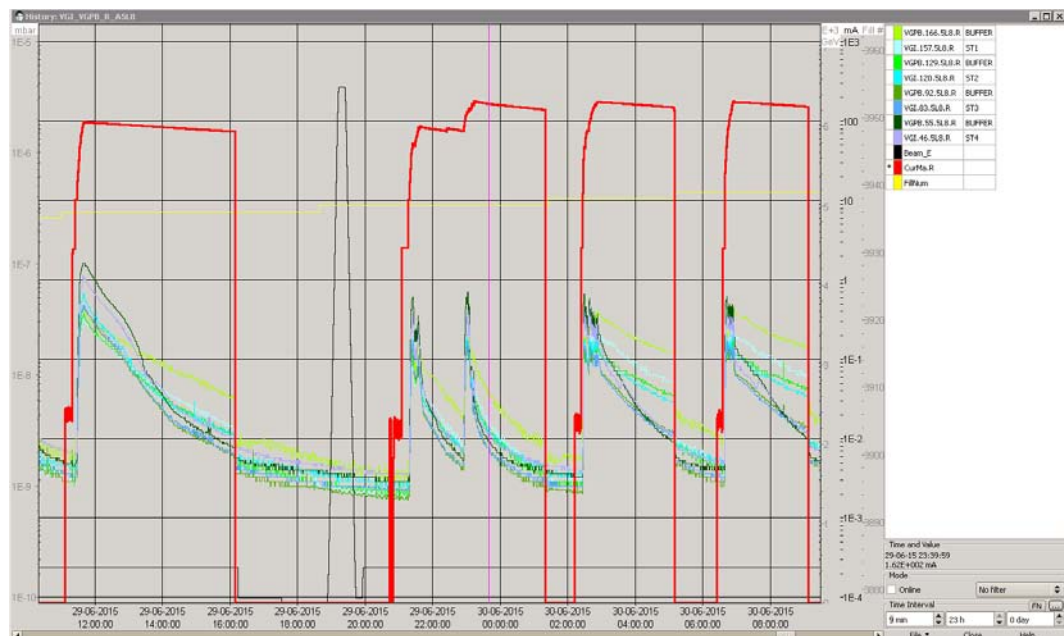
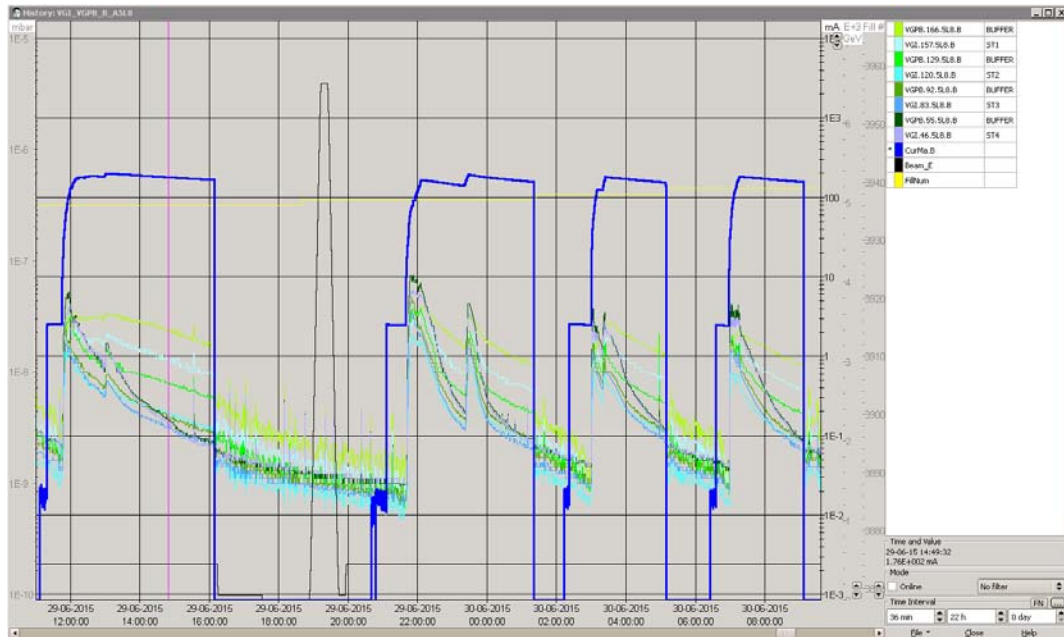


*Figure 5-5: Scrubbing effect: the pressure decreases very quickly.*

### 5.3 Second Scrubbing Run

The second scrubbing run uses 25 ns in order to have a stronger impact on the walls. All is presented with the same structure used above.

The general trend of beam current, blue or red, and the higher pressure, in green, are shown below (see *Figure 5-6*).

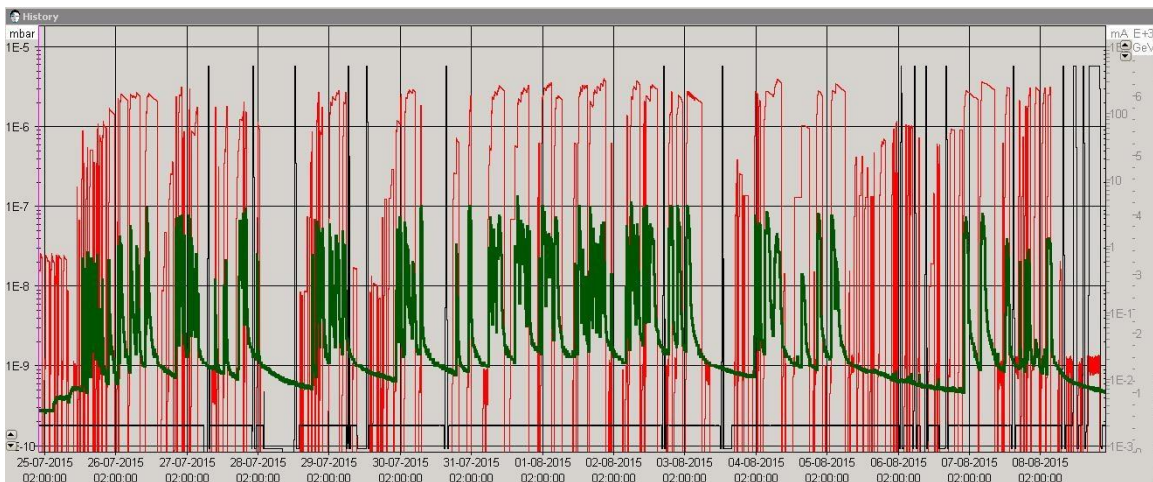
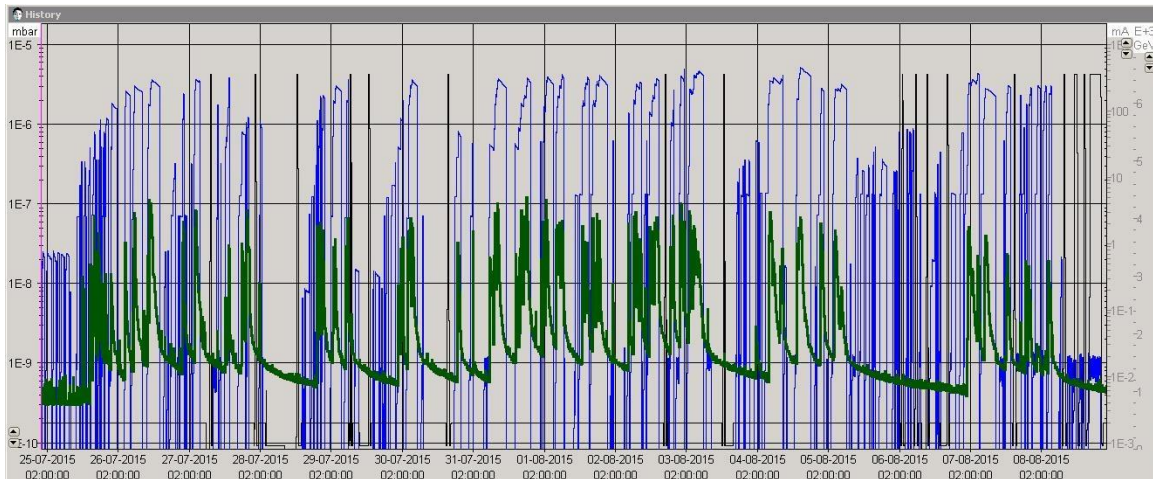


*Figure 5-6: Trend of pressure of Copper not baked (green), energy of external beam (blue) and internal beam (red), energy in LHC accelerator (black).*



Focusing on a determined fill number, it is possible to see that the trend of pressure starts linearly and, with a following injection, it becomes logarithmic (see *Figure 5-7*).

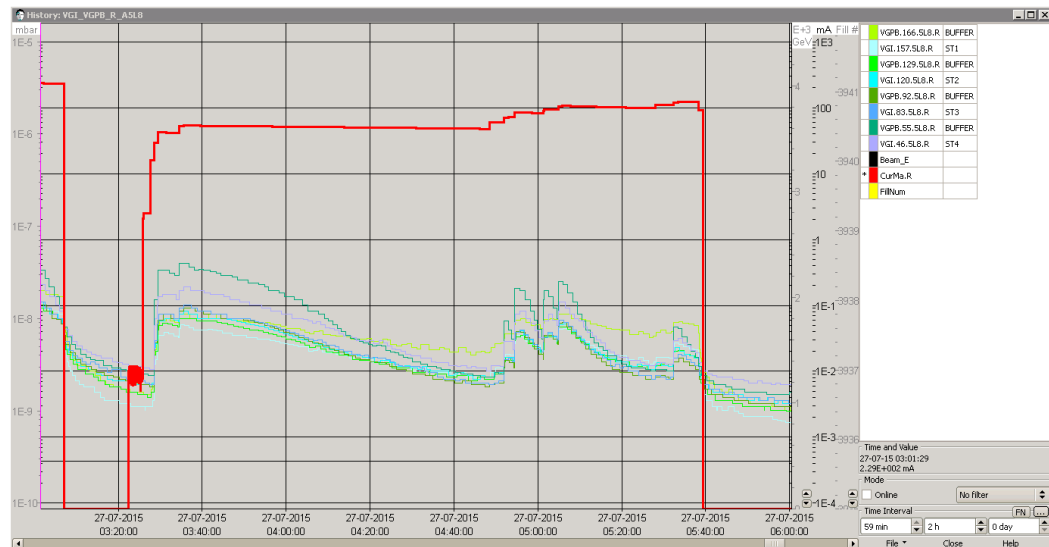
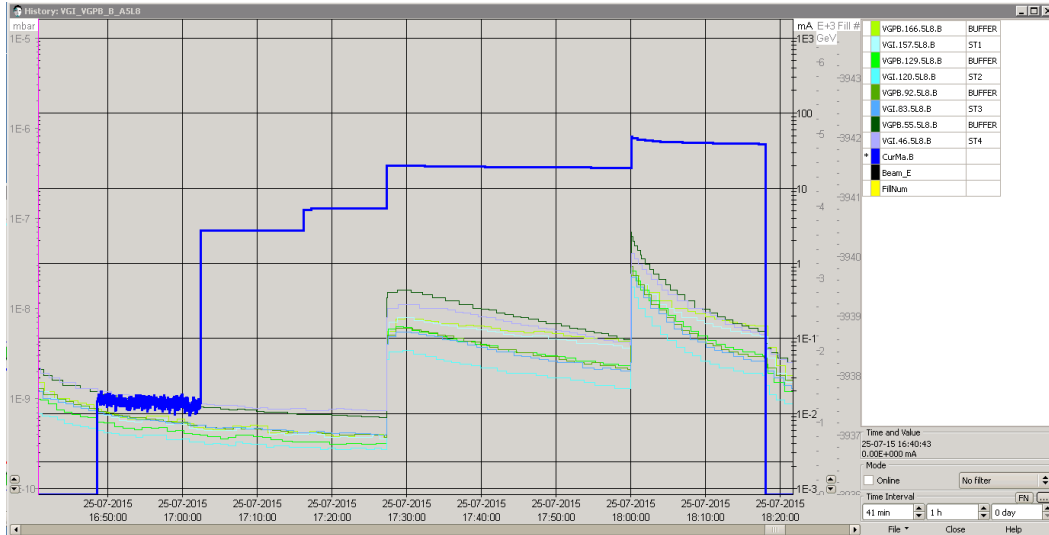
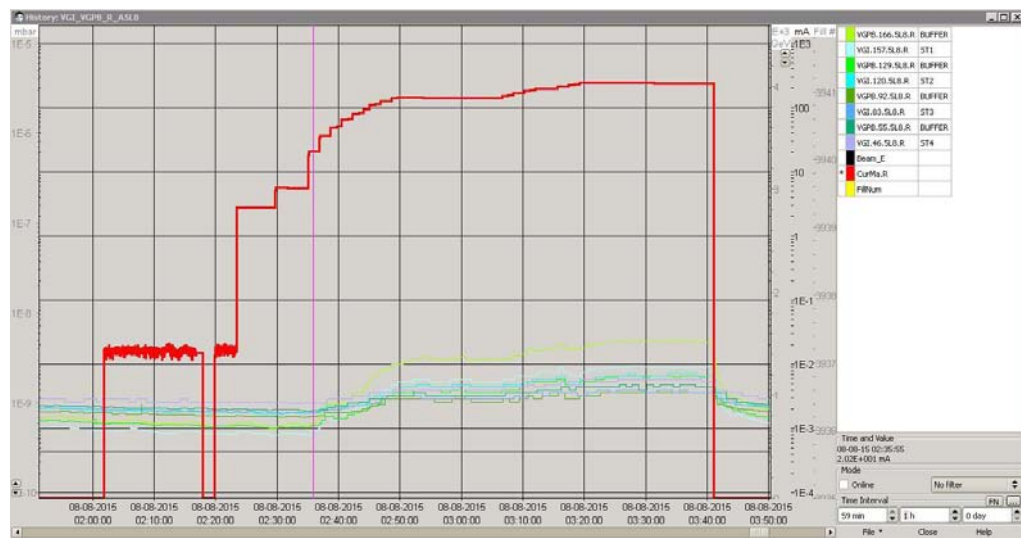
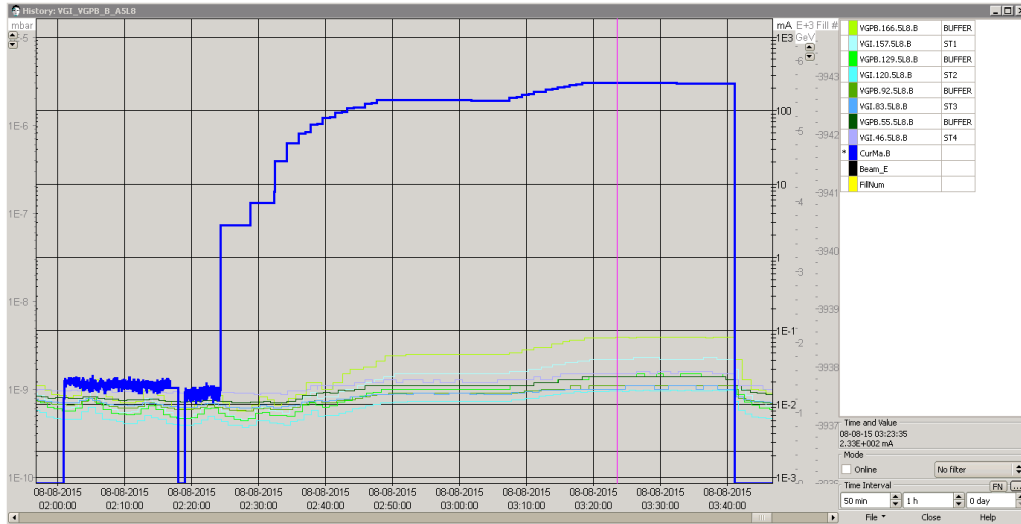


Figure 5-7: Trend of pressure during scrubbing run.

At the end of the scrubbing the increase of pressure is really lower than at the beginning. Here there is one of the last beams (see *Figure 5-8*).



*Figure 5-8: Scrubbing effect: the pressure doesn't rise up too much.*

## 5.4 Conditioning effect

Considering the values of the main picks of pressure of the eight stations divided by the respective beam current, it is possible to build the next graph (see *Figure 5-9*).

The ratio between pressure and current decreases due to the conditioning effect on the surface.

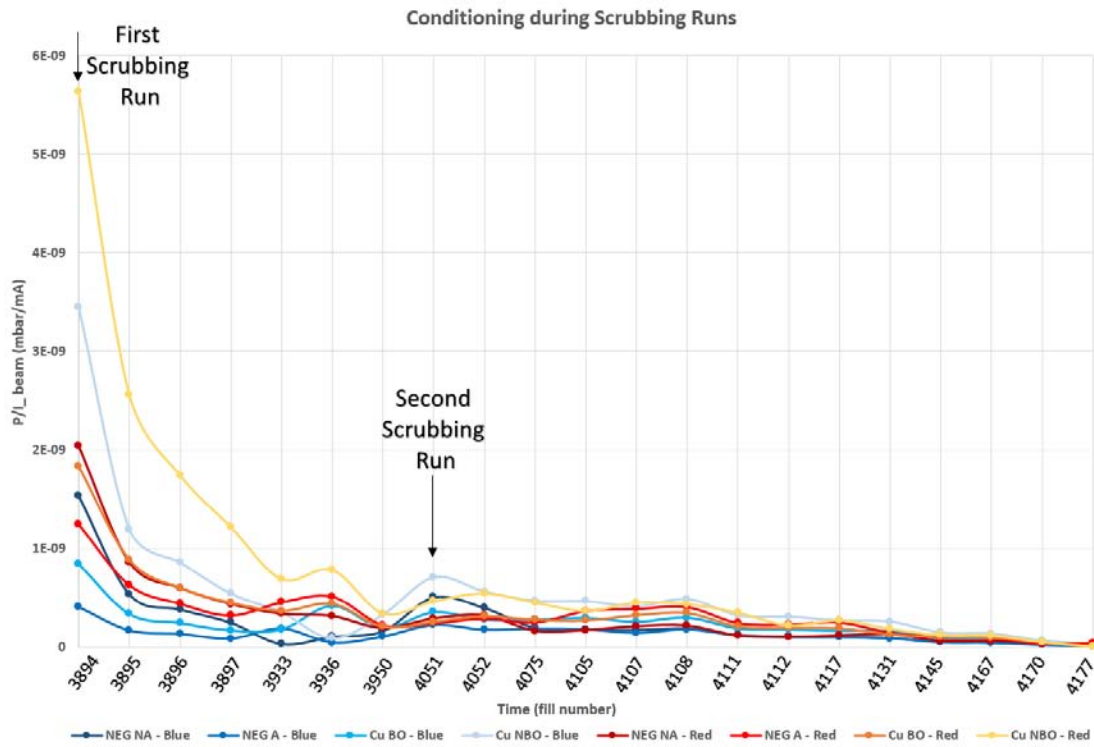


*Figure 5-9: Conditioning effect in VPS.*

As it is possible to see, there is a so called “memory effect” in between the two scrubbing runs. It is because in between LHC ramped up to the maximum energy.



## 6. ANALYSIS

Considering the tools in VPS and the objectives listed above, the main results are now presented. Due to issues of data acquisition, these data are concerning the period from 21/09/2015. It is not possible to know exactly all the history of this system speaking about conditioning of the liners, but it is possible to have information through pressure trend and VQM. (51) (52)

Concerning the errors on the following data, it is important to indicate that, thanks to the experience of my team on these kinds of data acquisition, a value of 10-15% is coherent with several instruments used.

### 6.1 Check the reliability of the electrical measurements (Keithley and SCOPE)

The electrical measurements done in VPS are acquired with Keithley and SCOPE. Starting with this last interface, only for simplicity reasons, it is possible to say that the electrical signals appear. It can read four channels. The first channel is linked to the unshielded pickup dedicated to the trigger on station 2 (Activated NEG) on the blue beam. The other three channel are shielded pick up of 7% of transparency located on blue pipe, respectively station 1 (Not Activated NEG), station 3 (Baked Copper) and station 4 (Not Baked Copper). In *Figure 6-1* and *6-2* is presented the acquisition system without beam and with beam.

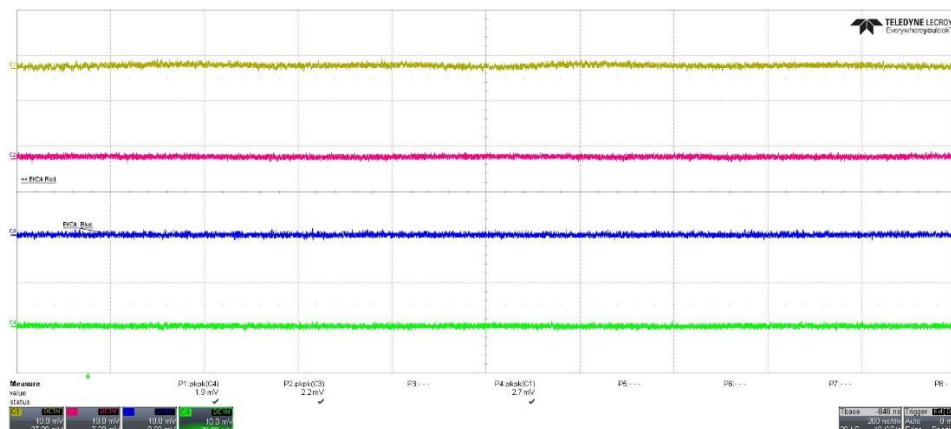


Figure 6-1: Main interface of SCOPE without beam.

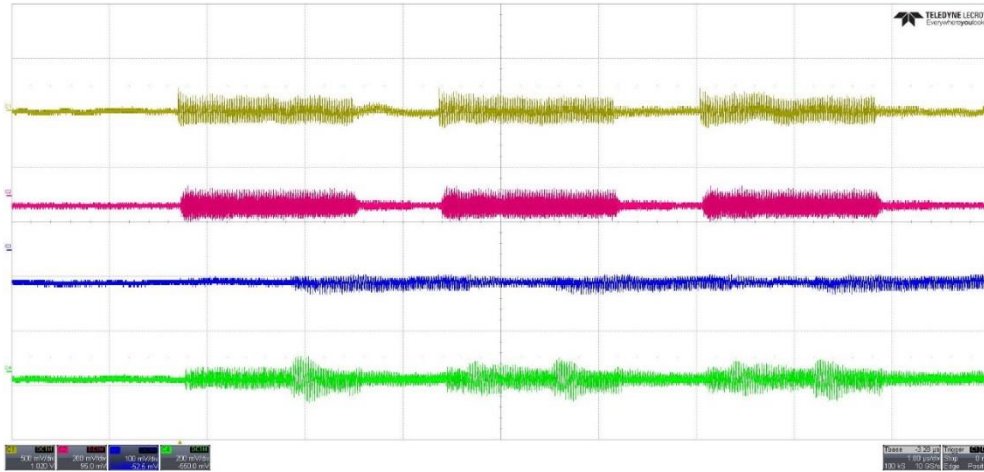


Figure 6-2: Main interface of SCOPE with beam.

Considering this last image, it is possible to see that the time resolution used is  $1\mu\text{s}/\text{division}$ , while for the y-scale it is different changing the channel. It is possible to regulate it thanks to the Menu. It is a value of voltage that, considering a resistance of  $1\text{M}\Omega$ , correspond to a direct current. Here the zoom of the values in  $\text{mV}/\text{division}$  (see Figure 6-3).



Figure 6-3: detail of SCOPE Parameters.

If you consider the intensity pick to pick of the example taken above, you can build this table for the SCOPE (see Figure 6-4).

SCOPE							
Channel	Grid	Station	Beam	Position Pick up	Surface	ensity pick to pick (n	equivalent current (A)
1	0%	2	Blue	External	NEGA	250	2.5E-07
2	7%	1	Blue	High	NEG NA	100	1.0E-07
3	7%	3	Blue	High	Cu BO	30	3.0E-08
4	7%	4	Blue	High	Cu NBO	70	7.0E-08

Figure 6-4: Levels of currents read by SCOPE.

Comparing the same example taken the 28.09.15 at 13:45 with the SCOPE with that of the Keithley, it is possible to see that the intensity of the electrical signals are quite in the same order of magnitude (see Figure 6-5, 6-6).

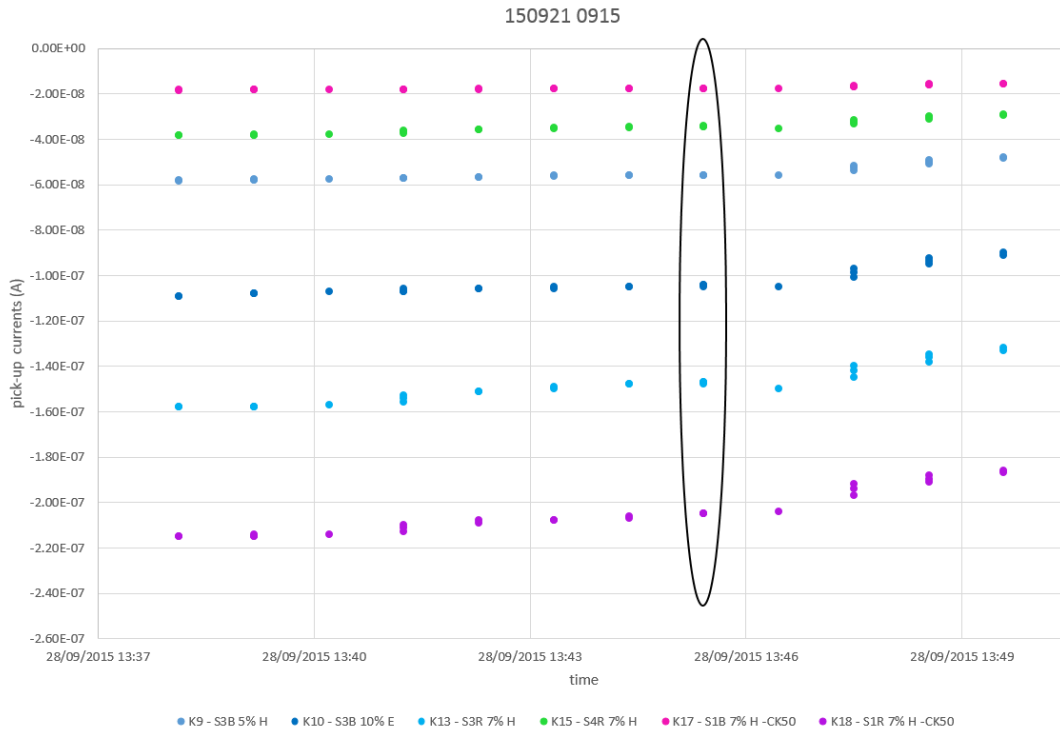


Figure 6-5: Graph of pressure read by Keithley.

KEITHLEY						
Channel	Grid	Station	Beam	Position Pick up	Surface	current (A)
K17	7%	1	Blue	High	NEG NA	-1.9E-08
K18	7%	1	Red	High	NEG NA	-2.0E-07
K9	5%	3	Blue	High	Cu BO	-5.6E-07
K10	10%	3	Blue	External	Cu BO	-1.0E-07
K13	7%	3	Red	High	Cu BO	-1.5E-07
K15	7%	4	Red	High	Cu NBO	-3.5E-08

Figure 6-6: Levels of currents read by Keithley.

Considering not activated NEG (pink), not baked Copper (blue) and Baked copper (green), it is possible to cross check that the values are compatible, between  $10^{-7} \div 10^{-8}$  A. The values of the SCOPE are not precise because it is a fast measurement, and it gives an idea of the amplitude of the phenomenon.

This check is important because it permits to be sure of the intensity of the phenomenon is going on. Usually Keithley is used as a safety way to record data, while SCOPE is a focus on the beam structure (bunches and batches) and on the build-up of electron cloud.

What it is necessary to solve in the future is the fact that for the moment is not possible to see the build-up of the electron cloud phenomenon on it.

Here an example of a train made by 15 batches on the blue pipe. It is taken on 28.06.15 at 17:05 (see *Figure 6-7*).



*Figure 6-7: Example on SCOPE.*

The same structure is possible to see from PVSS program, counting 15 batches, in which the first is smaller as shown in the SCOPE (see *Figure 6-8*).

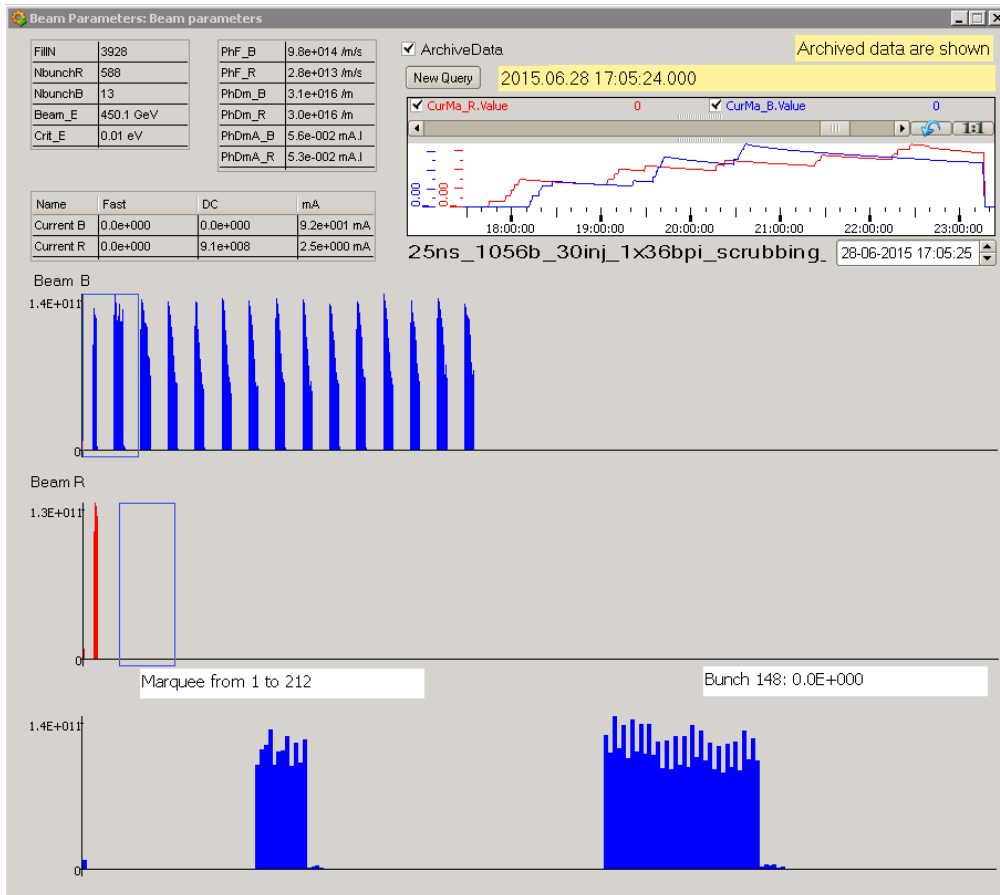


*Figure 6-8: Structure of the beam for the same example in PVSS.*

It is also possible to see the inner structure of a batch. Here it is an example taken the 31.07.15 at 7:54. The structure is exactly the same implemented in PVSS (see *Figure 6-9, 6-10*).

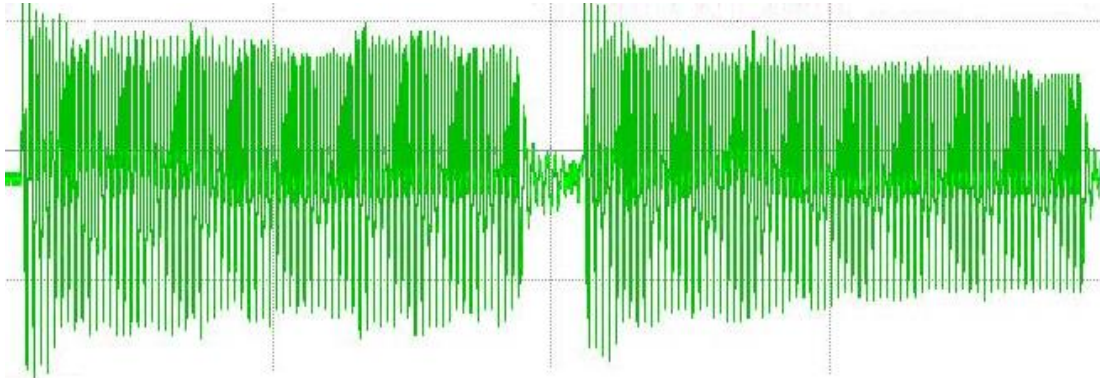


*Figure 6-9: Detail of an example taken from SCOPE.*

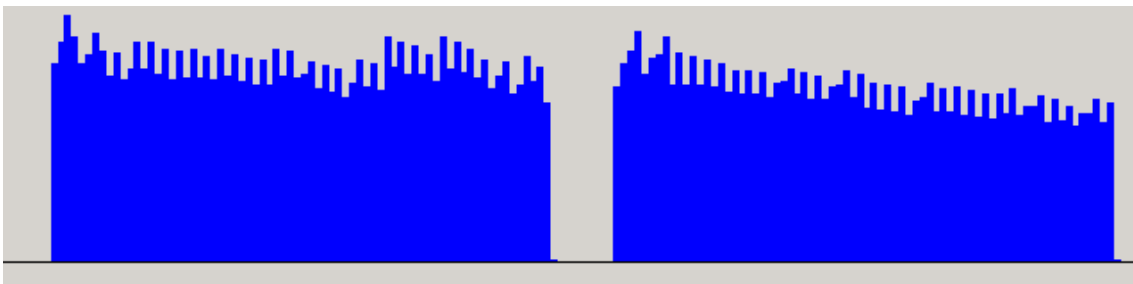


*Figure 6-10: Detail taken for the same example in PVSS.*

## 6.2 Study of the influence of the transparency of the grids of shielded pickup

Pick up with different transparencies are used in VPS. The influence of this parameter is important in order to understand the electrical signals. There are pick up of 5%, 7%, 10% or 0.2%. Each pick up is made of holes of 2mm of diameters.

Here there is the first example of data on station 2, activated NEG, on 21.09.15 at 19.15, in which it is possible to see that the number of holes influences the measurement. The electrical signals coming from external pipe are in blue, while the internal one are in red (see *Figure 6-11*).

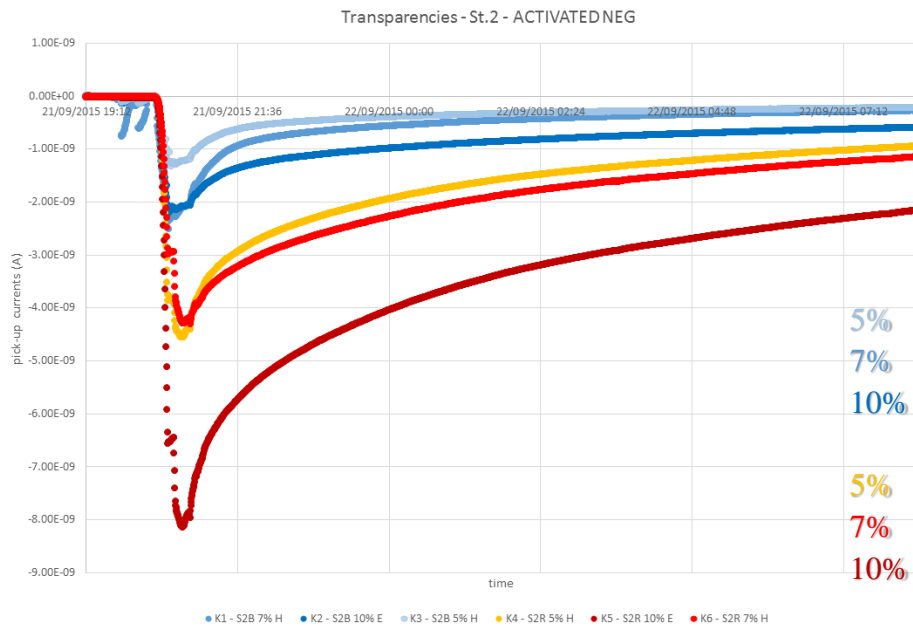


Figure 6-11: Influence of transparencies of grids on Station 2.

Considering the pick values and the ratio between each current and the 10% current, it is possible to build this table to see if the trend is linear(see Figure 6-12).

STATION 2	Blue beam			Red beam		
Transparency	5%	7%	10%	5%	7%	10%
Pick Current (A)	-1.32E-09	-2.48E-09	-2.14E-09	-4.56E-09	-4.32E-09	-8.14E-09
$I_x/I_{10\%}$	62%	116%	100%	56%	53%	100%

Figure 6-12: Table of relationships between transparencies and currents read by pickup.

The currents of the Keithley are increasing with the increase of the transparency. This currents seem to be proportional to the transparency in the blue line, but more than proportional in the red one (only for station 2- Activated NEG). This can be due to the photoelectrons impinging in the grid 10%. This means that the phenomenon is not killed by the rising number of holes.

Considering station 3, baked Copper, and station 4, not baked Copper, it is presented the same graph (see Figure 6-13, 6-14).

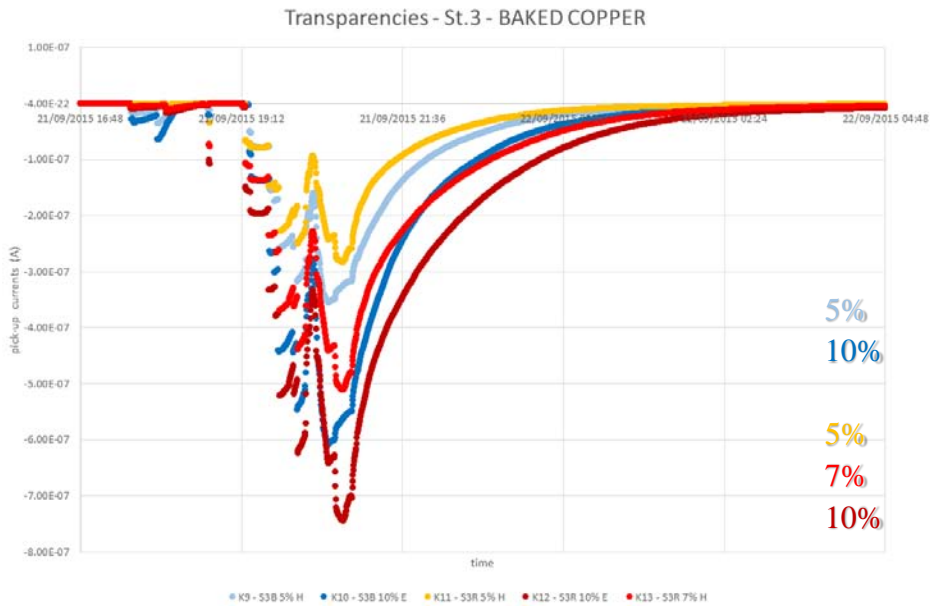


Figure 6-13: Influence of transparencies of grids on Station 3.

STATION 3	Blue beam		Red beam		
Transparency	5%	10%	5%	7%	10%
Pick Current (A)	-3.54E-07	-6.09E-07	-2.81E-07	-5.11E-07	-7.44E-07
I <sub>x</sub> /I <sub>10%</sub>	46%	100%	38%	69%	100%

Figure 6-14: Table of relationships between transparencies and currents read by pickup.

As it is possible to see, the signals are proportional to the transparency (see Figure 6-15, 6-16).

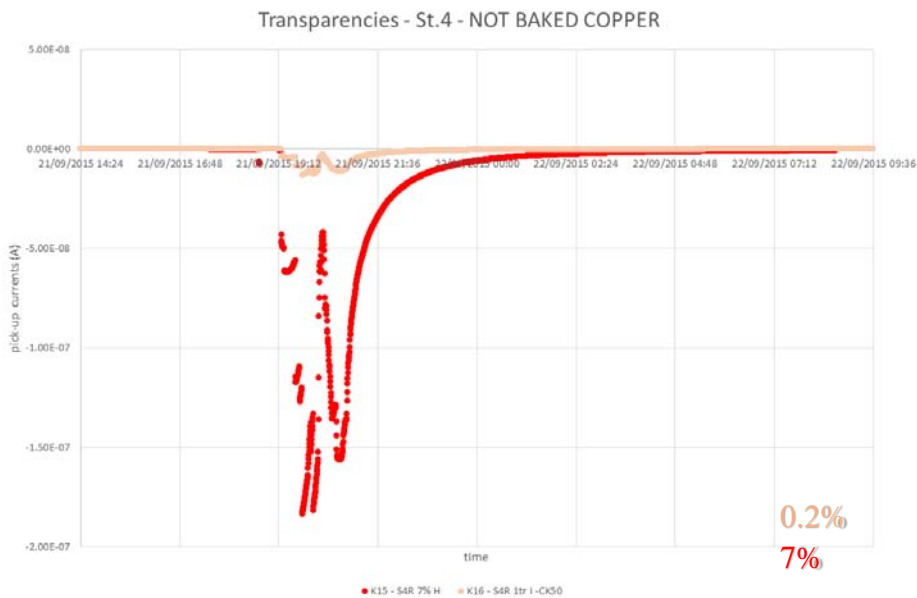


Figure 6-15: Influence of transparencies of grids on Station 4.

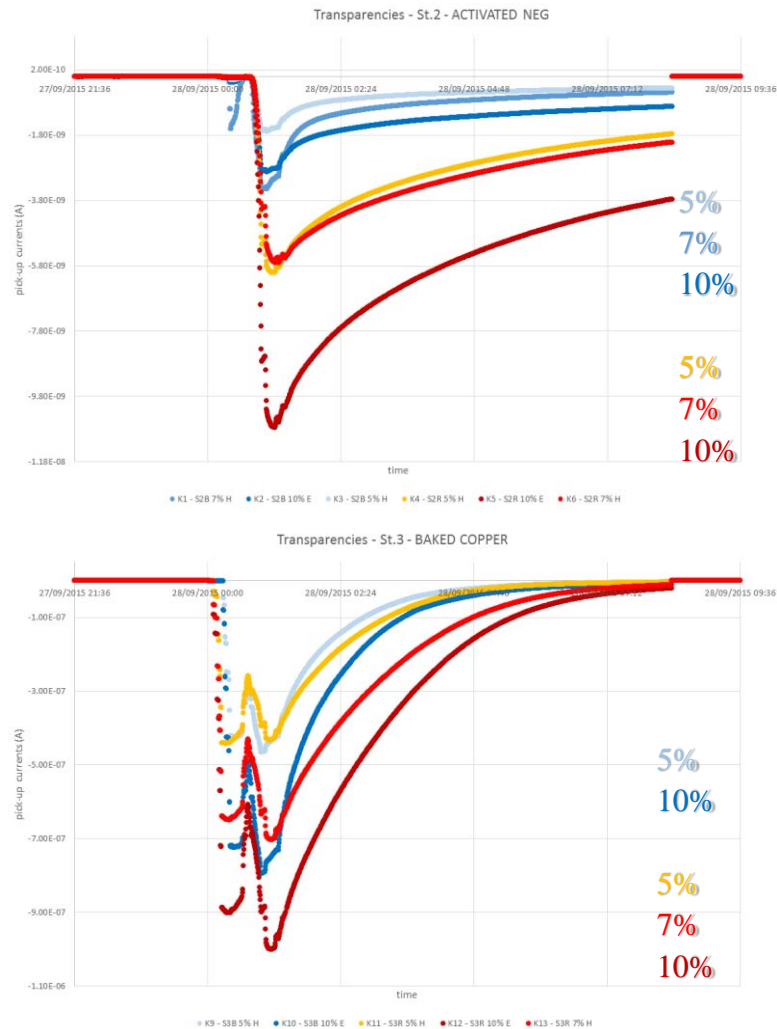
STATION 4	Red beam	
Transparency	0.2%	7%
Pick Current (A)	-1.11E-08	-1.56E-07
I <sub>x</sub> /I <sub>7%</sub>	7%	100%

Figure 6-16: Table of relationships between transparencies and currents read by pickup.

Considering that  $\frac{0.2}{7} = 2.85\%$ , the electrical signal read with 0.2% is higher than expected, comparing it with 7%. But in any case is not good enough.

Here two similar examples are reported with the same results.

Example 2, on 27.09.15 at 06:00 (see Figure 6-17, 6-18):





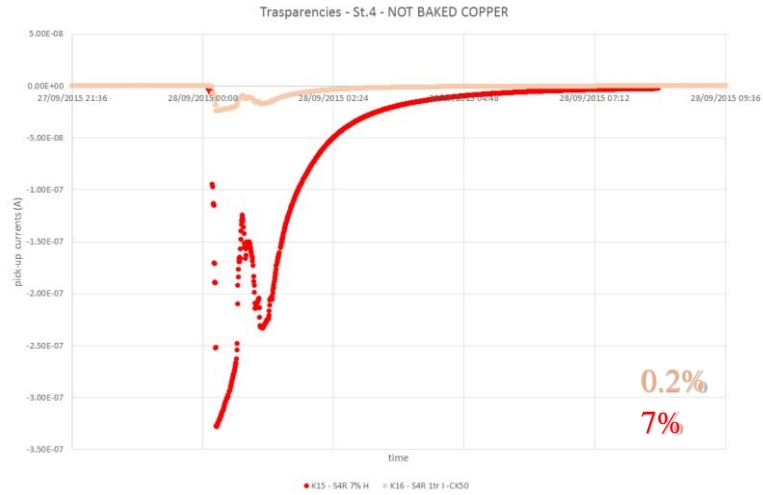


Figure 6-17: Influence of transparencies of grids on Station 2, 3 and 4.

STATION 2	Blue beam			Red beam		
Transparency	5%	7%	10%	5%	7%	10%
Pick Current (A)	-1.72E-09	-3.46E-09	-2.94E-09	-6.54E-09	-6.09E-09	-1.15E-08
I_x/I_10%	59%	118%	100%	57%	53%	100%

STATION 3	Blue beam		Red beam		
Transparency	5%	10%	5%	7%	10%
Pick Current (A)	-4.72E-07	-8.07E-07	-4.67E-07	-7.52E-07	-1.07E-06
I_x/I_10%	58%	100%	44%	70%	100%

STATION 4	Red beam	
Transparency	0.2%	7%
Pick Current (A)	-2.00E-08	-2.71E-07
I_x/I_7%	7%	100%

Figure 6-18: Table of relationships between transparencies and currents read by pickup.

Example 3, on 28.09.15 at 01:06 (see *Figure 6-19, 6-20*):

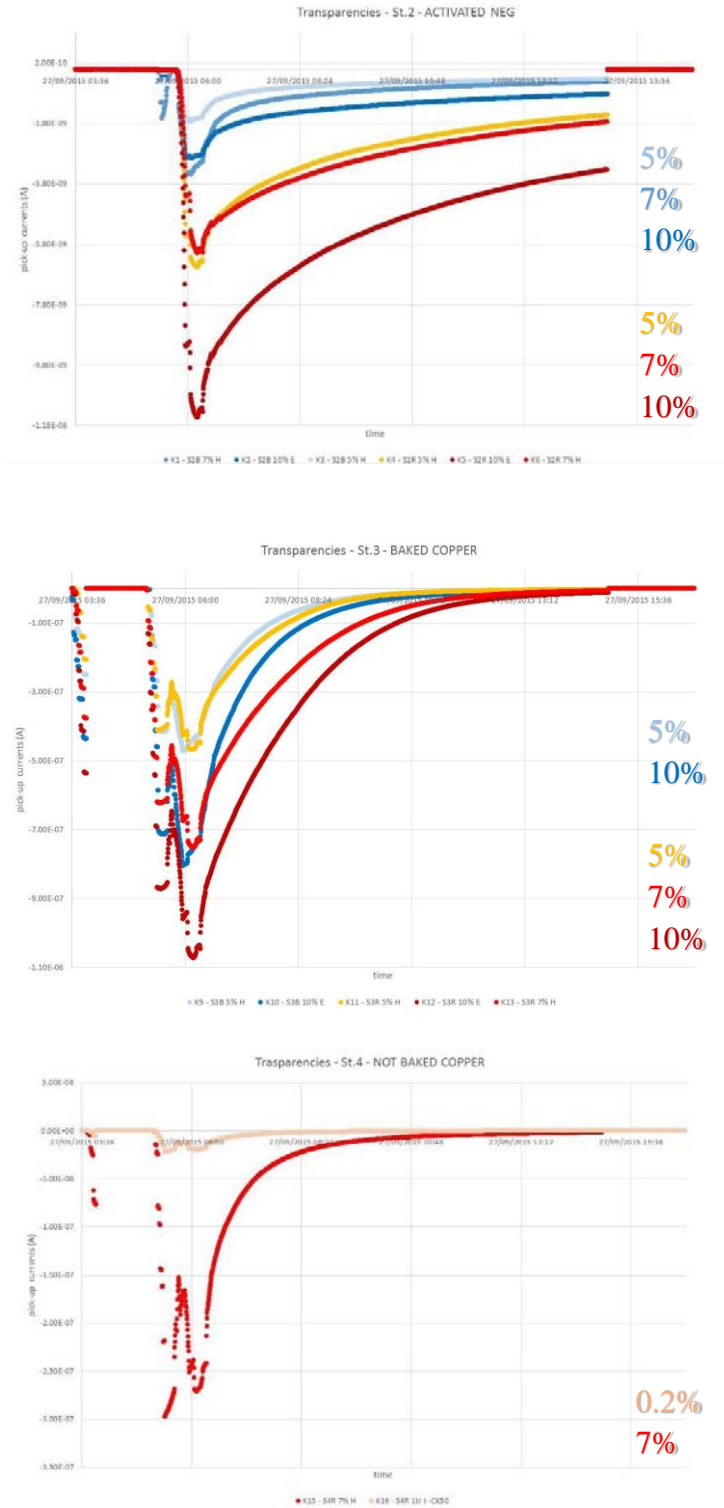


Figure 6-19: Influence of transparencies of grids on Station 2, 3 and 4.

STATION 2	Blue beam			Red beam		
Transparency	5%	7%	10%	5%	7%	10%
Pick Current (A)	-1.68E-09	-3.55E-09	-2.92E-09	-6.01E-09	-5.71E-09	-1.07E-08
I <sub>x</sub> /I <sub>10%</sub>	58%	122%	100%	56%	53%	100%

STATION 3	Blue beam		Red beam		
Transparency	5%	10%	5%	7%	10%
Pick Current (A)	-4.65E-07	-8.06E-07	-4.31E-07	-7.00E-07	-1.00E-06
I <sub>x</sub> /I <sub>10%</sub>	58%	100%	43%	70%	100%

STATION 4	Red beam	
Transparency	0.2%	7%
Pick Current (A)	-1.71E-08	-2.33E-07
I <sub>x</sub> /I <sub>7%</sub>	7%	100%

Figure 6-20: Table of relationships between transparencies and currents read by pickup.

In conclusion it seems that with 10% there is a higher signal so it means that the phenomenon is not reduced too much by a higher loss of electrons coming from the cloud due to a bigger amount of holes.

### 6.3 Check the effective conditioning of surfaces during the scrubbing runs in different coatings with shielded pick up

In order to check the conditioning effect for different surfaces, I compare four pickup having the same transparency (7%), being in the same position (High), concerning the same beam (red one). In yellow is presented the not activated NEG (Station 1), in blue the activated NEG (Station 2), in orange the baked Copper (Station 3) and in grey not baked Copper (Station 4).

The parameters studied are the currents coming from pick up and the beam current. The ratio between beam current and pick up current gives information about the conditioning effect.

It is important to remember that the currents of the pickup are composed by two phenomena: photoelectrons and electrons. Considering a stable beam current, if the beam Energy is above 3000 GeV, the signal due to photoelectrons is evident and is a stable contribute. This means that the increase of photons happens only during the energy ramp

between 450 GeV and 6500 GeV. In this case the ratio between a constant pick up current and a constant beam current is again constant.

If the electron cloud phenomenon is present, the pick up current is not any more stable and the ratio increases. This is a way to see, with time, the evolution of the surface behaviour and the conditioning effect. Here some examples are presented.

Example 1, on 21.09.25 at 20:30 (see *Figure 6-21, 6-22*):

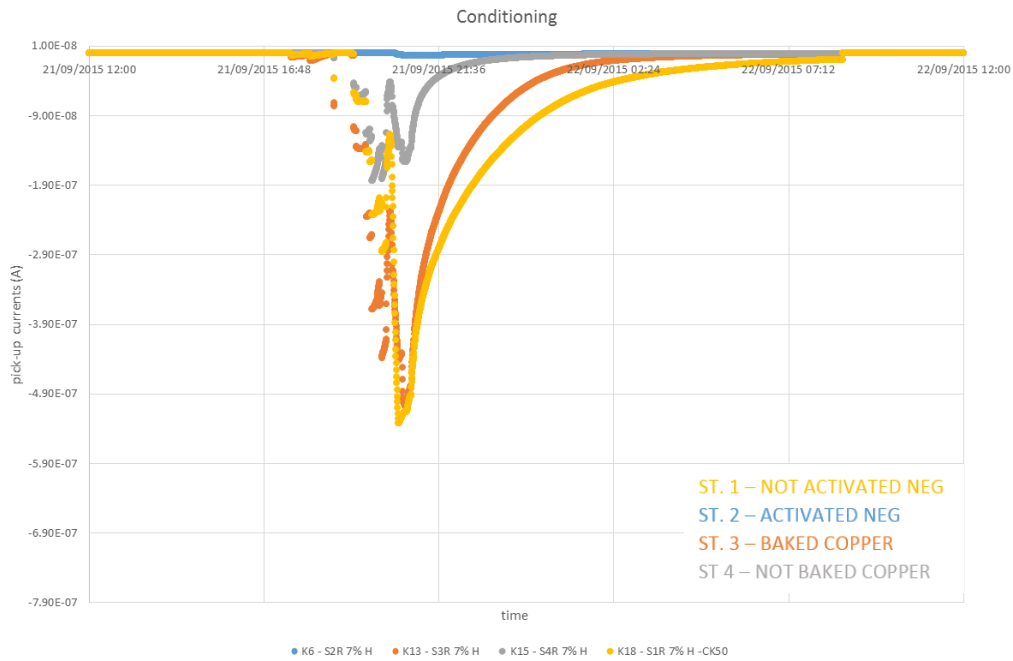


Figure 6-21: Pickup currents.

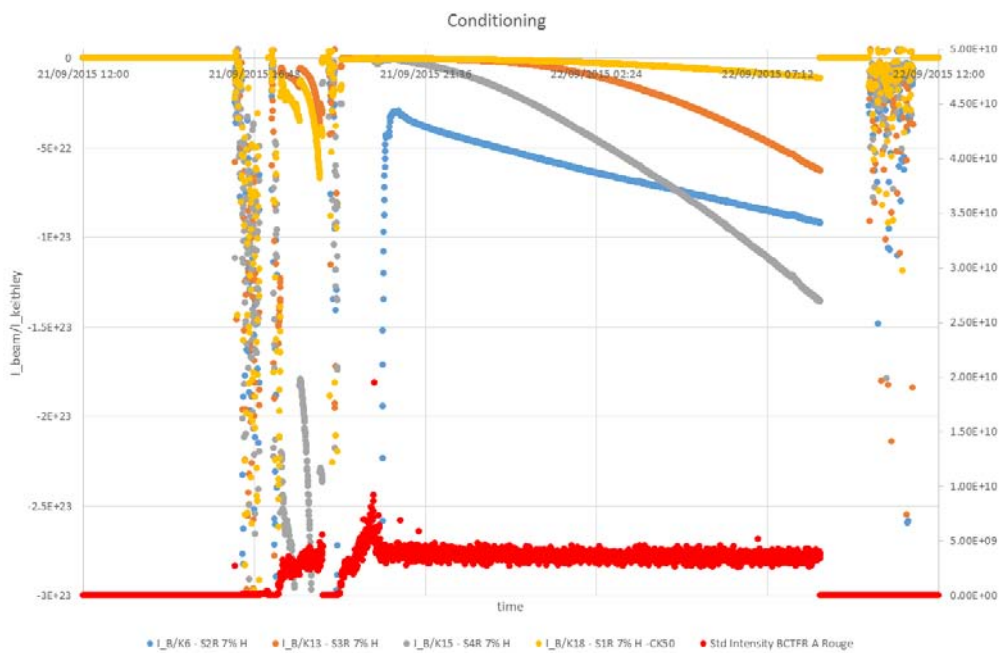
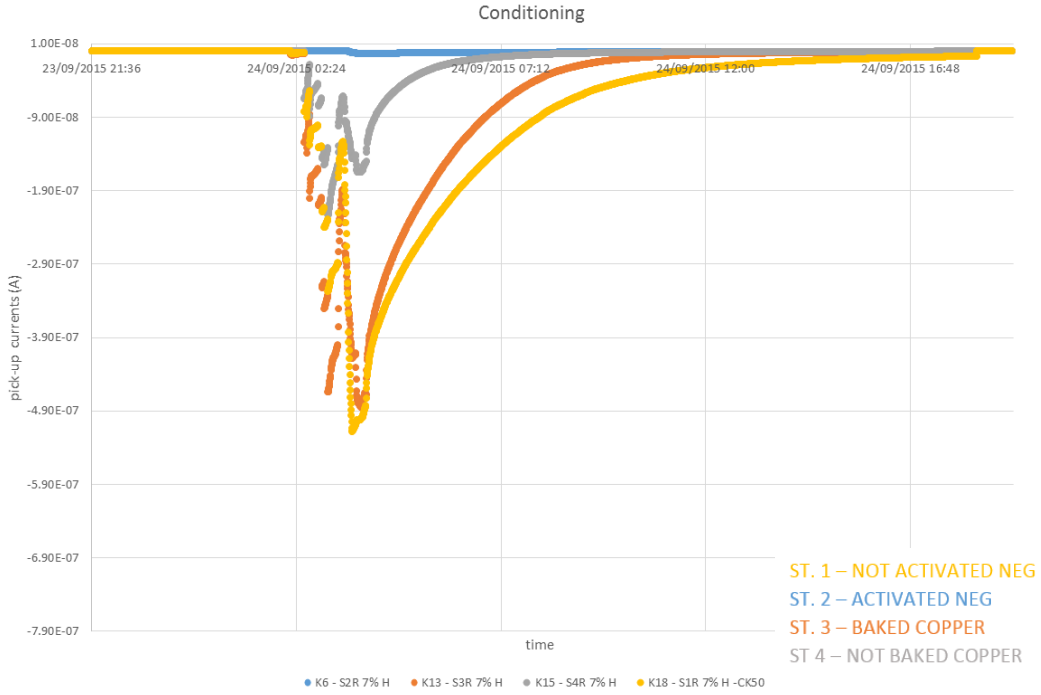
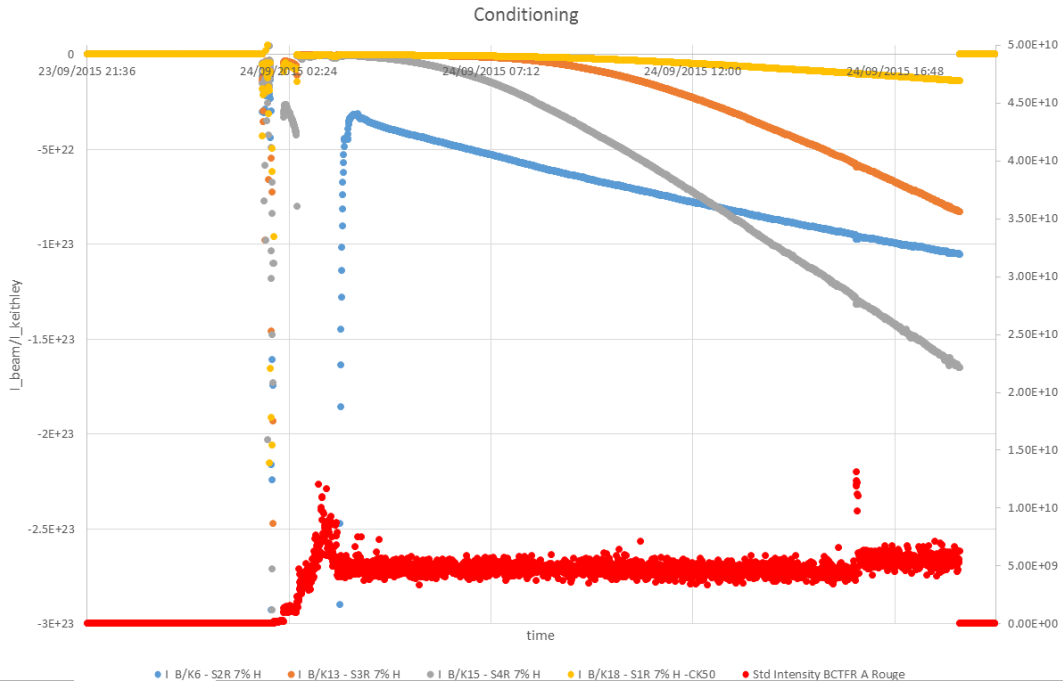


Figure 6-22: Ratio between the beam current and pickup currents.

Example 2, on 24.09.15 at 3:00 (see *Figure 6-23, 6-24*):



*Figure 6-23: Pickup currents.*



*Figure 6-24: Ratio between the beam current and pickup currents.*

Example 3, on 28.09.15 at 1:00 (see *Figure 6-25, 6-26*):

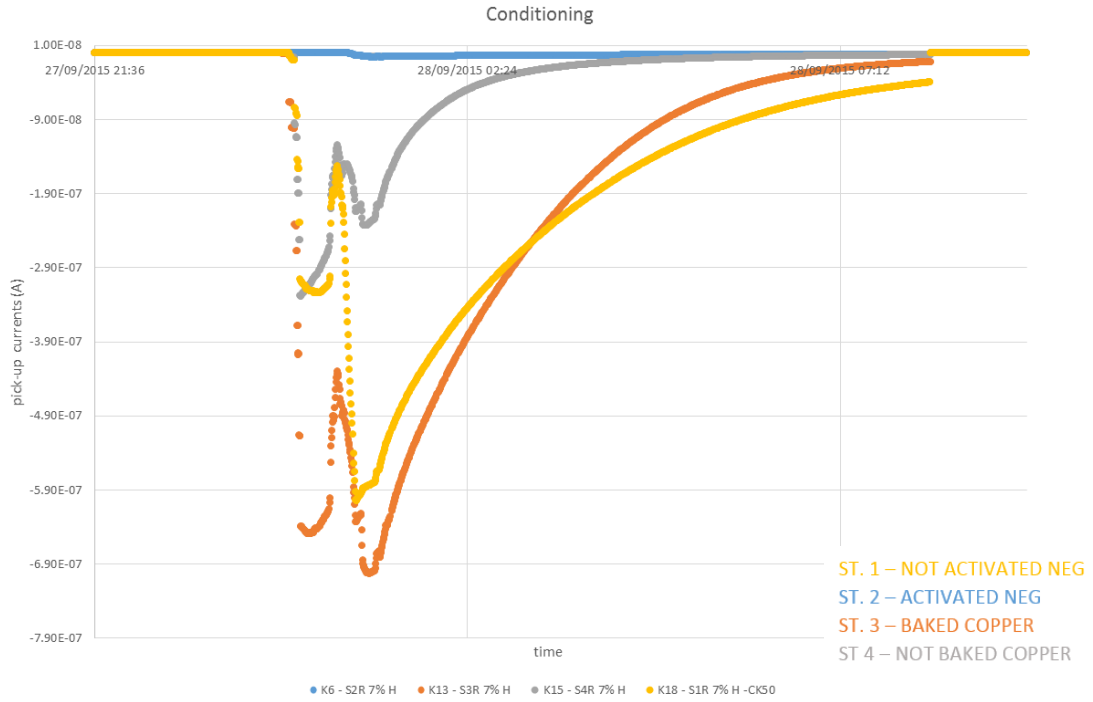


*Figure 6-25: Pickup currents.*

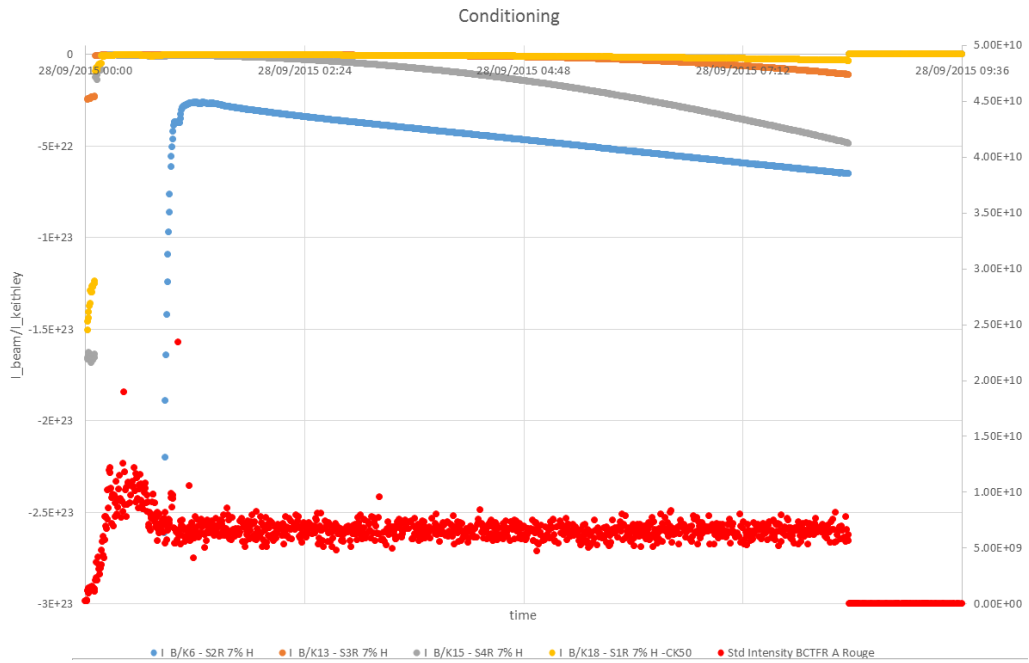


*Figure 6-26: Ratio between the beam current and pickup currents.*

As you can see, speaking about pick up currents, the baked Copper (Station 3) has the higher signal on Keithley, then not activated NEG (Station 1), not baked Copper (Station 4) and, as expected, a lower signal on activated NEG (Station 2). I was expecting that not activated Copper (Station 4) had the higher values of signals. Due to the fact that all the detectors are different and handmade, it is difficult to compare between them, but it is important to be able compare the evolution on the same pickup.

Speaking about the ratio, it is possible to notice that for both Copper stations (3 and 4) the slope is more evident because the phenomenon of electron cloud is stronger.

#### 6.4 Measurement of photons with unshielded pickup

In order to check the photon impact in blue and red beam, here there is a comparison between two unshielded pickup present on VPS. They are located in the station 1 (not activated NEG) in the external position.

An important remark: the SR, as explained before, is created thanks to the bending magnets present in the arc. Due to this, considering the configuration of LHC accelerator, it is possible to notice that VPS is on the right side of the arc 7-8 and on the left side of LHCb experiment in point 8. This means that more light, and so more signal, is expected from the blue beam, coming from the arc.

It is possible to have these signals only with 6500 GeV, not with the energy of 450 GeV used during scrubbing run. The minimum limit in order to have the photons production, in fact, it is around 2000-3000 GeV for LHC machine. In this system is around 2600 GeV (53) (54). Here some examples.

Example 1, on 21.09.15 at 20:30 (see *Figure 6-27*):

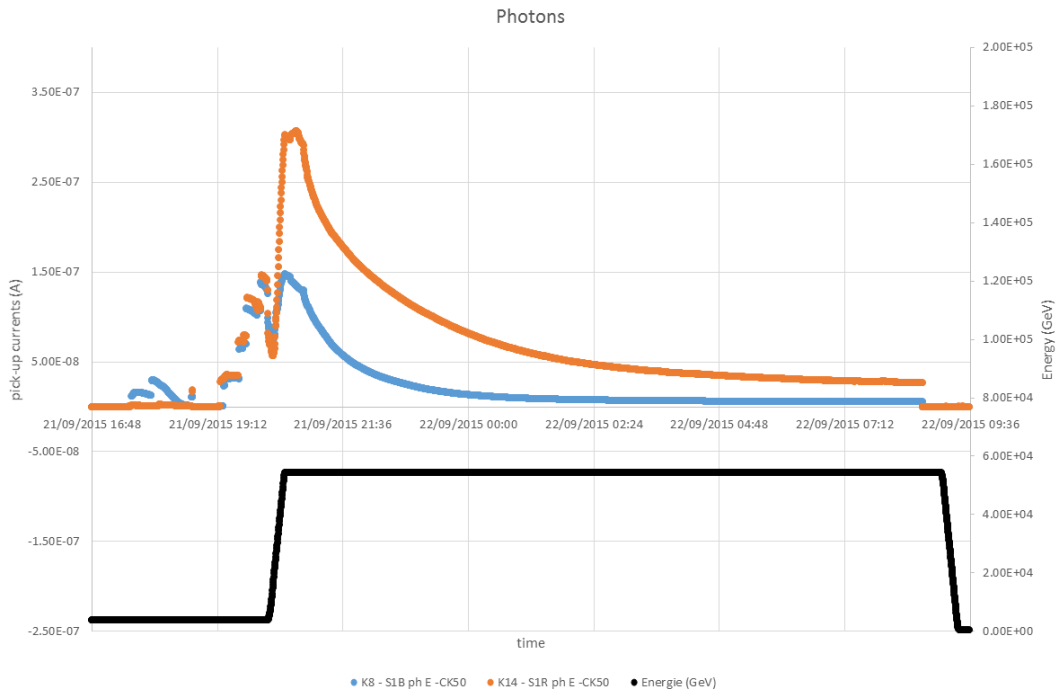


*Figure 6-27: Unshielded pickup currents.*

It is possible to read respectively  $1.5 \cdot 10^{-7} \text{ mA}$  for blue pipe and  $3 \cdot 10^{-7} \text{ mA}$  for the red one ( $\frac{I_{red}}{I_{blue}} = 2$ ).

From PVSS it is possible to read the pressure (light blue for external beam and orange for internal one) and cross check the contribution of pressure due to electron cloud and that due to photons. The energy is in black, while the beam currents are blue and red, like the beams (see *Figure 6-28*).

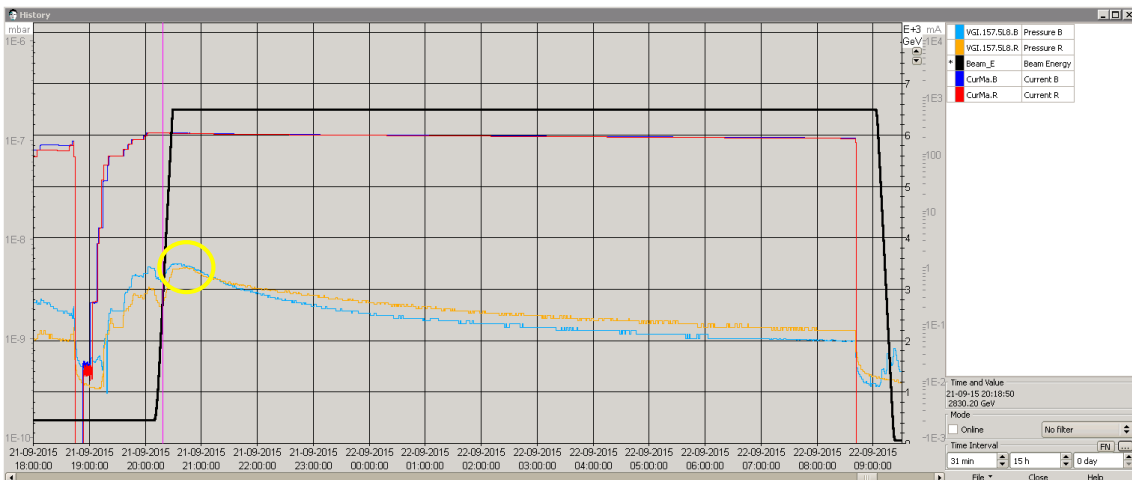


*Figure 6-28: PVSS: trend of pressure.*



It is possible to see that around 2600 GeV there is a bump of pressure due to photons (see *Figure 6-29*).

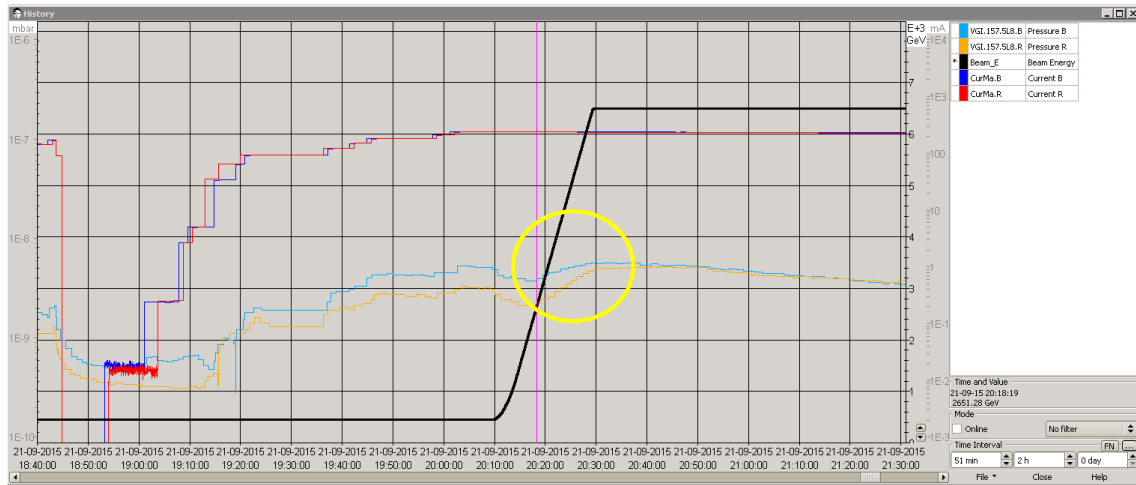


*Figure 6-29: PVSS: Detail of the increase of pressure due to photons.*

The blue pipe goes from  $3.7 \cdot 10^{-9} \text{ mbar}$  to  $5.6 \cdot 10^{-9} \text{ mbar}$  ( $\Delta P_{blue} = 1.9 \cdot 10^{-9} \text{ mbar}$ ), while for the red pipe goes from  $2.1 \cdot 10^{-9} \text{ mbar}$  to  $5 \cdot 10^{-9} \text{ mbar}$  ( $\Delta P_{red} = 2.9 \cdot 10^{-9} \text{ mbar}$ ). The ratio between them is  $\frac{\Delta P_{red}}{\Delta P_{blue}} = 1.5$ .

The electrical measurement is coherent with the pressure trend. In fact in both cases the red one is higher (1.5 ÷ 2 times more).

Example 2, on 24.09.15 at 3:00 (see *Figure 6-30, 6-31, 6-32*).

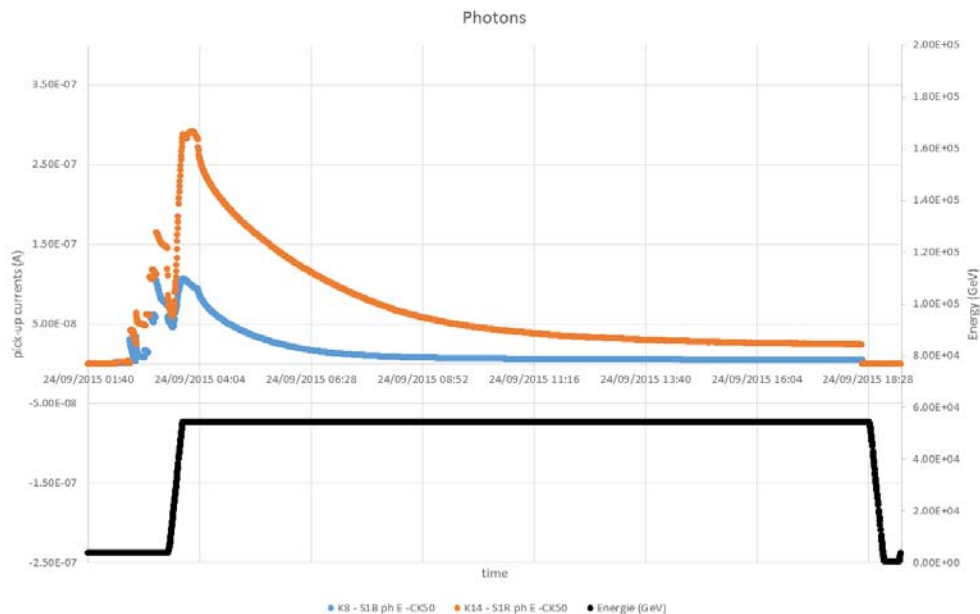


*Figure 6-30: Unshielded pickup currents.*

It is possible to read respectively  $1 \cdot 10^{-7} \text{ mA}$  for blue pipe and  $3 \cdot 10^{-7} \text{ mA}$  for the red one ( $\frac{I_{red}}{I_{blue}} = 3$ ).

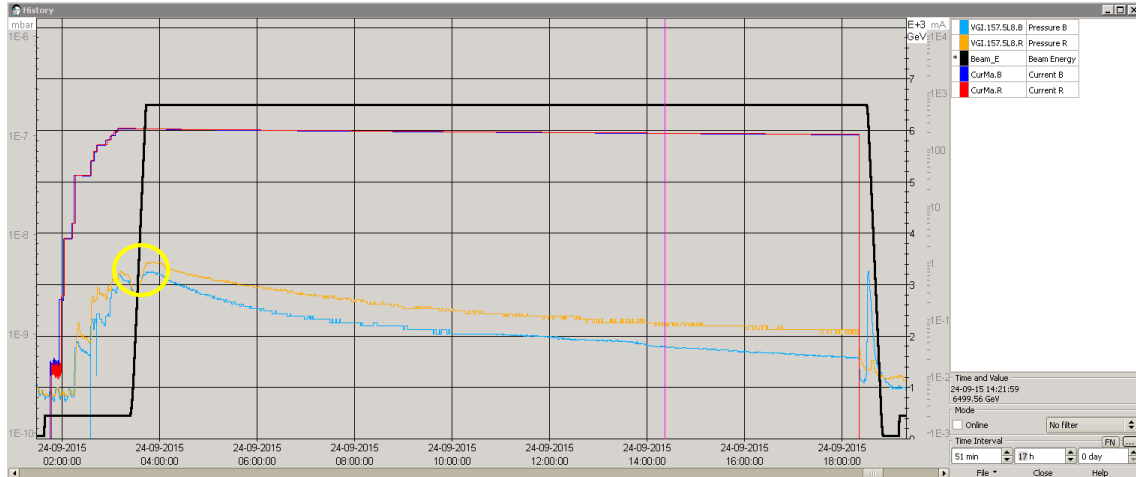


Figure 6-31: PVSS: trend of pressure.

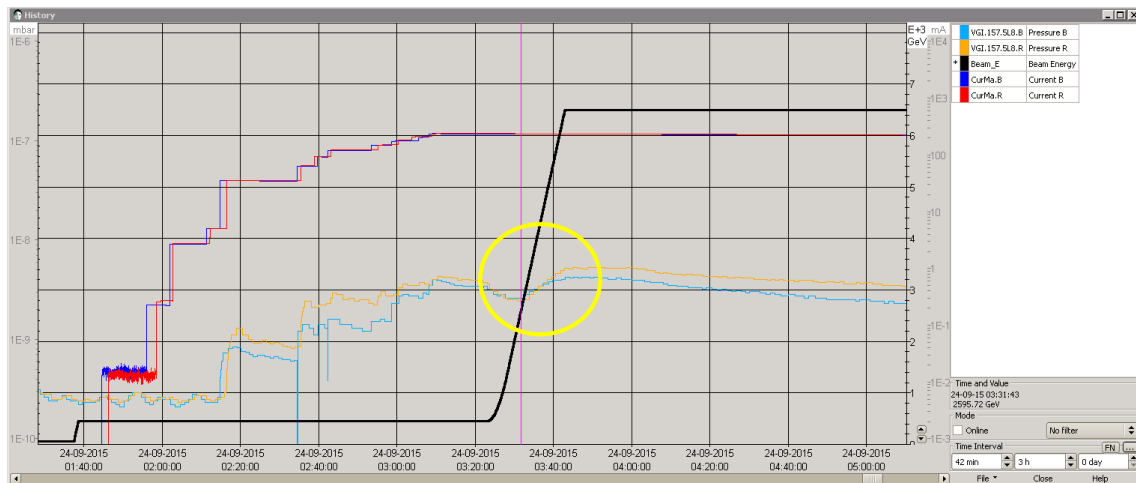
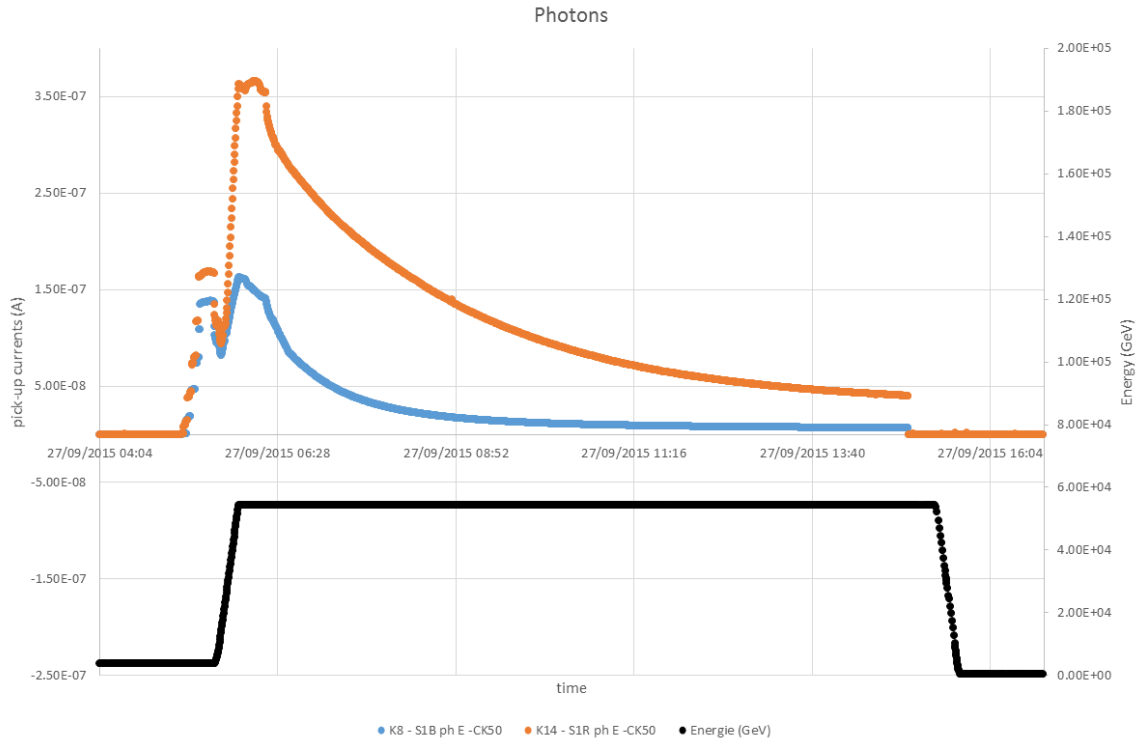


Figure 6-32: PVSS: Detail of the increase of pressure due to photons.

The blue pipe goes from  $2.6 \cdot 10^{-9} \text{ mbar}$  to  $4.2 \cdot 10^{-9} \text{ mbar}$  ( $\Delta P_{blue} = 1.6 \cdot 10^{-9} \text{ mbar}$ ), while for the red pipe goes from  $2.4 \cdot 10^{-9} \text{ mbar}$  to  $5.1 \cdot 10^{-9} \text{ mbar}$  ( $\Delta P_{red} = 2.7 \cdot 10^{-9} \text{ mbar}$ ). The ratio between them is  $\frac{\Delta P_{red}}{\Delta P_{blue}} = 1.69$ .

The electrical measurement is coherent with the pressure trend. In fact in both cases the red one is higher ( $1.7 \div 3$  times more).

Example 3, on 27.09.15 at 6:00 (see *Figure 6-33, 6-34, 6-35*).



*Figure 6-33: Unshielded pickup currents.*

It is possible to read respectively  $1.62 \cdot 10^{-7} \text{ mA}$  for blue pipe and  $3.62 \cdot 10^{-7} \text{ mA}$  for the red one ( $\frac{I_{red}}{I_{blue}} = 2.23$ ).

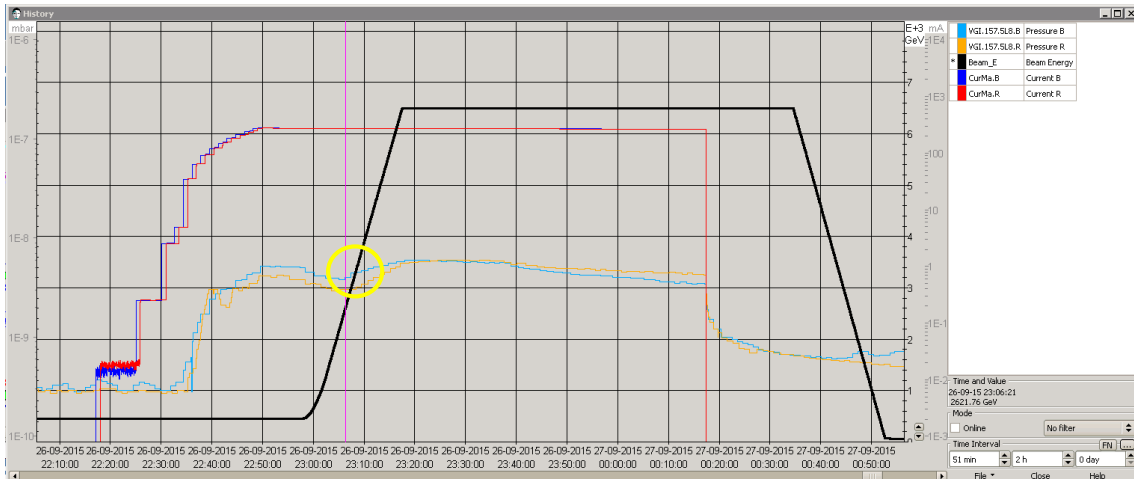


*Figure 6-34: PVSS: trend of pressure.*

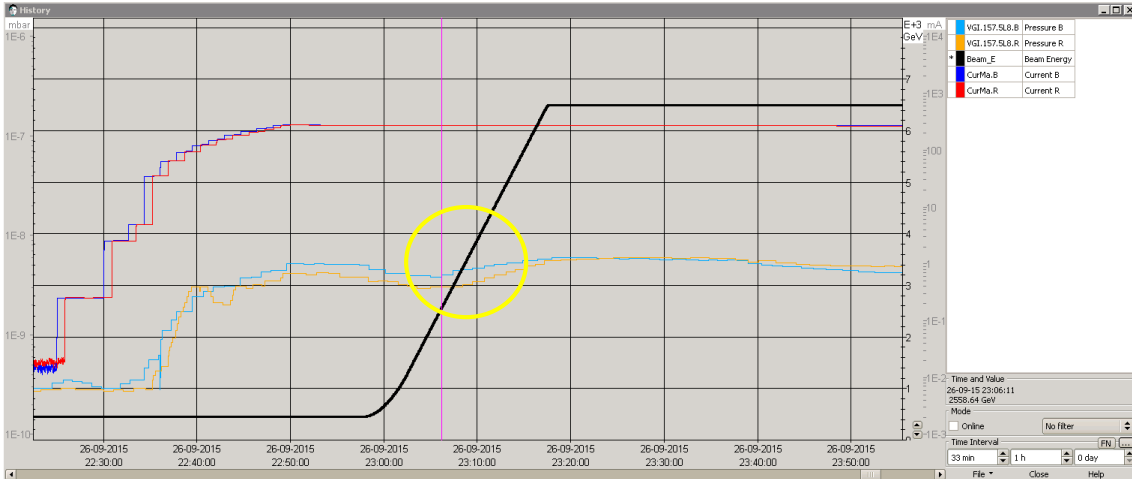


Figure 6-35: PVSS: Detail of the increase of pressure due to photons.

The blue pipe goes from  $3.8 \cdot 10^{-9} \text{ mbar}$  to  $5.7 \cdot 10^{-9} \text{ mbar}$  ( $\Delta P_{\text{blue}} = 1.9 \cdot 10^{-9} \text{ mbar}$ ), while for the red pipe goes from  $3 \cdot 10^{-9} \text{ mbar}$  to  $5.5 \cdot 10^{-9} \text{ mbar}$  ( $\Delta P_{\text{red}} = 2.5 \cdot 10^{-9} \text{ mbar}$ ). The ratio between them is  $\frac{\Delta P_{\text{red}}}{\Delta P_{\text{blue}}} = 1.32$ .

The electrical measurement is coherent with the pressure trend. In fact in both cases the red one is higher (1.3 ÷ 2.3 times more).

As you can see, the values of unshielded pick-up for photons from red beam are double than blue beam. This was not expected and will be study again in the future, thanks to the new planning involving photon pick up in many positions and with different surfaces.

## 6.5 Control the influence of the voltage in the electrical signals through a High Voltage Bias

The pickup present in VPS have usually a battery of 9 V. To understand if it is enough to grab the majority of the signal coming from the cloud, it is useful the use of High Voltage BIAS. 9V was chosen because secondary electrons have a very low energy of some eV, a value that usually is below 10 eV.

This tool is a variable battery that replaces the normal one. The system is attached to a shielded pick up, exactly 7% of transparency on the station 1 (not activated NEG) in the red beam.

Increasing the value of the voltage of the bias of High Voltage Bias is possible to catch also electrons with energy more than 9 eV.

In fact the value of current is increasing with the increase of voltage (it is needed to consider only positive voltage to grab electrons, so there is a negative current).

Here the unique example, changing the voltage from 0 V to 70 V (orange track), (see *Figure 6-36*).

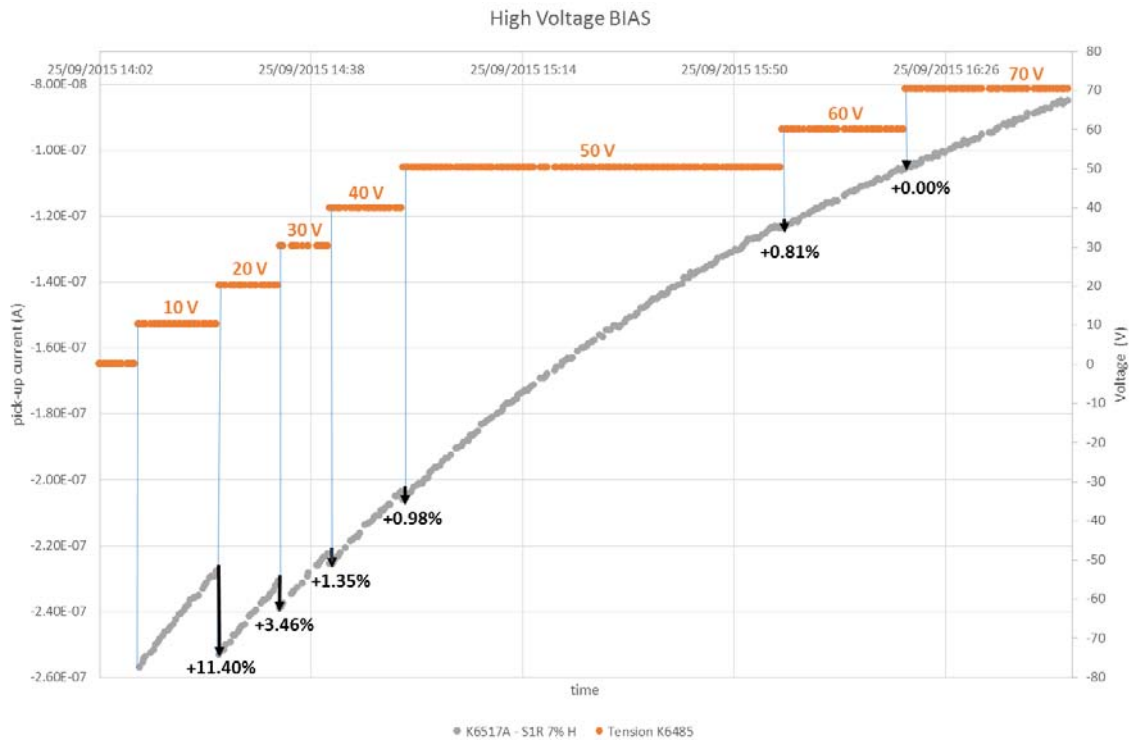


*Figure 6-36: Trend of currents using High Voltage Bias.*

With 0V, the current (grey track) is stable, around  $2.25 \cdot 10^{-8}$  A. When the voltage become positive, there is a negative current that increases with the increase of voltage.

As you can see from the next table, the percentage of electrical signal is increasing with the voltage (see *Figure 6-37*).

From	to	Percentage of added signal
10 V	20 V	11.40%
20 V	30 V	3.46%
30 V	40 V	1.35%
40 V	50 V	0.98%
50 V	60 V	0.81%
60 V	70 V	0.00%
<b>10 V</b>	<b>70 V</b>	<b>18.01%</b>

*Figure 6-37: Table of increase (%) of electrical signals compared to 9V used.*

It is possible to notice that, increasing the voltage from 10V to 70V, 18% of the electrical signal is gain. This is because the majority of the electrons have energy below 10 eV, but those responsible of multipacting have higher one.

I think it is interesting to improve the system using at least 20 or 30V in order to have a signal 15% higher on reading. This can help on the accuracy of the signal.

## 6.6 Scan the energy spectrum of electron cloud (EKD)

In the last years many studies were carried out in order to estimate the energy of the electrons. The next graphs is what theory and some experiments found (see *Figure 6-38*).

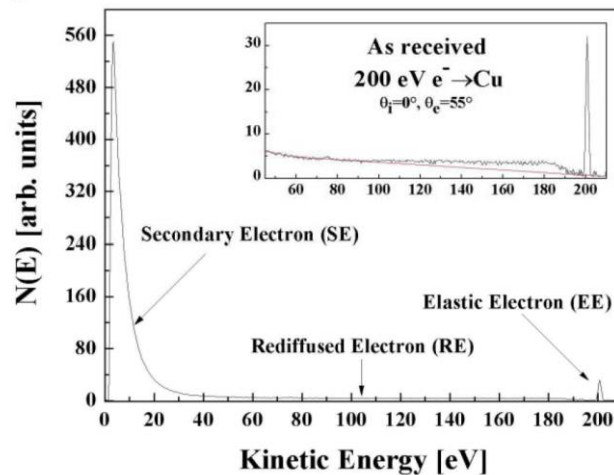


*Figure 6-38: Energy Spectrum of electron cloud.*

There are three main picks: the secondary electrons (with less than 10eV that form the electron cloud), the re-diffused electrons (around one hundred eV due to the acceleration they receive from the beam) and the elastic electrons.

Thanks to VPS, it is possible for the first time to graph this kind of data coming from LHC accelerator.

Using the Electron Kicker Detector (EKDk), it is possible to scan the voltage (V) of the grid in order to read a current (A) proportional to the number of electrons imping with more than the energy applied to the grid of the detector. The current is negative due to the negative charge of electrons. It is necessary to derive this curve to obtain the energy spectrum of electrons. Considering the fill number 4528 on 23.10.2015 at 10:00, the

current read by this instrument, changing the voltage from 0 to 1250 V and viceversa, is here represented, for both beams (see *Figure 6-39, 6-40*).

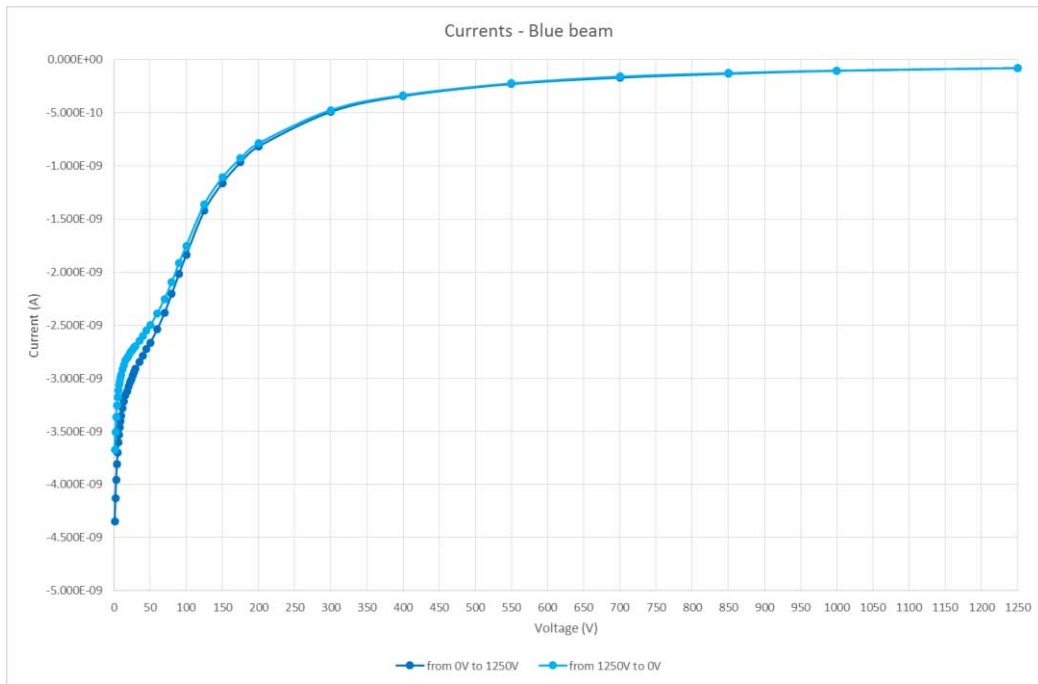


*Figure 6-39: Currents read by EKD in Blue pipe.*

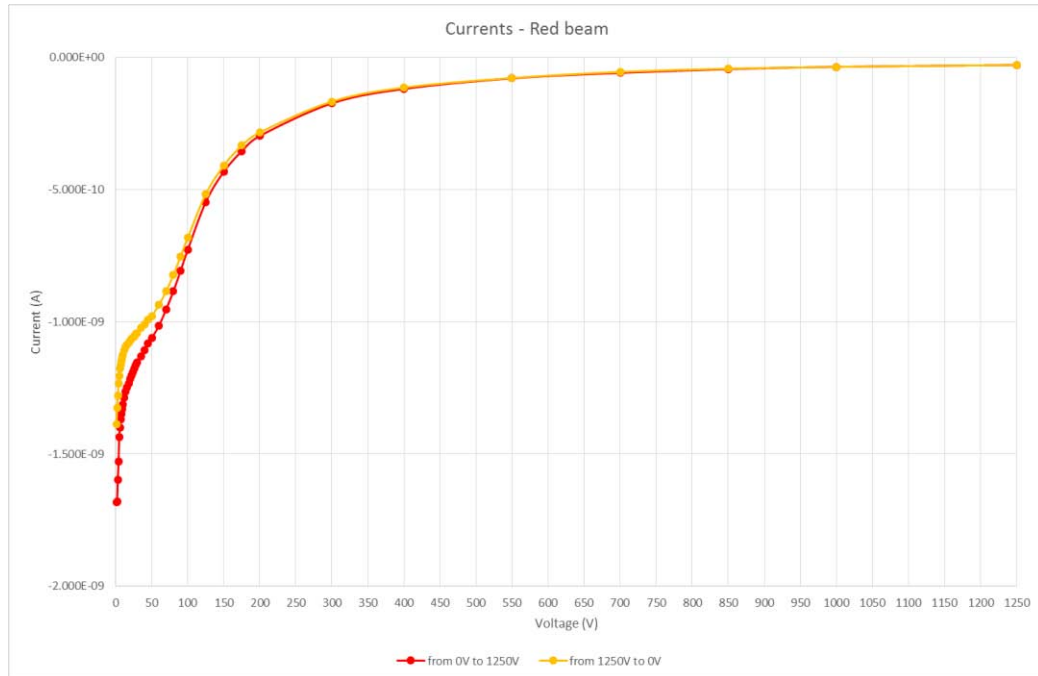


*Figure 6-40: Currents read by EKD in Red pipe.*

From these currents, it is possible through derivation, to see the energy distribution of the electrons (eV) (see *Figure 6-41*).

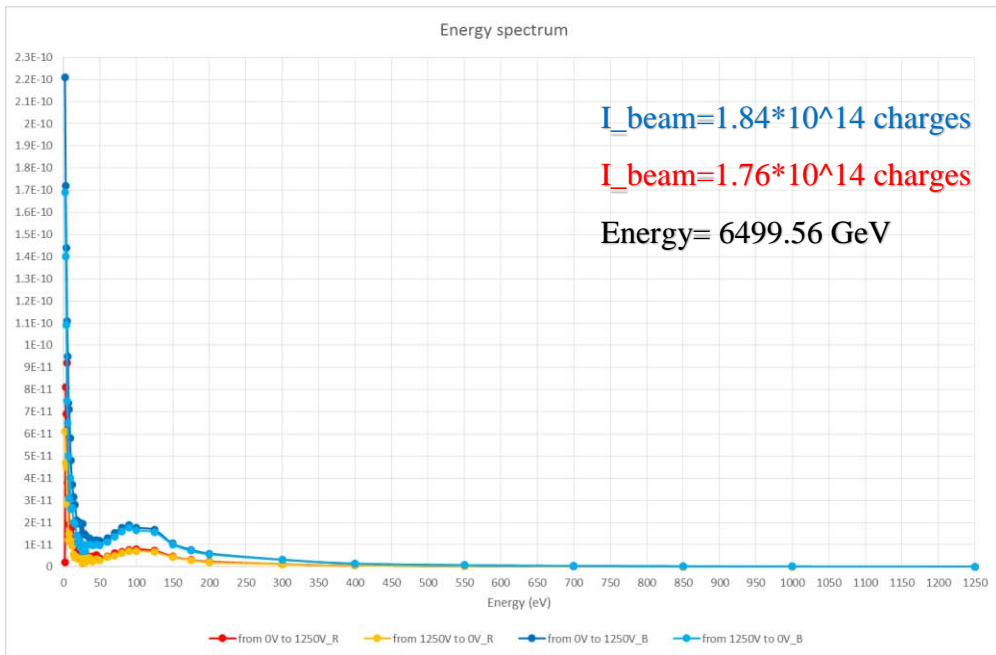


*Figure 6-41: Energy spectrum of electrons measured in VPS.*

It is possible to zoom to notice that there are two picks (see *Figure 6-42*): one at a very low energy (secondary electrons) and the second one around 100 eV. The last one are the electrons that receive the kick from the presence of the beam and create multipacting effect.

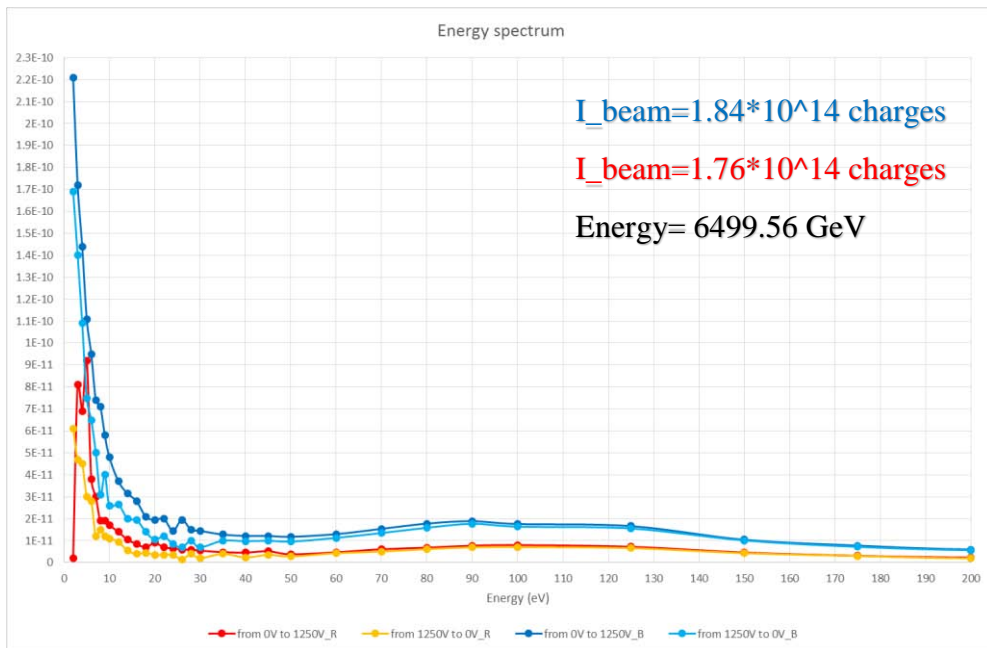


*Figure 6-42: Zoom of energy spectrum of electrons measured in VPS.*



## 6.7 Analyse the power deposition on the walls (Calorimeters)

One of the sensor present on the calorimeters is for calibration. Starting from this, without beam, I calibrated each of the two calorimeters in order to know the effective power deposition on them during a LHC run on a long straight section, LSS. This calibration sensor sends a tension (V) that is converted in heat transmitted from the squared plate to the support of the calorimeter.

The main heat equation to consider is the following:

$$\dot{Q} - R \cdot \Delta T - C \cdot \Delta \dot{T} = 0$$

Where  $\dot{Q}$  is the heat load on the liner,  $\Delta T$  is the difference of temperature between calorimeter plate and liner,  $R$  is the thermal resistance between calorimeter plate and liner,  $C$  is the thermal capacitance of the plate.

The differential equation that solves it is:

$$\Delta T(t) = \dot{Q} \cdot R \cdot \left(1 - e^{-\frac{t}{RC}}\right)$$

Considering no initially difference on temperature and at equilibrium  $\Delta \dot{T} = 0$ , with the time constant expressed by:

$$\tau = R \cdot C$$

And the slope by:

$$\frac{d\Delta T(t)}{dt} = \frac{\dot{Q}}{C} \cdot e^{-t/\tau}$$

Here a simple scheme of the thermal equation (see *Figure 6-43*). (36)

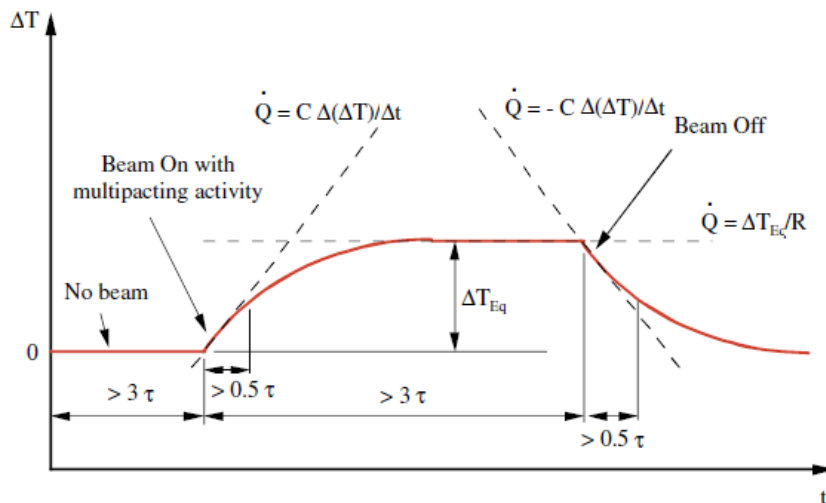


Figure 6-43: Parameters of the thermal equation of a Calorimeter.

In order to calculate the thermal resistance  $R$ , it is important to calculate the two resistances in parallel due to radiation and contact:  $R_{RAD}$  and  $R_{COND}$ .

$$R = \frac{R_{RAD} \cdot R_{COND}}{R_{RAD} + R_{COND}}$$

For small  $\Delta T$ , the radiative heat flow is:

$$Q_{RAD} = \sigma \epsilon S F (T^4 - T_{liner}^4) \approx \sigma \epsilon S F 4 T^3 \Delta T$$

Where the Stefan-Boltzmann constant is  $\sigma = 5.67 \cdot 10^{-8} \frac{W}{m^2 \cdot K^4}$ , the emissivity is  $\epsilon = 0.05$ , the view factor  $F$  is taken of 1, the surface  $S$  of the plate of  $930.25 mm^2$  (squared of 30.5mm per side).

So the radiative resistance is:

$$R_{RAD} = \frac{\Delta T}{Q_{RAD}} \approx \frac{1}{\sigma \epsilon S F 4 T^3}$$

The conductive thermal resistance  $R_{COND}$  is related to the electrical resistance, following this rule:

$$R_{COND} \approx \frac{R_{el}}{\lambda \cdot \rho}$$

Where the thermal conductivity is  $\lambda \approx 15 \frac{W}{m \cdot K}$  and the electrical resistivity is  $\rho \approx 7 \cdot 10^{-7} \Omega \cdot m$ .

The thermal capacitance  $C$  is made of liner mass  $M$  multiplied by specific heat of copper  $c$ :

$$C = M \cdot c$$

Considering the calibration, the following is an example of trend of data coming from the system and the equation (see *Figure 6-44*).

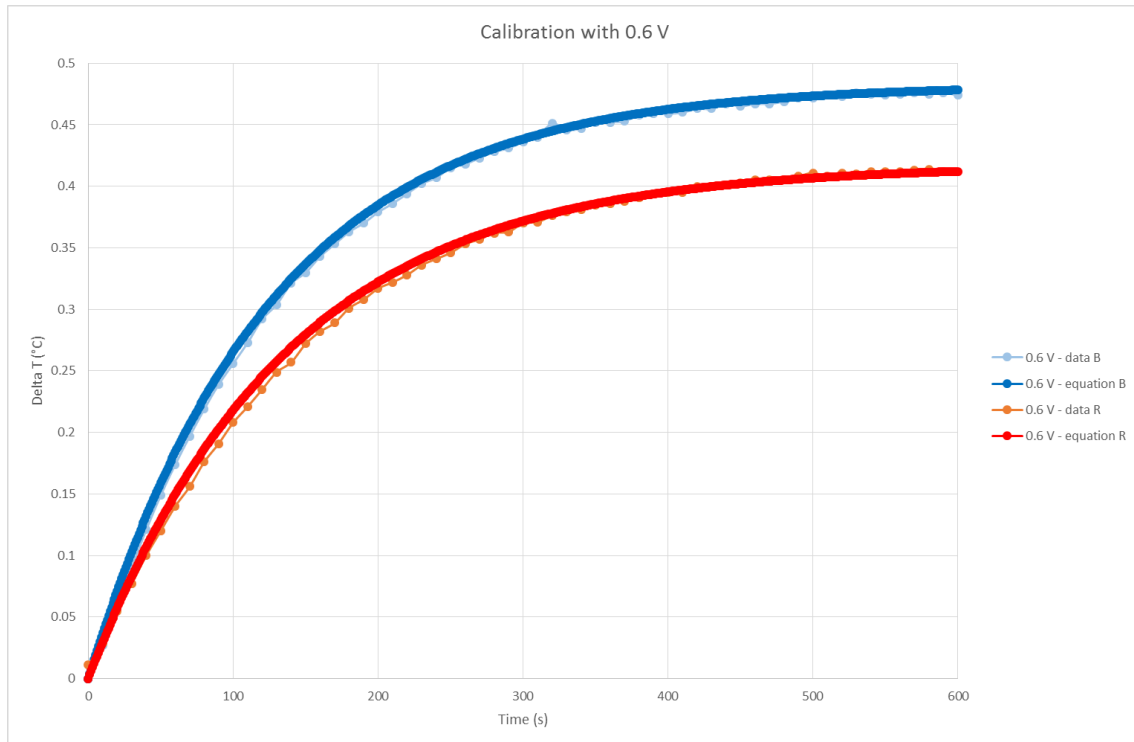


Figure 6-44: Calibration of calorimeters.

It is possible to notice that the values agree. The value of 0.6 V is chosen because with a voltage of around 0.63 V sent in the pt100 for calibration, the power deposition calculated is around 1 W/m. This has to be verified with the future analysis.

In fact, knowing the voltage on the plate, the  $\Delta T$ , the parameters of pt100 and the geometry of the system, it is possible to calculate the power deposition on the chamber. The resistance R (Ohm) changes with the temperature, following this rule:

$$R = 0.389 \cdot T + 100 \text{ (}\Omega\text{)}$$

Where 100 is the resistance at 20°C and T is the temperature reached by pt100.

The power (W) is measured considering that:

$$P = \frac{V^2}{R} \text{ (w)}$$

Then it is possible to calculate the thermal resistance (K/W):

$$R_{th} = \frac{\Delta T}{P} \left( \frac{K}{W} \right)$$

The last passage is done in order to convert the power in power per meter of chamber, value that is common as reference for LHC measurements (see Figure 6-45).

Due to geometry, the power has to be multiplied by a factor of 277 in order to find W/m.

These calculations are shown in the following table.

CALIBRATION of CALORIMETERS									
BEAM	Voltage (V)	T1 (°C)	Tsat (°C)	R (Ohm)	Power (W)	ΔT (°C)	Rth (K/W)	P_1m_chamber(W/m)	
0.1 V	blue	0.104	19.428	19.443	107.563	0.000101	0.015	149.173	0.028
	red	0.104	19.558	19.571	107.613	0.000101	0.013	129.343	0.028
0.2 V	blue	0.198	19.416	19.47	107.574	0.000364	0.054	148.173	0.101
	red	0.197	19.546	19.593	107.622	0.000361	0.047	130.336	0.100
0.3 V	blue	0.295	19.407	19.529	107.597	0.000809	0.122	150.839	0.224
	red	0.293	19.536	19.645	107.642	0.000798	0.109	136.670	0.221
0.4 V	blue	0.388	19.4	19.616	107.631	0.001399	0.216	154.428	0.387
	red	0.386	19.529	19.719	107.671	0.001384	0.190	137.302	0.383
0.5 V	blue	0.486	19.484	19.829	107.713	0.002193	0.345	157.332	0.607
	red	0.483	19.6	19.9	107.741	0.002165	0.300	138.551	0.600
0.6 V	blue	0.579	19.487	19.974	107.770	0.003111	0.487	156.556	0.862
	red	0.577	19.603	20.03	107.792	0.003089	0.427	138.249	0.856
0.7 V	blue	0.678	19.491	20.156	107.841	0.004263	0.665	156.007	1.181
	red	0.675	19.61	20.19	107.854	0.004224	0.580	137.296	1.170
0.8 V	blue	0.771	19.492	20.345	107.914	0.005508	0.853	154.853	1.526
	red	0.767	19.61	20.36	107.920	0.005451	0.750	137.585	1.510
0.9 V	blue	0.87	19.484	20.573	108.003	0.007008	1.089	155.391	1.941
	red	0.865	19.602	20.554	107.996	0.006928	0.952	137.407	1.919
1.0 V	blue	0.965	19.982	21.264	108.272	0.008601	1.282	149.056	2.382
	red	0.96	20.008	21.212	108.251	0.008514	1.204	141.422	2.358
1.1 V	blue	1.06	19.892	21.518	108.371	0.010368	1.626	156.827	2.872
	red	1.06	20.01	21.48	108.356	0.010370	1.470	141.761	2.872
1.2 V	blue	1.16	19.86	21.781	108.473	0.012405	1.921	154.858	3.436
	red	1.15	19.972	21.659	108.425	0.012197	1.687	138.309	3.379
1.3 V	blue	1.26	19.903	22.161	108.621	0.014616	2.258	154.488	4.049
	red	1.25	20.02	21.99	108.554	0.014394	1.970	136.865	3.987
1.4 V	blue	1.35	19.934	22.511	108.757	0.016758	2.577	153.781	4.642
	red	1.34	20.047	22.295	108.673	0.016523	2.248	136.053	4.577
1.5 V	blue	1.45	19.925	22.881	108.901	0.019307	2.956	153.108	5.348
	red	1.44	20.038	22.616	108.798	0.019059	2.578	135.262	5.279
1.6 V	blue	1.54	19.931	23.286	109.058	0.021746	3.355	154.280	6.024
	red	1.54	20.046	22.964	108.933	0.021771	2.918	134.030	6.031
1.7 V	blue	1.64	20.033	23.801	109.259	0.024617	3.768	153.066	6.819
	red	1.63	20.16	23.438	109.117	0.024349	3.278	134.626	6.745
1.8 V	blue	1.73	20.042	24.237	109.428193	0.027350356	4.195	153.3800894	7.576
	red	1.73	20.169	23.823	109.267147	0.027390667	3.654	133.4031057	7.587
1.9 V	blue	1.83	20.046	24.724	109.617636	0.030550741	4.678	153.1223092	8.463
	red	1.83	20.176	24.244	109.430916	0.030602869	4.068	132.9287128	8.477

Figure 6-45: Results of the calibration of the calorimeters.

This means that with 0.6 V the temperature increase of around 0.4 – 0.5 °C that corresponds to a power deposition of 1 W/m.

The main parameters founded through calibration are presented here (see *Figure 6-46*).

Beam	Pipe	Tau	Rth (K/W)	Cth (J/K)
Blue	External	125	153.62	0.81
Red	Internal	142	136.18	1.04

*Figure 6-46: Table of main parameters founded by calibration.*

Where Tau is in seconds and after 5 tau usually the exponential equation arrives to a steady-state. So it takes around  $125s \cdot 5 = 625s = 10'$  ( $\approx 600s$ ) for the blue calorimeter and  $125s \cdot 5 = 710s = 11'$  for the red one in order to reach the equilibrium. This is comparable with the calibration.

It is important to compare these data coming from calibration, to what theory says.

Considering the calorimeter **thermal capacitance**, it is done by the mass multiplied by the specific heat of copper:

$$C_{th\_calorimeter} = m \cdot c = 1.62g \cdot 10^{-3} \cdot 400 \frac{J}{kg \cdot K} = 0.648 \frac{J}{K}$$

Considering also the contribution of six stein steel ribbon:

$$m = 6 \cdot \delta \cdot V = 6 \cdot 7.85 \frac{g}{cm^3} \cdot (0.05 \cdot 5 \cdot 10 mm^3) = 0.1177g$$

$$C_{th\_stein\ steel} = m \cdot c = 0.1177g \cdot 10^{-3} \cdot 466 \frac{J}{kg \cdot K} = 0.055 \frac{J}{K}$$

So the total capacitance is:

$$C_{th} = C_{th\_calorimeter} + C_{th\_stein\ steel} = 0.648 + 0.055 = 0.702 \frac{J}{K}$$

This is compatible with that found through data, with an error of around 30%.

Only to have an idea, the capacitance of the liner is:

$$C_{th\_liner} = M \cdot c = 2.96kg \cdot 385 \frac{J}{kg \cdot K} = 1184 \frac{J}{K}$$

So, it is possible to say that there is a good contact between the sensor pt100 and the plate.

In this way the heat is dissipated through radiation and conduction along the liner.

Considering the **thermal resistance** it is possible to see that:

$$R_{COND} \approx \frac{R_{el}}{\lambda \cdot \rho} = \left( \frac{\rho \cdot L}{S} \cdot \frac{1}{6} \right) \frac{1}{\lambda \cdot \rho} = \left( \frac{7 \cdot 10^{-7} \Omega m \cdot 0.01 m}{0.00002 m \cdot 0.005 m} \cdot \frac{1}{6} \right) \frac{1}{15 \frac{W}{m \cdot K} \cdot 7 \cdot 10^{-7} \Omega m}$$

$$= 0.0117 \Omega \cdot \frac{1}{15 \frac{W}{m \cdot K} \cdot 7 \cdot 10^{-7} \Omega m} = 1111.11 \frac{K}{W}$$

$$R_{RAD} = \frac{\Delta T}{\dot{Q}_{RAD}} \approx \frac{1}{\sigma \epsilon S F 4 T^3} = \frac{1}{5.67 \cdot 10^{-8} \frac{W}{m^2 \cdot K^4} \cdot 0.05 \cdot 930.25 mm^2 \cdot 1 \cdot 4 \cdot 293^3}$$

$$= 3768.64 \frac{K}{W}$$

$$R = \frac{R_{RAD} \cdot R_{COND}}{R_{RAD} + R_{COND}} = \frac{1111.11 \cdot 3768.64}{1111.11 + 3768.64} = 858.11 \frac{K}{W}$$

Considering the data, the resistance is around  $135 \div 155 \frac{K}{W}$ .

If I consider that NEG buffers are around the copper liner, the emissivity coming from the buffers is dominating and increases up to 1 because it is comparable to a black body, so the radiative resistance is:

$$R_{RAD} = \frac{\Delta T}{\dot{Q}_{RAD}} \approx \frac{1}{\sigma \epsilon S F 4 T^3} = \frac{1}{5.67 \cdot 10^{-8} \frac{W}{m^2 \cdot K^4} \cdot 1 \cdot 930.25 mm^2 \cdot 1 \cdot 4 \cdot 293^3}$$

$$= 188.43 \frac{K}{W}$$

In this case:

$$R = \frac{R_{RAD} \cdot R_{COND}}{R_{RAD} + R_{COND}} = \frac{1111.11 \cdot 188.43}{1111.11 + 188.43} = 161.11 \frac{K}{W}$$

All seems to be coherent with the data found.

Considering the **power losses** (W/m), here the relation between voltage and power deposition on the chambers (see *Figure 6-47*).

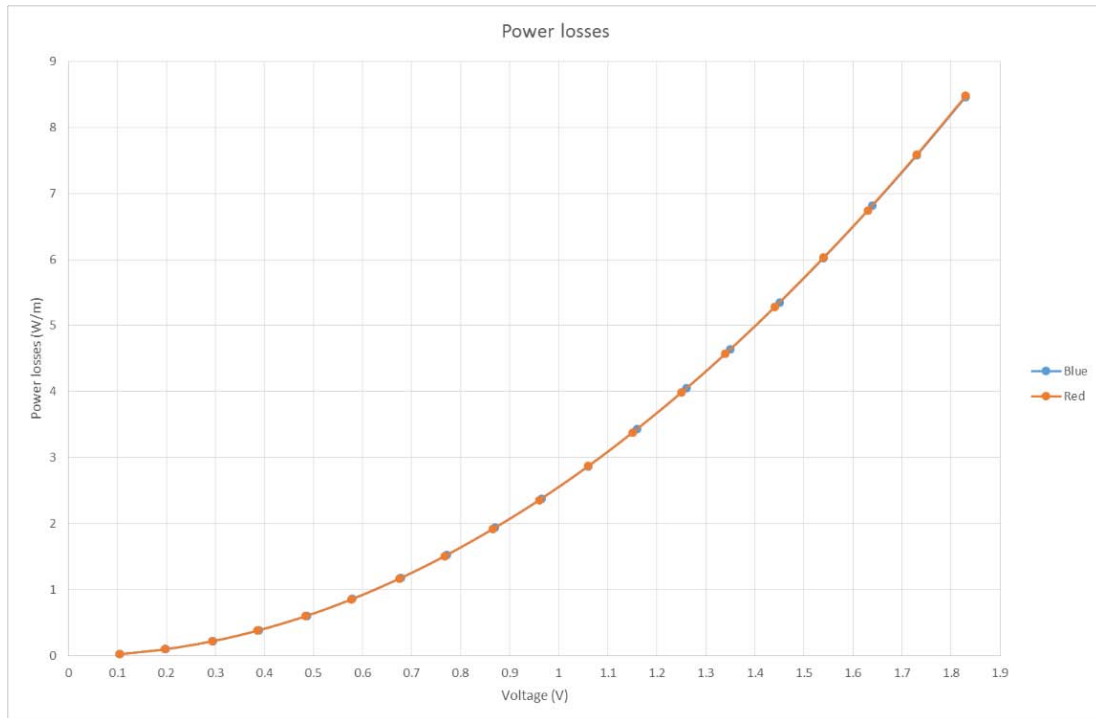


Figure 6-47: Power deposition (W/m) related to the voltage applied to the calorimeter.

More analysis have to be done in order to analyse the LHC data in order to compare them with this calibration.

### 6.8 Analyse the gas spectrum (VQM)

Another important analysis done for the first time in LHC machine is the spectrum of gasses released from the wall of the beam pipes. This is done thanks a special device called VQM, already presented along the tools, that doesn't suffer of electrical problems and interaction with beam, that affect the common gas analysers. Being quite a new tool, the data can give an idea of the partial pressure and the ratio between the gasses, while the value of the current is less meaningful.

Considering an event with beam and without, it is possible to see that the spectrum changes. This is because the beam has an impact on the environment it passes through.

Considering the material science, it is important to focus the following table that associates at each interesting mass one or more molecules (see *Figure 6-48*).

Mass	Gas	Mass	Gas
1	H	17	OH
2	H <sub>2</sub>	18	H <sub>2</sub> O
12	C	28	CO, N <sub>2</sub>
14	N	32	O <sub>2</sub>
15	O <sup>-</sup>	40	Ar
16	O, CH <sub>4</sub>	44	CO <sub>2</sub>

Figure 6-48: Table that associates a gas/ gasses to a mass value.

It is important to consider that in this system there are four VQM analysers that are located in Activated NEG (Station 2) and Copper not baked (Station 4), for both beam.

Considering an example on 25/09/2015, in which are presented many scans for the same gage, shifted in mass to make seen the intensity of the main picks (2 and 28). To have a reference, each scan is shifted of a unit in mass on the right respecting the previous measurement, so the blue line is shifted of 1, the orange of 2, the grey of 3 on the right. The first scan is taken before the beam, while the other three are taken in sequence with the beam. The current of the beam is quite stable, around  $1.4 \cdot 10^{14}$  charges. This is repeated in four graphs for each gage (see *Figure 6-49, 6-50, 6-51, 6-52*).

It is possible to verify that, with the time, the values of the picks decreases because of beam conditioning. The main pick for NEG is Hydrogen, while for Copper is Carbon Oxide. It is also possible to notice that in NEG the amount of gas is concentrated only on Hydrogen (2) and Carbon Oxide (28), while for Copper there is also a release of Carbon (12), Oxygen (16), Water (18) and Carbon Dioxide (44).



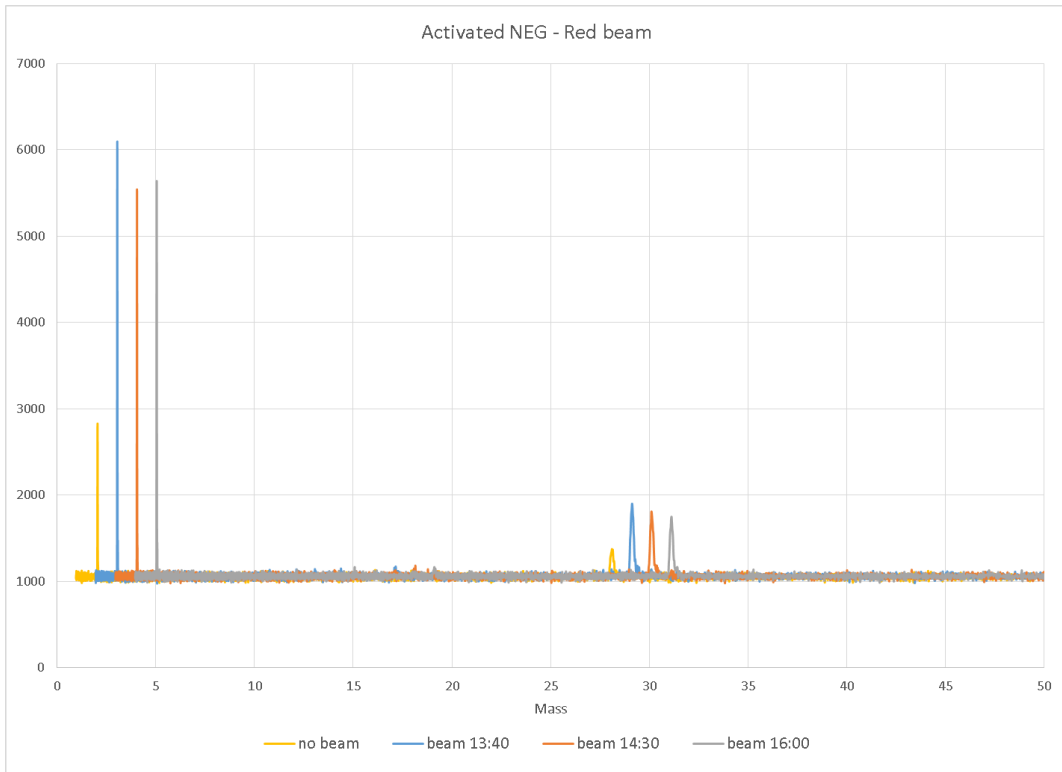


Figure 6-49: Activated NEG spectrum on Red beam.

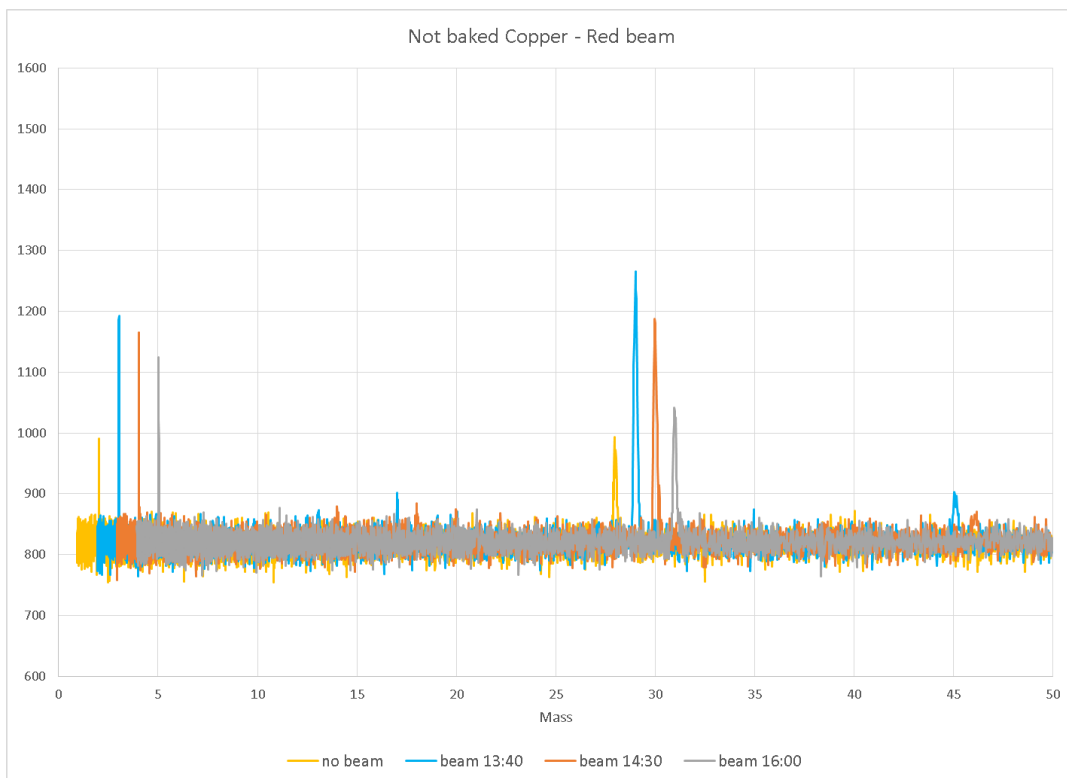


Figure 6-50: Not baked Copper spectrum on Red beam.

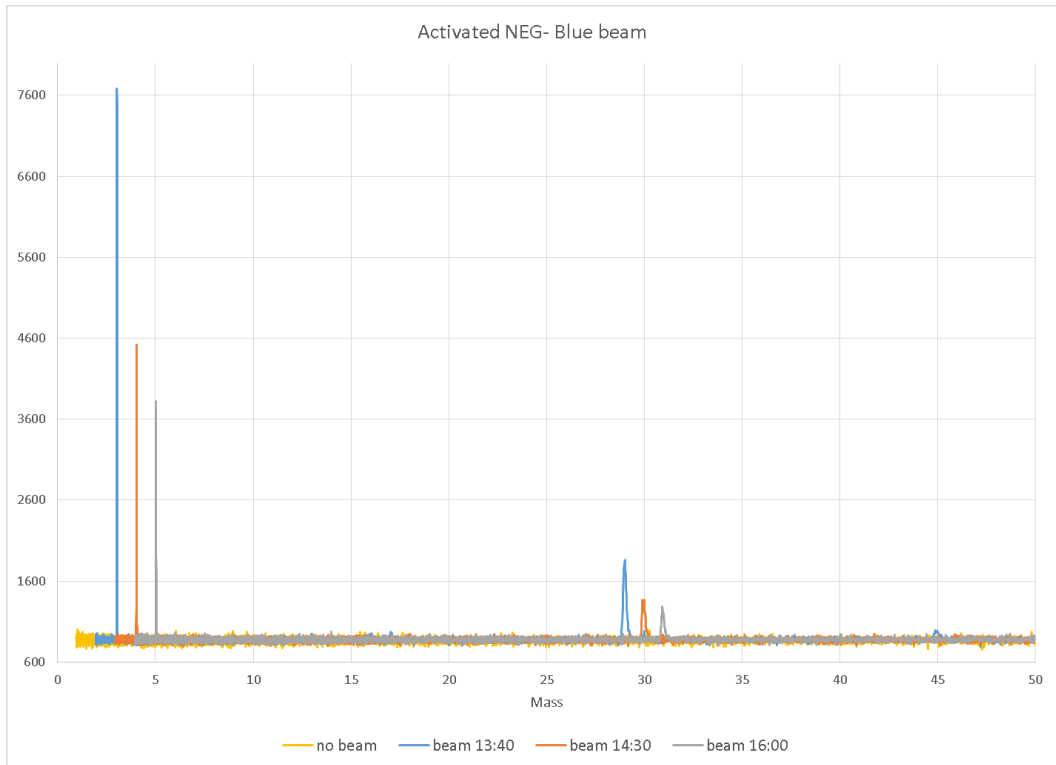


Figure 6-51: Activated NEG spectrum on Blue beam.

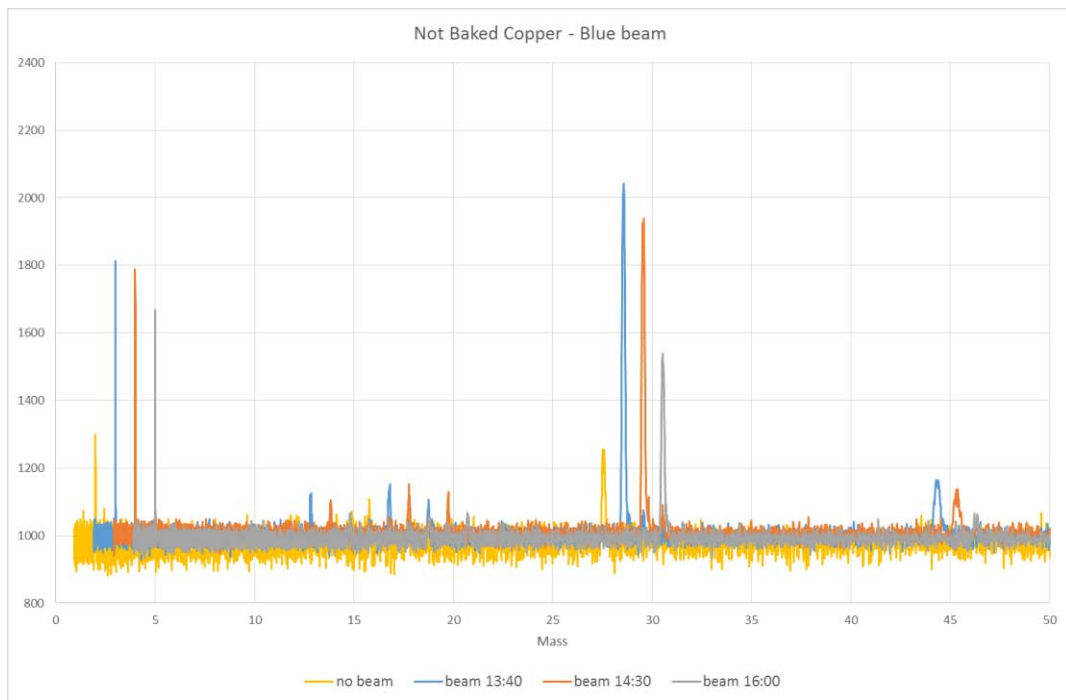


Figure 6-52: Not baked Copper spectrum on Blue beam.

## 6.9 Gas Injections

The injections on old VPS are done in two different moments: at the beginning of the installation (2014) and at the end (January 2016), before being changed by the new system presented above.

### 6.9.1 Injection 2014

It is possible to start from the first injections on VPS, happened in 2014, just when the system was installed in LHC tunnel. The injection is done in the middle of the system, in the left side of station 3. The injection involves two gasses, hydrogen ( $H_2$ ) and methane ( $CH_4$ ). The first is used to check if the activated NEG on liners and on buffers is still activated, due to its capacity of pumping many gasses, a part for methane. The second gas is used to check if the ion pumps are working.

Here many important graphs are shown: the first and the second are the pressure distribution on the blue and the red pipe (see *Figure 6-53, 6-54*), then the third is about the spectrum of gasses released (see *Figure 6-55*) and the last two are the calculation of the transmission coefficient (see *Figure 6-56, 6-57*), done considering the ratio of pressure between the injection and the pressure in each place. This is useful to understand the conditioning effect on surfaces and what this involves.

It will be possible to notice that speaking about  $CH_4$  two orders of magnitude are gained between the injection and the extremities of the system thanks to the pumps, while for  $H_2$  there is around one order of magnitude.

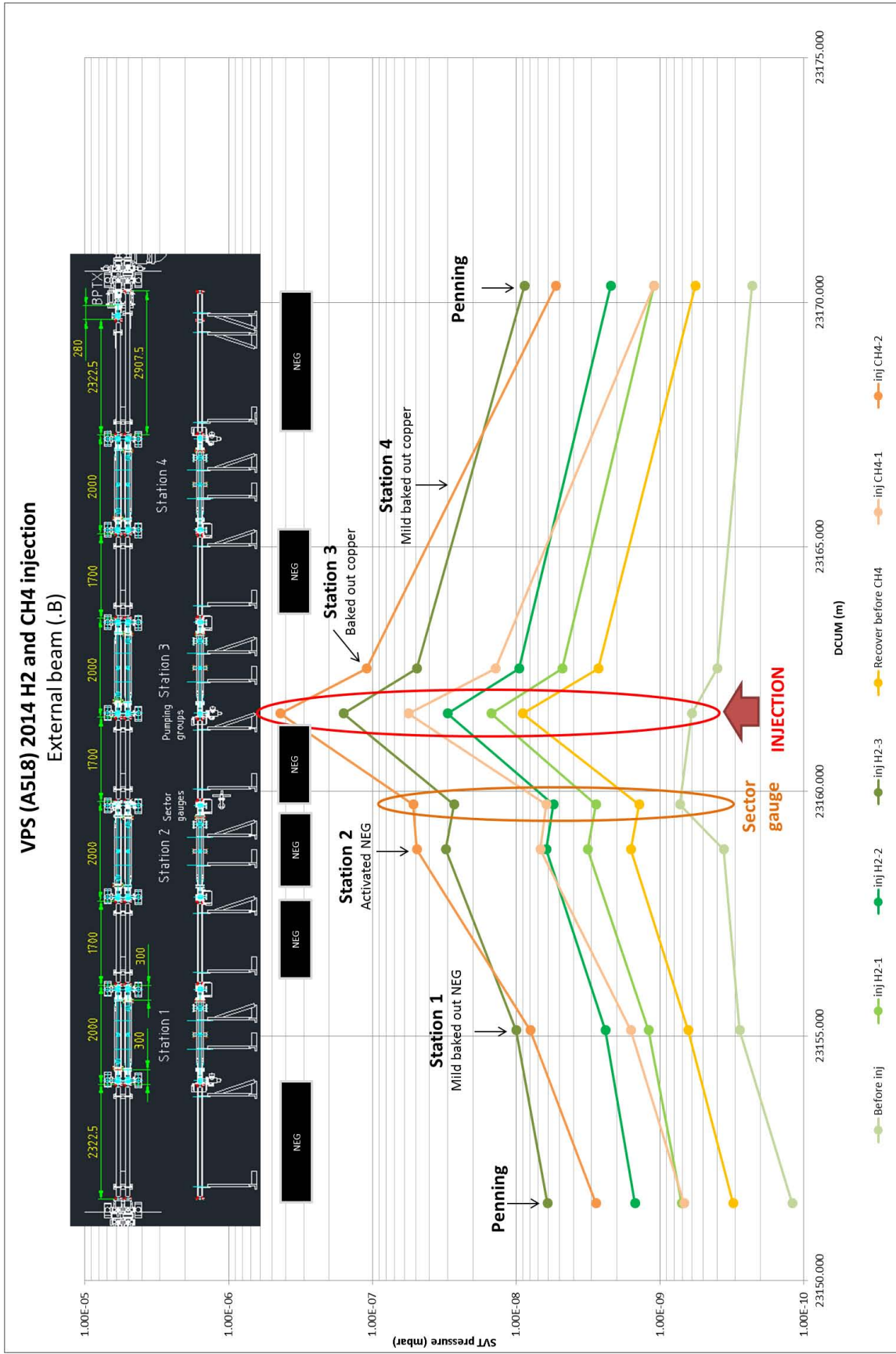


Figure 6-53: Pressure trend during injection 2014 in Blue pipe.

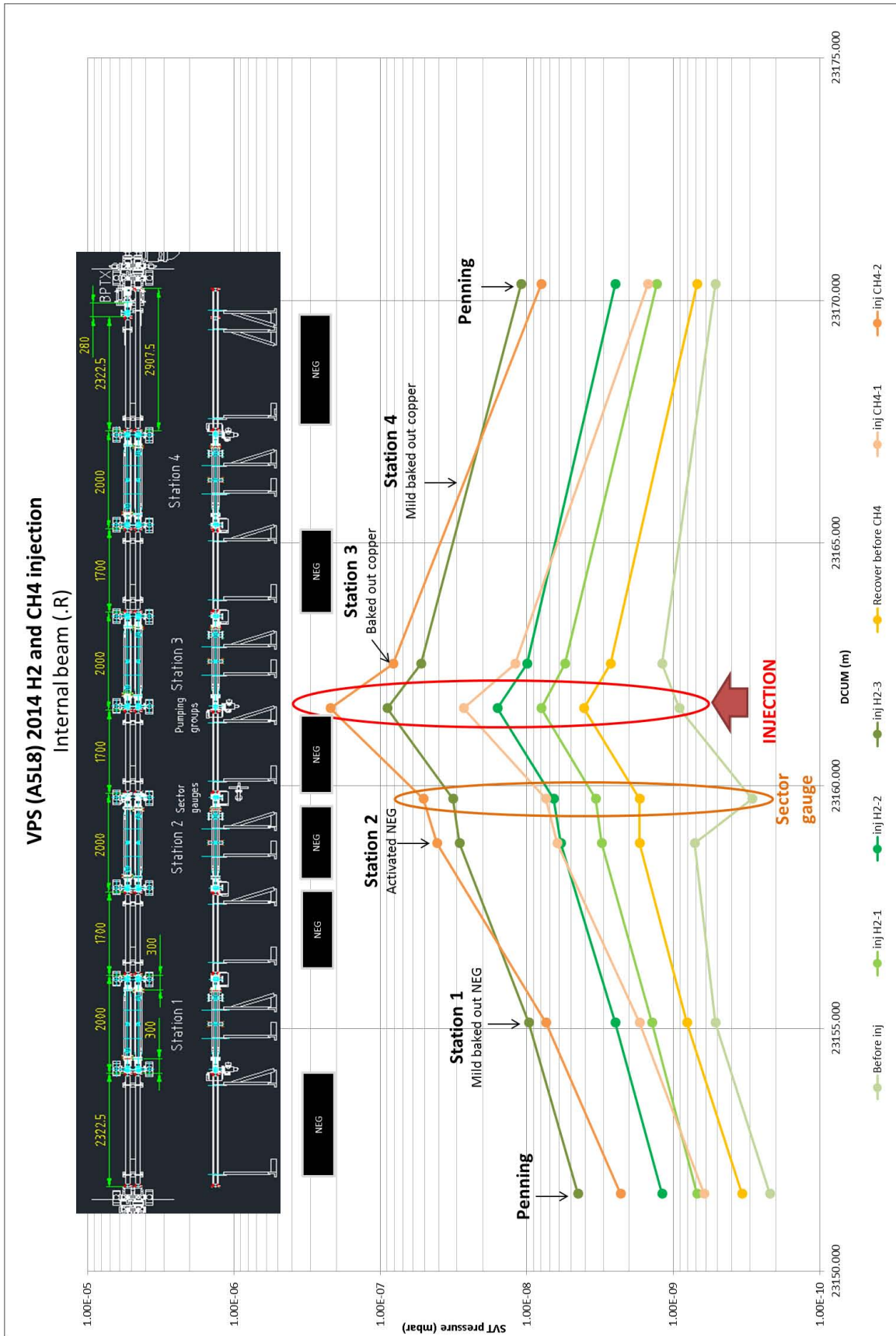


Figure 6-54: Pressure trend during injection 2014 in Red pipe.

It is possible to notice that the pick of the injections of  $H_2$  (m=2) is two orders of magnitude higher than the others picks, while  $CH_4$  (m=16) injection gains one order of magnitude comparing with  $H_2$ .

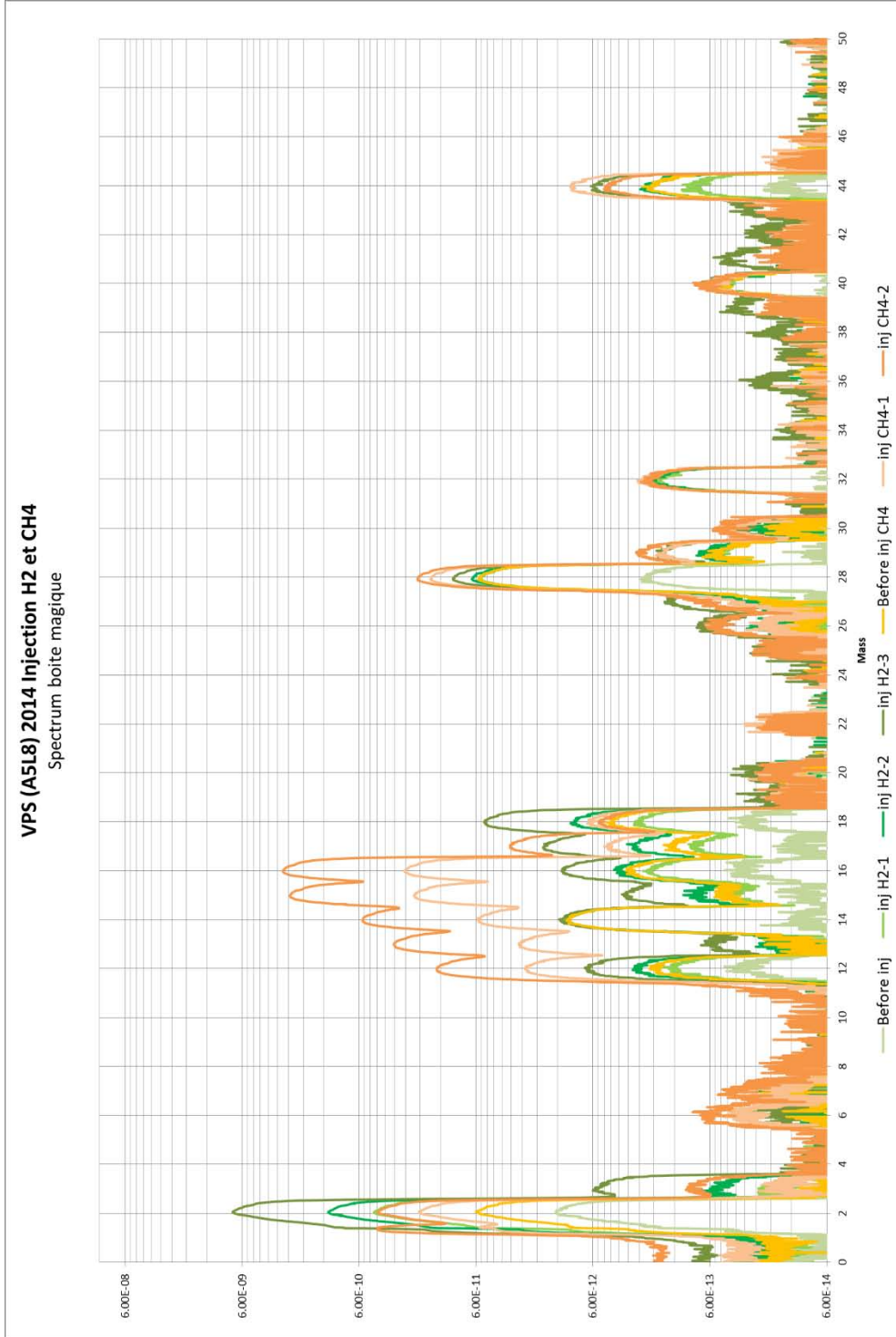


Figure 6-55: Spectrum of injections 2014 taken from injection system called “boite magique”, in common for the two beam pipes.

The most important parameter is the ratio between the pressure at the injector and the pressure in each place considered. This can give an idea of the pumping speed of ion pumps and also of the buffers (made of activated NEG) in the case of  $H_2$  injections.

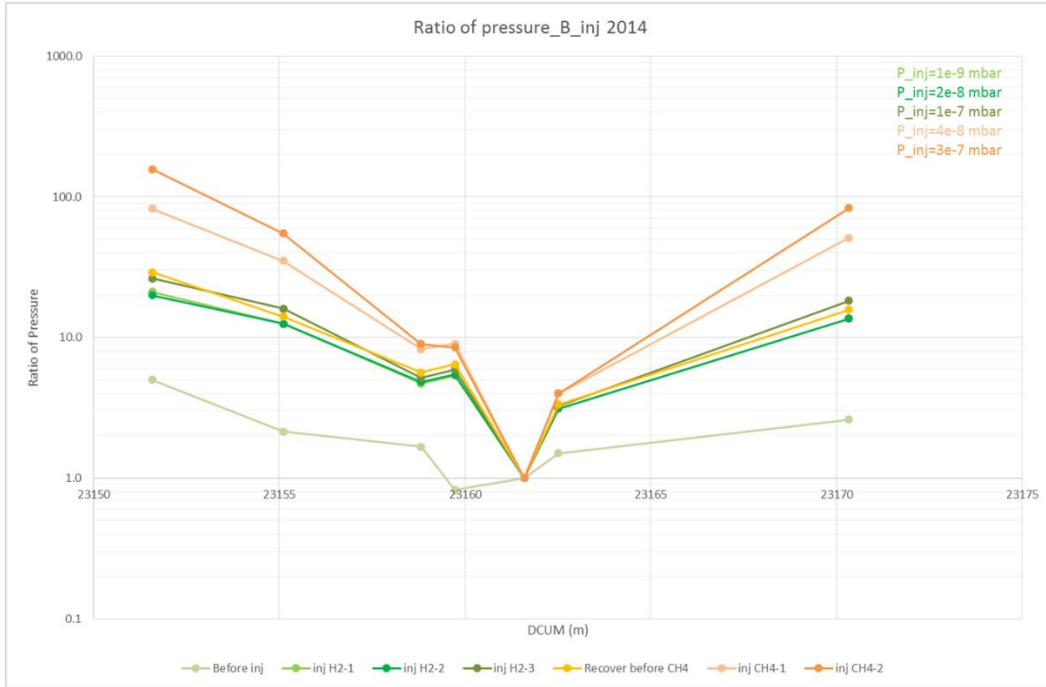


Figure 6-56: Ratio of pressure during injection 2014 in Blue pipe.

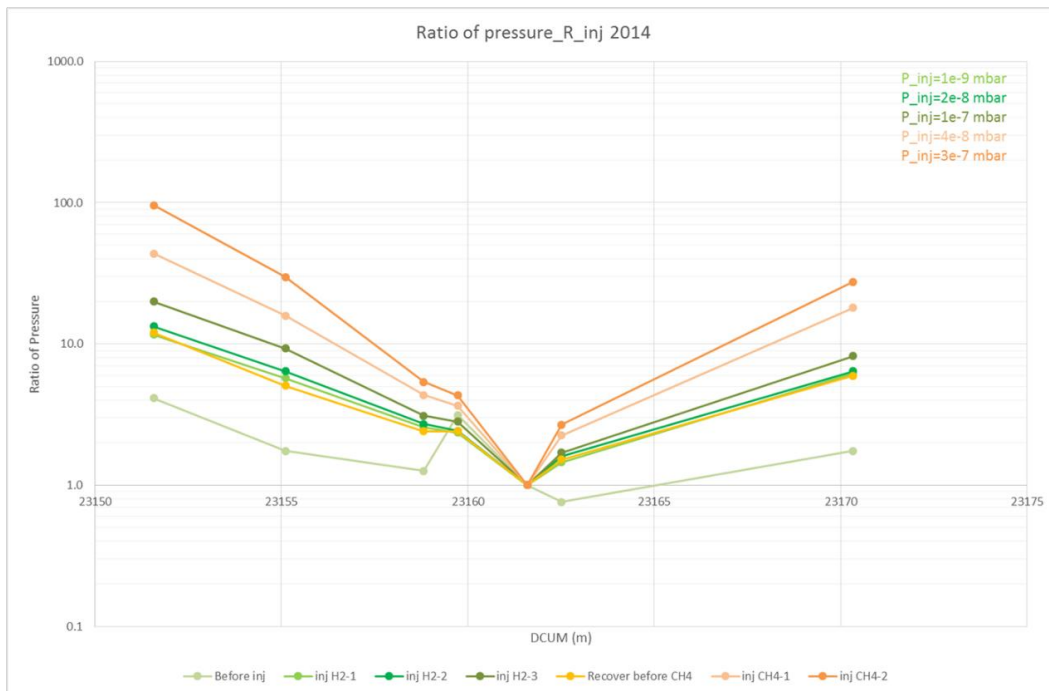


Figure 6-57: Ratio of pressure during injection 2014 in Red pipe.

A factor 10 is gained in the extremities of the system with  $H_2$  injections, while a factor 100 happens for  $CH_4$ . This can be because the injection of Methane were carried after Hydrogen injections and the second reference pressure is higher.

### 6.9.2 Injection 2016

It is possible to compare the analysis just presented with the injections on VPS, happened in 2016, just before the dismounting of the system. This is done to see if the condition changed the surface and the transmission properties of the surfaces. The same structure is kept.



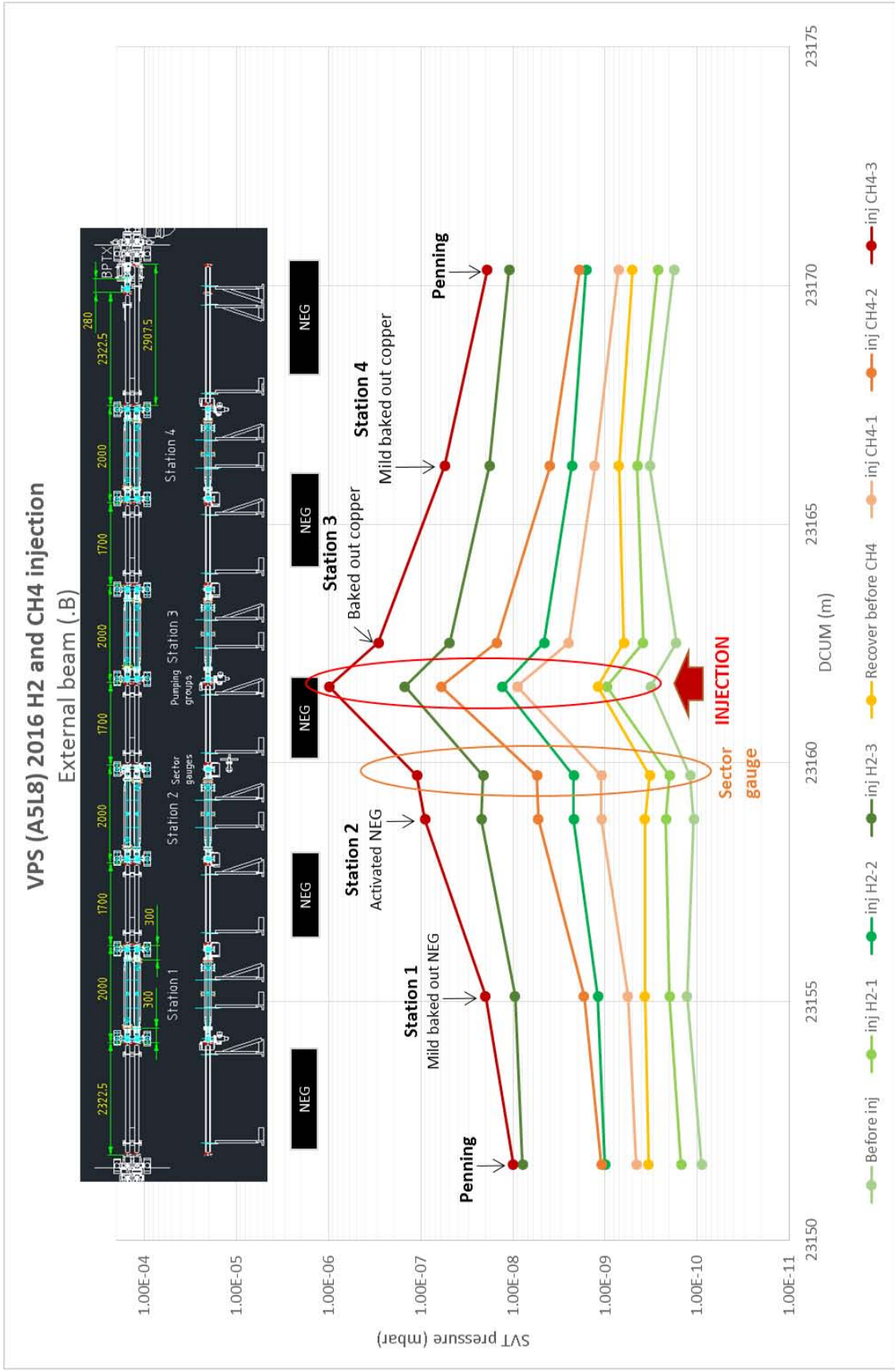


Figure 6-58: Pressure trend during injection 2016 in Blue pipe.

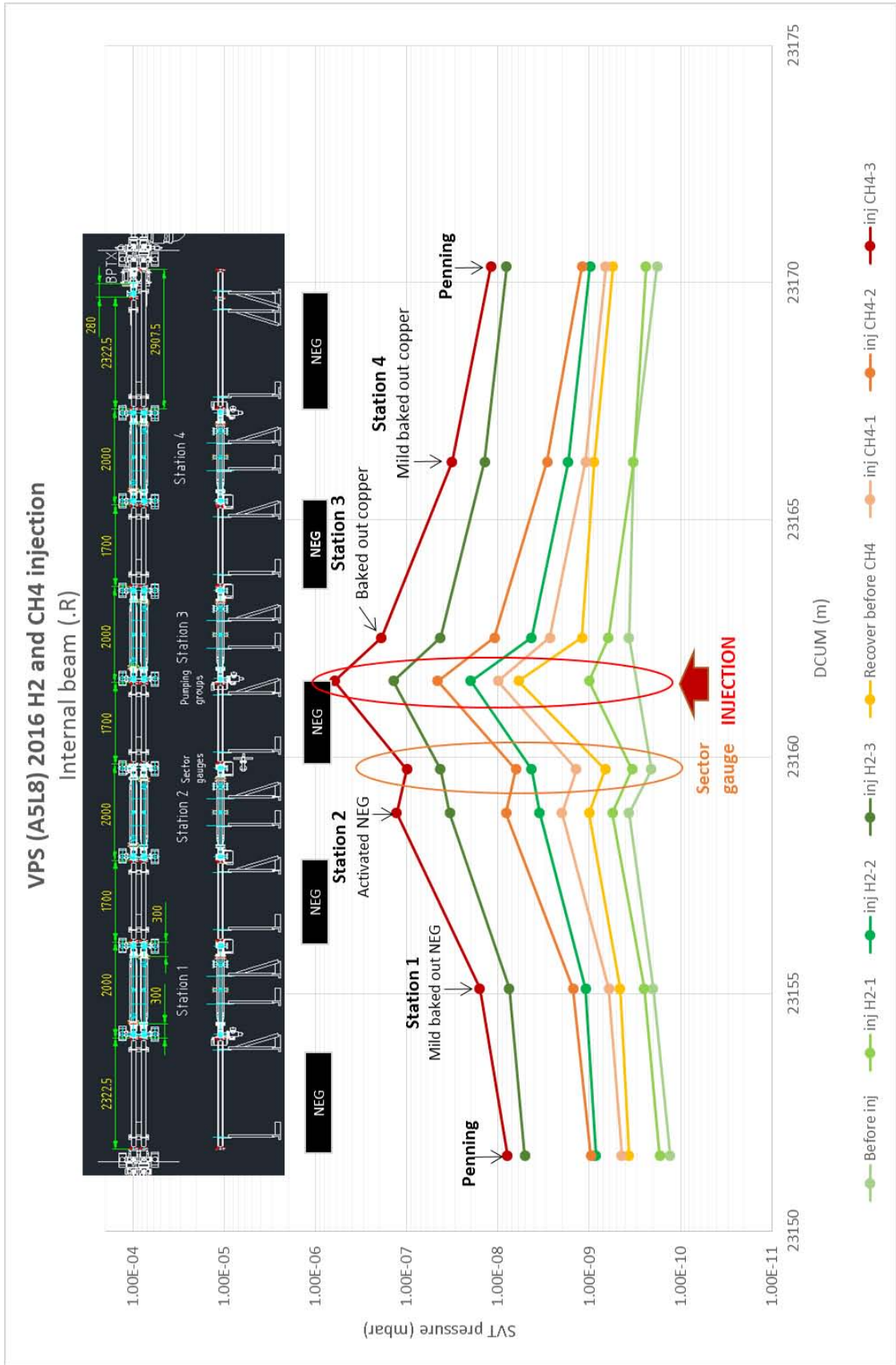


Figure 6-59: Pressure trend during injection 2016 in Red pipe.

It is possible to notice that also this time the pick of the injections of  $H_2$  ( $m=2$ ) is at least two orders of magnitude higher than others, while  $CH_4$  ( $m=16$ ) injection gains one order of magnitude comparing with  $H_2$ , because the same Methane can break some bonds and gives origin to hydrogen (see *Figure 6-60*).

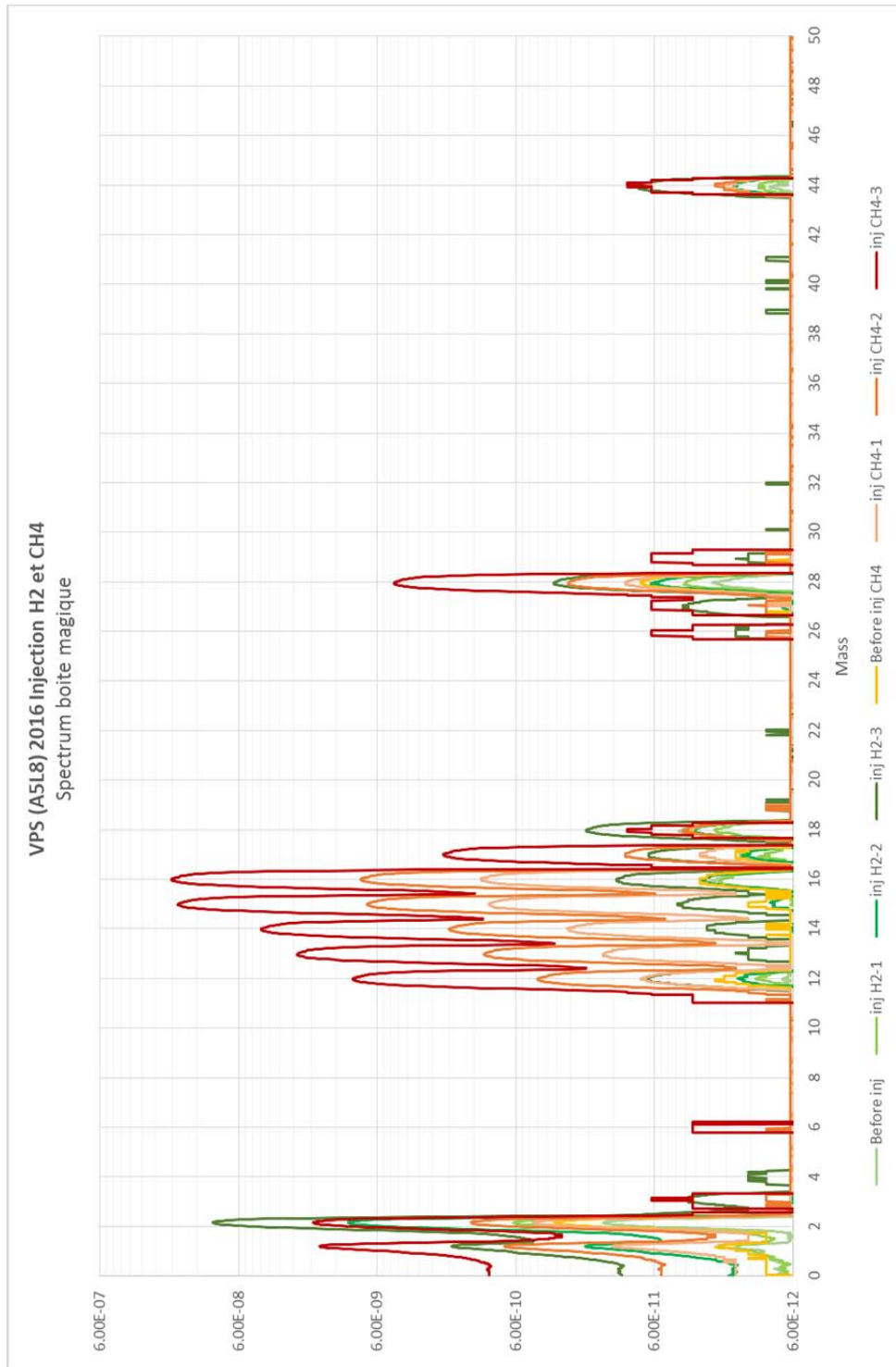


Figure 6-60: Spectrum of injections 2016 taken from injection system called "boîte magique", in common for the two beam pipes.

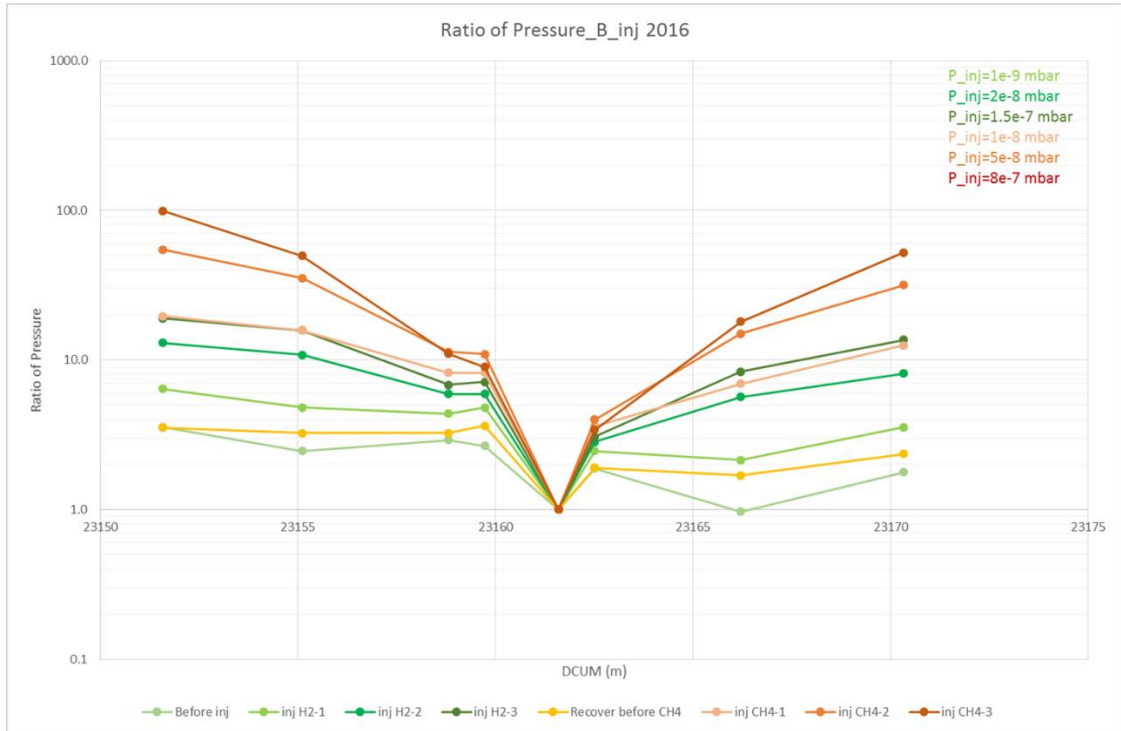


Figure 6-61: Ratio of pressure during injection 2016 in Blue pipe.

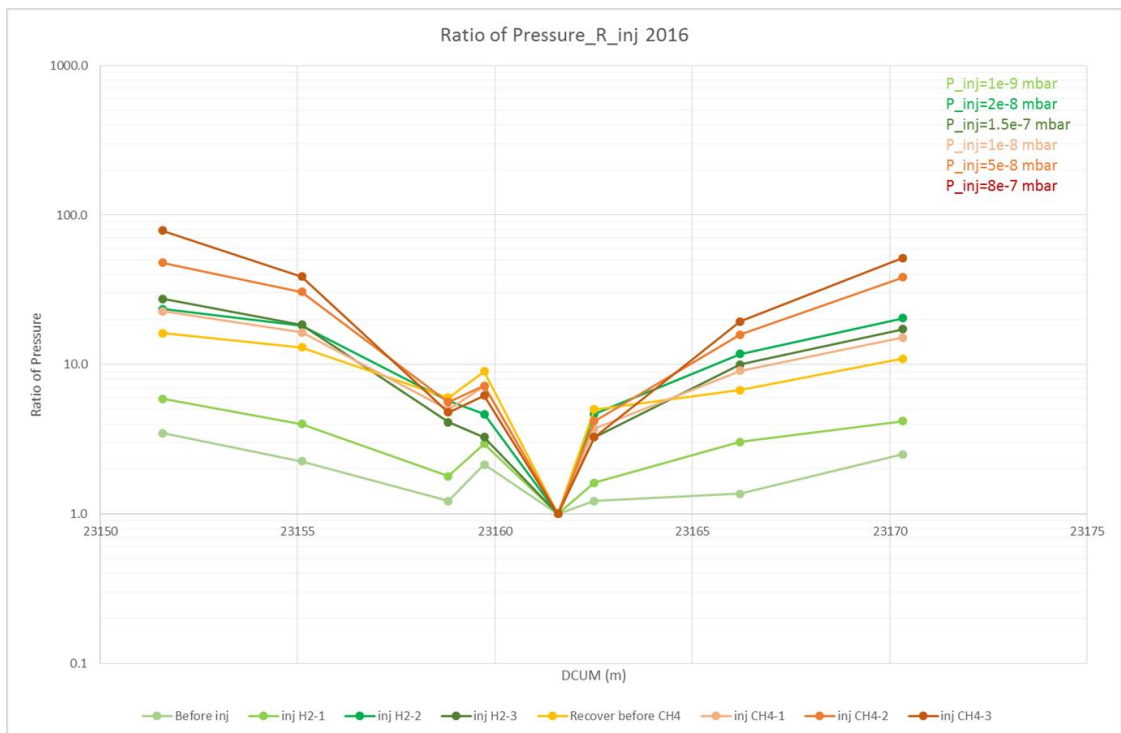
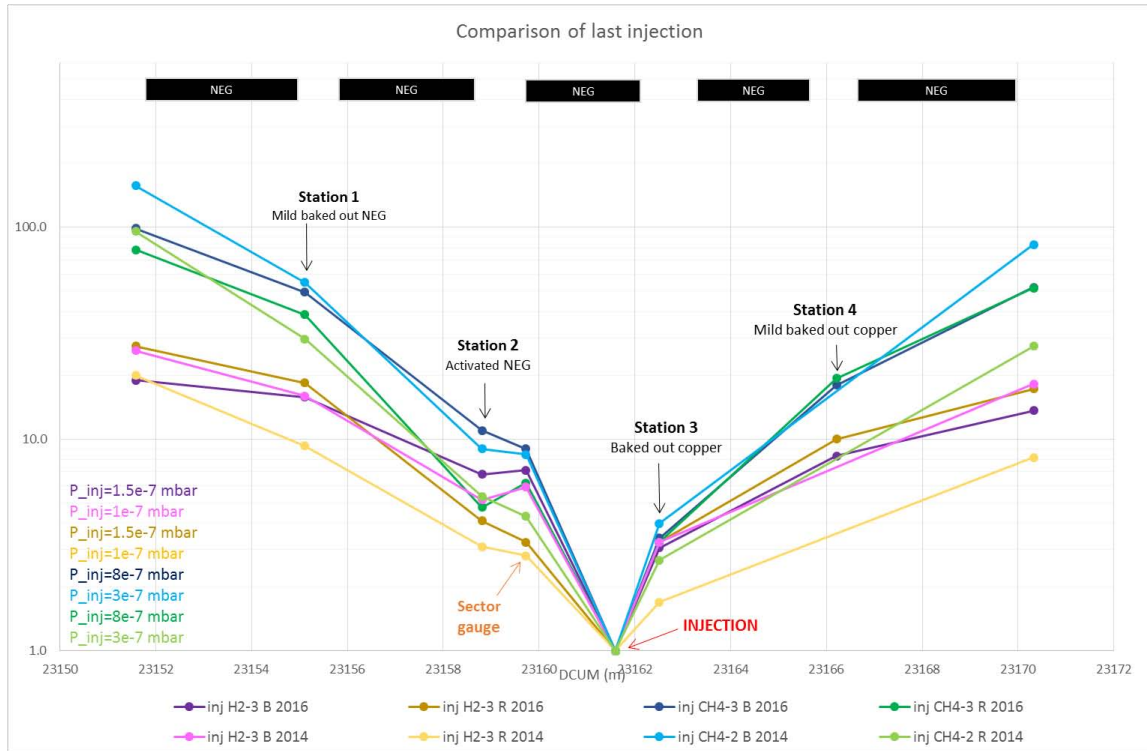


Figure 6-62: Ratio of pressure during injection 2016 in Red pipe.

Looking at these data, it seems that no a big difference is in between them. Now it is possible to see in details the comparison, in order to understand if the buffers are still working (see *Figure 6-63*).



*Figure 6-63: Comparison of injection ratio between 2014 and 2016.*

From this graph is possible to compare the two different injections (2016 and 2014) of Hydrogen and Methane, considering two beam pipe (B and R). Due to the fact that the pressure reached at injection of Hydrogen and Methane are different, also this ratio is influenced.

It is evident that no big differences happened and it seems that buffers work as at the beginning.



## 7. PLAN FOR THE NEW INSTALLATION

The first goal of this study is to understand the responses of the instruments in relationship to the phenomenon. In fact the deeper aim is to get and build a well-functioning system in which it will be possible to characterize the behaviors of several materials for accelerators, tested in the laboratory previously. After the analysis the second important part of this thesis is the new configuration of VPS. The idea is to install it between December 2015 and February 2016.

### 7.1 Plan for VPS 2016

After many initial projects, the following is the official one. The idea is to keep the same system with four stations per beam: three of them new and one old. The aim of keeping the last one, made of not baked copper, after one year of conditioning, is because in this way it is possible to compare it with a new one, with the same surface, but without a long period of beam conditioning. In fact it is possible to study each kind of surface, considering that before it has to be tested in the laboratory, in order not to pollute all the accelerator. The liners have the same shape, as for the chambers, but the windows in which the tools are attached, are shifted in different places and orientations. This is due to the optimisation done thanks to analysis. The symmetry between blue and red liners is respected, as before.

The surfaces are respectively: Activated NEG vented with air (1.5-2micron of thickness), Carbon coating (400-600nm of thickness), not baked Copper (new liner), and the old one with not baked Copper (see *Figure 7-1*).

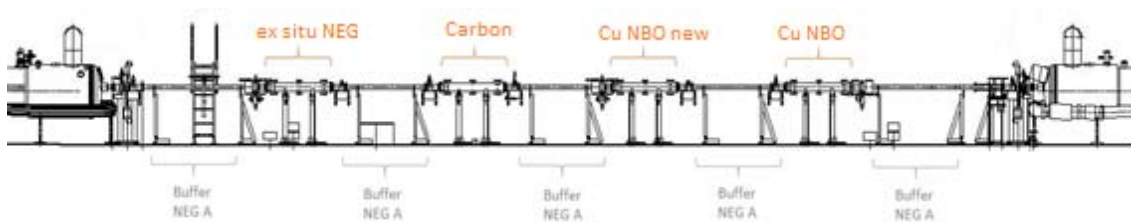


*Figure 7-1: VPS new schematic specifying the surface studied.*



These material are chosen because:

- It is interesting to investigate an Activated NEG that after the venting looks like a Not Activated one. Here it is possible to see the results on NEG of X-ray photoelectron spectroscopy (XPS) after the coating, before the activation (see *Figure 7-2*). (55)

Chamber	Surface C [at. %]	Surface O [at. %]	Surface pollutant [at. %]	Surface metallic composition [at. %]			Activation (carbon area decrease) $\Delta C(RT-250^\circ C)/C(RT)$ [%]	Activation Carbide/total C (250°C) [%]	Activation (oxygen area decrease) $\Delta O(RT-250^\circ C)/O(RT)$ [%]
				Ti	Zr	V			
ref LSS 16-4 CR000044	23.4	52.9	---	24.2	41.7	34.1	52.7	78.8	74.5
S0115 b XPS-TE-VSC-SCC-20151210	11.9	53.6	N(3.22), Cu(6.257)	28	38	34	38.4	83.6	82.9

Good properties
problems
comments on the sample

min		16.0	30.0	25.0		40.0	66.0
max	40	35.0	51.0	42.0			

*Figure 7-2: Main results for NEG coating analysis. The presence of Nitrogen and Copper is not dangerous.*

- Carbon has a very low SEY, around 1 (see *Figure 7-3*). (56)

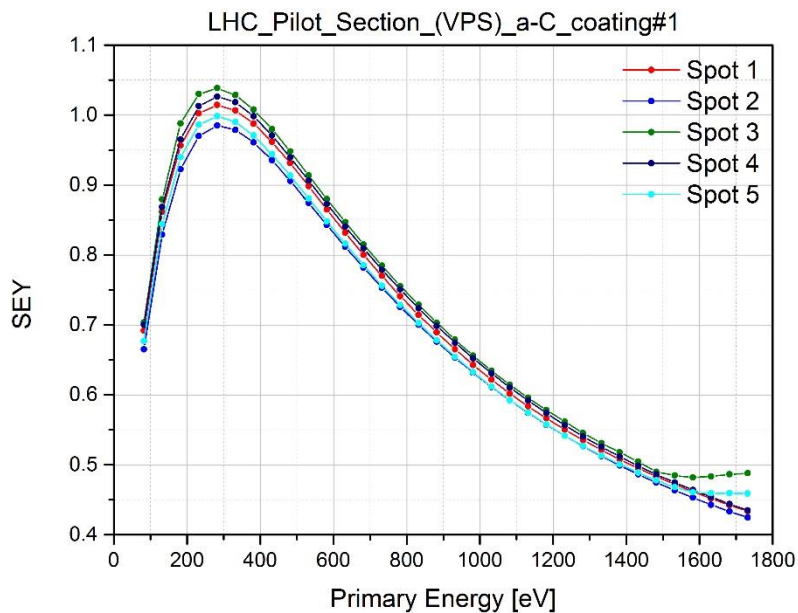


*Figure 7-3: SEY of Amorphous Carbon on VPS liners.*

- The new Not Baked Copper can be compared with the old one to see the effect of the conditioning of the beam.



Here it is possible to see a flat drawing of the new liners that are different from the old one (see *Figure 7-4*).

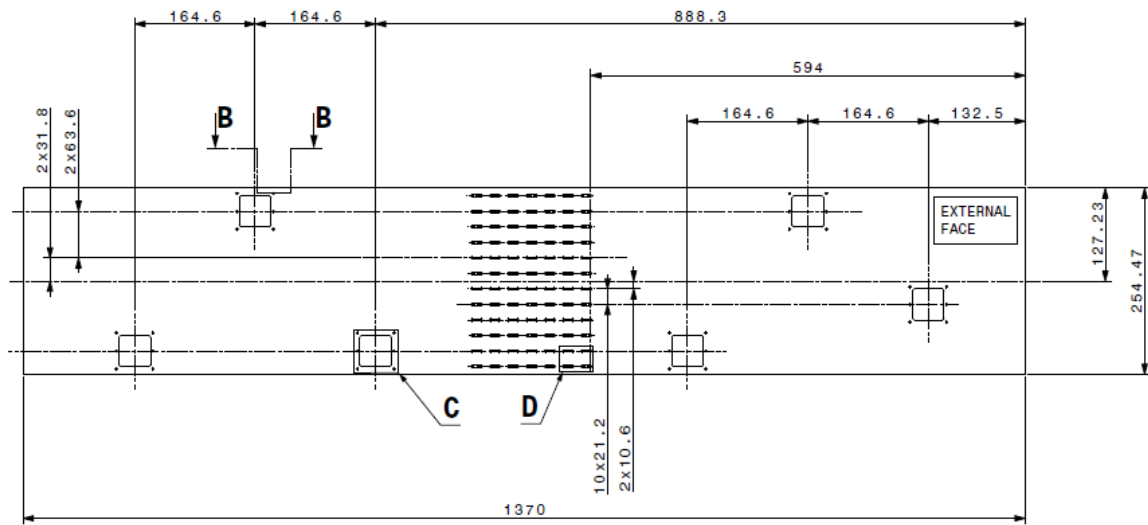


*Figure 7-4: Flat drawing of a liner.*

Following there is an image of a liner with the first stage of detectors (see *Figure 7-5*).



*Figure 7-5: Rolled drawing of a liner.*

Here the main table of the detectors on VPS 2016 (see *Figure 7-6*).

Stations		1		2		3		4		
Faisceau Bleu	Extérieur	Connecteur	Connecteur	Connecteur	Connecteur	Connecteur	Connecteur	Connecteur	Connecteur	
	Surface	ex situ NEG	CARBON COATING	CARBON COATING	Cu NBO new	Cu NBO old				
	Type of liner	A	A	A	A	First				
	N° Liner	B 21	B 23	B 26	B 26	7				
	N° Chambre	13	11	9	9	12				
	N° BAG	40	401	703	703	50				
	N° VQVM	835A00440 (843-10)	835A00676	835A00676	NA	835A00679				
Equipement	Entrée (Gauche)	E11	ph	1 / 111 / K1	ph	1 / 211 / K4	Trig	1 / 311 / Sc1a		
		I12	ph	2 / 112 / K2	ph	2 / 212 / K5	50%	2 / 312 / K7		
		B13	cal1.in	Canon 1-12	cal2	Canon 1-12	cal3	Canon 1-12		
		H		100.03 Ohm		99.97 Ohm		99.98 Ohm	7%	
		E							1 / 411 / K10	
	Sortie (Droite)	I							NU	
		B21	7%	3 / 113 / K3	7%	3 / 213 / K6	7%	3 / 313 / K8	1 trou=0.2%	
		I22	7%	4 / 114 / Sc4a	7%	4 / 214 / Sc4a	7%	4 / 314 / Sc2a		
		B23	cal1.out	Canon 13-25	NU		15%	6 / 315 / K9 (SHV1)		
		H		100.03 Ohm					cal4	Canon 1-12
							EKDK	6 / SHV1		
							EKD	2 / 412 / K12, 5 / SHV2		
Faisceau Rouge	Intérieur	Connecteur	Connecteur	Connecteur	Connecteur	Connecteur	Connecteur	Connecteur		
	Surface	ex situ NEG	CARBON COATING	CARBON COATING	Cu NBO new v2	Cu NBO old				
	Type of liner	B	B	B	B	First				
	N° Liner	R 22	R 25	R 27	R 27	8				
	N° Chambre	7	15	14	14	16				
	N° BAG	636	398	474	474	326				
	N° VQVM	835A00456 (831-9)	835A00705	835A00705	NA	835A00675				
Equipement	Entrée (Droite)	E11	ph	1 / 121 / K13	ph	1 / 221 / K16	Trig	1 / 321 / Sc1b		
		I12	ph	2 / 122 / K14	ph	2 / 222 / K17	50%	2 / 322 / K2_7		
		B13	cal1.in	Canon 1-12	cal2	Canon 1-12	cal3	Canon 1-12		
		H		100.03 Ohm		99.98 Ohm		99.98 Ohm	cal4	Canon 1-12
		E							EKD	1 / 421 / K2_2, 5 / SHV4
	Sortie (Gauche)	I							EKD	6 / SHV3
		B21	7%	3 / 123 / K15	7%	3 / 223 / K18	7%	3 / 323 / K2_6		
		I22	7%	4 / 124 / Sc4b	7%	4 / 224 / Sc4b	7%	4 / 324 / Sc2b		
		B23	cal1.out	Canon 13-25	NU		15%	6 / 325 / K2_1 (SHV1)		
		H		100.03 Ohm					7%	2 / 422 / K2_3
								NU		
								1 trou=0.2%	3 / 423 / K2_4	

Figure 7-6: Main table of VPS information.

As it is possible to see from the table, the station one and three have the same structure of tools (two photon pickup, calorimeter and two 7% grid pickup), while for the second one has the trigger and other transparencies to check. The fourth one is exactly the same of

before. The same interpretation of the old main table can be used to codify the meaning of the values and numbers

## 7.2 Production of new pieces

Since the beginning of August, after the period of the second Scrubbing Run, the plan and the production of new liners started. From simple sheets of copper to the final rolled, welded and cleaned liners.

In particular my job was that of taking care about the organisation and the timing of all the steps, and from October the building and welding of the pickup and calorimeters, and the assembling of each liner with the planned configuration of tools.

In November the coating workshop started to do surface treatments of NEG and Carbon. Later the liners were mounted and bolted to the chambers, the vacuum tests took place. In December injection experiments on the old liners started in the tunnel of LHC, just before the dismounting. From January the new liners I planned were installed in LHC Accelerator.

Considering the job I personally did, the techniques and the tools used are going to be explained, in order to be able to replicate them in the same way in the future. As I told before I used many machines in order to build my pieces.

### 7.2.1 Rolling of tools and making hole plates

The first two machines are tools in order to bend metals. I used the first to bend roll patches (see *Figure 7-7*) and the second one to bend plates with the help of technicians (see *Figure 7-8*). The pressure applied was that of 5 tons metric.



Figure 7-7: Rolling machine.

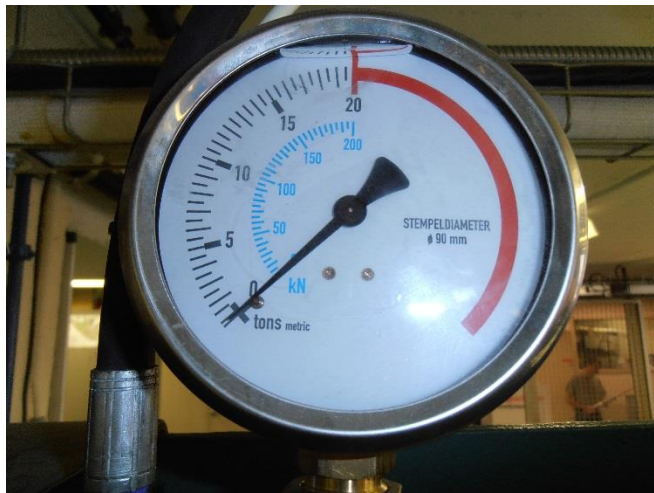


Figure 7-8: Bending machine for electrodes.

In order to do a hole in the centre of them, another machine was used (see Figure 7-9).



Figure 7-9: Me making holes in the electrodes for photon pickup.

### 7.2.2 Cleaning of Stain steel ribbon

In order to clean stain steel ribbon I used a machine in which an ultrasonic bath was done. The pieces have to be immersed in Acetone for 20 minutes and subsequently in Alcohol for 20 minutes (see *Figure 7-10*).



*Figure 7-10: Ultrasonic machine.*

### 7.2.3 Welding of detectors

The welding concerns calorimeters and pick up of different transparencies. The first are the calorimeters (see *Figure 7-11*). In order to build one of them, it is necessary to weld small stripes of stain steel INOX (10\*0.5\*0.05mm) on a thin copper (30\*30\*0.2mm), attaching the temperature sensors, Pt100. After it is needed to attach this to the copper plate (68.2\*60mm) and then attach the last Pt100 on it.

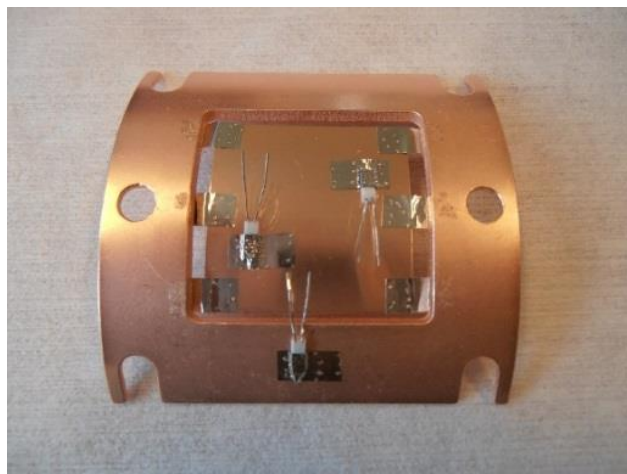


*Figure 7-11: Calorimeter built by me.*



Speaking about pick up, because of the fact that copper on copper is very difficult to weld, I had to weld a small stripe of stain steel INOX al around the grid in order to easily do the job (see *Figure 7-12*). After it is needed to attach this on the copper plate.

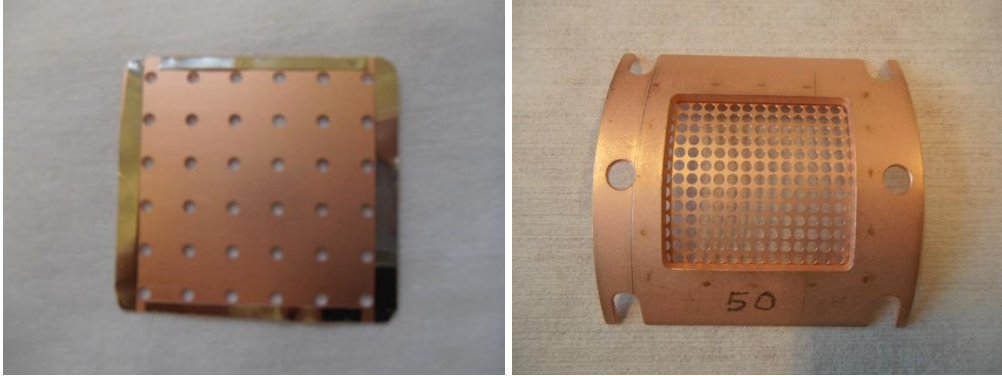


*Figure 7-12: Building of pickup: grids with stain still stripes welded to make easier the welding Copper on Copper.*

In order to weld I used two machine, one less powerful for small welding between stain steel ribbon (thickness 0.05mm) and a thin copper (thickness 0.2mm), while for a stronger welding I used the second one.

The parameters used are the following:

- 1<sup>st</sup> machine to weld INOX on thin Copper: 1.5KA, 1.6 slope, 4ms.
- 2<sup>nd</sup> machine to weld grids on Copper plate: 3.5 Power, 10 time shift, 4s.
- 2<sup>nd</sup> machine to weld INOX on Copper plate: 4 Power, 2.5/3 time shift, 3s.

Here it is possible to respectively see the two machine. The first has smaller electrodes (diameter of 1÷2mm), (see *Figure 7-13*) and it is used to weld very thin layers, while the second one is stronger (electrode diameter of 5mm), (see *Figure 7-14*).

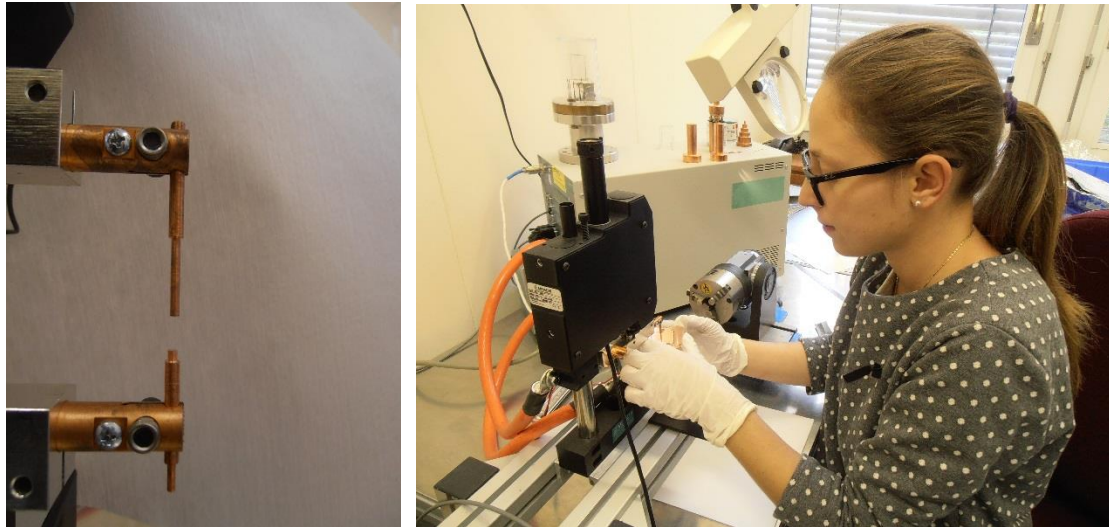


Figure 7-13: Small machine to weld and me at work.

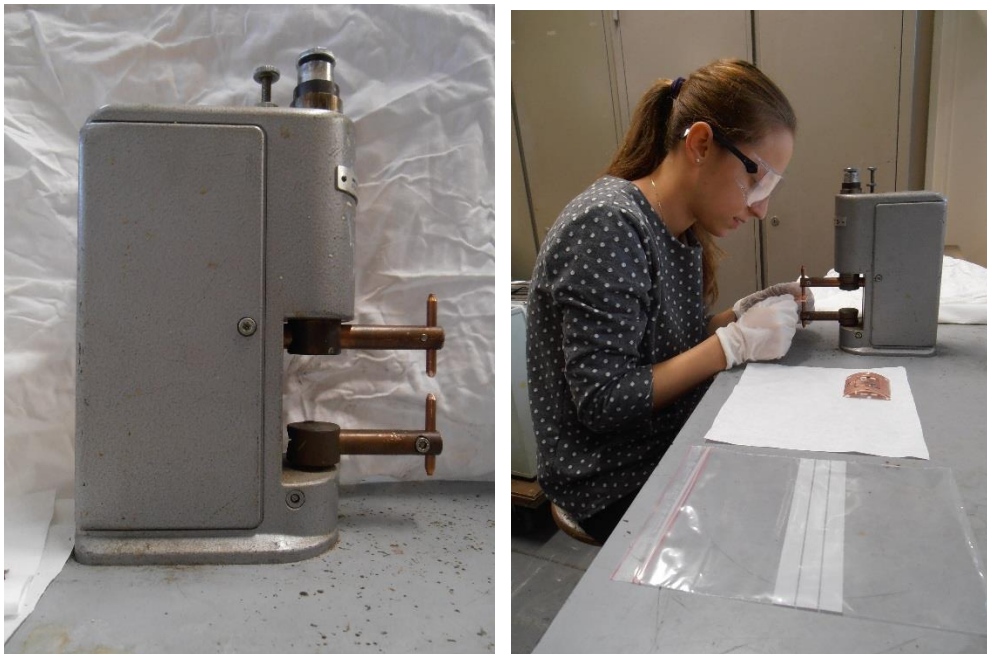


Figure 7-14: Stronger welding machine and me at work.

#### 7.2.4 Assembly of detectors on liners

Each liner, as the plan explained above in *Paragraph 6.1*, needs different detectors. On the windows carved on them, calorimeters and pick up have to be installed.

For the shielded pick up, for example, are necessary three layer (see *Figure 7-15*): the first one is the grid (see *Figure 11-8*), the second is the electrode that acquires the electrical signal (*“Detector sheet”*, see *Figure 11-12*), and the third is the hood in order to shield from RF and to avoid short circuit between the electrode and the vacuum

chamber (“Cover sheet”, see Figure 11-13). The grids and the hoods are grounded, while the electrode sees the signal coming from the beam.

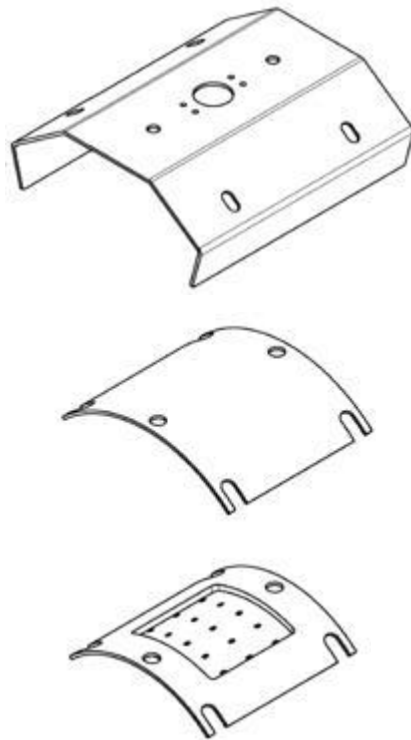


*Figure 7-15: From the bottom the order of mounting a shielded pickup: a grid, the electrode and the hood.*

In order to give an estimation, the time necessary to assembly one liner with 6 windows (see Figure 11-5) is around one day of work. Further, to do the wiring other 2 hours are needed.





Figure 7-16: me mounting the pickup and calorimeters on liner in b. 113.

In order to recognize the liners and write a reference on each window, a printmaker for metals is used. It is used also to write the number of the transparency of the grid. Here it is the machine (see Figure 7-17). Usually the level of power used was 4.



Figure 7-17: Printmaker used.

In order to control the insulation of the electrode from the grids and the liner, a high voltage test is used (see Figure 7-18). All the detectors are tested and they resist up to 2 KV. This is a safety way to control the system.



Figure 7-18: High voltage test.

### 7.2.5 Bake out of chambers and wires

The chambers need to be covered with a jacket in order to do the bake out before the coating (see Figure 7-19). This is done by expert on it.



Figure 7-19: Bake out jacket for a chamber.

In general, the bake out is a procedure used to clean the surfaces. Heating up the system, a big amount of gas is released. Each part has a different temperature that can reach in order not to damage it.

All the Kapton wires used for connections of pick up and calorimeters are cut and baked in this system at 150 degree for 32h in order to release the water captured by the insulator (see Figure 7-20). From a pressure of  $10^{-3}$  mbar with the pieces inside the chamber, during the heating it went up to  $10^{-2}$  mbar. After the bake out it reached  $10^{-7}$  mbar.

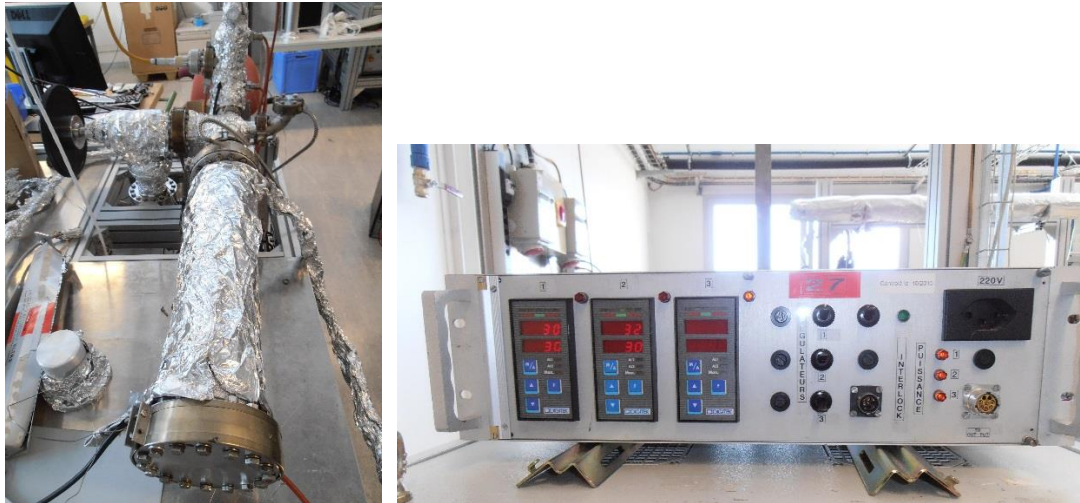


Figure 7-20: Bake out system for Kapton wires.

### 7.2.6 Vacuum Tests in the laboratory

Once the liners are inserted on the chambers, it is time for bake out and vacuum test, before bringing the pieces in the tunnel.

The tests were done in two benches in the building 113. Each kind of surface of coating is individually tested. On the first bench the two Copper stations are installed and in parallel the two NEG on the second bench made for. Once copper is ready, it is removed to leave the place for Carbon once.

The bench used to test Copper and Carbon is made of two pumps (primary and turbomolecular one), BAG (SVT1), Penning (VGP Dome) and RGA in the fixed system, a BAG at the beginning of the vacuum test (SVT2), (see *Figure 7-21*).

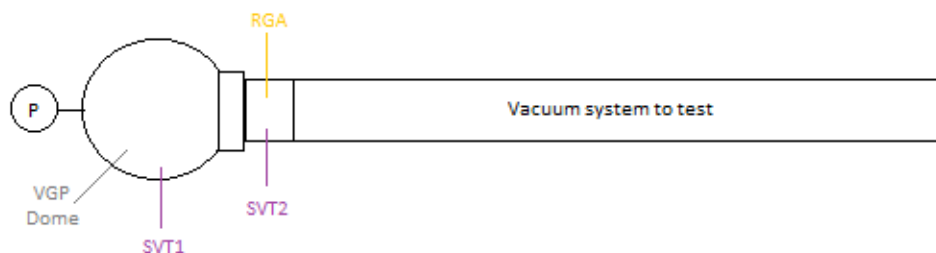


Figure 7-21: Scheme of the bench used for Copper and Carbon stations.

Carbon and Copper liners are baked at 80°C in order to make Kapton wires degas from water and hydrocarbons.



Speaking about **Copper**, it was heated up to 50 °C and then to 80°C. The process and spectra are shown on it. The pressure reached in the end of the vacuum system is  $3 \cdot 10^{-7} \text{ mbar}$  (see *Figure 7-22*).

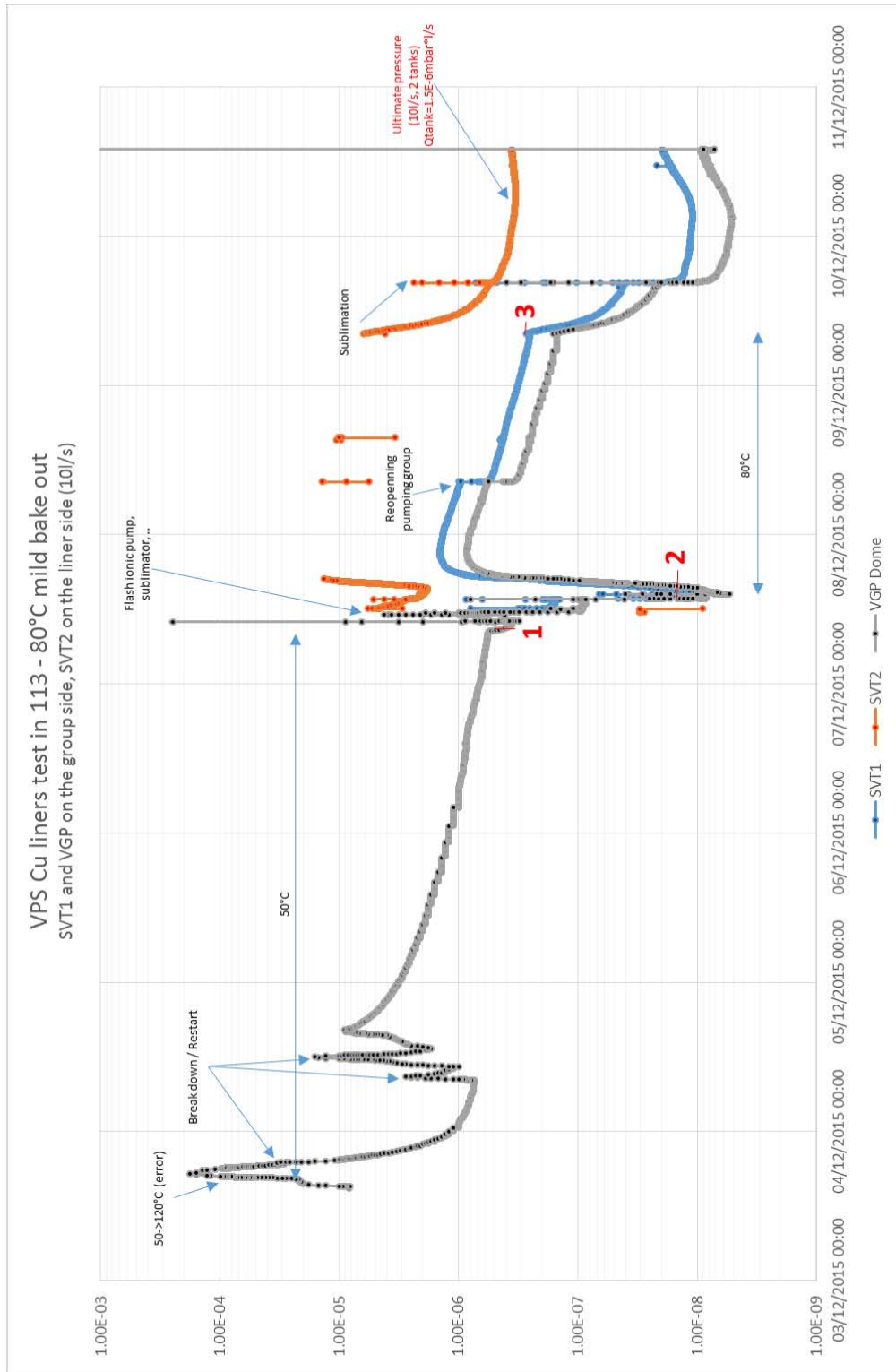
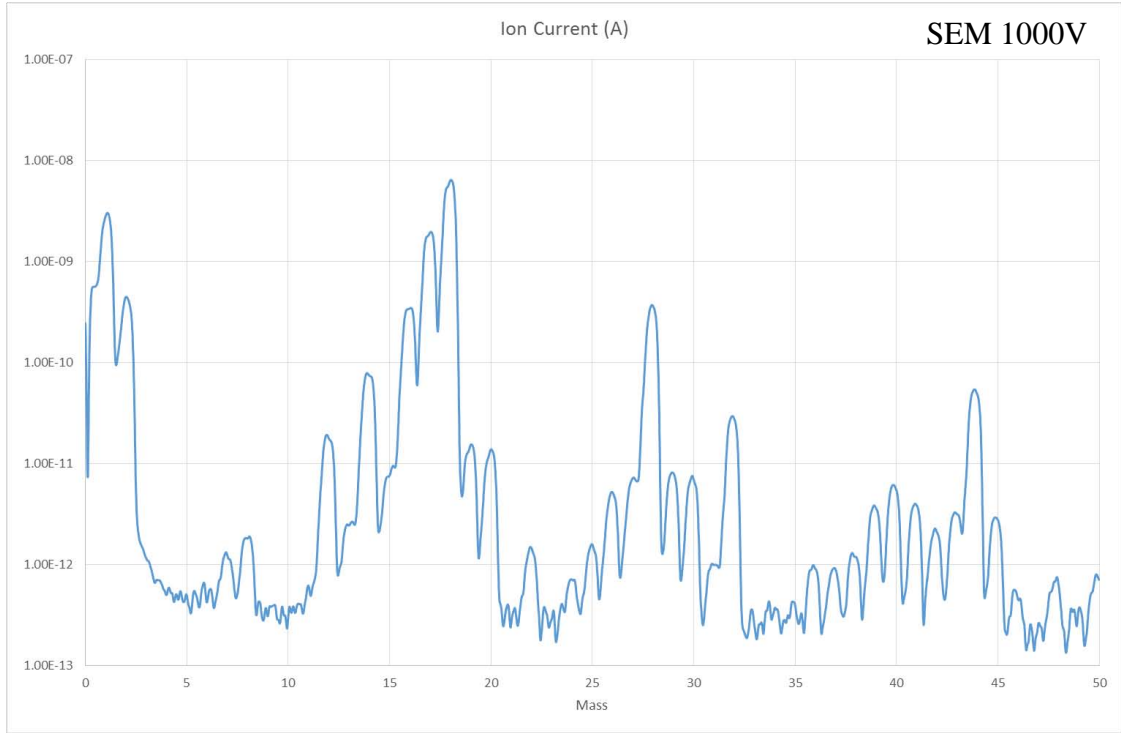


Figure 7-22: Vacuum Tests for Copper liners.

Example 1, 07.12.15 at 09:56: heating at 50°C (see *Figure 7-23*).



*Figure 7-23: RGA spectrum on Copper liners at 50°C.*

Example 2, 08.12.15 at 15:23: during mild bake out of 80°C (see *Figure 7-24*).

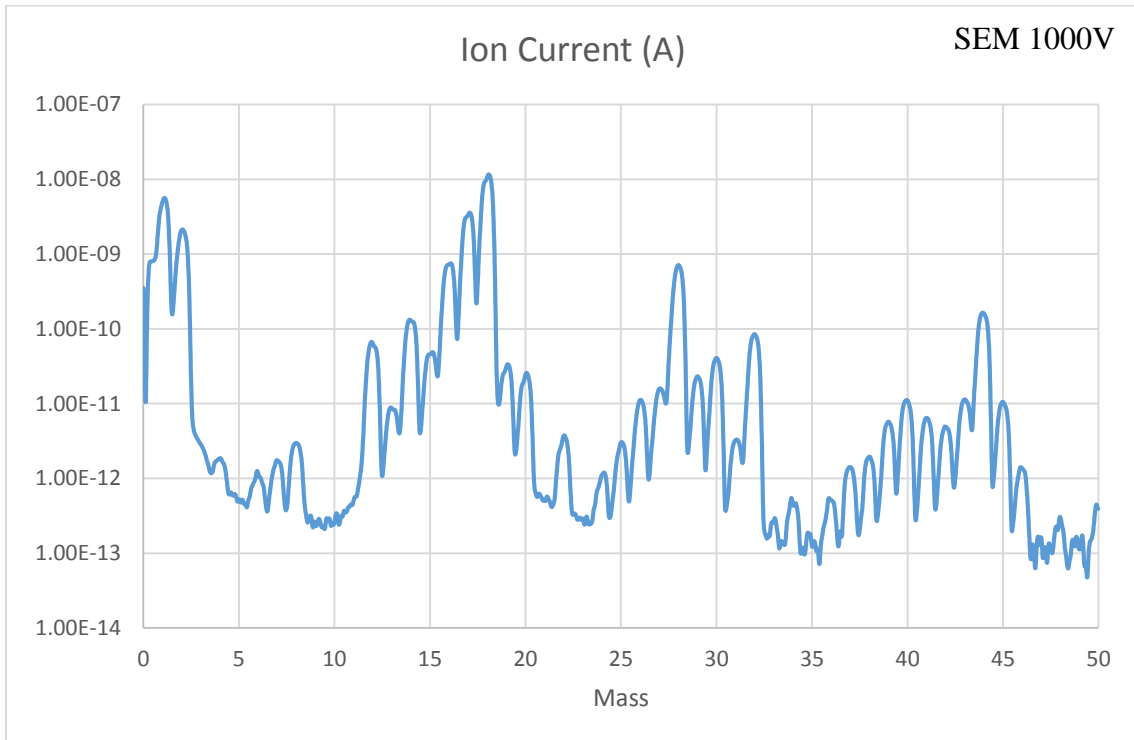


*Figure 7-24: RGA spectrum on Copper liners during bake out at 80°C*

Example 3, 09.12.15 at 08:24: after mild bake out of 80°C (see *Figure 7-25*).

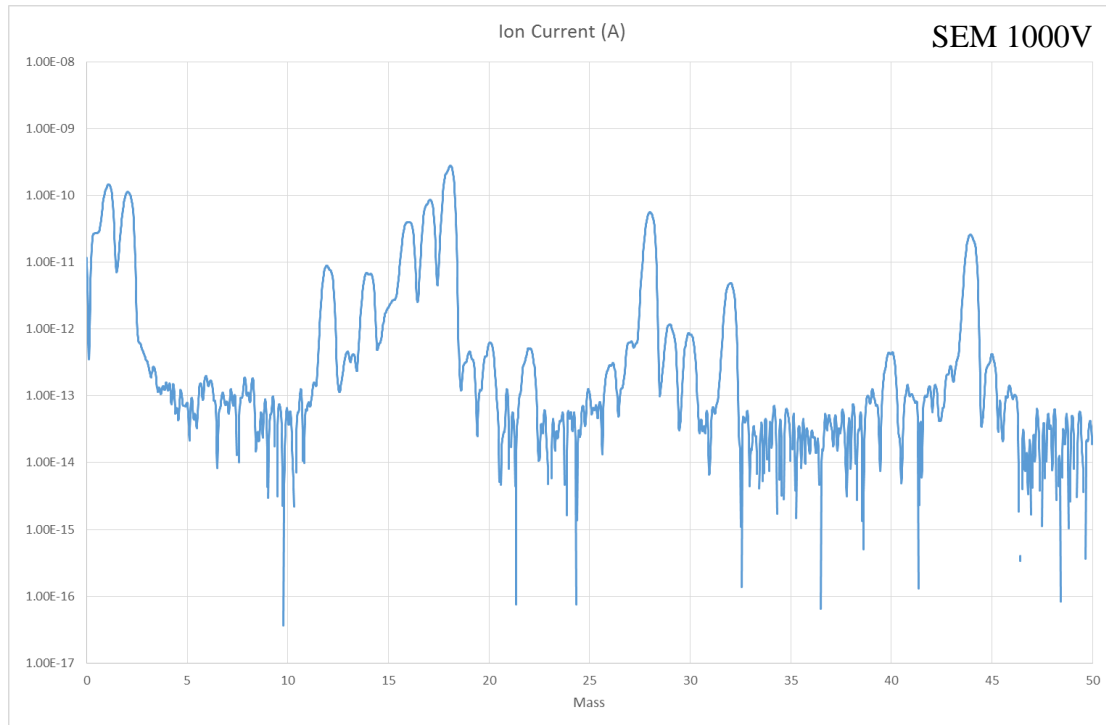


*Figure 7-25: RGA spectrum on Copper liners after bake out.*

As it is possible to see the presence of a leak, probably in the fix system, or a “virtual” leak due to a big amount of Kapton wires attached to the liner. This is evident due to:

- Mass 14 (*N*) is higher than 15 (*O*),
- High pick of mass 32 (*O*<sub>2</sub>),
- Masses 14 and 28 in proportion of one tenth,
- High pick of mass 40 (*Ar*).

It is possible to notice that the amount of mass 1, (*H*<sup>+</sup>) is reducing after the bake out.

Speaking about **Carbon**, tested in the same bench, a similar spectrum is present. The process is similar to the previous one, so it will be not presented, but here there are the spectrum during and after the mild bake out.

Example 1, 14.12.15 at 08:32: mild bake out of 80°C. Pressure of the chamber:  $6 \cdot 10^{-6}$  mbar (see Figure 7-26).

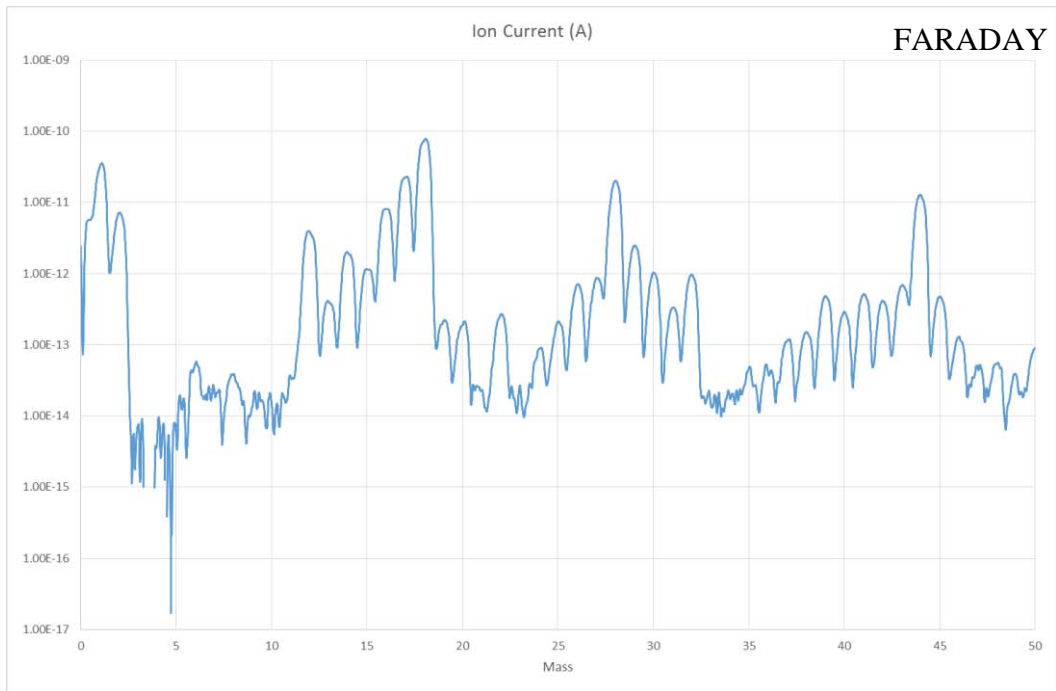


Figure 7-26: RGA spectrum on Carbon liners during bake out at 80°C.

Example 1, 16.12.15 at 17:46: after mild bake out of 80°C. Pressure of the chamber:  $2.5 \cdot 10^{-7}$  mbar (see Figure 7-27).

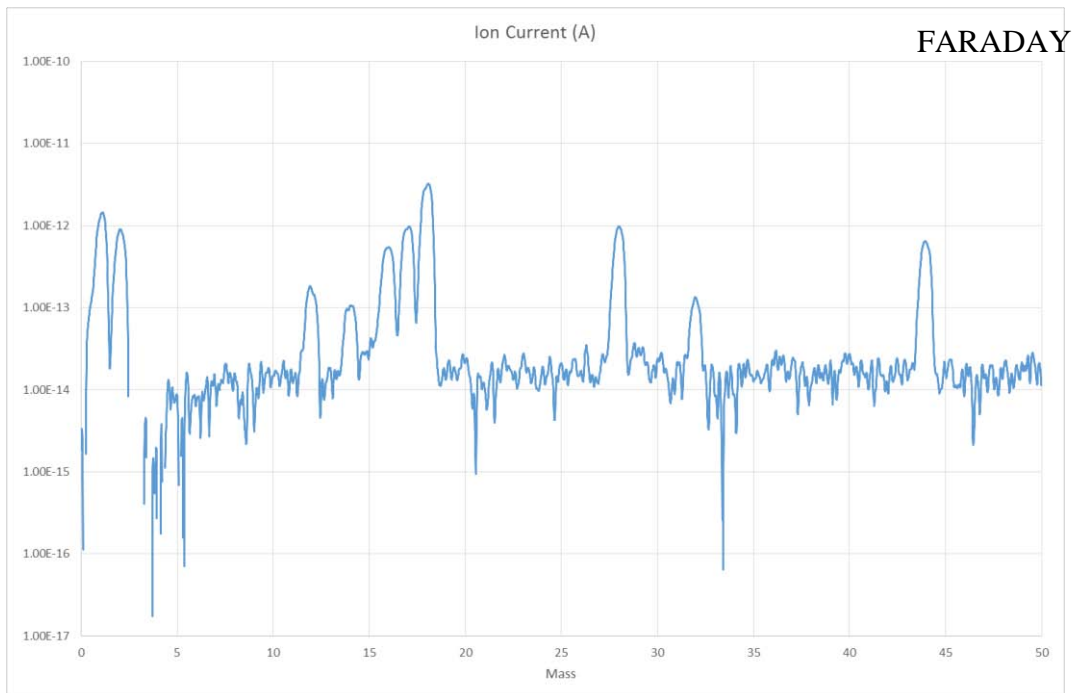
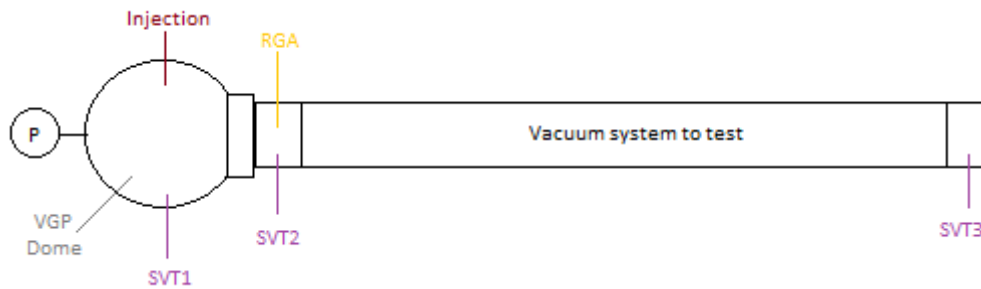


Figure 7-27: RGA spectrum on Carbon liners after bake out.

The **NEG** bench has three pumps (primary, turbomolecular and also ionic one), BAG (SVT1), Penning (VGP Dome) and RGA in the fixed system, a BAG at the beginning of the vacuum test (SVT2) and one at the end of the chamber to be tested (SVT3) (see *Figure 7-28*).



*Figure 7-28: Scheme of the bench used for NEG stations.*

NEG is baked and activated at 230°C for 24 hours. Here the process is presented. Some spectra from RGA are taken in different moments marked on the drawing (see *Figure 7-29*).



VPS NEG liners test in 113 - 230°C bake out for 24 h  
 SVT1 and VGP on the group side, SVT2 on the liner side (10l/s), SVT3 at the end the the liners

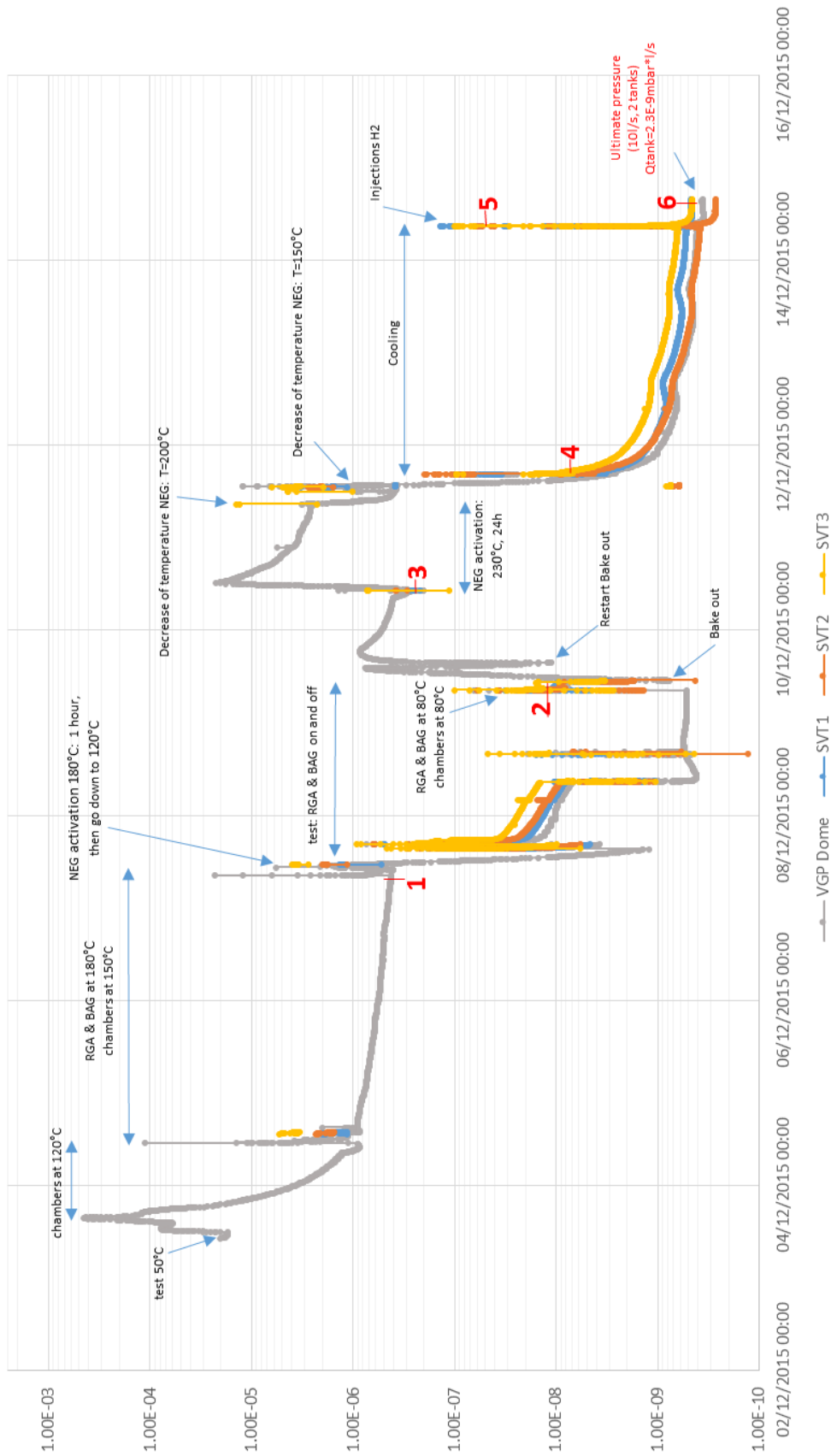
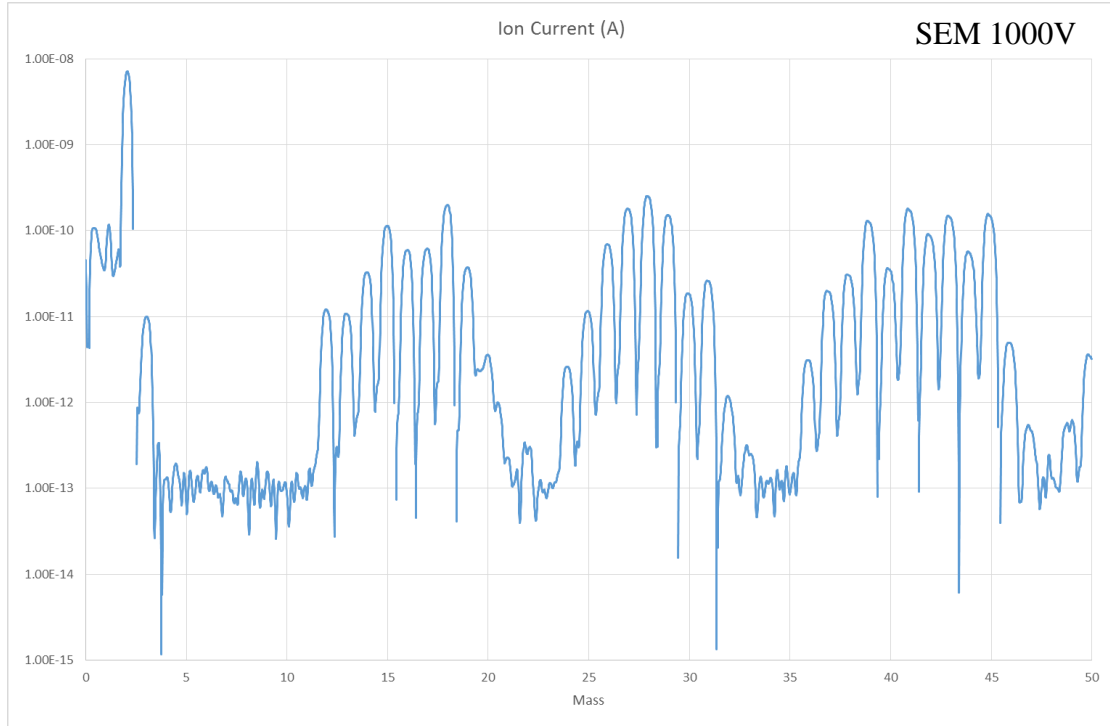


Figure 7-29: Vacuum Tests for NEG liners.

Example 1, 07.12.15 at 09:43: activation 180°C (see *Figure 7-30*).



*Figure 7-30: RGA spectrum on NEG liners during bake out and activation at 180°C.*

Example 2, 09.12.15 at 08:38: before bake out (see *Figure 7-31*).

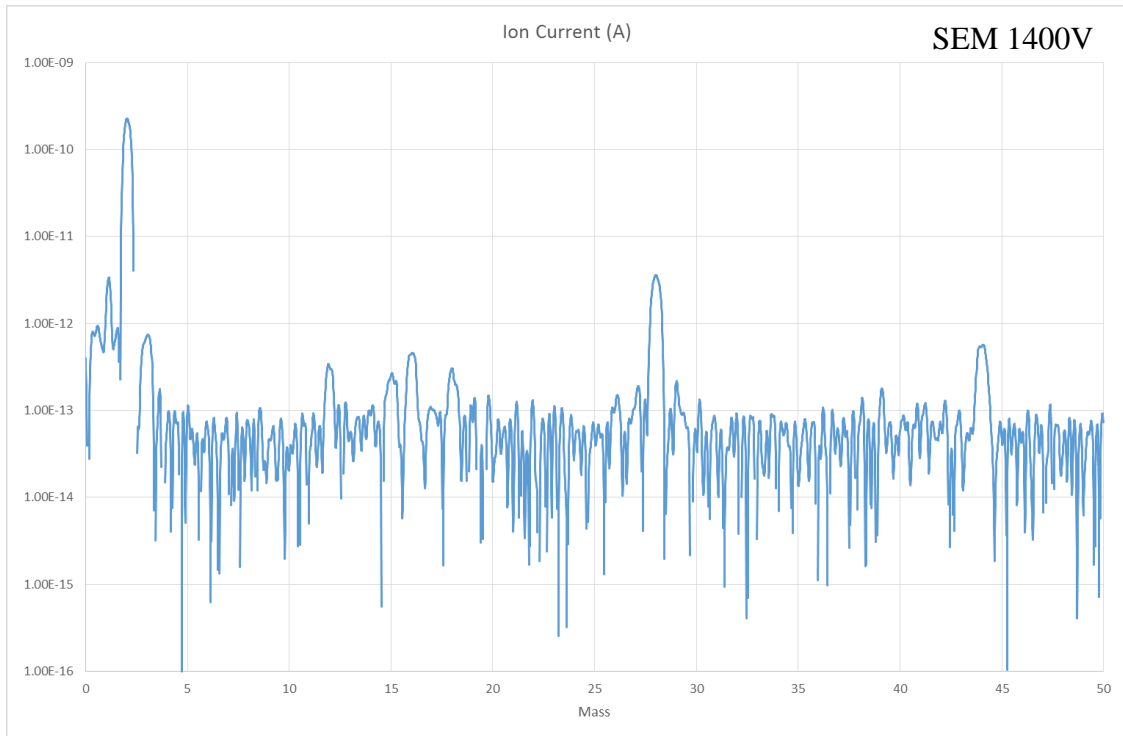


*Figure 7-31: RGA spectrum on NEG liners before bake out..*

Example 3, 10.12.15 at 10:18: during bake out (see *Figure 7-32*).

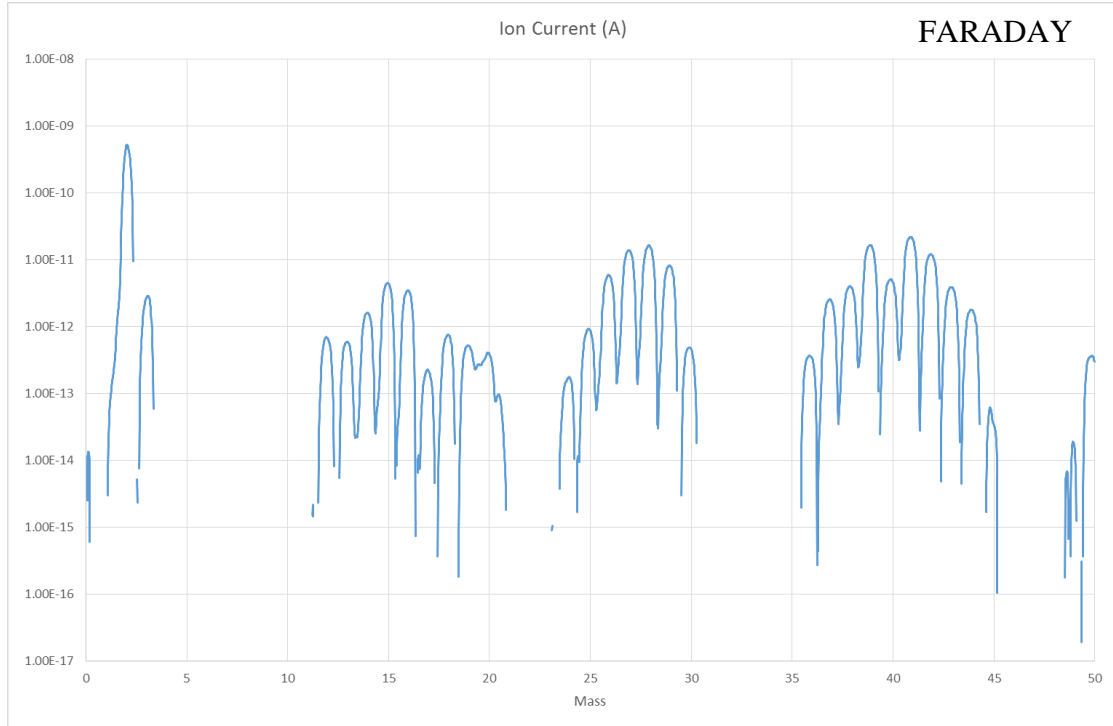


*Figure 7-32: RGA spectrum on NEG liners during bake out and activation at 180°C.*

Example 4, 11.12.15 at 16:55: after bake out (see *Figure 7-33*).

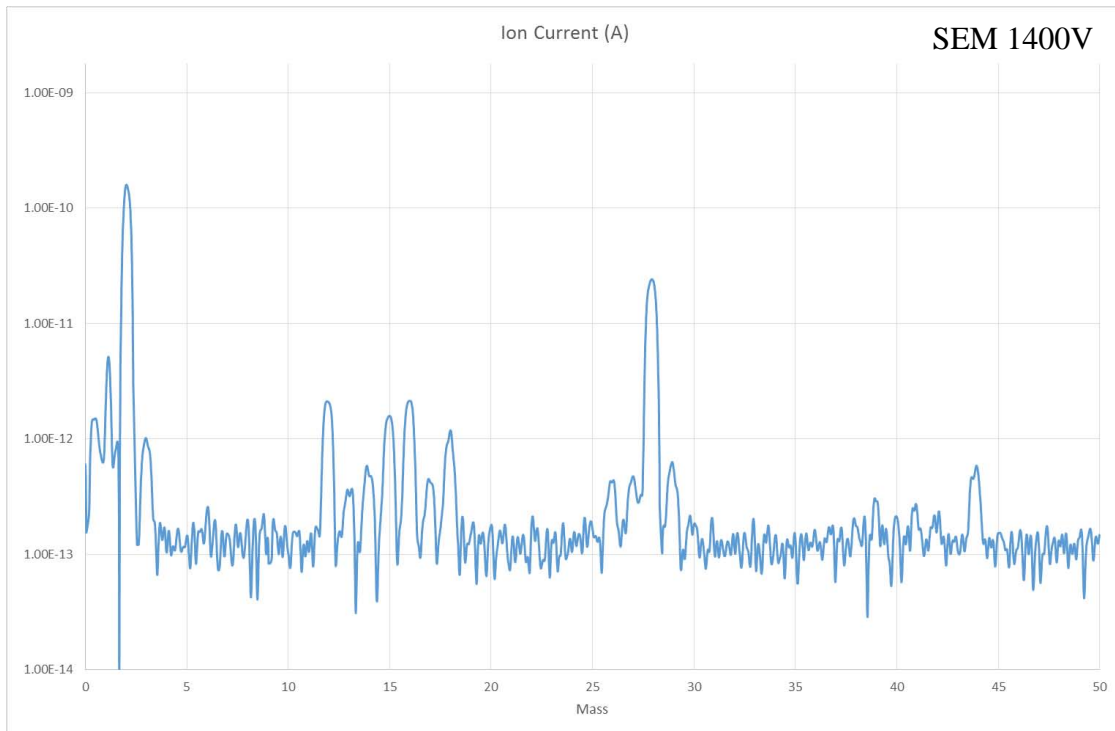


*Figure 7-33: RGA spectrum on NEG liners after activation.*

Example 5, 14.12.15 at 08:58: during injections (see *Figure 7-34*).

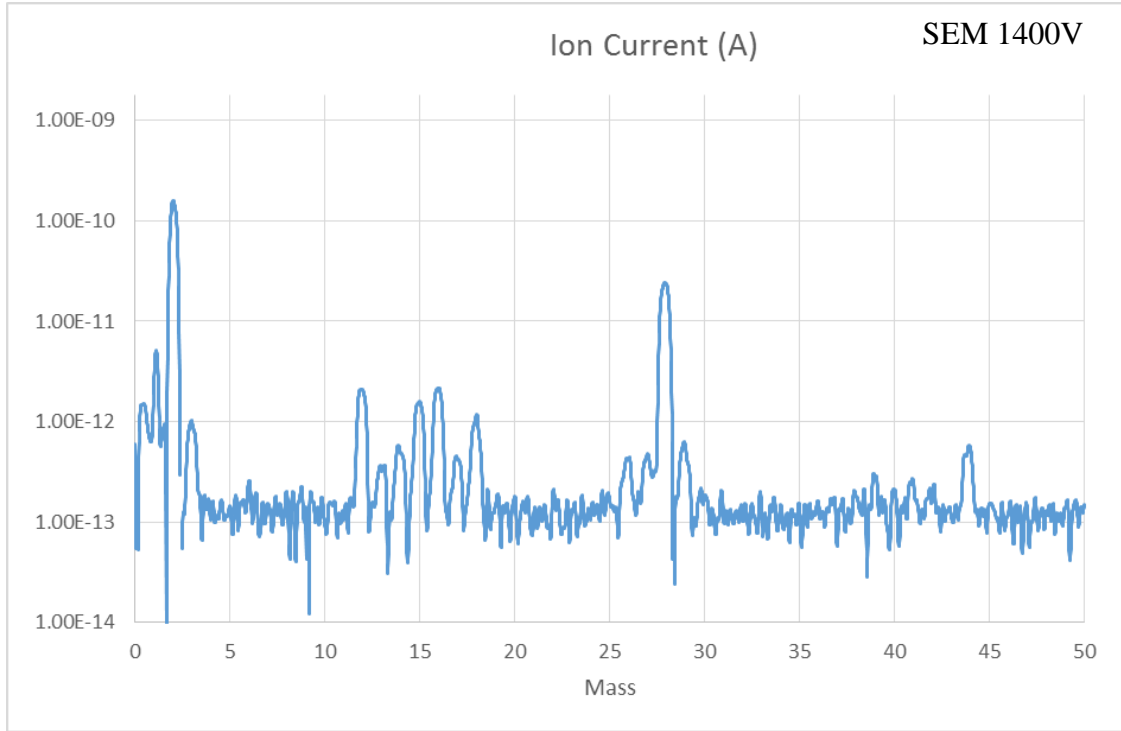


*Figure 7-34: RGA spectrum on NEG liners during injections of H<sub>2</sub>.*

Example 6, 14.12.15 at 14:19: after injections (see *Figure 7-35*).

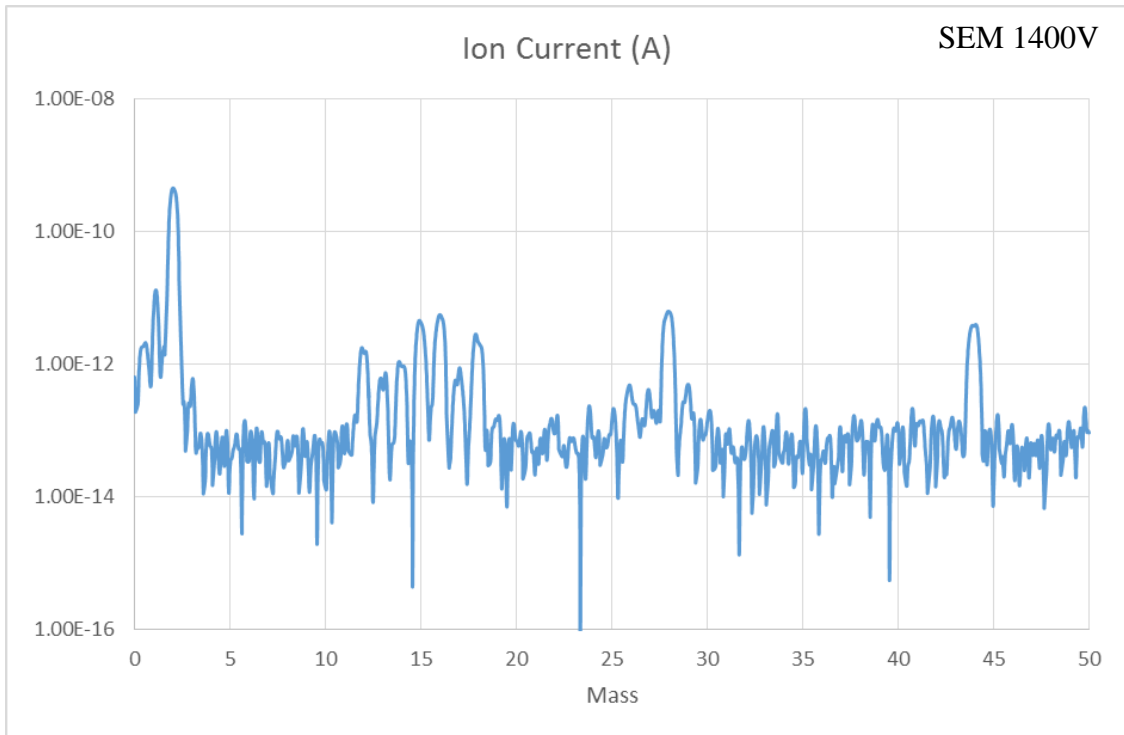


*Figure 7-35: RGA spectrum on NEG liners after injections of H<sub>2</sub>.*

Considering these spectra, it is possible to notice that hydrocarbons are present. The bake out and activation release many of these (examples 1 and 3).

Considering the pressure during injections, an important parameter to calculate is the sticking factor. It depends on the geometry (length divided by the radius) and on the ratio of pressure between the pressure of injection (SVT2) and the pressure at the end of the system to test (SVT3). It explains the capacity of a surface to pump some gasses.

Using Inventor and Molflow is possible to do a simulation and build a reference curve considering  $L=2756\text{mm}$ , that is the length of two chambers in series, and  $r=40\text{mm}$ , this is the result. Once the ratio of pressure is known, is possible to enter in the graph and discover the value of sticking factor (see *Figure 7-36*). (57)

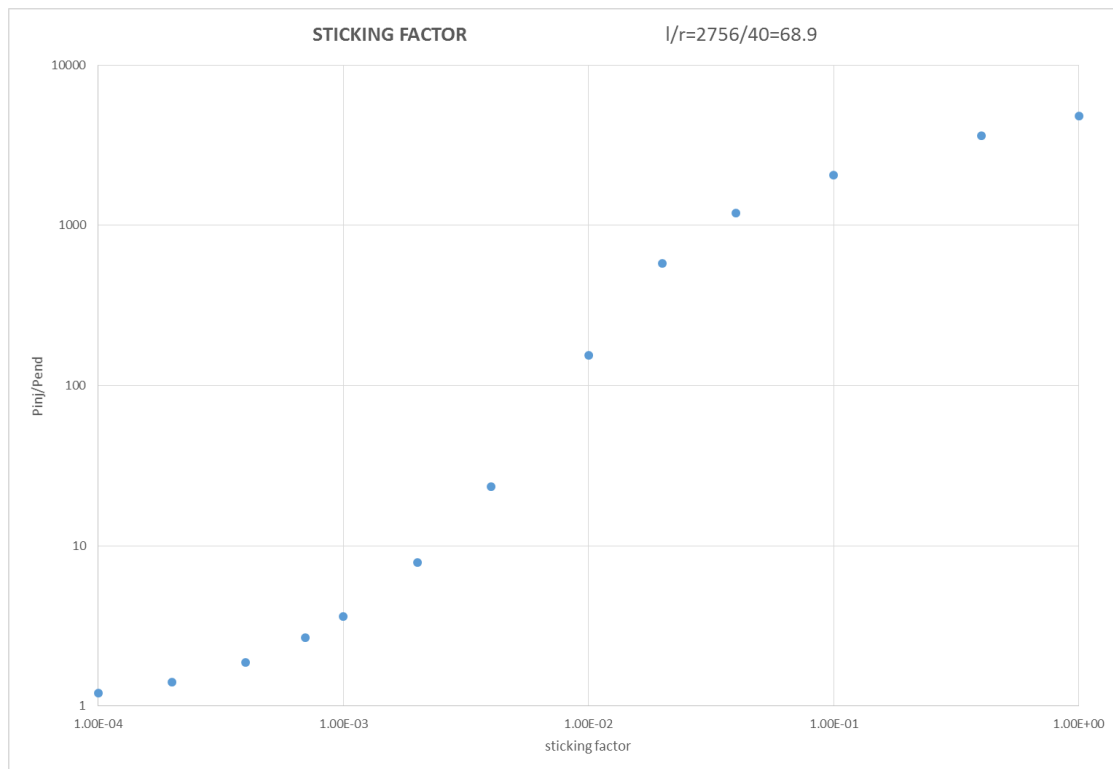


*Figure 7-36: Sticking factor in function of the geometry of the tube.*

Usually a good value is between  $10^{-2} \div 10^{-3}$ , while in this case the value is really lower. This means that NEG is not well activated or saturated by the injection or is “dead”, i.e. some reactions occurred and created chemical strong bounding with the surface. The most probable hypothesis is that the activation, due to a high amount of Kapton cables, is not successful.

### 7.3 Installation of new system

Thanks to the help of my team and an external company called “40-30 Air liquid” (58) the old VPS is dismantled in the tunnel. In the same time the new VPS is dismantled from the laboratory and, after nitrogen injections and around 30h of ventilation in air, is mounted in LHC tunnel. Then a leak test is done. (59)

Here a photo of mine, (see *Figure 7-37*), while tightening a flange on station 2, blue pipe.

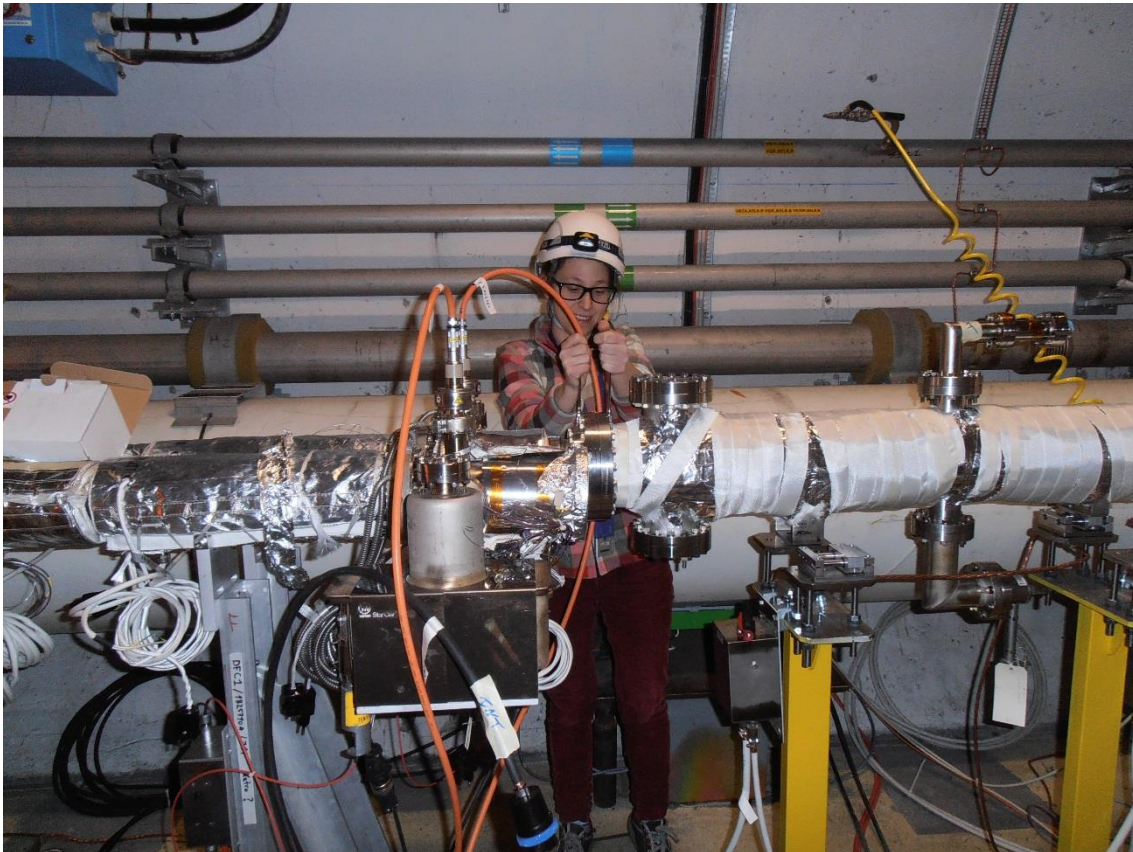


*Figure 7-37: Me during the installation of new VPS.*

After the installation the bake out takes place. As told in *Paragraph 7.2.5*, depending on the material there are different programs to use in order to heat up the system without damaging delicate parts.

This heating of VPS is done in three steps: the first in which the liners and the buffers are heated up respectively to 80°C and 120°C in order to degas the higher amount of water kept in the Kapton wires.

After some days the “bake out” can start when the temperature of gages reach 350°C, stainless steel and Penning gages reach 250°C, VQM up to 180°C, sector valves and NEG cartridge up to 140°C.

The third step is the “Activation” of NEG buffers that are in between the stations up to 230°C.

All this procedure are shown in the following table (see *Figure 7-38, 7-39*), in which there are the ramp rate in °C/h, the temperature of the constant state to keep for at least one day.

BAKE OUT					
Part	Program	Step	Ramp rate	Plateau	
			°C/h	°C	h
NEG coated pats	1	1	50	120	24
		2	60	230	24
		3	80	20	24
stainless steels, magic box, penning	2	1	75	250	24
		2	50	150	24
		3	100	20	24
CF flange of NEG chambers	3	1	50	180	24
		2	50	250	24
		3	80	20	24
Sector Valves, NEG cartridge	4	1	50	140	24
		2	50	140	24
		3	100	20	24
SVT,RGA	5	1	75	350	24
		2	50	180	24
		3	60	20	24
BPM C	6	1	50	200	24
		2	50	120	24
		3	100	20	24
BPM T	7	1	50	180	24
		2	50	120	24
		3	100	20	24
Liners	8	1	50	80	24
		2	50	80	24
		3	50	20	24
VQM	9	1	50	180	24
		2	50	180	24
		3	60	20	24
Collars transition	10	1	50	120	24
		2	50	120	24
		3	60	20	24

Figure 7-38: Bake out trend guidelines for VPS.

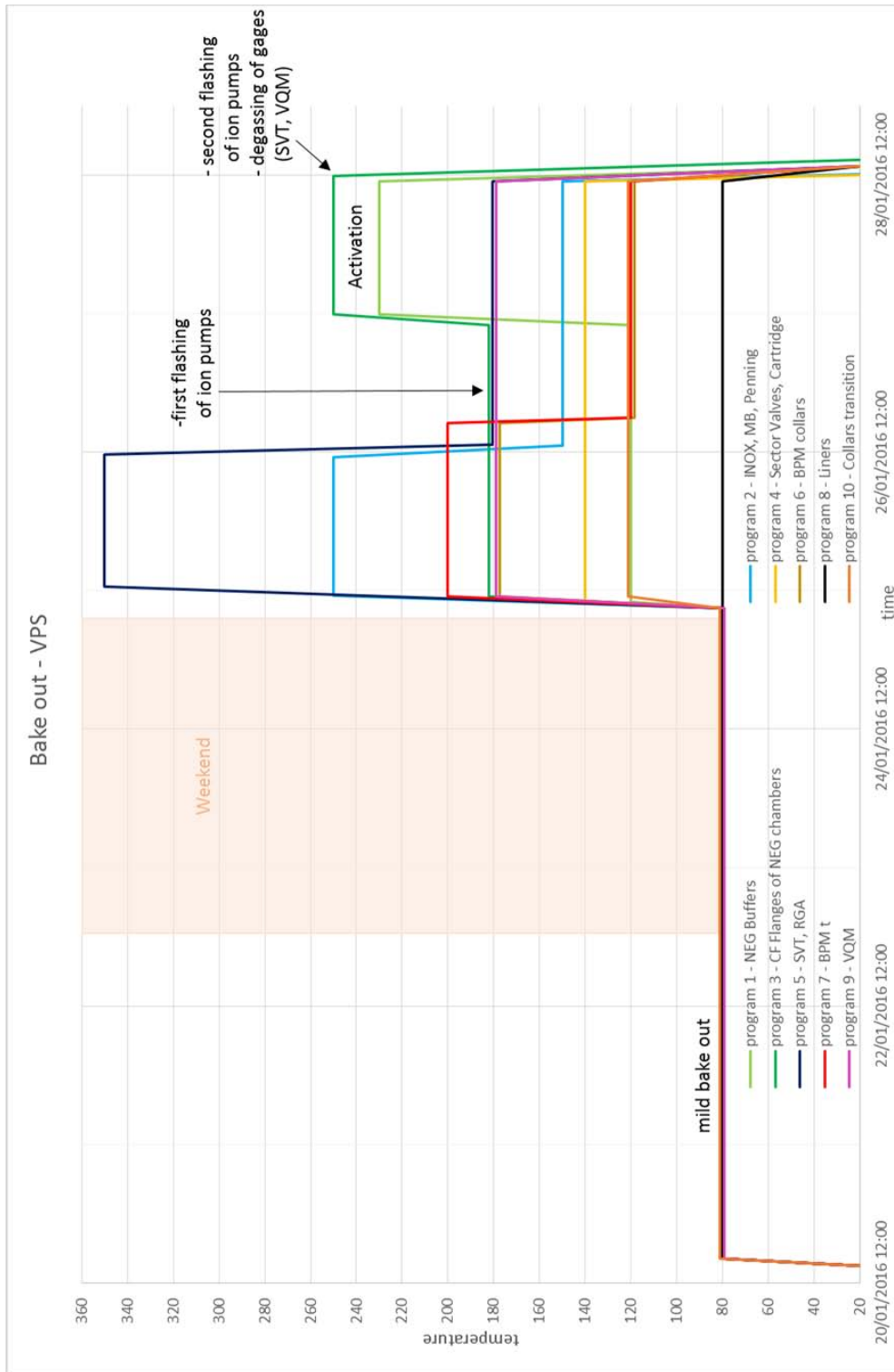


Figure 7-39: Bake out trend.

After this, the gas injections takes place, but they will not be presented in this work, due to the proximity of my graduation. In the next step of my career during my PhD at CERN the results and comparison will be present.



## 8. CONCLUSIONS

Here it is possible to find the main remarks of the analysis, considering both scrubbing runs and normal run of LHC, the difficulties encountered during the data acquisition and the production of the new version of the VPS and the next steps.

### 8.1 Achievements in brief

There are the main works followed by me during my job at CERN from March 2015 till now. The first consists on the monitoring of the scrubbing run from CCC with the relative analysis, the second are the analysis done considering all the detectors of VPS and the last is the optimisation and the build-up of the new set up that is installed in LHC accelerator from the beginning of 2015.

Speaking about Scrubbing Run results, I confirm that the conditioning was efficient, thanks to the decrease of pressure that is possible to see from my analysis on *Chapter 5*. The ratio between the pressure and the beam current decreases of about one order of magnitude from the beginning to the end of the scrubbing. In the future more has to be done in order to reduce the number of proton losses per batch to have a better conditioning. The next Scrubbing Run will be in April 2016 with the new VPS installed.

Speaking about analysis, it is possible to confirm some points:

- Keithley and SCOPE are working in the same range of values. Checked this, the new VPS was planned and installed with shielded pickup in order to read the total current with the Keithley and, thanks to the fast measurement (SCOPE), to see the build-up of the electron cloud in the new VPS (*Chapter 6.1*).
- There is a relationship of proportionality between the transparency of the grids (from 5% to 10%) and the currents of shielded pickup read. It was decided for the new VPS to increase some of the grid transparencies up to 50% in order to see if

in this new range the currents are proportional without killing the phenomenon (*Chapter 6.2*).

- The effective conditioning of the four stations is evident mainly for the copper ones, due to a high slope of the ratio between the beam current and the Keithley current. This is a double check of the real conditioning effect on the surfaces, happened during the Scrubbing Runs (*Chapter 6.3*).
- It is possible to confirm that the major presence of the protons starts around 2500-3000 GeV (*Chapter 6.4*).
- The intensity of the battery in Volt, used for the shielded pickup, influence the measurement because 9V is not enough to grab all the electrons. It should be more interesting to use 30V in order to increase the electrical signal of 15%. For the new VPS it is thought to use a 30V battery before the switch. This doesn't match with the necessity of unshielded pickup for photons that need -9V to operate. Due to the fact the switch is in common, the solution for the moment is to leave the actual batteries and play again with the High Voltage BIAS in order to investigate better this subject (*Chapter 6.5*).
- For the first time in LHC accelerator, a scan of the energy of the electrons is done and confirm the theory and experiments done in laboratories. The majority of electrons has energy less than 10eV, but some of them, called "reflected" have around 100eV, and are the reason of the multipacting effect (*Chapter 6.6*).
- Speaking about the calorimeters, the calibration gives information about the parameters (Rth and Cth) of the calorimeters. More has to be done in order to compare the amount of power deposition on the walls in this system present in a LSS, with the heat load of the arcs (*Chapter 6.7*).
- For the first time a gas analyser is used in LHC machine. It confirms that the main gasses released from Copper in a LHC run are water, carbon oxide and dioxide, methane and hydrogen. For NEG the significant picks are only methane and hydrogen, due to a better behaviour. The presence of the beam, increasing the pressure, increases the number of molecules released from the walls and so the picks are higher. With time, these picks decrease because the beam is doing a conditioning process on the surfaces. More has to be done to be able to compare

this VQM with a normal gas analyser that, in the accelerators, is not possible to use for electronic problems (*Chapter 6.8*).

- Considering the gas injections on the old system, it is evident that there is no a big change from the beginning of the installation to the end. It means that buffers are still pumping Hydrogen, thanks to activated NEG. (*Chapter 6.9*).

Speaking about the build-up of the new system, I planned and managed some of the steps, starting from a flat copper to the final liners. I learned a lot on welding, cleaning and building the liners. Thanks to technical instructions given by experts I succeeded on building the detectors, in particular calorimeters and pick up, to prepare the Kapton wires used to connect the detectors to the acquisition system and to mount all. These jobs increased my manual capabilities and permitted me to understand better the way in which instruments operate. For me, as Engineer, it was a very important opportunity to implement and realize improvements in this new version of the project. The new VPS is currently in the LHC accelerator and it will be studied by me for the next three years, before the technical stop in 2019.

I estimate the amount of time in which I studied and analyzed data from the office, I worked in CCC, the time in which I physically worked in the tunnel and in the laboratory, building detectors and mounting the liners, the time for training and courses in the following pie chart (see *Figure 8-1*).

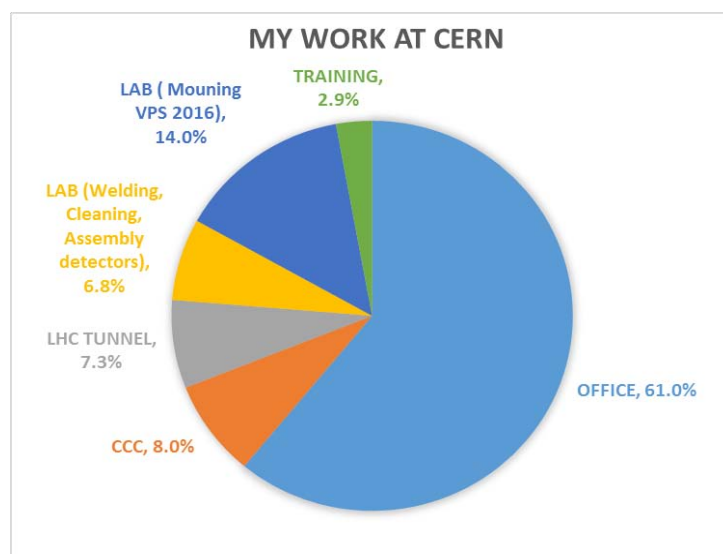


*Figure 8-1: Types of works I carried out during my permanence in CERN.*

It is possible to see that in 12 months working at CERN, I passed around 60% in the office (studying, reading articles, analyzing data, planning the new VPS), around 20% between the construction of detectors (welding, cleaning, assembling calorimeters and pickup) and the mounting of them in the liners, 7% for maintenance, cabling and mounting the new setup in the tunnel, the same amount in CCC during scrubbing runs and some units for training. This gives an idea of the kind of work done, concerning the very important practical experience I acquired in the last year.

## 8.2 Next steps

The next step for this new version of VPS in LHC accelerator is to follow the data acquisition in the next three years. I will have the opportunity to continue to work under a PhD with the University of Paris Saclay - Paris Sud.

I will also assembly a mock up in the new laboratory in order to do some calibrations and experiments to verify the truth of the data coming from LHC.

I will dedicate more time to do simulations, not only to verify the acquired data, but also to foreseen the behaviour of electron cloud phenomenon with different configurations, as for example for HL-LHC, the future improvement of the main accelerator. Also new coatings, as Laser treatment, will be studied. (60) (61) (62)

Here the schedule for the next runs of LHC and the following accelerators (see *Figure 8-2*). (63)

# New LHC roadmap: according to MTP 2016-2020

LS2 starting in 2019 => 24 months + 3 months BC  
 LS3 LHC: starting in 2024 => 30 months + 3 months BC  
 Injectors: in 2025 => 13 months + 3 months BC

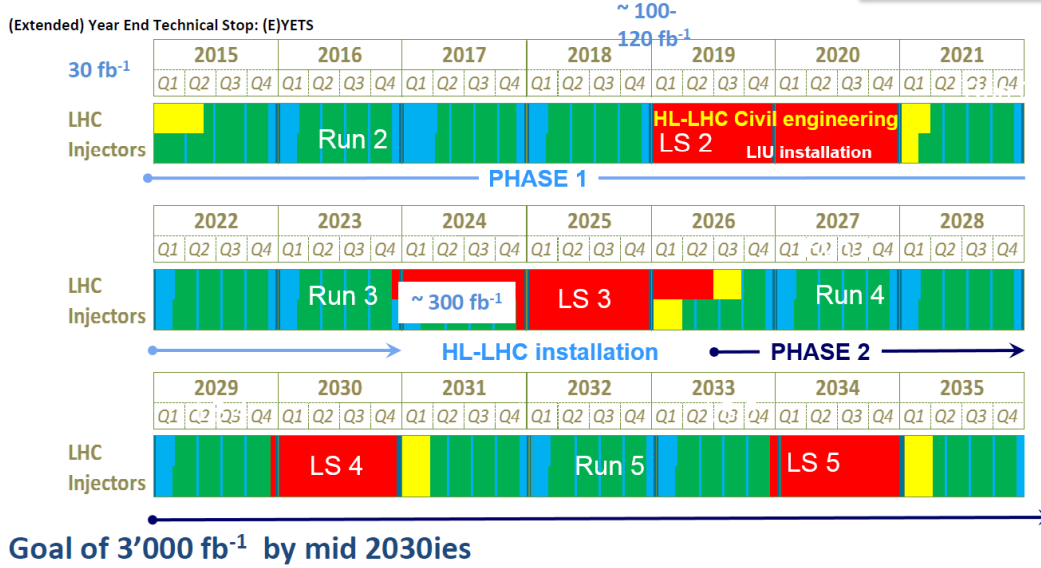
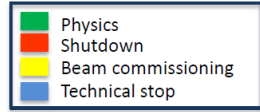


Figure 8-2: LHC roadmap until 2020.



## 9. BIBLIOGRAPHY

1. **L. Evans, P. Bryant.** *LHC Machine*. s.l. : ION Publishing Ltd and SISSA, 2008.
2. **Myers, .** *The Large Hadron Collider 2008-2013*. 2013. International Journal of Modern Physics A, Vol. 28, No. 25.
3. **CERN.** *http://home.cern/*.
4. **Virdee, .** *The LHC project: The accelerator and the experiments*. s.l. : Elsevier, 2010.
5. **B. Southworth, G. Boixader.** *Le monde des particules*. s.l. : CERN, 2000.
6. **Grobner, .** *Overview of the LHC vacuum system*. s.l. : Pergamon, 2001. Vacuum 60 (2001) 25-34.
7. **Baglin, .** *Vacuum Systems*. 2014. CAS - Introduction to Accelerator Physics, Prague, Czech.
8. **Chiggiato, .** *Vacuum issues*. CAS Intensity Limitations - Presentation.
9. **Sonato, .** *Lezioni di Scienza e Tecnologia del Vuoto*. Padova : s.n., 2005.
10. **Brabdt, .** *CAS - CERN Accelerator School - Vacuum in accelerators*. Geneva : CERN, 2007.
11. **Ricci, .** *Dispense di Fisica e Tecnologia del Vuoto*. Roma, Italia.
12. **Mazzolini, .** *The use of NEG Pumps and Coatings in Large Vacuum Systems: Experience and limitations*. Trieste, Italy : s.n., May 2006. CAS.
13. **Iadarola, .** *Electron cloud studies for CERN particle accelerators and simulation code development*. Geneva : CERN , March 2014. CERN Thesis 2014-047.
14. **G. Bregliozzi, V. Baglin, P. Chiggiato, P. Cruikshank, J.M. Jimenez, G. Lanza.** *Observations of electron cloud effects with the LHC vacuum system*. 2011. Proceedings of IPAC2011, San Sebastian, Spain.

15. **G. Iadarola, H. Bartosik, G. Rumolo, G. Arduini, V. Baglin, D. Banfi, S. Claudet, O. Dominiguez, J. Esteban Muller, T. Pieloni, E. Shaposhnikova, L. Tavian, C. Zannini, F. Zimmermann.** *Analysis of the electron cloud observations with 25ns bunch spacing at the LHC.* 2014. Proceedings of IPAC2014, Dresden, Germany.
16. **V. Baglin, O. Bruning, R. Calder, F. Caspers, I.R. Collins, O. Grobner, N. Hilleret, J.-M. Laurent, M. Morvillo, M. Pivi, F. Ruggiero.** *Beam-induced electron cloud in the LHC and possible remedies.* s.l. : CERN, 1998. LHC Project Report 188.
17. **R. Cimino, Theo Demma.** *Electron cloud in accelerators.* s.l. : World Scientific Publishing Company, 2014. International Journal of Modern Physics A, Vol 29, No. 17.
18. **Jimenez, J. M.** *SPS: scrubbing or coating?* s.l. : CERN, 2012. Proceedings of Chamomix 2012 workshop on LHC Performance.
19. **Y. Tanimoto, T. Honda, M. Ady, R. Kersevan, P. Chiggiato.** *Vacuum Properties of NEG and Carbon Coatings Exposed to Synchrotron Radiation.* 2015. Presentation.
20. **Chiggiato, .** *Vacuum properties of non-evaporable getter thin film coatings.* Presentation.
21. **W.H. Hartung, D.M. Asner, J.V. Conway, C.A. Dennett, S. Greenwald, J.-S. Kim, Y. Li, T.P. Moore, V. Omanovic, M.A. Palmer, C.R. Strohman.** *In-situ measurements of the secondary electron yield in an accelerator environment: Instrumentation and Methods.* USA : Elsevier, 2015.
22. **M. T. F. Pivi, G. Collet, F. King, R. E. Kirby, T. Markiewicz, T. O. Raubenheimer, J. Seeman, F. Le Pimpec.** *Experimental observations of in-situ secondary electron yield reduction in the PEP-II particle accelerator beam line.*
23. **J. J. Fijol, A. M. Then, G. W. Tasker, R. J. Soave.** *Secondary electron yield of SiO<sub>2</sub> and Si<sub>3</sub>N<sub>4</sub> thin films for continuous dynode electron multipliers.* 1990. USA.
24. **J. Barnard, I. Bojko, H. Hilleret.** *Measurements of the Secondary Electron Emission of Some Insulator.* s.l. : CERN, 1997.



25. **V. Baglin, J. Bojko, O. Grobner, B. Henrist, N. Hilleret, C. Scheuerlein, M. Taborelli.** *The secondary electron yield of technical materials and its variation with surface treatments.* EPAC 2000, Vienna, Austria.
26. **B. Henrist, N. Hilleret, C. Scheuerlein, M. Taborelli, G. Vorlaufer.** *The variation of the secondary electron yield and of the desorption yield of copper under electron bombardment: origin and impact on the conditioning of the LHC.* s.l. : CERN, 2002. Proceedings of EPAC 2002, Paris, France.
27. **V. Baglin, G. Bregliozzi, J.M. Jimenez, G. Lanza.** *Vacuum Performances and lessons for 2012.* s.l. : CERN, 2012. Proceedings of Chamonix 2012 workshop on LHC Performance.
28. **B. Henrist, V. Baglin, G. Bregliozzi, P. Chiaggiato.** *The LHC Vacuum Pilot Sector Project.* 2014. IPAC14.
29. —. *The LHC vacuum pilot-sector project.* 2014. Proceedings of IPAC2014, Dresden, Germany.
30. **Balzers.** *Measure de pressions partielles dans la technique du vide.* Liechtenstein : A. Pfeiffer GmbH, Assier. BG 800 169 PF (8310).
31. **Stanford Research Systems.** *Bayard-Alpert Ionization Gauges.* [www.thinkSRS.com](http://www.thinkSRS.com).
32. **Arun Microelectronics Ltd.** *UHV Bayard-Alpert Gage Manual.* 2015. KAIG17MANUSR.
33. **J.-M. Laurent, U. Irizo Ariz.** *Particle collectors for electron cloud studies.* s.l. : CERN, 2003. Vacuum Technical Note 03-05.
34. **J. Sikora, Y. Li, M. Palmer, S. De Santis, D. Munson.** *A shielded pick-up detector for electron cloud measurements in the CESR-TA ring.* Proceedings of BIW10, Sante Fe, New Mexico, US.

35. **S. Gerstl, R. Voutta, S. Casabuoni, A. W. Grau, T. Holubek, D. Saez de Jauregui, R. Bartolini, M. P. Cox, E. C. Longhi, G. Rehm, J. C. Schouten, R. P. Walker, G. Sikler, M. Migliorati, B. Spataro.** *Cold vacuum chamber for diagnostics: Instrumentation and first results.* 2014. Physical Review Special Topics - Accelerator and Beam, 17, 103201.
36. **V. Baglin, B. Jenninger.** *CERN SPS electron cloud heat load measurements and simulations.* CERN : s.n., 2003. Physical Review Special Topics - Accelerators and Beam, V. 6, 063201.
37. **L. Wang, A. Chao, H. Fukuma.** *Energy spectrum of an electron cloud with short bunch.*
38. **J.-M. Laurent, H. Song.** *Electron cloud energy and power measurements in SPS.* s.l. : CERN, 2004. Vacuum Technical Note 04-02.
39. **M. Commisso, T. Demma, S. Guiducci, L. Ping, A. Raco, V. Tullio, G. Viviani, R. Cimino, P. Vilmercati.** *A retarding field detector to measure the actual energy of electrons participating in e-cloud formation in accelerators.* Proceedings of EPAC08, Genoa, Italy.
40. **D. Saez de Jauregui, S. Casabuoni, A. Grau, M. Hagelstein, R. Cimino, M. Commisso, E. Mashkina, R. Weigel.** *Spectrum of the low energy electrons bombarding the wall in the anka storage ring.*
41. **Research Board.** *2015 Injector Accelerator Schedule.* s.l. : CERN, 2015.
42. —. *LHC Schedule 2015.* s.l. : CERN, 2015.
43. —. *LHC Schedule 2016.* s.l. : CERN, 2015.
44. **G. Iadarola, G. Arduini, V. baglin, H. Bartosik, J. Esteban Muller, G. Rumulo, E. Shaposhnikova, L. Tavian, F. Zimmermann, O. Dominguez, G.H.J. Maury.** *Electron cloud and Scrubbing studies for the LHC.* s.l. : JaCoW, 2013. Proceedings of IPAC2013, Shangai, Cina.

45. **O. Bruning, F. Caspers, I.R. Collins, O.Grobner, B. Henrist, H. Hilleret, J.-M. Laurent, M. Morvillo, M. Pivi, F. Ruggiero X. Zhang.** *Electron cloud and beam scrubbing in the LHC.* s.l. : CERN, 1999. LHC Project Report 290.
46. **G. Iadarola, G. Arduini, V. Baglin, H. Bartosik, J. Esteban Muller, G. Rumolo, E. Shaponshnikova, L. Tavian, F. Zimmermann, O. Dominguez, G. H. I. Maury Cuna.** *Electron Cloud and Scrubbing Studies for the LHC.* s.l. : CERN, 2015.
47. **G. Rumolo, G. Iadarola, O. Dominguez, G. Arduini, H. Bartosik, S. Claudet, J. Esteban Muller, F. Roncarolo, E. Shaposhnikova, L. Tavian.** *LHC experience with different bunch spacing in 2011 (25, 50 and 75ns).* 2012. Proceedings of Chamonix 2012 workshop on LHC Performance.
48. **C. Yin Vallgren, G. Bregliozzi.** *Scrubbing Runs and MDs 2015.* 2015. Presentation.
49. **Iadarola, .** *2015 LHC Scrubbing: goals, strategy, schedule and requirements.* mAY 2015. LBOC meeting.
50. **G. Bregliozzi, G. L anza, V. Baglin, J.M. Jimenez.** *Vacuum pressure observations during 2011 proton run.* s.l. : CERN, 2011. pages 177-182.
51. **G. Iadarola, H. Daerau, S. Gilardoni, G. Rumolo, G. Sterbini, C. Yin Vallgren.** *Electron cloud studies for the upgrade of the CERN PS.* 2013. Proceedings of IPAC2013, Shangai, China.
52. **G. Arduini, V. Baglin, T. Bohl, B. Jenninger, J.M. Jimenez, J.-M. Laurent, F. Ruggiero, D. Schulte, F. Zimmermann.** *Electron-cloud build-up simulations and experiments at CERN.* 2004. Proceedings of EPAC 2004, Lucerne, Switzerland.
53. **V. Baglin, G. Bregliozzi, J.M. Jimenez, G. Lanza.** *Synchrotron radiation in the LHC vacuum system.* 2011. Proceedings of IPAC2011, San Sebastian, Spain.
54. **F. Meot, L. Ponce, J. Bossler, R. Jung.** *Diagnostic with synchrotron radiation of the LHC proton beams.* 2002. Proceedings of EPAC 2002, Paris, France, pages 1945-1947.

55. **Sapountzis**, . *X-ray photoelectron spectroscopy (XPS) report*. s.l. : CERN, 2015. For VPS.
56. **Taborelli**, . *Carbon coatings for particle accelerator applications*. Chester : s.n., 2015. Presentation.
57. **V. Bencini, G. Bregliozi, C. Yin Vallgren, R. Kersevan, P. Chiggiato**. *Measurements of NEG coating performance variation in the LHC after the first long shutdown*. 2015. Proceedings of IPAC2015, Richmond, VA, USA.
58. **Air Liquide - 4030**. [http://sparesby4030.com/en/68\\_air-liquide](http://sparesby4030.com/en/68_air-liquide).
59. **P. Sonato, S. Dal Bello**. *La ricerca delle perdite con cercafughe ad elio*. Padova : s.n., 2004. Consorzio RFX.
60. **Wevers**, . *Outgassing of Laser Engineered Surface Structures*. 2016. Presentation.
61. **R. Cimino, A. Romano, S. Petracca, M. R. Masullo, S. O'Connor, G. Bregliozi, V. Baglin**. *Search for new e-cloud mitigator materials for high intensity particle accelerators*. 2014. Proceedings of IPAC2014, Dresden, Germany.
62. **Kato**, . *Caron Coating on Aluminium, Copper and Steinless Steel Chambers for e-Cloud Mitigation*. KEK (Japan) : s.n., 2015.
63. **Baglin**, . *HL-LHC: Where are we? Where do we go?* 2015. Presentation.
64. **G. Rumolo, G. Iadarola, O. Dominiguez, G. Arduini, H. Bartosik, S. Claudet, J. Esteban Muller, F. Roncarolo, E. Shaposhnikova, L. Tavian**. *LHC experience with different bunch spacing in 2011 (25, 50 and 75ns)*. 2012. Proceedings of Chamonix 2012 workshop on LHC Performance.

## **10. APPENDIX: ACRONYMS**

AGD: Argon Glow Discharge

ALICE: A Large Ion Collider Experiment

CERN: Conseil Européen pour la Recherche Nucléaire, European Organisation for  
Nuclear Research

CCC: CERN Control Centre

CMS: Compact Muon Solenoid

EC: Electron Cloud

HL-HLC: High Luminosity Large Hadron Collider

LHC: Large Hadron Collider

LHCb: Large Hadron Collider beauty

LSS: Long Straight Section

NEG: Not Evaporable Getter

OFC: Oxygen-free Copper

PS: Proton Synchrotron

Pt100: Sensor of temperature in Platinum

RF: Radio-frequency

SR: Synchrotronic radiation (light)

SEY: Secondary Electron Yield

SPS: Super Proton Synchrotron

TE: Technology Department

VPS: Vacuum Pilot Sector

VSC: Vacuum, Surfaces and Coatings group

VSM: Vacuum Studies and Measurement section



## 11. APPENDIX: DRAWINGS

Here it is possible to find the drawings of VPS used for the old and the new configuration.

- VPS layout
  
- Vacuum chamber
- Vacuum chamber and liner – old version
  
- Liner – old version
- Liner – new version
  
- Grid sheet for pickup
- Patch sheet for pickup and calorimeters
- Grid and patch sheet assembly for pickup
  
- Grid sheet for filter (75%)
- Patch sheet for filter (75%)
- Grid and patch sheet assembly for filter (75%)
  
- Detector sheet
- Cover sheet
- Module layers
  
- Full Patch sheet
- Patch layer











Liner – new version

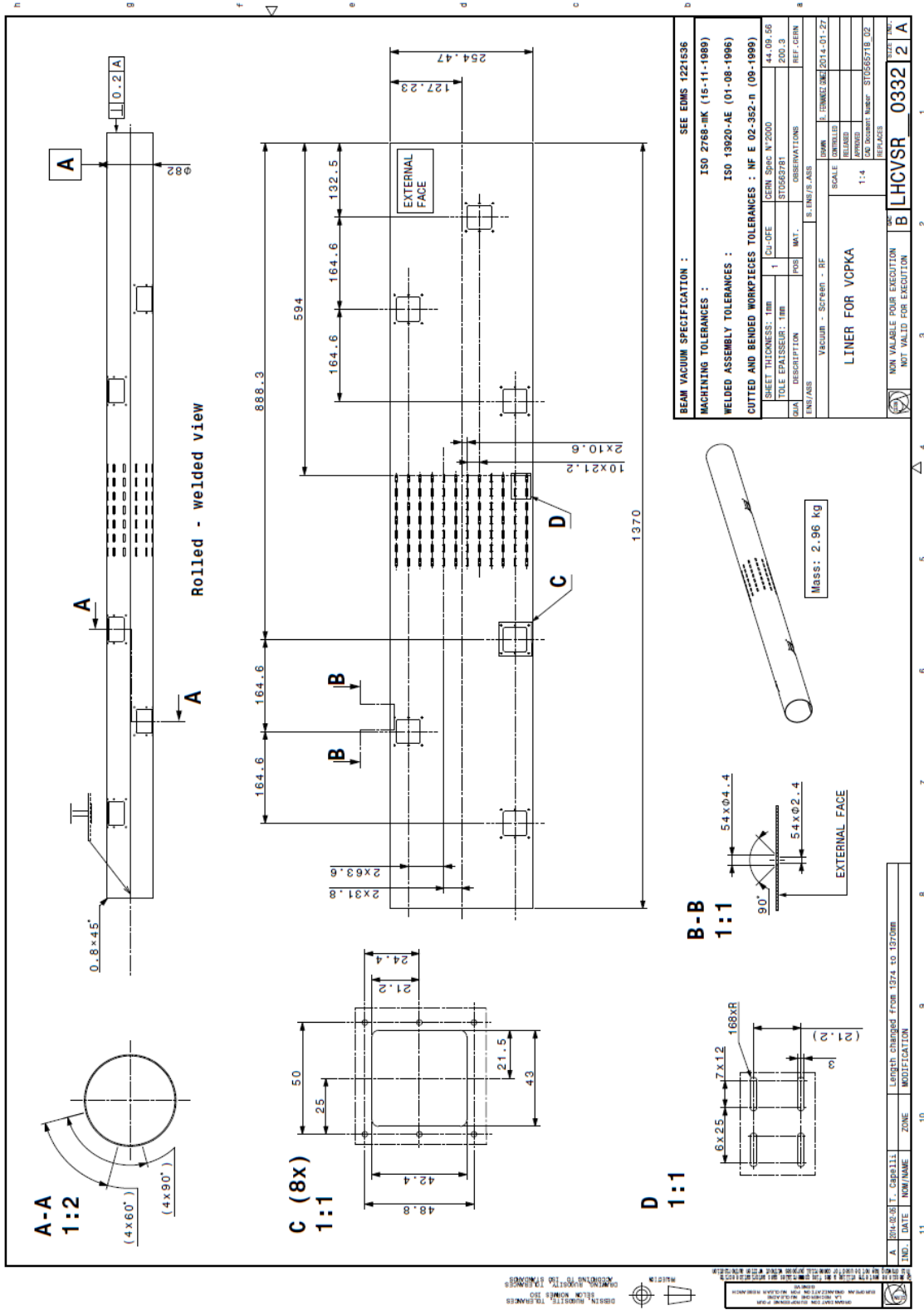


Figure 11-5: Liner – new version used since 2016

Grid sheet for pickup

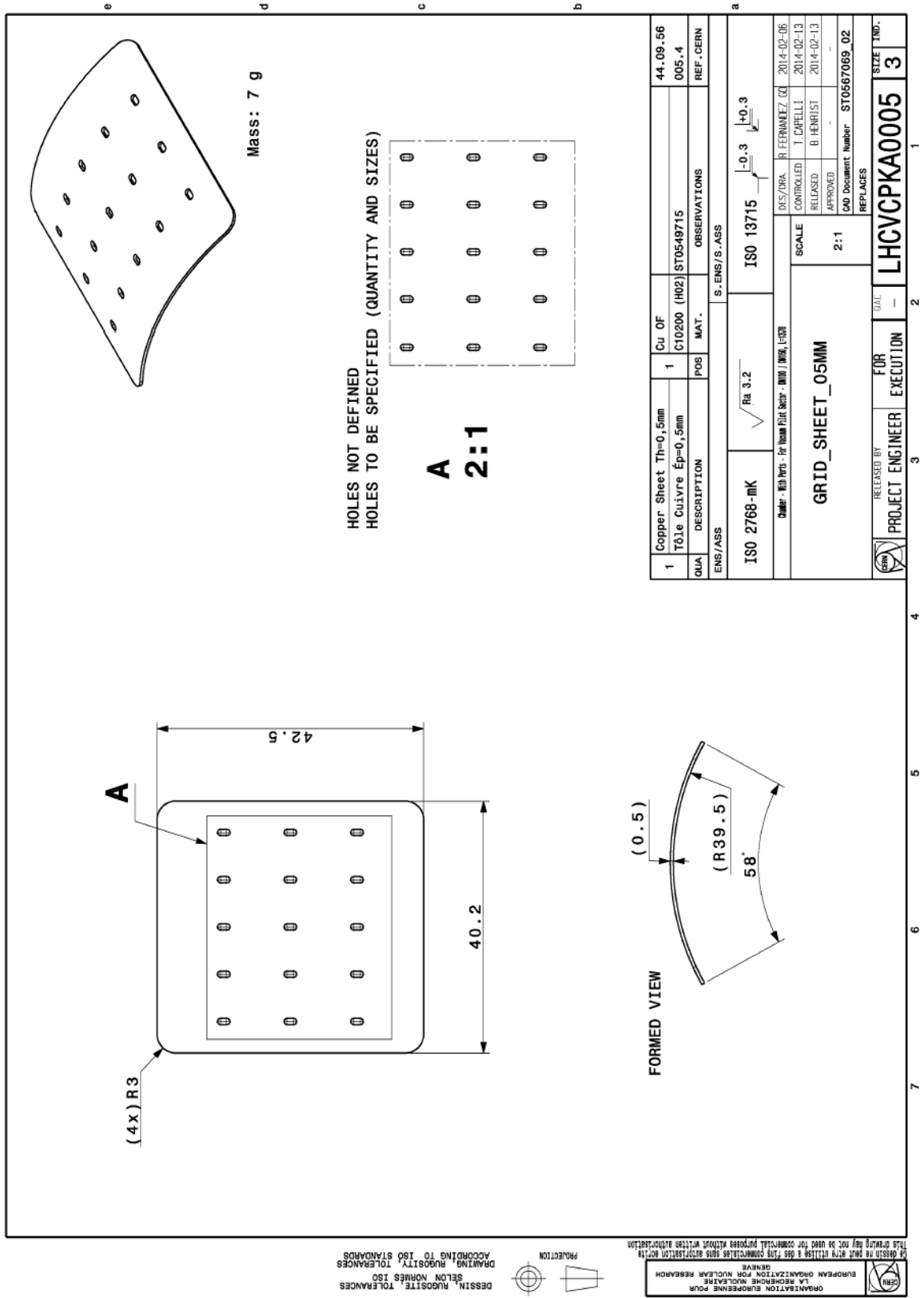


Figure 11-6: Grid sheet for pickup



Grid and patch sheet assembly for pickup

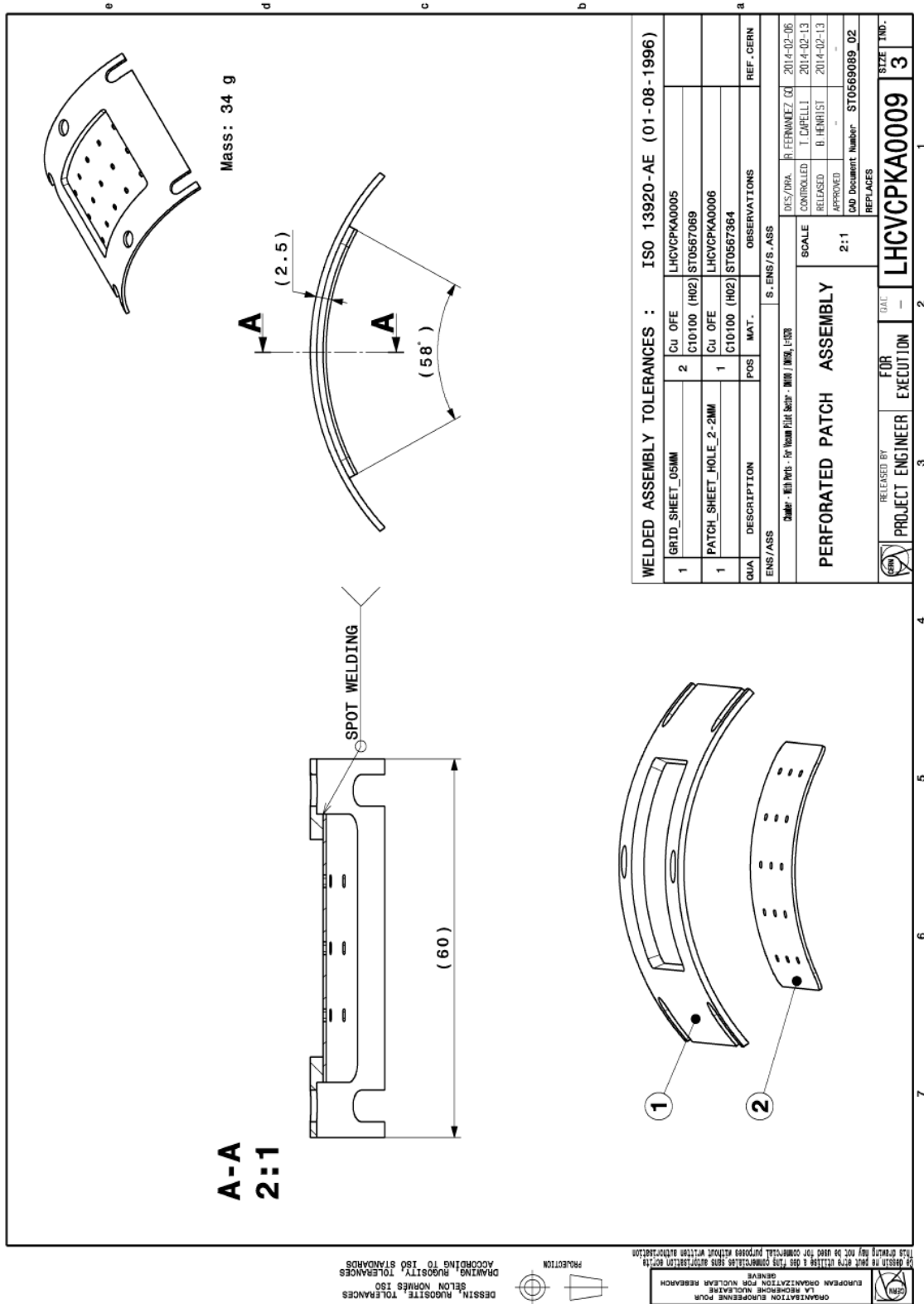


Figure 11-8: Grid and patch sheet assembly for shielded pickup: the grid is welded on the patch

Grid sheet for filter (75%)

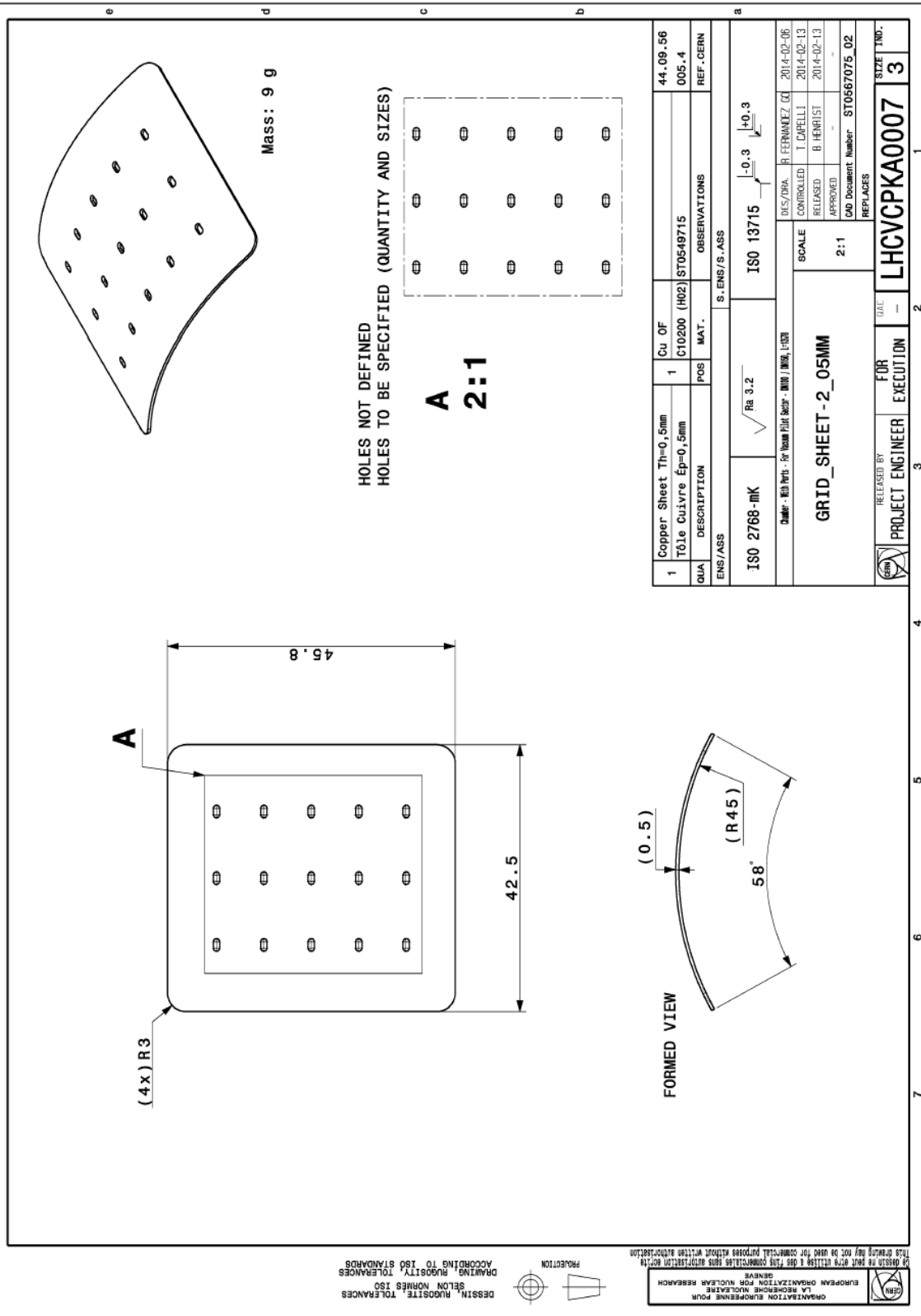


Figure 11-9: Grid sheet for filter (75%)







Detector sheet

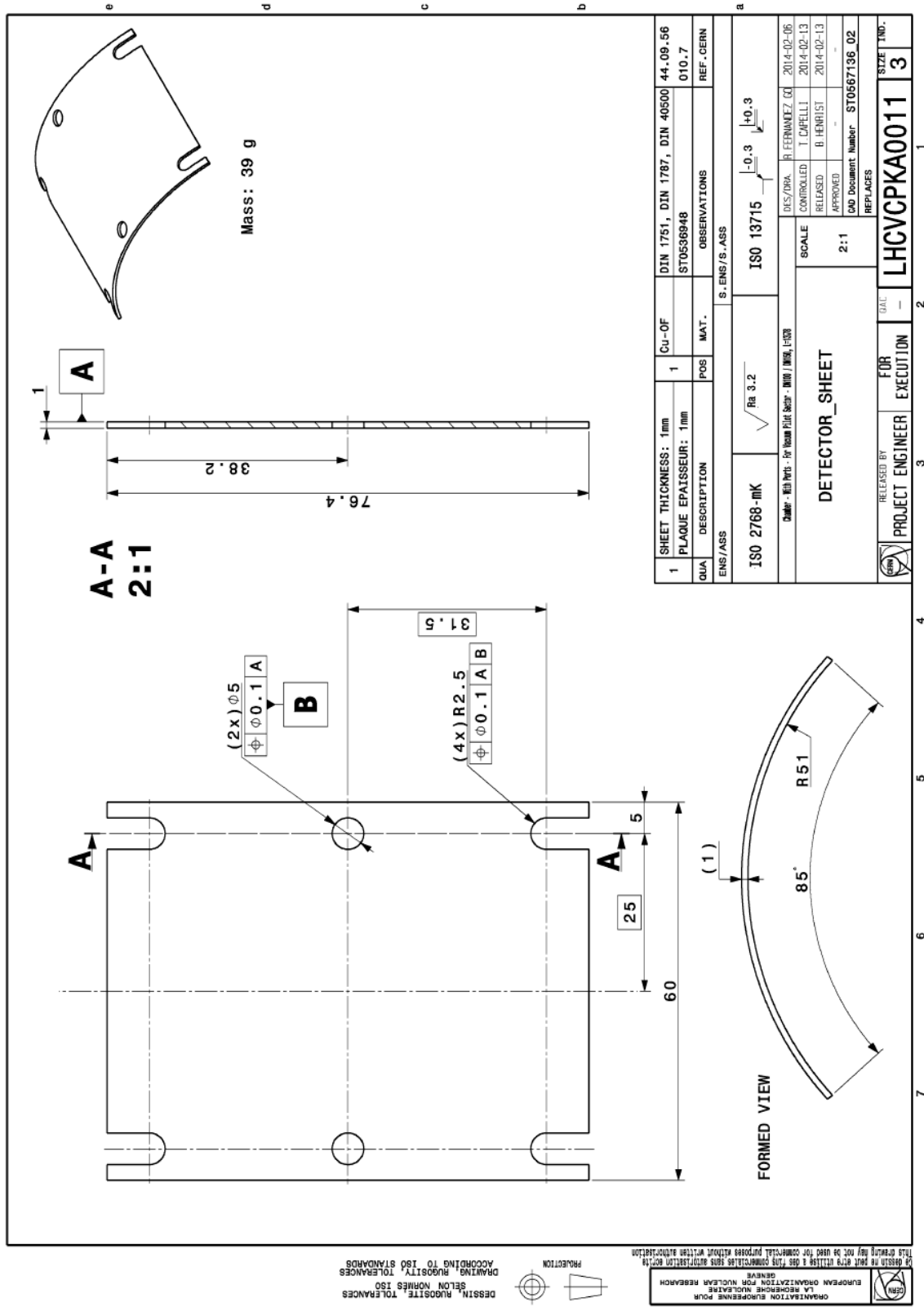


Figure 11-12: Detector sheet is the electrode that measures the currents for shielded pickup





Full Patch sheet

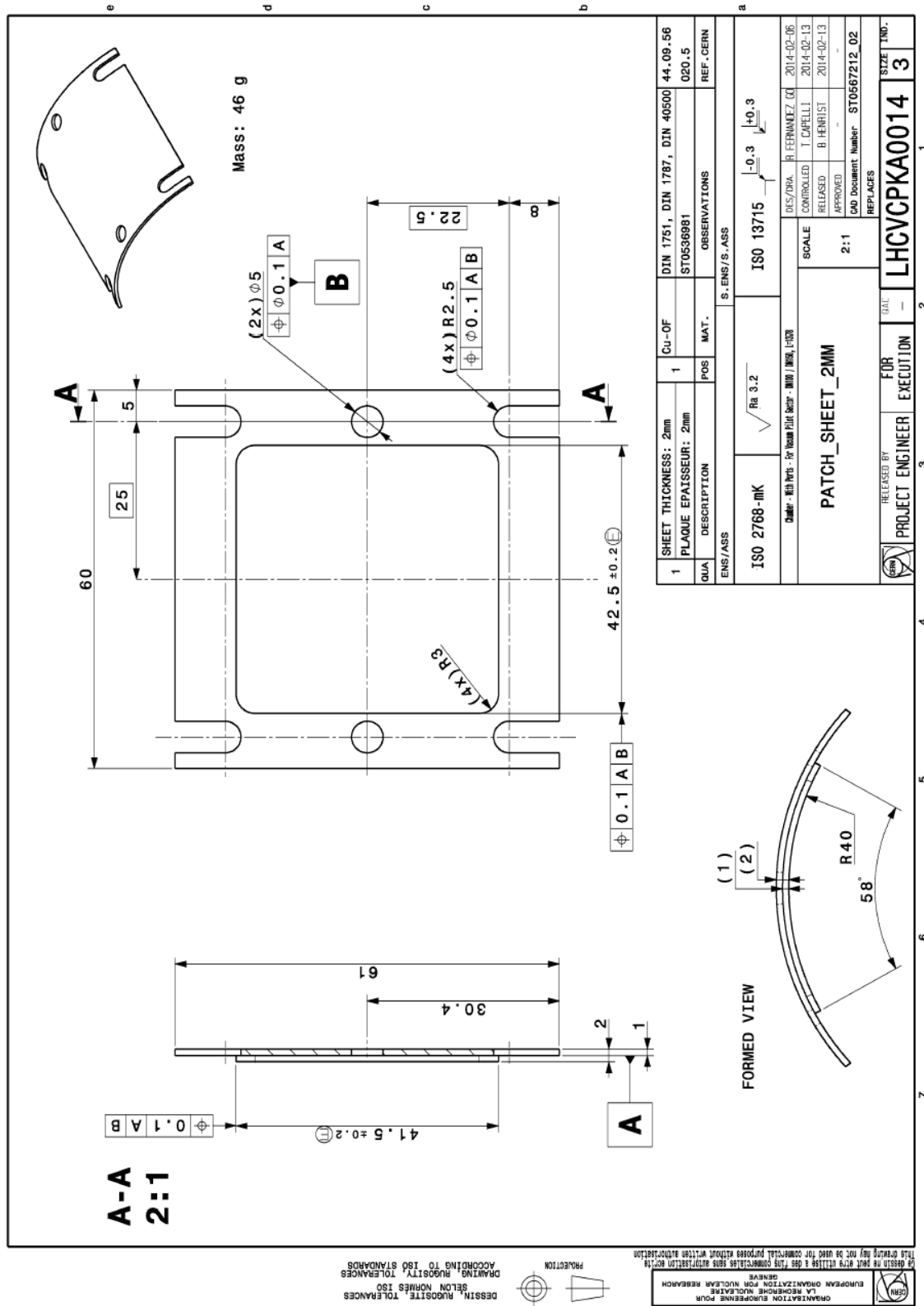


Figure 11-15: Full Patch sheet is present when a window on the liner is not used

# Patch layer

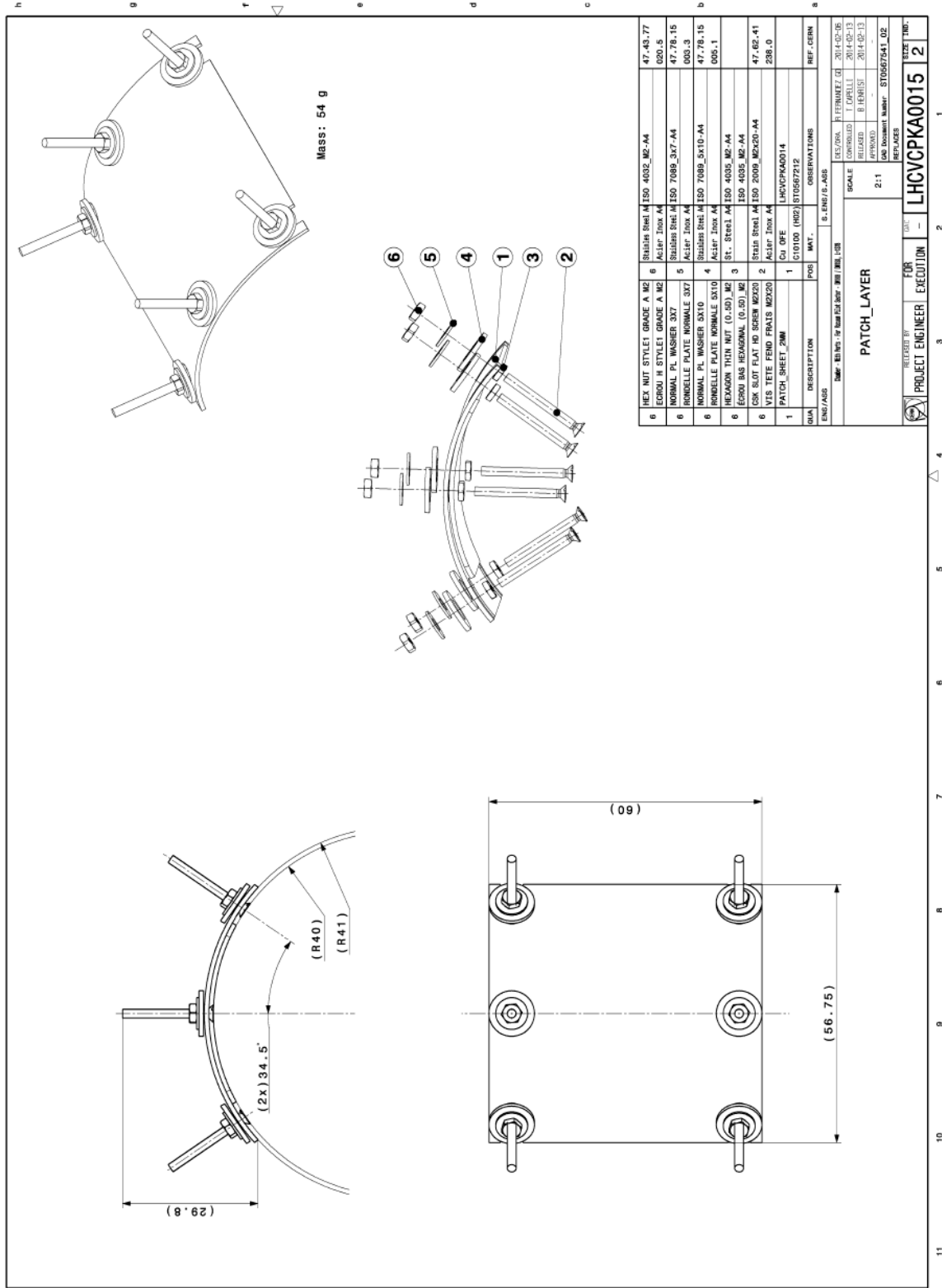


Figure 11-16: Patch layer assembly with screws





## 12. ACKNOWLEDGMENTS

I would like to Thank all the people who supported and helped me to achieve this wonderful experience at CERN, a dream, from my childhood, that became true.

First of all I would Thank Prof. Piergiorgio Sonato who transmitted me the love for the science, in particular for vacuum and plasma research. Thanks also to Dr. Gianluigi Serianni who sustained me in order to do this application.

Coming at CERN, I begin Thanking my group Leader, Paolo Chiggiato, and my Supervisor, Vincent Baglin, for the possibility they gave me, choosing me as Technical student.

A big Thank goes to Bernard Henrist, a skilled engineer who taught me quite everything about VPS, from theoretical part to practical experience, replying to my many questions.

Thanks also to Ivo Wevers for the great help in CCC and with VQM analysis.

Thanks the patient and kind engineer who shared the office with me, helped me in the building of new liners and taught me French, Philippe Lancon.

Thanks also to Berthold Jenninger who replayed to my several questions.

Thanks to Anne-Laure Lamure and Roberto Saleme, fellows, with whom I shared information and laugh.

I want to Thank also Giuseppe Bregliozzi and Christina Yin Vallgren with whom I collaborated during Scrubbing Runs.

I have to say a big Thank to technicians, Herve Rambeau and Hendrik Kos, who provided me their workshops and tools to realize new pieces for VPS.

I would like to Thank all the other Physicists, Engineers and Technicians who helped me during my work at CERN in order to understand a little bit more of this amazing world and to learn a method of scientific job through the team work.

Thanks to my parents, Anna and Francesco, my brother Matteo and my family because they were the first people who approved this experience and encouraged me to continue, following my dreams.

Thanks to all my friends, old and new ones, from each part of the world, because they remember me that fight for what I like to do is hard, but with their support is really rewarding.

I would like to conclude my work with this meaningful sentence:

“A: Why, what do you imagine to be able to find?

B: I believe I would simply like the idea of discovering something, of doing something unique that nobody has ever done before.”

From the Film: “*Garden State*”

“A: Perché, che cosa immaginate di poter trovare?

B: Credo che mi piaccia semplicemente, chissà, l’idea di scoprire qualcosa, di fare qualcosa di straordinariamente unico che nessuno ha mai fatto prima.”

Dal Film: “*La mia vita a Garden State*”

Thanks,

Filippo Burattini

My Section: TE-VSC-VSM 2015







My Group: TE-VSC 2015

